

ISSN: 1813-1786 (Print)
ISSN: 2313-7770 (Online)
Volume No. 21

Indexed & Abstract in:

- PASTIC SCIENCE ABSTRACTS
- AGRIS DATABASE
- ProQuest Products
- EBSCO DATABASES
- Library of Congress, USA
- OCLC World Cat

- Aluminum Industry Abstracts
- ANTE: Abstracts in New Technology & Engineering
- Ceramic Abstracts
- Civil Engineering Abstracts
- Computer and Information Systems Abstracts (Module)
- Copper Technical Reference Library
- Corrosion Abstracts
- Earthquake Engineering Abstracts
- Electronics & Communications Abstracts

- Engineering Research Database
- Engineered Materials
- Environmental Engineering Abstracts
- Environmental Science and Pollution Management
- Materials Research Database
- Mechanical & Transportation Engineering Abstracts
- Solid State and Superconductivity Abstracts
- Metadex

TECHNICAL JOURNAL

(Quarterly)

for online access please visit <http://web.uettaxila.edu.pk/techjournal/index.html>

2016



University of Engineering and Technology
Taxila, Pakistan

AIM & SCOPE

“Technical journal is a multidisciplinary journal in the field of engineering science and technology that offers platform for researchers, engineers and scientists to publish their original and to date research of high scientific value. It is a double blind peer-reviewed open access academic journal, published quarterly by University of Engineering & Technology, Taxila, Pakistan. Articles published in the Journal illustrate innovations, developments and achievements in the field of engineering and technology. The journal is being published electronically as well as in print form.”

Technical Journal

A Quarterly Journal of University of Engineering & Technology (UET) Taxila, Pakistan
Recognized by Higher Education Commission (HEC)
Y Category

ISSN: 1813-1786 (Print) ISSN: 2313-7770 (Online)

Volume No. 21 (Quarterly)

No. II (Apr - Jun)

2016

Phone: 92 - 51 - 9047896

Fax: 92 - 51 - 9047420

E-Mail: technical.journal@uettaxila.edu.pk

Chief Editor

Dr. Hafiz Adnan Habib

Managing Editor

Muhammad Anwar

Editor

Asif Ali

EDITORIAL OFFICE:

Editor Technical Journal

Central Library, University of Engineering and Technology (UET) Taxila, Pakistan

EDITORIAL BOARD

● INTERNATIONAL MEMBERS

Peter Palensky

Austrian Institute of Technology, Energy
Department, 1210 Wien, Österreich
peter.palensky@ait.ac.at

Patric Kleineidam

Lahmeyer International GmbH
Head of Department - Wind Energy, Friedberger
Strasse 173, 61118 Bad Vilbel, Germany
Patric.Kleineidam@de.lahmeyer.com

Brian Norton

Dublin Institute of Technology, Aungier Street
Dublin2, Ireland
president@dit.it

Assefa M. Melesse

Department of Earth and Environmental, ECS 339
Florida International University, Florida
melessea@fiu.edu

Jianzhong Zhang

School of Science, Harbin Engineering University,
Harbin, China
zhangjianzhong@hrbeu.edu.cn

Rodica Rameer

Micro Electronics, School of Electrical
Engineering & Telecommunication, University of
New Southwales Sydney, Australia
ror@unsw.edu.au

Jun Chang

School of Information Science and Engineering,
Shah Dong University, Jinan, China.
changjun@sdu.edu.cn

G. D. Peng

School of Electrical Engineering &
Telecommunication, University of New Southwales
Sydney, Australia
g.peng@unsw.edu.au

● NATIONAL MEMBERS

Abdul Ghafoor

Department of Mechanical Engineering, NUST
Campus, Islamabad
principal@smme.nust.edu.pk

M. Mazhar Saeed

Research & Development,
Higher Education Commission Pakistan
mmazhar@hec.gov.pk

Farrukh Kamran

CASE, Islamabad
farrukh@case.edu.pk

Haroon ur Rasheed

PIEAS, P.O. Nilore, Islamabad
haroon@pieas.edu.pk

Abdul Sattar Shakir

Faculty of Civil Engineering, UET Lahore
shakir@uet.edu.pk

Sarosh Hashmat Lodi

Civil Engineering & Architecture, NED UET,
Karachi
sarosh.lodi@neduet.edu.pk

Khanji Harijan

Department of Mechanical Engineering,
Mehran University of Engineering & Technology,
Jamshoro.
khanji1970@yahoo.com

Iftikhar Hussain

Industrial Engineering, UET Peshawar
iftikhar@nwfpuet.edu.pk

Ahsanullah Baloch

Faculty of Engg. Science and Technology, ISRA
Univ. Hyderabad
csbaloch@yahoo.com

● LOCAL MEMBERS

Niaz Ahmad Akhtar

UET Taxila
vc@uettaxila.edu.pk

Abdul Razzaq Ghuman

Faculty of Civil & Environmental. Engineering,
UET Taxila
abdul.razzaq@uettaxila.edu.pk

Mohammad Ahmad Ch.

Faculty of Electronics & Electrical Engineering,
UET Taxila
dr.ahmad@uettaxila.edu.pk

Shahab Khushnood

Faculty of Mechanical & Aeronautical
Engineering, UET Taxila
shahab.khushnood@uettaxila.edu.pk

Mukhtar Hussain Sahir

Faculty of Industrial Engineering, UET Taxila
Mukhtar.sahir@uettaxila.edu.pk

Adeel Akram

Faculty of Telecom & Information Engineering,
UET Taxila
adeel.akram@uettaxila.edu.pk

Mumtaz Ahmad Kamal

Faculty of Civil & Environmental Engineering,
UET Taxila
dr.kamal@uettaxila.edu.pk

M. Shahid Khalil

Faculty of Mechanical & Aeronautical
Engineering, UET Taxila
shahid.khalil@uettaxila.edu.pk

CONTENTS

	Page No.
SECTION: A	
1. Hill Torrent Management in Southern Punjab of Pakistan: Historic Perspective and New Trends M. M. Qureshi, M. U. Rashid, M. A. Shah, M. A. Baluch	02
2. Performance and Comparison of Crumb Rubber Modified and Conventional Mixes under Varying Temperature and Stress Levels M. A. Kamal, S. Shahid, M. U. Arshid, I. Hafeez	10
3. Investigation of Jatropha Biodiesel production on Experimental scale M. M. Tunio, S. R. Samo, Z. M. Ali, K. Chand	14
4. The Economic Analysis of Portable Photo-Voltaic Reverse Osmosis (PVRO) System H. Bilal, A. H. Alami, M. Farooq, A. Qamar, F. A. Siddiqui	19
SECTION: B	
6. Hybrid Power Analysis Approach for Electronic System Design Y. A. Durrani, A. Ahmad	26
SECTION: C	
7. Design and Analysis of Prototype Tesla Turbine for Power Generation Applications I. Zahid, A. Qadir, M. Farooq, M. A. Zaheer, A. Qamar, H. M. A. Zeeshan	33
8. Impact of swept volume ratio in designing a beta type Stirling engine F. A. Siddiqui, I. A. Chaudhry, M. Farhan, I. Sanaullah, M. Asim, M. F. Hanif, T. Ambreen	39
9. Off Shore Wind Turbines: A Solution To Energy Crisis In Pakistan M. M. A. Bhutta, M. A. M. Qureshi, M. A. Ahmad, S. A. Ahmad, A. A. Bhutti	49
10. Load Dispatch Management using Trend Analysis of Demand and Generation in Pakistan A. Ali, M. A. Chaudhary, S. Khushnood, M. Hussain	57
11. Knowledge management: Awareness and adoption in the Oil and Gas Automation industry in Pakistan M. P. Mughal, B. Ahmad	68
12. Process Improvement for PET Bottles Manufacturing Company Using Six Sigma Approach M. Ullah, A. M. Khan, R. Nawaz, R. Akhtar	76
13. Casagrande liquid limit testing of Jamshoro soil by One Point method M. Aslam, S. N. R. Shah, S. H. Otho	85
SECTION: D	
13. Classification of Brain States using Subject-Specific Trained Classifiers N. Irtiza, H. Farooq	96
14. Co-Design of Dual-Band Low Noise Amplifier Operating in 900MHz/1800MHz Bands for Multi-standard wireless Receiver S. Mudassir, J. Muhammad, J. Akbar, T. Mir, R. Zeeshan	107

Discover papers in this journal online <http://web.uettaxila.edu.pk/techjournal/index.html>

Views expressed in this journal are exactly those by authors and do not necessarily reflect the views of
University of Engineering and Technology Taxila or Chief Editor

Section A

CIVIL, ENVIRONMENTAL,
ARCHITECTURE,
TRANSPORTATION ENGINEERING
CITY AND REGIONAL PLANNING

Hill Torrent Management in Southern Punjab of Pakistan: Historic Perspective and New Trends

M. M. Qureshi¹, M. U. Rashid², M. A. Shah³, M. A. Baluch⁴

¹Department Civil Engineering, Quaid-e-Azam College of Engineering and Technology, (QETC), Pattoki Campus

²University of Management and Technology, Lahore

³National Engineering Services, Lahore

⁴University of Engineering & Technology, Taxila

¹mubashirengg@yahoo.com

Abstract-Hill torrents (locally known as Rodh Kohi) are distinct type of waterways in which water drains from the mountains and hit the localities and infrastructure in its way with enormous speed. More than 200 hill torrents originate from the west of Suleiman Range and hit Taunsa, Dera Ghazi (D.G.) Khan and Rajanpur Districts of Punjab in Pakistan. Among these, 13 hill torrents are having large catchment areas and flood potential. These Hill Torrents after crossing fan area locally named as "Pachad area" crosses D.G. Khan Canal through 22 numbers cross drainage structures and frequently creates disaster up to River Indus. Hill Torrents generally associated with uncertain flood flows have kept D.G. Khan and Rajanpur Districts Hill Torrent fan area socio economically very weak. Most often catastrophic flood events cause loss of billions of rupees to infrastructure, houses and irrigated lands. Conversely huge area, about 2.02 hectares, cultivable piedmont (Pachad) area fails to receive valuable irrigation water. Since the ancient times, diversion embankments of small size have been utilized by local people for diverting flood flows to their irrigation fields. These earthen embankments usually fail for high flow events but effectively divert low floods. A number of studies and plans were suggested to manage the Hill Torrent Floods since 1929 to date. It has been noted that these projects have shown some improvements in terms of utilization of Hill Torrent water for irrigation to uplift the economy of the area. It has been observed that piedmont area of the hill torrents is very fertile but due to erratic nature of floods land utilization is very low. The flood water due to its erratic nature one side destroys the infrastructure while on the other side barren land in piedmont area (Pachad area) is deprived off water for agriculture. This situation demands that there is a lot of space to improve the management of Hill Torrent floods. In this study existing management practices and appraisal of previous studies for Hill Torrents management in southern Punjab have been discussed with focus on additional prospective for sustainability of initiatives to gain full benefits of Hill Torrent water with an improved protection against flood vulnerabilities.

Keywords-Hill Torrents, Catastrophic Floods, Flood Water Management, Piedmont Area Irrigation

I. INTRODUCTION

The term torrent is utilized for water carrier channels carrying flash water flows; the term is mostly utilized for steep mountainous rivers generating rapid runoff. Locally these types of channels are termed as "Rodh Kohi". The torrential area of Dera Ghazi (D.G.) Khan and Rajanpur Districts of Punjab province is situated between the Indus River and the Suleiman range surrounded by province of Sindh, Baluchistan in the west and Khyber Pakhtunkhwa (KPK) in the North. About forty five percent of the total catchment areas lie in the two districts and the remaining 55% in the province of Baluchistan. The area in the west (on the right side of the Indus River) which is unirrigated by local canal Irrigation network is piedmont area locally known as "Pachad" area and is fertile due to unexploited sediment deposits of the mountains brought down with flood water. Pachad area is considered to be an area between darrah (the point after which torrent enters the plains) and the right bank of Indus River. The torrential area of the two districts consists of thirteen (13) major Hill torrents extending from Kaura and ending at Sori Janubi as shown in Figure 1. These torrents after crossing the piedmont area hits the cross drainage structures constructed across the Chashma Right Bank, D.G. Khan under construction Kacchi canals and ultimately enters to Indus River. The piedmont area of these torrents is situated in the arid zone of the country and only source of agriculture water is floods and rains. The rainfall pattern is such that it causes erratic and uncontrolled floods during Monsoon months (June to August). The flood water in monsoon at one side destroys the infrastructure in D.G. Khan Canal / Chashma Right Bank Canal command area due to erratic nature of flows while on the other side barren land in piedmont area are deprived off water for agriculture [1].

Various studies conducted on optimum use of flash flood water for irrigation purpose and minimize the drought effect for Hill Torrent's concluded that the

provision of storage reservoirs, diversion structures and cross drainage structures utmost important [ii-iv]. Conventionally agriculture growers in hill torrents regions use low flows of torrents by building small embankments locally named "Gandaz". It has been noted that flash floods break small embankments and not allow the farmers to use this precious water. 80 % agriculture contribution of Pakistan is supported from Punjab therefore it has a key role in Pakistan's economic life. More than 90% agronomic production in Punjab is through irrigated land exploiting a major part of its conventional water resources and land. Now with increasing population and reducing land resources, demands utilization of barren lands that only rely on the flood water irrigation. It has been noted that cropping intensity in piedmont area of hill torrents fluctuates significantly according to the level and frequency of inundating. Sorghum and Millets are sown on maximum of the cropped area on flood dampness and afterwards oil seeds are grown. For the occasions when flood period ends, late and optimal soil dampness is there in the soil from previous inundating, wheat is cultivated in the month of November. The flood water and silt of Pitok and Sori Shumali is brackish so injurious for plant growth. The piedmont area of remaining eleven hill torrents is very fertile because it has been developed by the continuous silt accumulation carried out by flood water. It has been noted that the yields per unit area are low which may be attributed to erratic and insufficient water availability and poor management practices [v].

The use of GIS was found effective for integrated way of conserving the excess water to minimize the flash flood risk and its use for irrigation purposes. Earthen reservoirs were proposed using GIS to achieve both the objectives [vi]. In order to uplift the quality of life for the people inhabiting the piedmont areas of these torrents and to avoid destruction of valuable infrastructure due to sudden floods, this research work investigated existing water management practices, various previous studies and implementation programs, conducted various site visits to the piedmont area to evaluate the outcome of existing management efforts and proposed new development strategies. Previous reports have been discussed keeping in view the management of floods of all 13 torrents and due to limited space, scope of evaluation for existing management practices and proposed development strategies have been discussed only for Kaha hill torrent. Kaha hill torrent has been selected for discussion as this torrent bring maximum discharge ($Q_{100} = 6440 \text{ m}^3/\text{s}$ at darrah) among the 13 torrents and has maximum potential of agricultural growth.

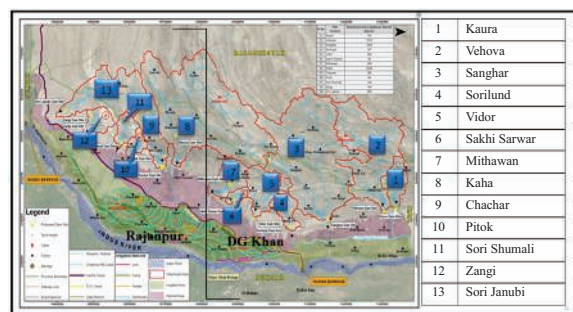


Fig. 1. Location of Hill Torrents of Rajanpur and D.G. Khan Area of Punjab, Pakistan

II. EXISTING WATER MANAGEMENT OF HILL TORRENTS

For cultivating the seasonal crops flood Irrigation is conventionally utilized for diverting flow of hill torrent into areas to be irrigated. The agricultural practices are developed keeping in view the extreme occasions of inundations and droughts and a unique irrigation system for hill torrent area is being practiced, known locally as "Kamara Irrigation". In this system sequential water rights are enforced and irrigation pattern are dictated starting higher to lower riparian, without concern of the period and amount of flows generated through storms. Due to this arrangement distant lower riparian's could not get irrigation water throughout a year of low flow. For utilizing the flood water generally embankments of earthen material are constructed through the stream with big water passage on one or both sides of the stream. Traditionally earthen embankments and arrangement of water delivery were built by the local peoples on their own by utilizing their customary expertise. It has been noted that locals, prepare field by constructing embankments of about 1.8 m high to store the water by keeping in view the soil type, share in water and various other local factors. As soon as water dried up in the field, crops are sown which flourish due to the moisture stored in the soil. No further irrigation is possible except rain if it occurs.

This arrangement is barely proficient of handling the small flows, upon which moderate and large flows destroy the earthen embankments of farmers and frequently cause unprecedented damages to the local economy. These sudden floods are causing not only the wastage of irrigable flows but from centuries are causing loss of human lives, edible, potable and cashable agricultural production.

Cropping intensity is defined as the percentage ratio of the cultivable command area to the cropped area. For evaluating the existing system cropping data from revenue record from concerned offices of Rajanpur and Dera Ghazi Khan Districts has been collected (2010-2013) and average cropping intensity has been computed. The computed cropping intensities for each torrent are shown in Fig. 2 below.

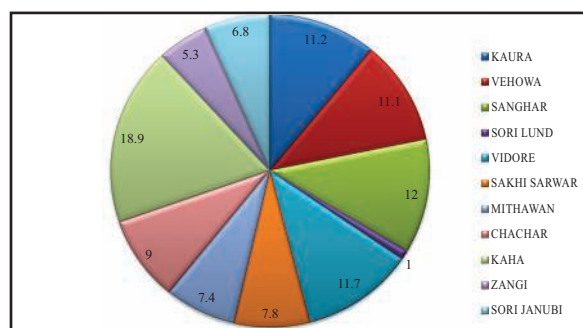


Fig. 2. Existing Cropping Intensity of Hill Torrents of Punjab Province, Pakistan

The analysis indicates the annual cropping intensity of the area is from 19% for Kaha to as low as 1 % for Sori lund. According to the amount and frequency of inundation in piedmont area, large variation in the cropping intensity has been noticed. Sorghum and Millets are sown on maximum of the cropped area on flood dampness and afterwards oil seeds are grown. Hill Torrent wise existing crop yields have also computed by analyzing field investigations and deliberations with officials of agriculture department functioning in the area. Published reports on Agricultural Statistics of Punjab for districts of Dera Ghazi Khan and Rajanpur were also consulted and compared for determining the existing crop yield levels. The crop yields estimated for Oil-Seeds, Pulses, Wheat, Bajra and Sorghum are 305, 280, 495, 242 and 293 kg/acre respectively. The overall yields are low that may be attributed to erratic and insufficient water supplies. Socio-economic situation of the agricultural community can be deteriorated without flood protection and proper management of water resources.

In order to improve the socio-economic condition of the local people of piedmont area various studies and implementation plans were initiated by various governmental agencies. In this research effort various previous reports have been studied and their recommendations are discussed below.

III. REVIEW OF PREVIOUS REPORTS

Following previous reports have been studied to review the previous development plans;

- NESPAK (1984), Flood Management of Dera Ghazi Khan Hill Torrents [vii]
- JICA (1992), Feasibility Study (FS) on Development of Irrigation based upon Flood Flows of Dera Ghazi Khan Hill Torrents [viii]
- NESPAK, (1998). Master Feasibility Studies for Flood Management of Hill Torrents of Pakistan, Flood Flows of D.G. Khan Hill Torrents, Federal Flood Commission, Ministry of Waters and Power, Govt. of Pakistan, [ix]
- NESPAK, (2005). Chashma Right Bank Irrigation

Project (Stage-III) Updating Feasibility Study on Hill Torrents Management Plan in CRBC Area in Dera Ghazi Khan District, Irrigation & Power Department, Punjab, [x]

After reviewing the above reports following are the inferences;

- It was identified [vii] that recommended strategy should be, “utilizing the maximum quantities of floodwaters in areas where they are generated”. For utilizing the flood waters gabion dispersion structures were proposed and no structure for storage or delay action dams was planned.
- It was proposed [viii] that catchment management techniques will cater sediment production of upper catchment for sustainable and long term solution for hill torrent management difficulties. The study proposed some dispersion structures for Vidore as case study.
- It was adopted [ix] to build suitable flood dispersion and diversion structures sustained by a system of surface drains to securely take the left over flow to the Indus River. In this study also no storage/delay action dam structure was proposed with the reason that dams may fill immediately due to heavy sediment loads.
- Six alternatives were evaluated [x] and finally recommended approach was Diversion /Distribution Options for attaining flood mitigation and irrigation purposes in the piedmont area. This study has also not considered dam structure in mountains with the same reason as mentioned above.

The outcomes of previous reports suggested that almost all the studies have considered distribution/diversion of floods in piedmont area with gabion dispersion structures and have not considered dams - either delay action or storage option - in mountain area.

The probable reason of ignoring dam structures in mountain area may be techniques of reservoir flushing were not mature at the stage when these reports were prepared. Now, with the current engineering knowledge it is possible to flush reservoir by adopting suitable techniques. Therefore, in the present study, development plan is to consider flood management at two stages i.e.

- in mountains by constructing delay action/storage dams with suitable flushing arrangement and
- in the piedmont area by constructing dispersion structures/regular canal irrigation.

IV. PERFORMANCE EVALUATION OF EXISTING STRUCTURES OF KAHA HILL TORRENT

Kaha Hill Torrent is one of the main hill torrents of Dera Ghazi Khan. It originates in the area lying within administrative territory of Balochistan Province and

drains an area of over 57, 00 sq km of Suleman Range. Kaha leaves mountains, upstream of Harand and fans out into numerous small channels known locally as wahs in downstream area. Flows of Kaha are managed with the help of 13 dispersion structures as shown in Figure 3. Recently under annual development program almost all the structures were modified from wire crate gabion structures to rigid PCC structures.

It has been noted that all the flood water dispersion structures across the flows are now rigid and constructed using PCC instead of conventionally used earthen embankments. It was informed by the local officials of the government agencies that, these rigid structures were constructed from year 2011 to 2013 under the annual development program and were according to the suggestions of various studies conducted in the past. These structures generally comprise of following components;

- Construction of a weir along whole width of hill torrent flow path which is a dispersion structure
- Upstream, downstream and central cut off walls on the basis of worst scour.
- Abutments, wing walls and retaining walls.
- Off taking channels on right and left side
- Protection bunds / embankments.
- Bed stabilizer on downstream of main weir.

For the purpose of performance evaluation of existing structures although several sites were visited as part of this study but in this paper two representative sites i.e. Muhammad Wah and Jindra Wah have been discussed and shown in Figures 4 and 5.

It has been noted that upstream side of the structures are filled with sediments after two flood seasons. This filling is as per design and will improve

the water entry to the off-taking channel (wah). On the downstream side gabion crating is provided at glaxis. It has been observed and reflected from the figure that gabion crates are damaged due to high velocity torrential flows. It has been noted that around downstream cutoff walls high speed flood water caused erosion as shown in the Figure 5. On the downstream side of the newly constructed structures these problems arise as energy dissipation phenomenon probably has not been considered in the design. It has been noted that no permanent structure has been provided for the off take of irrigation channels (Wahs). Drawback of this practice is that during high flows usually these earthen off takes could not perform properly and sometimes beds of wahs near off-take are subjected to heavy erosion and on other hand sediment accumulate at the mouth of wah and restrict the entry of water. It has been observed that upstream guide banks are constructed of local material and for preparing embankment it is not compacted as shown in Fig. 4. Disadvantage of this practice is that during high flows these embankments could not sustain the pressure of water and usually cause breaches. Due to breaches in guide bank water will disperse wildly instead of passing through the structures.

Although no data is available to compare the performance of these rigid dispersion structures to the historic earthen structures in terms of increase in cropping intensity or crop production. But from the discussions with local people it has been noted that these rigid structures are useful in improving the water diversion and reduced the annual efforts of the local people that they have to put after each flood in term of reconstruction of diversion weirs.

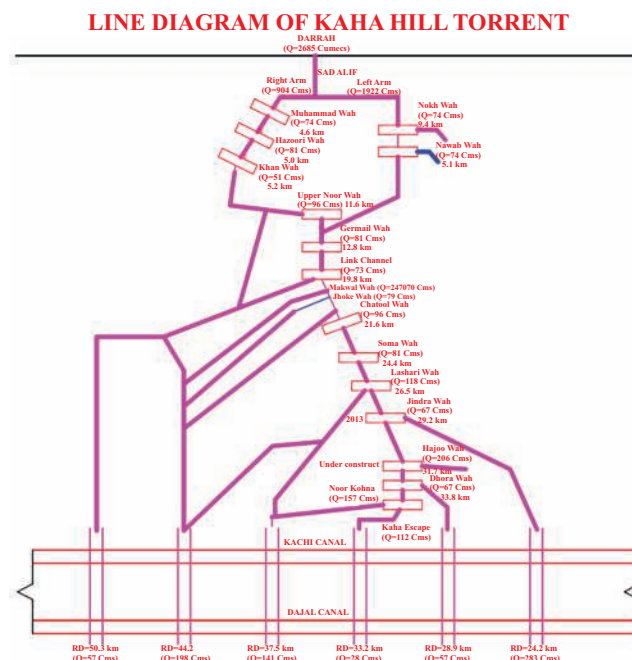


Fig. 3. Line Diagram of Kaha Hill Torrent



Fig. 4. Muhammad Wah (at 4.60 km) Kaha Hill Torrent



Fig. 5. Jindra Wah (at 29.20 km) Kaha Hill Torrent

V. PRESENT DEVELOPMENT PLAN FOR KAHA HILL TORRENT

Present development plan of the Kaha hill torrent has been proposed by keeping in view two issues i.e. to substantially reduce the flood peaks and to improve the irrigation agriculture of the area. For this purpose Kaha watershed was visited and identified a potential location for multipurpose dam near Nilakund village. The latitude and longitude of the site are $29^{\circ} 33' 46''$ and $69^{\circ} 48' 39''$ and it is about 18 miles upstream of Kaha darrah. For evaluating the storage potential of the site, freely available SRTM digital elevation data has been acquired and elevation area capacity curve prepared as shown in Fig. 6.

Hydrological studies at the dam site consist of computing the water availability and flood hydrographs. For this purpose rainfall runoff analysis has been done by utilizing the HEC-HMS computer software. The computed flood hydrographs at the dam site are shown in Fig. 7.

Dam height and its appurtenant structures like low level outlets and spillways at the selected site has been designed in such a way that created reservoir has

enough volumes to store the discharges that attenuate the peak of 100 year return interval discharge to 50% and to increase the cropping area from existing 6854 ha to designed 36180 ha. The salient features of the dam and its appurtenant structures are presented below.

Inflow Flood

Inflow Design Flood = $6440 \text{ m}^3/\text{s}$ (100 year Return Period)

Dam / Reservoir

Top of Dam Embankment = El. 684.4 m asl

Height of Dam = 124.0 m (El. 684.4 El. 560.4)

Reservoir Dead Storage (El. 575.7 m asl) = 0.11 Million m^3

Reservoir Gross Storage at MCL (El. 674.7 m asl) = 1227.62 Million m^3

Live Reservoir Storage = 1227.51 Million m^3

Spillway

Spillway width = 152.3 m

Crest Level = El. 674.7 m asl

Maximum Conservation Level (MCL) = El. 674.7 m asl

Low Level Outlets

Invert Level of LLOs = El. 575.7 m asl

Flushing Outlet

No. of Outlets = 4 No.

Size of Outlet = 2.74 m x 2.74 m

Total Discharge Capacity of Outlets at MCL = 924 m³/s

Water Availability

Average Annual Availability = 250 Million m³

Annual Agriculture Demand = 160 Million m³

Proposed Cropping Period = Whole year

Total CCA = 36180 ha

Cropping Intensity = 70% per annum

Agricultural Shortages = 10.0%

By utilizing the elevation~area~capacity, outflow rating of the dam outlet works and the inflow

hydrograph of 100 yr return Fig. 6. Elevation~Area~Capacity Curve at Selected Dam Site in Kaha Hill interval reservoir routing studies have been conducted by utilizing the MS Excel sheet program. The output of the reservoir routing study was an outflow hydrograph and is shown in Figure 8 below. It is evident from the figure that peak of the hydrograph is attenuated from 6440 m³/s to 3216 m³/s.

It is clear from the above analysis that if the development plan proposed as part of this study is implemented it will not only improve the irrigation agriculture of the area but also ensure safety of the downstream areas from the hazards of sudden floods.

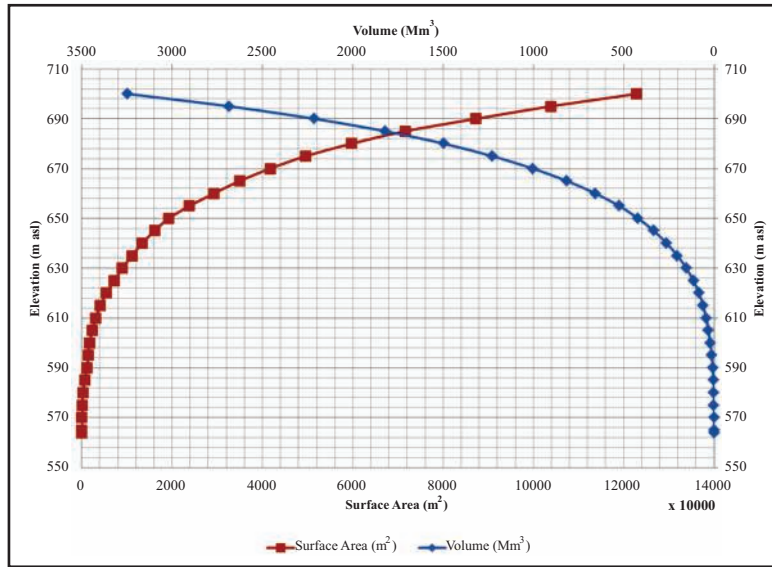


Fig. 6. Elevation~Area~Capacity Curve at Selected Dam Site in Kaha Hill Torrent

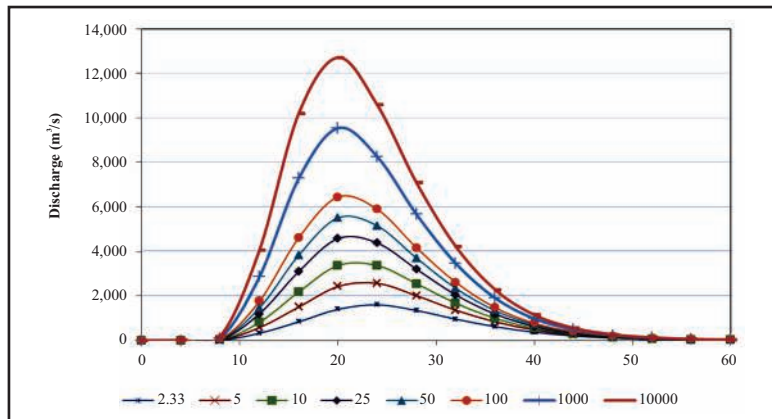


Fig. 7. Flood Hydrographs at Selected Dam Site in Kaha Hill Torrent

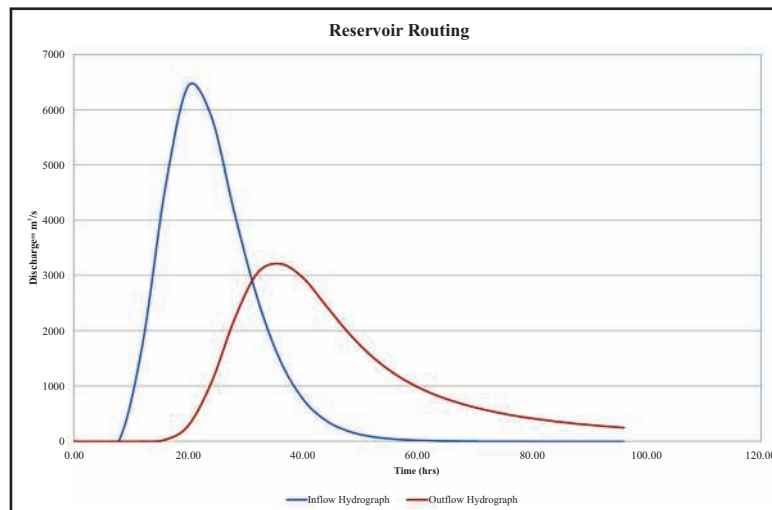


Fig. 8. Inflow and Outflow Hydrographs for Kaha Dam

VI. CONCLUSIONS AND RECOMMENDATIONS

Following are the main conclusion and recommendations of the study;

- The piedmont area of the hill torrents despite of having fertile lands in general is producing low value crops. The land utilization per year varied from torrent to torrent. Maximum existing cropping intensity is 19% in Kaha to as low as 1% in Sori lund.
- Historically, flood waters of hill torrents were diverted by using earthen embankments that washed away in even low to medium floods. Now, due to intervention of governmental agencies there is trend of constructing rigid dispersion structures instead of old flexible embankments.
- Newly constructed rigid structures cause improvement in diverting the flood waters to irrigation fields. Beside this there is need to improve the design of downstream energy dissipation arrangements according to the state of the art engineering practices.
- Presently flexible structures have been provided for the off take of irrigation channels (Wahs). It is recommended that these off takes should be designed as rigid structures to withstand high floods.
- It is recommended to improve the existing rigid dispersion structure by keeping in view their present performance.
- Present development plan of the Kaha hill torrent involve construction of 124 m high dam. Implementation of this development plan can cause appreciable reduction in flood peaks and will increase the cropping area by 5 times as compared to existing.
- It is recommended to initiate a comprehensive

feasibility study for the construction of dams in the mountain areas of the hill torrents.

ACKNOWLEDGMENTS

Writers are thankful to Punjab Govt. for providing relevant information / data. The amenities provided by the National Engineering Services Pakistan, Lahore during this study are also acknowledged thankfully.

REFERENCES

- [i] M. Shafiq, "Hill Torrent Management Initiatives In Southern Part of Punjab an Overview, Impact Analysis & Way Forward", Proceedings of 72nd Annual Session of Pakistan Engineering Congress. Paper No. 746, Pg (289-314), 2013.
- [ii] M. A. Kamran, T. Shamshad, "Impacts of Hill Torrents Management on Socio Economic Conditions of Arid Land Farmers: a Case Study of Tehsil DG khan". Asian Journal of Humanity, Art and Literature. Vol 1, No 3, 2014.
- [iii] M. S. Mirjat, A. J. Soomro, K. H. Mirjat, M.U. Mirjat, A.S. Chandio, "Potential of Hill Torrent Spate Irrigation in the Kohistan Areas of Sindh "A case Study"." Pakistan journal of Agriculture Engineering 27 (2) 100-114. 2011.
- [iv] F. N. Saher, M. A. Nasly, T. A. A. Kadir, N.K.E.M. Yahaya, W.M.F. Wan Ishak, "Managing Flood Water OF Hill Torrents as Potential Source for Irrigation". Journal of Flood Risk Management. Volume 8, Issue 1 March 2015 Pages 87-95
- [v] GoP, (1990). Harnessing Hill Torrents In Dera Ghazi Khan, Irrigation and Power Dept. Punjab
- [vi] Z. Yasin, G. Nabi, "Alternative Management Plan for Flash Floods and Flow of Mithawan Hill Torrents in Pakistan". International Journal

- of Scientific & Engineering Research, Volume 5, Issue 12, December-2014.
- [vii] NESPAK, (1984). Flood Management of D.G. Khan Hill Torrents, Federal Flood Commission, Ministry of Waters and Power, Govt. of Pakistan
- [viii] JICA, (1992). Feasibility Study on Development of Irrigation based upon Flood Flows of D. G. Khan Hill Torrents, Federal Flood Commission, Ministry of Waters and Power, Govt. of Pakistan
- [ix] NESPAK, (1998). Master Feasibility Studies for Flood Management of Hill Torrents of Pakistan, Flood Flows of D. G. Khan Hill Torrents, Federal Flood Commission, Ministry of Waters and Power, Govt. of Pakistan
- [x] NESPAK, (2005). Chashma Right Bank Irrigation Project (Stage-III) Updating Feasibility Study on Hill Torrents Management Plan in CRBC Area in Dera Ghazi Khan District, Irrigation & Power Department, Punjab

Performance and Comparison of Crumb Rubber Modified and Conventional Mixes Under Varying Temperature and Stress Levels

M.A. Kamal¹, S. Shahid², M.U.Arshid³, I. Hafeez⁴

² Civil Engineering Department, UET Taxila, Pakistan

³usman.arshid@uettaxila.edu.pk

Abstract-Laboratory investigations were carried out in terms of resistance against rutting and assessing resilient modulus of Crumb Rubber Modified Mixes (CRMM) and conventional mixes (60/70 pen) at varying temperatures (55, 40, and 25 °C) and stress levels (500, 300 and 100 kpa). The specimens were tested using UTM (5P) and a comparison of the rutting resistance and resilient modulus (Mr) of both the mixes were made. CRMM showed better performance in terms of rutting resistance and increased resilient modulus compared to that of conventional mixes (CM) under same stress and temperature conditions.

Keywords-Resilient Modulus, Asphalt, Accumulated Strain, Modified Bitumen

I. INTRODUCTION

Quality of bitumen is important in evaluating the properties of bituminous concrete mixes in terms of its performance. In Pakistan, growth of commercial vehicles, uncontrolled axle loads, and substantial changes in daily and seasonal pavement temperatures are accountable for an early breakdown of flexible pavements in most areas of the country. Local refineries meet the current specifications of bitumen. However, mainly the failure of flexible pavements before the expected time is due to the design compatibility of conventional asphalt mixes with the continual application of wheel load under local environmental conditions.

Various studies have indicated that performance of Asphalt mixes can be greatly improved with the introduction of modifiers. It is hypothesized that by improving the binder stiffness at high service temperature and reduced stiffness at lower service temperatures, an improved binder can be developed. Polymers introduced as binders create a lattice within the asphalt by combining small molecules into larger ones. These larger molecule lattices are more stable under high and low temperatures and thus resist thermally induced cracking at low service temperature and permanent deformations and rutting at high

temperatures [i] and [ii] reported that hot rolled asphalt surfacing showed improved performance with the addition of organic polymers. While [iii] has also identified beneficial properties of modified bitumen.

One such form of modified bitumen is Crumb Rubber Modified Bitumen (CRMB) also called Asphalt Rubber, introduced in Pakistan by M/s Phoenix Commercial Company (Pvt.) Limited in collaboration with an Indian manufacturer. Full scale trial sections were laid using CRMB and their performance under extreme loading and environmental conditions was studied by [iv]. They reported better performance of CRMM mixes than that of conventional mixes in terms of their resilient modulus and pavement deflection.

Similar findings have already been reported by [v]-[xii] that performance of asphalt mixes with crumb rubber compared to the conventional mix is better.

II. PROBLEM STATEMENT

High traffic intensity of commercial vehicles, overloading, inflated tire pressures, substantial change in daily and seasonal temperatures, low maintenance, limited budgets are few of the problems resulting in premature failure of flexible pavements. Consequently, huge Govt. exchequer is being incurred to keep the road to an expectable service level. National Highway Authority incurred a mammoth expenditure of Rs. 5.951 Billion for operation and maintenance of 9098 km of its network during 2007-08. This includes Rs. 1,417 Million on rehabilitation of 114 km roads, Rs. 1,638 Million on structural overlays, Rs. 1,676 Million on functional overlays of 514 km, Rs. 810 Million on routine maintenance of 8183 km of roads and Rs. 410 Million on highway safety [xiii].

India having the identical environment as in Pakistan has revealed that properties of bitumen and bituminous mixes can be improved to meet the requirements of pavement with the incorporation of certain additives. Crumb Rubber Modified Bitumen is one such effort in this regard which improves complex modulus and elastic response of bitumen at higher temperatures [xiv]. It is the time to adopt alternate

technologies to address the frequent pavement failures. The use of modified bitumen has been reported to offer solution to reduce the maintenance rate; consequently, treatments stand for a longer time. Additionally at elevated temperatures bitumen modifier increases the resistance of asphalt concrete against permanent deformation. This could be achieved by either stiffening the bitumen so that total visco-elastic response of the asphalt is reduced with a corresponding reduction in permanent strain or by increasing the elastic component of the bitumen, thereby reducing the viscous component, again resulting in reduction of permanent strain.

III. EXPERIMENTAL WORK

A. Aggregate Gradation & Asphalt Content

In this research work, mixes were prepared using aggregate gradation of National Highway Authority (NHA), Government of Pakistan Class-A specification for Wearing Coarse, as shown in Table I. Optimum asphalt contents were worked out using Hot Mix Asphalt Design approach and reported to be 4.2% for conventional mix (60/70 pen) and 4.3% for CRMB [xv].

TABLE I
GRADATION OF AGGREGATES

Sieve Size	%age Passing	JMF Limits	NHA Specs Limits
1"	100	100	100
3/4"	94.6	88.6-100	90-100
3/8"	63.4	57.4-69.4	56-70
No. 4	44.4	38.4-50.4	35-50
No. 8	28.9	24.9-32.9	25-35
No. 50	8.8	4.8-12.8	5-12
No. 200	4.4	2.8-6.8	2-8

Bitumen (60/70 pen and Crumb rubber ranging from 0.15 mm to 0.60 mm particle size were heated to 150 °C and mixed by wet process at a rate of 15% by mass at a low speed, for about five minutes. The blend was then heated at a temperature between 175 °C to 185 °C and stirred at a speed of 3000 rpm with a high speed mixture for about 45 minutes. Heated up to 165 °C, Crumb Rubber Modified Binder was stirred smoothly to prevent segregation and mixed in a batching plant finally to transport on site. The product was then laid by conventional asphalt paver [iv].

B. Repeated Load Uniaxial Strain Test

Repeated Load Uniaxial Strain Tests were performed as per British Standard Institute to measure the amount of accumulated and resilient strains against repeated loading. The tests were performed using

Universal Testing Machine, UTM-5P. Initially, static conditioning stress (10 kpa) was applied to the specimen for a specified conditioning time (100 sec). A fixed time delay was maintained following the conditioning period, during which the applied stress was set to zero. Once the delay time expired, the specimens were then subjected to repeated pulse loading for loading stresses of 100, 300 and 500 kpa against varying temperatures of 25, 40 and 55 °C. Pulse period was set as 2000 ms and pulse width of 500ms with terminal pulse count of 1800 [iv].

The accumulated resilient strains were measured against applied stresses and varying temperature conditions. Strains during both the conditioning and pulsed loading conditions were measured along the same axis as the applied stresses using two Linear Variable Differential Transducers (LVDTs).

The tests results were based on an average of three specimens for varying load and temperature conditions both for conventional and CRMB mixes and are shown in Fig. 1.

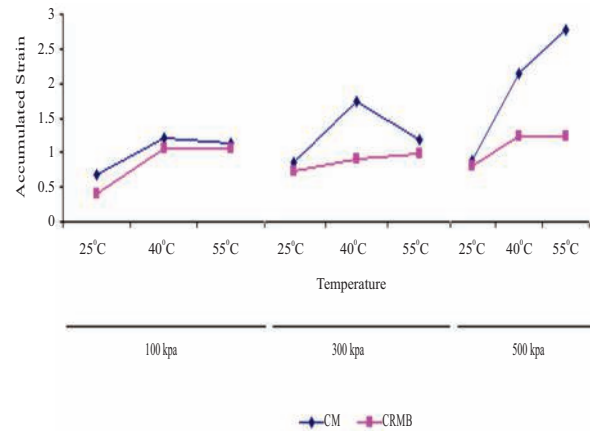


Fig. 1. Accumulated Strains for Conventional Mix (CM) and Crumb Rubber Modified Bitumen (CRMB)

It can be observed from Fig. 1 that CRMB mix showed less accumulated strain at all temperatures and stress level advocating better performance against permanent deformation and rutting. Accumulated strains of CRMB mix was about 55% less than that of the conventional mix (CM) at extreme stress level of 500 kpa and at a temperature of 55 °C

C. Repeated Load Indirect Tensile Test

The five pulse Repeated Load Indirect Tensile Test was performed as per ASTM D4123 to determine resilient modulus of bituminous mixtures [xvi]. The test was carried out by applying compressive loads with haversine waveforms, a pulsed diametral loading force was applied to a specimen and the resulting total recoverable diametral strain was then measured on axes 90 degrees from the applied force.

Tests were performed with five condition pulses for a period of 2000 ms followed by a Peak Loading Force of 100N. The test pulse period was kept as 1000 ms with pulse width of 400 ms. Since strain was not measured on the same axes, therefore Poisson's ratio of 0.4 was assumed to calculate the resilient modulus.

Modulus of Resilience (M_r) is directly associated to the load spreading ability of a material giving a relationship between applied stresses and corresponding strains. It is affected by density, temperature, particle size, shape and gradation as well as lateral confinement. The resilient modulus test is used in structural analysis of layered pavement system and determines the stiffness of pavement materials under stress conditions by simulating wheel loads on pavement.

Tests were performed for combination of varying loads (100, 300 and 500 kpa) and varying temperatures (25, 40 and 55 °C). Each combination was tested 3 times and average values were taken. In total 27 tests with 9 different loading and temperature combinations were performed.

Average values of resilient modulus of conventional bituminous mix and CRMB against varying loads and temperatures are shown in Fig. 2

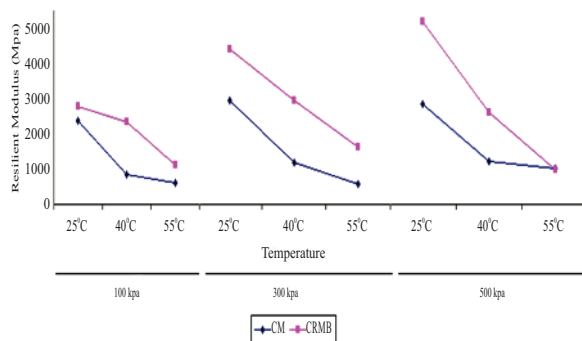


Fig. 2. Resilient Modulus for Conventional Mix (CM) and Crumb Rubber Modified Bitumen (CRMB)

A higher value of M_r for CRMB Mix to that of conventional mix can be observed at the tested temperatures and loading conditions. It can also be observed that resilient modulus values increase with the increase in applied load and decrease with increase in temperature.

I. CONCLUSIONS

Following conclusions have been drawn;

Crumb Rubber Modified mixes showed better performance with lesser accumulated strains at all the tested temperatures and stress levels.

Resilient Modulus of CRMM mixes showed higher values to that of the Conventional mixes at all temperatures and loading conditions.

Overall performance of CRMM was better than that of the conventional mixes in terms of resisting against rutting and higher resilient modulus.

REFERENCES

- [i] T. Sharif. "Modified Bituminous Mixes to Minimize Pavement Rutting", Department of Civil Engineering, Highways Group, University of Birmingham, UK. 1992.
- [ii] J. H. Denning and J. Carswell "Improvement in rolled asphalt sampling by the addition of organic polymers", TRRL Report, Crowthorne, Berkshire, UK. 1989.
- [iii] D. C. Douglas, and H. Zhu. "Asphalt Rubber – An Anchor to Crumb Rubber Markets", Third Joint UNCTAD / IRSG Workshop on Rubber and the Environment, International Rubber Forum, Veracruz, Mexico. 1999.
- [iv] M. A. Kamal, F. Shazib, and B. Yasin, "Resilient Behaviour Of Asphalt Concrete Under Repeated Loading & Effects Of Temperature," Journal of the Eastern Asia Society for Transportation Studies, vol. 6, pp. 1329–1343, 2005.
- [v] J. Harvey and C. L. Monismith, "Effects Of Laboratory Asphalt Concrete Specimen Preparation Variables On Fatigue And Permanent Deformation Test Results Using Strategic Highway Research Program A-003a Proposed Testing Equipment," Transportation Research Record, No. 1417. pp. 38-48, 1993.
- [vi] W. Daly and I. Negulescu, "Characterization of asphalt Cements modified with Crumb rubber from discarded tires," Transportation Research Record: Journal of the Transportation Research Board, vol. 1583, pp. 37–44, Jan. 1997.
- [vii] M. Hossain, S. Swartz, and E. Hoque, "Fracture and tensile characteristics of asphalt-rubber concrete," Journal of Materials in Civil Engineering, vol. 11, No. 4, pp. 287–294, Nov. 1999.
- [viii] S. K. Palit, K. S. Reddy, and B. B. Pandey, "Laboratory evaluation of Crumb rubber modified asphalt mixes," Journal of Materials in Civil Engineering, vol. 16, No. 1, pp. 45–53, Feb. 2004.
- [ix] Wong, C. Ching. and W. Wong, "Effect of Crumb Rubber Modifiers on High Temperature Susceptibility of Wearing Course Mixtures", Construction and Building Materials, pp. 1741-745. Vol. 21 2007.
- [x] W. Haibin, Q. He, Y. Jiao, J. Chen, and M. Hu. "Evaluation of anti-icing performance for crumb rubber and diatomite compound modified asphalt mixture." Construction and Building Materials 107(2016): 109-116.
- [xi] X. Ouming, F. Xiao, S. Han, S. N. Amirkhanian, and Z. Wang. "High temperature rheological

- properties of crumb rubber modified asphalt binders with various modifiers." *Construction and Building Materials* 112 (2016): 49-58.
- [xii] K. B. Vural, M. Yilmaz, and M. Akpolat. "Performance evaluation of crumb rubber and paraffin modified stone mastic asphalt." *Canadian Journal of Civil Engineering* 43, no. 5 (2016): 402-410.
- [xiii] Ministry of Finance, Govt. of Pakistan. "Pakistan Economic Survey". 2007-08. Source: http://www.finance.gov.pk/survey_0708.html
- [xiv] P. Kumar, H. C. Mehndiratta, Singh, and K. Lakshman, "Rheological properties of crumb rubber modified bitumen-a lab study," *Journal of Scientific and Industrial Research (JSIR)*, Vol 68, No. 9, pp 812-816. Sep. 2009.
- [xv] National Highway Authority, General Specification, Ministry of Communications, Government of Pakistan, 2000.
- [xvi] ASTM D4123-82 (Re-approved 1995). "Standard Test Method for Indirect Tension Test for Resilient Modulus of Bituminous Mixtures", American Society for Testing.

Investigation of Jatropha Biodiesel Production on Experimental Scale

M. M. Tunio¹, S. R. Samo², Z. M. Ali³, K. Chand⁴

^{1,2,4}Energy & Environment Engineering Department, QUEST Nawabshah

³Chemical Engineering Department, MUET- Jamshoro, Pakistan

³zeenat.ali@faculty.muett.edu.pk

Abstract-Jatropha is most promising non edible seed for biodiesel production. The Jatropha oil was extracted from pretreated Jatropha seed. The Jatropha oil was analyzed prior to Jatropha biodiesel production. The Jatropha oil contains total saturated fatty acid, mono unsaturated fatty acid and poly unsaturated fatty acids 19.45, 41.88 and 38.25 in weight% respectively. The Jatropha oil was converted to Jatropha biodiesel by two step transesterification reaction using methylate at 50 °C at 600 rpm in 30 minute reaction time. The prepared Jatropha Biodiesel was analyzed by Gas Chromatography on FID detector using Nitrogen as carrier gas. The research concluded that Jatropha Biodiesel was the best alternative of fossil biodiesel.

Keywords-Jactopha Oil, Biodiesel, Nitrogen, Chromatography, Acid

I. INTRODUCTION

The increasing population, urbanization, and industrial development increase the energy demand. Today's need is the continuous and cost effective energy supply. The energy has significant role in running the industrial units and machineries. It needed for powering our homes, vehicles, lighting our villages and towns. The industrial wheel can be stops and daily life activities would be affected if the energy would be beyond the access of common man [i-ii].

The renewable energy obtained from virtually inexhaustible or regenerative source exists in environment. The wind, solar and tidal energy are the renewable energy or non conventional energy. They are easily accessible round the clock, in real means they are the gift of nature. The non renewable energy sources depend to their exploration. That need the manpower, machinery, management, money and most important it's marketing. The marketing feasibly can be analyzed by its exploration cost verse the selling cost [iii]. The coal, petroleum, natural gas and fossil fuels are non renewable energy sources and exist beneath the earth surface.

The Pakistan is under the developing stage. The energy generation infrastructure nor fully developed or equipped with latest technology neither manage properly. The 60% energy generated from fossil fuels

and 36% were from biomass including the animal dung, wood and agricultural waste. The commercial energy shares was as 1.2% from nuclear, 7.6% from coal, 11.0% from hydro, 50.3% from gas and 29.8% from oil [iv]. The primary energies are based on gas, oil and hydro. The biomass plays a role in primary energy generation in Pakistan and contributes the 36% of total energy matrix. The Pakistan posses the high bio fuel potential to meet the 80% of total bio fuels requirement of country which presently fulfills by their imports. In 2004-05 the energy consumption was 425kWh. In 2009-10 the energy supply decline 0.64 % and per capita 3.09 % compared to lasts few years. The country paid approximately \$8 billion in 2006-2007 in respect of exporting the diesel and petrol [iv]. The biodiesel consumption is increasing by 437.06 thousand barrels/day [v]. In early period of 1930-1940 all the vehicles were running on fossil fuels because it was plentiful and less expensive than after its scarcity and depletion were noted. Hence from 1970 the attentions were paid towards the generation of biofuels from non edible feedstocks [vi].

Pakistan existed on Asian south region with land area 888, 0000 km. The 70% population about 140million people belonging to agricultural land cultivation and earn about US\$ 480 per capita and contribute 35% of total agricultural GDP[vii]. As the Pakistani's are agriculturalist hence the need is to explore the biomass which have high tendency to replace the fossil fuel and fulfils the country's energy demand. The non woody, woody, non edible seeds and edible seeds are the biomass and had conversion capability to biofuels. The biofuels are advantages because of their versatility, lower carbon emission, , cost effective, renewable , reduce the fossil fuel dependency and green house gases.

The biofuels (biodiesel and bioethanol) produced from crops, seeds, microorganism and organic waste. The researchers are engage to develop the biofuels from non edible crops and animal feed [vii-viii] that are environmentally and socially sustainable.

The Jatropha, neem, moringa, trisperma, castor beans and candlenut, linseed, rapeseed (Fig.1) are non edible seeds having high potential to biodiesel production [ix].

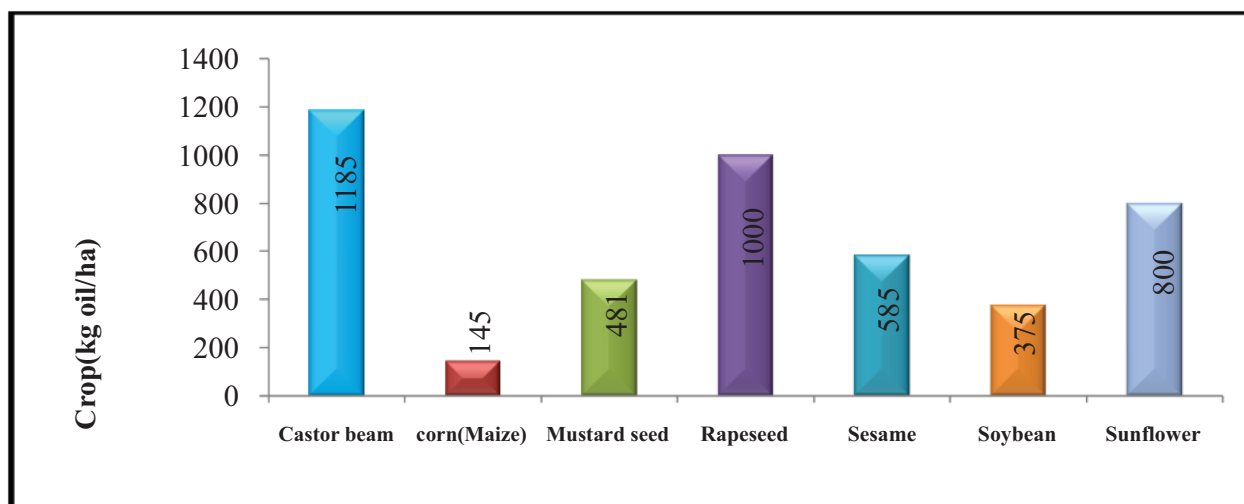


Fig. 1. The Comparison of potential energy crops for biodiesel production

The *Jatropha* is non edible feedstock and preferable because of 14% free fatty acid content and 80 % unsaturated fatty acid [x] which can be converted into biodiesel by estrification reaction and gave 90-85% yield. The less moisture and saponifiables were favorable in biodiesel production [xi-xii]. The estrification reaction is the reaction in which the unsaturated free fatty acids converted into biodiesel. The high biodiesel production puts remarkable impact on country and enhanced the rural economy [xiii].

The vehicles are the main consumer of diesels. The *Jatropha* biodiesel can be applicable in pure or in blended form without alteration of engine and toxic emission. [xiv- xv]. The performance, emission and combustion characteristics were comparable to fossil diesel. The brake thermal efficiency, brake specific fuel consumption and power output were within the allowable range. The emissions of carbon monoxide, carbon dioxide, un-burnt hydrocarbon, oxides of nitrogen and smoke were found satisfactory [xvi- xvii].

This research paper focused the synthesis of biodiesel from non edible feedstock “*Jatropha*”. The attempt was made to minimize the free fatty acid content from *Jatropha* oil by two step transestrification reaction. The synthesized *Jatropha* biodiesel was analyzed and its characteristics were compared to

petroleum diesel. The objective of study was to highlight the *jatropha* biodiesel as best substitute of petroleum diesel.

II. BIONOMICAL DESCRIPTION OF *JATROPHA*

The bionomical name of *Jatropha* is *Jatropha caucas* belonging to spurge family. The *Jatropha* is flowering plant with height of around 6m and was cultivated in tropical and subtropical regions. It became mature and yielding in 9-10 month and 2-3 times per year. On the maturation the *Jatropha* plant appeared with green rounded shaped seeds. Then turn into light blue or purple colored hard shells. The oil bearing mass was inside the shells known as meat or Kernels (Fig. 2). The oil recovered by screw pressing mechanically.

III. METHODOLOGY

The *Jatropha* seeds were obtained in bulk quantity from Pipri Model farm Karachi owned by PSO Pakistan. The *Jatropha* seeds were hard and of blue color. The *Jatropha* seeds were fresh and possessed the high moisture content. It was pretreated before oil expelling. The dirty white oil bearing mass was appeared after shell cracking



Fig. 2. The non edible feedstock “*Jatropha caucas*”

VI. JATROPHA OIL EXTRACTION

The Jatropha seeds were pretreated in order to avoid the impurities and unwanted foreign particles and agrochemical sprays which were adhere the seed's outer surface. The pretreatment is necessary for maintaining the accuracy and precession in research process [xviii]. The pretreatment of Jatropha oil extraction was started from the collection of Jatropha seeds. The seeds was sorted and washed twice with double distill water. As the moisture was unfavorable for biodiesel production so it was minimized by sun drying to make the process more economical. The Jatropha seeds were dried in open air for 72 hours.

By drying the tensile and compression strength were lower down and needs less energy for crushing. After deseeding the stream were screened 10mm screen. Before that it was shuffled for separation of seeds coat and seed meat or Kernels. The screening process promotes the uniform oil extraction process. The shells were discord and meat portion or Kernels were collected and introduced in mechanical oil expeller. The Jatropha oil was collected in air sealed glass bottles. Prior to that glass bottles were sterilized, rinsed with double distilled water and oven dried. The yield of Jatropha oil extraction was 38% verses the 51% press cake.

V. SYNTHESIS OF JATROPHA BIODIESEL

The Jatropha Biodiesel was produced by Transesterification reaction. At first stage the triglycerides were converted to triglycerides, then to monoglycerides and finally to glycerol. The biodiesel was the methyl esters of long chain fatty acids present in Jatropha oil. The 800ml preheated (50 °C) Jatropha oil and sodium methylate (200 ml) was mixed in reaction vessel. The Sodium methylate was prepared

by dissolving the 5.0gram Sodium Hydroxide (Merck Company) in methanol (BDH 99%). The mixture was kept in magnetic stirrer for 30 minutes stirring at 600 rpm with fixed temperature of 50 °C. Then it was cooled at room temperature and transferred in separating funnel for settling. After 24 hours settling the two distinct layers were obtained. The upper layer was biodiesel which was recovered while the lower layer was crude unwanted Glycerin. The collected Biodiesel was washed twice with Glacial acetic acid (BDH) and water (0.002: 1) to dissolve the organic matters. The pH was 7.8 (JENCO Model 6010N pH meter) was lies slightly alkaline. It was neutralized by acid washing. The synthesized Jatropha Biodiesel was heat at 100 °C to remove the moisture content. Filter by filter paper (Double Rings Filter Paper 11.5 cm) and filtrate was collected in sample bottle for further analysis.

VI. JATROPHA BIODIESEL ANALYSIS

The Gas Chromatographic technique was applied for determination of free fatty acid content in synthesized Biodiesel. Biodiesel sample of biodiesel was directly injected into Gas Chromatograph (Fig 3). The ester content of the biodiesel was determined with gas chromatography (GC-FID). The filtered samples were injected into Perkin Elmer 8700. The RT -2560, 100 m (0.25 mm, internal diameter and 0.2 µm film thicknesses) column was used to separate the esters. The GC was set up according to the following conditions: Nitrogen was used as carrier gas with a linear velocity of 35 cm/s; 1 µL samples were injected into the column. The temperature profile was as follows: 280°C inlet temperature; 130 °C ramp at 4 °C/min up to 220 °C and hold for 10 min; A flame ionization detector (FID) was used at 300°C.

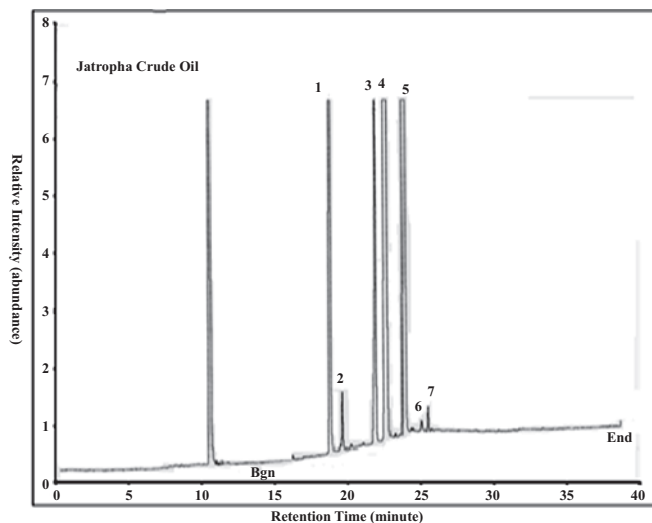


Fig. 3. Gas chromatogram of Biodiesel from Jatropha seed oil fatty acid methyl esters. 1. Palmitic acid 2. Palmitoleic acid 3. Stearic acid 4. Oleic acid 5. Linoleic acid 6. Eicosenic acid 7. Gamma-linolenic acid

VII. RESULTS AND DISCUSSION

The fatty acid played important role in Biodiesel production from Jatropha oil. It was directly taken part in estrification reaction. The free fatty acids are long chain molecules their molecular weight varies on molecular length. The Jatropha oil contents the saturated, mono unsaturated and poly unsaturated fatty acids. The free fatty acids content in Jatropha oil given

in Table I. The Total fatty acids (Palmitic acid) content was 14.7% by weight. The Eicosenic and Behinic acids were present in small and nearly in equivalent quantity. The Oleic acid and Palmitoleic acid were present 41.39% and 0.499% by weight respectively. The Linoleic acid conjugated and Alpha-Linolenic acid are the poly unsaturated fatty acid present in trace quantity.

TABLE I
THE FATTY ACID CONTENT IN JATROPHA OIL

Total Saturated Fatty acids (Weight %)	Palmitic acid (C ₁₄ H ₂₈ O ₂)	Steric acid (C ₁₈ H ₃₆ O ₂)	Eicosenic acid (C ₂₀ H ₃₈ O ₂)	Behinic acid (C ₂₂ H ₄₄ O ₂)
	14.7	4.407	0.160	0.183
Total MUFA* (Weight %)	Palmitoleic acid (C ₁₆ H ₃₀ O ₂)		Oleic acid (C ₁₈ H ₃₄ O ₂)	
	0.499		41.39	
Total PUFA** (Weight %)	Linoleic acid non conjugated (C ₁₈ H ₃₂ O ₂)		Gamma-Linolenic acid (C ₁₈ H ₃₀ O ₂)	
	37.952		0.307	

MUFA*= mono unsaturated fatty acid

PUFA**= poly unsaturated fatty acid

The quality of Jatropha biodiesel strongly influence by native Jatropha nature and Process condition. Another important factor was the viscosity. The Biodiesel became viscous because of long chain structure of Jatropha oil. The Jatropha seed was pretreated to minimize the unwanted contents.

The extracted oil was processed at optimum experimental condition for conversion of Jatropha oil into biodiesel. The sodium Hydroxide was used as catalyst. Through gravitational settling in separating funnel the biodiesel was collected and analyzed on Gas chromatography. The Gas Chromatographic tests were done in Centre of Excellence in Analytical Chemistry, University of Sind Pakistan.

The chromatograph showed the Jatropha Biodiesel contained palmitic acid, palmitoleic acid, stearic acid, Oleic acid, Linoleic acid and Eicosenic acid and gamma – linolenic acid. The sharp peaks showed the distinct separation of fatty acid.

VIII. CONCLUSION

The industries and some house hold appliances needed continuous supply of diesel. As the resources of fossil diesel are limited that is why efforts are made to switch on Jatropha biodiesel. The research is going on to synthesize the Jatropha biodiesel on laboratory scale and then after scale up on commercial level.

The diesel engines design in the line of stable and knocking free fuel under variety of operating condition and have clean and smoke free burning. The main advantage of biodiesel was that it can directly used in diesel engines without any engine alteration and can be

blended with any ratio to generate the required properties [xix]. The first and second generation bio diesel was feasible for long run at can be scale up [xx].

The present study lightened the Jatropha Biodiesel production on Laboratory scale. It is suggest that Laboratory data should be scale up on national level to over the energy crises. The Jatropha Biodiesel is best alternative to fossil diesel. The double estrification reaction was followed to convert the Jatropha oil to Jatropha biodiesel. The results fatty acids were found satisfactory. The study revealed that jatropha biodiesel is feasible to blend with petroleum diesel with various ratios in internal combustion engine without modification.

ACKNOWLEDGMENT

The authors are highly thankful to Mr. Obaidullah Dahar Assistant Professor Govt: Degree College Sakrand, Mr. Jawaid Akhtar Channa Manager New Business Department and office bearers of PSO Karachi for providing labrotory facilities and all technical support.

The authors deeply acknowledge the Dr. Farah Naz Talpur, Professor, Centre of excellence in analytical chemistry, University of sindh for her support in Gas Chromatographic analysis.

The research work is part of PhD thesis named” Production of biodiesel, analysis and testing the performance of biodiesel engine by using indigenous resources”.

Conflict of Interest

The authors declared that there is no conflict of interests.

REFERENCE

- [i] R. Raza, S. A. Hayat, M. A. Chaudhry, J. Muhammad. The 3rd International Conference of Materials for Advanced Technologies (ICMAT 2005); 2005
- [ii] U. K. Mirza, N. Ahmad, T. Majeed, K. Harijan. "Wind energy development in Pakistan". *Renewable and Sustainable Energy Reviews*. vol.11, 2007, no. 9, pp. 2179-2190
- [iii] T. A. lok Kumar, K. Akhilesh, R. Hifjur. "Biodiesel production from Jatropha oil (J. curcas L.) with high free fatty acids: an optimized process". *Biomass and Bioenergy*. vol. 31, no. 6, 2007, pp. 569-575
- [iv] M. Asif, "Sustainable energy options for Pakistan". *Renewable and Sustainable Energy Reviews*. vol.13, no. 4, 2009, pp. 903-909
- [v] S. Shaima Meryem, S. S. Ahmad, N. Aziz. "Evaluation of biomass potential for renewable energy in Pakistan using LEAP model". *Inter. Jour. of Emerging Trends in Eng. and Develop.*, vol.1, no.3, 2013, pp. 243-249
- [vi] K. B. Dilip, D. C. Baruah. "Performance of diesel engine using 1 obtained from mixed feed stock". *Renewable and Sustainable Energy Reviews*. vol. 16, no. 8, 2012, pp. 5479-5484
- [vii] http://www.iptu.co.uk/content/pakistan_clusters_enviro.asp
- [viii] R. Cheng- Jiang, X. Wei-He, A. Jaime, T. da Silva. "Potential of five plants growing on unproductive agricultural lands as biodiesel resources". *Renewable Energy*. vol.41, 2012 pp. 191-199
- [ix] M. Carlos, M. Andres, M. Giraldo, C. Eugenio, D. Herminia, P. C. Juan. "Fractional characterization of jatropha, neem, moringa, trisperma, castor and candlenut seeds as potential feedstocks for biodiesel production in Cuba". *Biomass and Bioenergy*. vol.34, no. 4, 2010, pp. 533-538
- [x] B. C. Arjun, S. T. Martin, M. B. Suzanne, K. Chris Watts, M. Rafiqul Islam. "Non-Edible Plant Oils as New Sources for Biodiesel Production" *Int. J. Mol Sci.*, vol.9, 2008, pp.169-180
- [xi] P. S. Pramanik, R. Konwarh, K. Sagar, B. K. Konwar, N. Karak. "Bio-degradable vegetable oil based hyperbranched poly (ester amide) as an advanced surface coating material" vol. 76, no. 4, 2012, pp. 689-697
- [xii] B. S. Chauhan, N. Kumar, YD Jun, KB Lee, "Performance and emission study of preheated Jatropha oil on medium capacity diesel engine," *Energy*, vol. 35, 2010. pp. 2484-2492
- [xiii] K. B. Dilip, D. C. Baruah. "Assessment of tree seed oil biodiesel: A comparative review based on biodiesel of a locally available tree seed" *Renewable and Sustainable Energy Reviews*" vol. 16, no.3, 2012, pp. 1616-1629
- [xiv] M. Satyanarayana and C. Muraleedharan. "A comparative study of vegetable oil methyl esters (biodiesels)", *Energy*, vol. 36, no. 4, 2011, pp. 2129-2137
- [xv] P. V. Rao "Experimental investigations on the influence of properties of Jatropha biodiesel on performance, combustion, and emission characteristics of a DI-CI Engines" *World academy of science, engineering*. vol.5. 2011 pp.03-23
- [xvi] I. B. Muhit., D. Baidya., Nurangir Nahid. "Prospect of Algal Biodiesel Production in Bangladesh: Overview from Developed Countries" vol.11, no.1, 2011, pp. 49-54
- [xvii] R. K. Singh and Saroj K Padhi. "Characterization of jatropha oil for the preparation of biodiesel". *Natural product Radiance*, vol.8, no. 2, 2009, pp 127-132
- [xviii] D. P. Prafulla, G.G. Veera Gnaneswar, K. R. Harvind, M. Tapaswy, D. Shuguang. "Biodiesel Production from Waste Cooking Oil Using Sulfuric Acid and Microwave Irradiation Processes". *Journal of Environmental Protection*, vol 3, 2012, pp. 107-111
- [xix] M. Satyanarayana and C. Muraleedharan, "A comparative study of vegetable oil methyl esters (biodiesels)". *Energy*. vol. 36, 2011, pp. 2129-2137
- [xx] N. A. Khan and H. Dessouky. "Prospect of biodiesel in Pakistan" *Renewable and sustainable energy reviews*, vol. 30, 2008, pp.12-15

The Economic Analysis of Portable Photo-Voltaic Reverse Osmosis (PVRO) System

H. Bilal¹, A. H. Alami², M. Farooq³, A. Qamar⁴, F. A. Siddiqui⁵

^{1,2}University of Sharjah, Sustainable Renewable Energy Program-College of Engineering, Sharjah, UAE

^{3,4}Mechanical Engineering Department, University of Engineering & Technology Lahore, Pakistan KSK Campus

⁵Mechanical Engineering Department, Bahaudin Zakaria University Multan, Pakistan

³enr.farooq@uet.edu.pk

Abstract—A reverse osmosis system was designed and powered by photovoltaic panels for the production of potable water. Elements of system design and integration were identified and optimized. These include capacity planning, standalone capabilities by providing battery storage system and economic analysis. The experimentation on the system, performed in the premises of Mechanical Department of UET Lahore-KSK Campus has proven that unit operated with successful throughput of 5.9 l/h for 5 hours with battery based and 3.8 l/h for 7 hours using battery less system. The battery-powered and direct solar operation modes were tested and in either case the system proved its worthiness. The cost comparison has been presented as well which clearly identifies that it as a cost effective energy efficient portable desalination system.

Keywords—Battery Based, Battery Less; Desalination; Photovoltaic; PVRO.

I. INTRODUCTION

Most of the water on earth is either saline or undrinkable without extensive processing [i-iii]. Clean water supplies are not sufficient to cover the daily need of potable water for all the people in the world. The alternate solution to address this problem, is processing the sea or brackish water for excess salt content removal, so that it can be used to compensate the need [iv]. The desalination process involves excess investment on infra-structure, and high energy consumption as well. Using a desalination process in remote areas is also quite difficult and there is no viable solution which can replace it [v]. Hence there is a need to optimize the desalination set-up for use in arid areas. The economic feasibility of Photo-Voltaic Powered Reverse Osmosis (PVRO) plants has slowly proved its competitiveness and feasibility with advances in photovoltaic and Reverse Osmosis (RO) setups, each in its respective field [vi-viii]. The cost of the PVRO plants compare reasonably with the diesel fuel plants but do not compete in efficiency at some limited periods where solar radiation is either unavailable or unpredictable. Although the initial cost of the PVRO

plants is high as compared to that of diesel based RO plants but in turn the maintenance and operation cost of the PVRO plants is relatively low. Moreover, skilled man-power at remote areas is also a problem. Operating a PVRO is ease as compared to diesel RO plants [ix]. The energy consumption directly affects the cost-effectiveness and feasibility of using desalination technologies for drinking water production [x]. Bilton and Wiseman have described the feasibility of the PVRO plant in comparison to RO plants that work on diesel. The economic evaluation is done by comparing the cost of water used for PVRO plant and the cost of the water used for RO plants working on diesel as a fuel. It was found out after the analysis of a typical site that if the solar energy is abundant, the PVRO is appropriate to use while working with either sea water or under-ground water [xi]. Small scale PVRO plants can provide water in remote areas where drinking water is a problem and supply of drinking water is either costly or difficult due to some restrictions. Variation in solar resource, local government policies, water type can affect the feasibility of plants installed. Natural resource of water could be a problem [xii]. The economic feasibility of PVRO plants is a function of location. The efficiency of such plants differs from location to location. Geographical location of areas does matter a lot. Also increasing the feasibility of the PVRO plants can extend their feasibility to currently marginal or unfeasible locations. To date no general method of feasibility of PVRO plants have been introduced. This paper introduces this method to generalize the feasibility and effects of locations and solar resource on plants. For different conditions analyzed it was concluded that PVRO plants are more feasible than Diesel powered RO systems due to high fuel cost which in turn results in high water cost for many locations [xiii]. By using innovative methodologies and intelligent system control it is possible to reduce the cost of PVRO plants. Moreover the configuration of the PV panel is an important aspect. Natural conditions like ambient temperatures, solar resource of the area and the time since the last rainfall also contribute to the evaluations of the locations and the feasibility of the systems. Every single parameter should be examined to utmost care

and should be satisfied for the operations of such plants whether it is related to operation or the basic control. It should be mentioned that the feasibility of the RO systems degrade with time because with the passage of time, some organic or in-organic material deposit themselves on the membrane module and at time, it becomes very difficult to remove them completely. A keen control and continuous inspection of deposition of such particles is very important, especially in remote areas where skilled man power is minor in numbers. All such aspects should be taken into consideration while designing a PVRO plant [xiv]. Mohamed and Papadakis compares the Photovoltaic SWRO (Sea Water Reverse Osmosis) in their paper which is directly coupled to that which uses battery powered by solar systems. Photovoltaic brackish water RO desalination plants have proved more efficient to supply water to remote areas and isolated communities. Whereas Sea-Water PVRO plants cost too much, this is due to the high energy demand of the plant. This in turn increases the maintenance and operating cost which is due to the fact that many SW-PVRO plants do not have energy recovery devices. Also, the solar batteries cost a lot and their use is required for maintaining constant pressure & flow rate through the membranes [xv]. After the test and analysis it was observed that direct coupled Sea water RO was more efficient than a small Solar Battery powered SW-PVRO plant. However large battery bank (>1500Ah) can improve the battery based system behavior but this would in turn be harmful for environment. This would also increase the operating and maintenance cost which would prove to be much costly in remote areas [xvi]. Al Sulemani & Niar describe the study of experimentation done by the Ministry of Water Resource at a particular site 900km south from Muscat, Oman's capital in their research work. The water pumped out of the well is treated first, dosing of water to balance the pH and reject water evaporation pond. The studies done over the years demonstrate that Photovoltaic RO plants are a good option for remote areas where fuel, power or portable water is a problem. The cost of the PVRO plants compare reasonably with the diesel fuel plants but do not compete in efficiency at some limited periods. Although the initial cost of the PVRO plants is high as compared to that of diesel based RO plants but in turn the maintenance and operation cost of the PVRO plants is relatively low. Moreover, skilled man-power at remote areas is also a problem. Operating a PVRO is an ease as compared to diesel RO plants [xvii]. According to them, for remote areas where power as in form of electricity is not an option, difficult access by road is also an issue or where the ground water is brackish such Solar operated RO plants can turn out to be a useful way to solve the water problems for the related community [xviii]. Tamim and Kimberly's research work deals with the desalination techniques through different means and processes. According to them,

there are three basic technologies used for the desalination of water namely, Chemical Processes, Membrane Technology and Distillation Processes [xix]. There are some plants which use a combination of these technologies to perform operations. Many future technologies are also discussed which can be more efficient in terms of maintenance and operation cost. The paper also states that energy consumption directly affects the cost-effectiveness and feasibility of using desalination technologies for drinking water production. They concluded that the major disadvantage of renewable energies is the lack of continuity and consistence in the supply [xx]. Lee & Glaser's discuss the desalination of agricultural water drained out of the system while using the membrane system. This drained water can contain a lot of mixed chemicals and micro-organisms. So the operations require a lot of considerations like feed water supply, membrane quality and operating conditions [xxi]. Two different RO plants were installed which were having the capacity of feed water of about 38,999 gpd. It was explained by them that during the selection of membrane, one has to carefully compromise between the decrease in bio-fouling potential and the performance of membrane. Also the permeate flux and the salt rejection capacity of membrane go hand in hand [xxii]. Kang & Cao says that with the development about RO membranes resistant to fouling. As RO is the widely and most popular method to produce fresh water from saline water, so the membranes used in RO process should be more efficient as they are at present. The major challenge faced by this technology at present is the membrane fouling. Therefore, research was initiated to produce membranes for RO process which can run for a longer period of times as compared to the present membranes in operation. Researchers are working on antifouling RO membranes, including the selection of new starting monomers, improvement of interfacial polymerization process, surface modification of conventional RO membrane by physical and chemical methods as well as the hybrid organic/inorganic RO membrane [xxiii]. Many new techniques have been discussed and considered in the paper. To start with the modification of the surface of RO membranes currently in operation is a way to go. If the surface of the current RO membranes can be modified, it can result in more efficient and fouling resistant membranes. But the use of this method either physical or chemical results in a decline of water flux. Other than that improvement in the polymerization process of membrane manufacturing is also a gate way towards producing fouling resistant membranes. Addition of polymers during the process can produce membranes much resistant to fouling [xxiv]. Another way is the addition of some inorganic compound during the process in polymeric RO membranes in a new direction to think about. The hybrid organic or inorganic membranes show a promising permeability

properties and anti-fouling nature. This can be extensively used on commercial scale for the time to come. In fact, Nano composites membranes have already been introduced and can be used for commercial purposes in near future. But in getting all this to commercial market is also a challenge that should be taken over [xxv]. Many new ideas and innovative technologies are currently under research for the producing anti-fouling membranes and are only limited for the purpose due to high operation cost. Researching on such innovative ideas is the need of the hour. Sooner or later we have to fight these challenges in order to survive and thrive on this planet. This planet has not much too offer in coming years if we talk about fresh drinking water, basic necessity of life [xxvi].

Many researchers have contributed for the high capacity water production using the photovoltaic system but almost never, a system is being prepared for the smaller capacities like l/h. This is really a challenge when it comes to size and portability. To deal with this problem, a renewable energy based set-up for the desalination system has been designed and analyzed for its performance in remote locations. The results taken through this experimental set-up has been evaluated and examined for future recommendation and modifications [xxvii].

The objective of this research is to evaluate the performance of a compact water desalination system, powered by solar energy. In cases of energy abundance and low demand on water, excess energy is to be stored in battery backup systems. The distillation technique used for this work is a RO system, powered by photovoltaic (PV) modules. RO requires less input energy than thermal desalination processes and is ideal for small water throughput requirements.

II. MATERIAL AND METHODS

A. Materials

A brief analysis for the type of membrane through this chart.

TABLE I
TYPE OF MEMBRANE [xiv]

Parameter	Plate & Frame Module	Hollow Fiber Modules	Tubular Module	Spiral Wound Module
Cost (\$/m2)	50-200	2-10	50-200	5-50
Pressure drop across permeate	Low	High	Low	Moderate
Suitability for High Pressure	Marginal	Yes	Yes	Marginal
Membrane specific type material restriction	No	Yes	No	No
Concentration Polarization Fouling Control	Good	Poor	Very Good	Moderate

The above table clearly indicates that the choice of Spiral-Wound module is the feasible choice with respect to all the aspects. Although Hollow fibre is also a good choice with respect to cost but due to high pressure drop across permeate and poor control against polarization fouling make it less appropriate against Spiral Wound module. Hence the module selected for RO membrane is Spiral-Wound.

Before proceeding to select the type of filtration needed before the RO system, the analysis of the sample water is required. After the sample water analysis, it becomes easy to predict about the pre-treatments and filtration stages.

The RO unit for the system is a spiral wound membrane of 3" diameter, 0.0005 micron pore size with Pre filter#1 of 5 micron pore size, GAC-Granular Activated Carbon as filter #2 and micro filtration of 1 micron pore size as filter #3. The temperature of raw water was 35-40°C. Two PV modules of 75W & 120W were used. To help circulate water within the system, a 24V and 1.7A DC pump was used. The designed system is shown in Fig. 1.

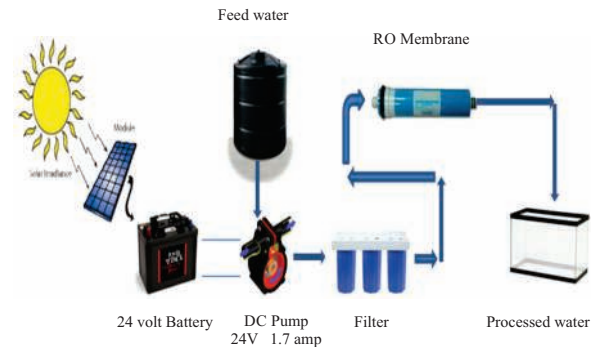


Fig. 1. Schematic of Portable Photovoltaic Desalination Unit

B. Measurement of design parameters

The solar irradiance was measured by the control console incorporated with solar panel. The output flow rate measurement would be simple by taking the volume in measuring cylinder and counting the time. Desalination unit has a DC Diaphragm pump, for which the load requirement was measured and then a factor of safety is taken into account. The included equations are as follows;

$$\text{Volume flow rate} = Q = \frac{\text{Volume of output water (V)}}{\text{Time (t)}}$$

Where Q is in liter/sec.

Load requirement of pump = $L = \text{Current (I)} \times \text{Voltage (V)}$

Load requirement of pump = $L = 1.7 \times 24 = 41 \text{ W}$

Power of Photovoltaic Panel chosen:

$$P = FS \times L = 1.75 \times 40.8 \approx 75 \text{ W}$$

(Where 1.75 is Factor of Safety (FS))

C. Experimental procedure for PVRO Desalination System

The data was collected in June-2012, at Coordinates: 31°45'N74°14', for solar irradiance in the specific location. A reference PV module was used as a reference to compare the enhancements that a second system would gain with an added battery storage system. The solar irradiance was measured to have the estimate of the input energy was analyzed with respect to the output water flow rate and the quality and then output of water.

During the first five days, the system was run by using the battery as the energy storage source. In the chart, there is no output seen in the first couple of hours because of not enough sunlight. Meanwhile, the battery was charging and once it got charged and ample sunlight was there, the system started to work with good output till about five hours. The flow rate is in Litre/hour. The results are shown below.

III. RESULTS AND DISCUSSION

The experiments were conducted for 10 days as it is quite enough for any variations in the weather conditions. In the summer season, it is the maximum output that can be achieved and this time duration provides good statistical evidence to prove our results. Following is the data collected for the solar irradiance (W/m^2) during the operational timings. Wp of the panel is 75W for battery based system and 120W for battery less system. Results are evaluated quantitatively, qualitatively and economically. Output power and solar irradiance of the battery based system has been explained in Fig. 2. It can be observed from the graph that the maximum power output is around noon times where as it is minimum during morning and evening times. The corresponding values of the solar irradiance are indicated on the right side of the graph. For the battery based system the solar irradiance is least in the morning & evening times.

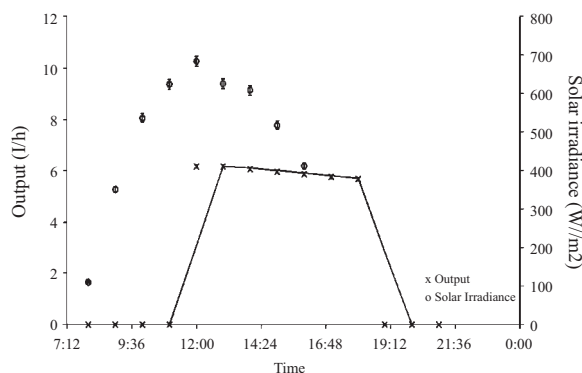


Fig. 2. Battery-Based System with 75W PV Panel

The RO unit produces 6.6 l/h using electricity whereas using the battery-based PV panel of 75W, the output flow rate of the desalination unit was

approximately 5.9 l/h for 5 hours. This implies that one day output of battery-based PV panel would be 29.5 l/day. However by using the battery-less PV panel of 75W, the desalination unit has maximum output flow rate ≈ 3 l/h for peak hours only.

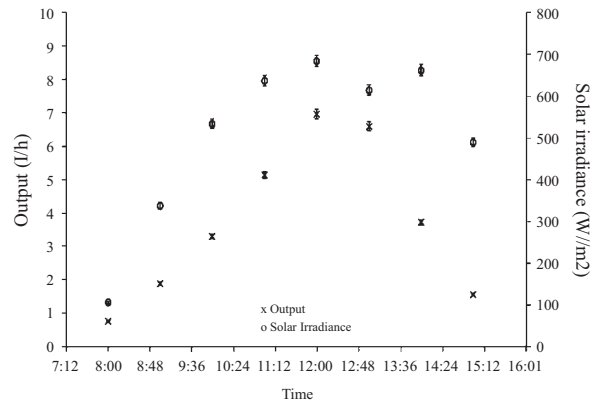


Fig. 3. Battery-Less System with 120W PV Panel

That is why instead of using 75W panel, 120W panel was used for direct connection, which gave us the output flow rate of 3.8 l/h for 7 hours. So one day output of battery-less PV panel is approximately 26.6 l/day.

TABLE II
QUALITY OF DIFFERENT TYPES OF WATER [xiii]

Parameter	Raw Water KSK	RO Water KSK	Guideline WHO
PH	7.2	7.1	6.5-8.5
Chlorides (mg/L)	530	40	250
Calcium(mg/L)	24	12.8	-
Total Dissolve Solid (mg/L)	1000	14	1000
Magnesium (mg/L)	24	9.7	-
Sulfate (mg/L)	350	15	250
Total Hardness (mg/L as $CaCO_3$)	160	72	500

The designed unit is portable and can be easily operated by a layman even so there is no specific cost involved for the labor using this system as compared to other heavy duty installation required distillation systems. There is almost negligible maintenance and operational requirement for the designed system. Only the quarter yearly cost for replacing the RO membrane could be considered. The life span varies from area to area and raw water quality, but roughly it will be workable up to 20-25 years keeping the regular maintenance required for the different parts in mind.

IV. CONCLUSION

The successful design and testing of a water purification system operating on solar energy is presented. For remote/disaster-stricken areas having abundant solar energy and unavailability of access to pure underground drinking water, this system proves key to confront the scarcity of potable water and fulfills the needs of a small population. The photovoltaic arrays generate energy that is environmentally friendly that reduces the environmental and noise pollution of comparable diesel generators. The difference between the battery less and battery based system is only 17 - 18% excess energy which makes us consider the battery less system. For a specific available solar energy, the battery-based system produces only 9.8% more product water. Hence the battery-based or battery-less systems, both can be used, but battery-less system is more cost effective with just small decrement of output flow rate than battery-based system.

V. RECOMMENDATIONS

Improvements in the designed unit can be done by incorporating the photovoltaic panel with solar tracking device. In this way, the efficiency of the system will be increased. If instead of coupling a big photovoltaic panel, two small panel of equal output can be coupled in series, then the price can further be reduced because larger the photovoltaic panel, more will be the cost. To address the decreasing rate of drinkable fresh water globally, many human rights organizations are funding research on desalination to facilitate people with adequate drinkable water. Thermal desalination systems can also be employed with the collaboration of such organizations for industrial-scale water purification because their production ability is massive. For better efficiency, the filters for pretreatment of feed-water at Reverse Osmosis water treatment plants must be cleaned every few days (back washed) to clear accumulated sand and solids. In particular, the research should be conducted to reduce the process energy consumption, as well as to minimize the harmful effects of scaling and fouling on membranes and to obtain higher water flux membranes. The modified models for Desalination Plants may be applied to have the Hybrid solar desalination. The main idea is to employ the solar power in both form, PV and Thermal, or to incorporate the PVRO Designed system with some other renewable energy as well. The system was tested using brackish water, it can be modified to use for the purification of sea water. The results can be analyzed to check the feasibility of the system.

VI. APPLICATIONS

The system designed is feasible for using in the areas which is vulnerable to natural disasters. In this

way, the availability of electricity is impossible to be available and so the system is compatible to work within such region. Keeping in view the disaster of Earth Quake 2008 in Northern areas of Pakistan, it has been found that the cost of supplying fresh water is always greater than producing water out of PVRO System. The designed unit is portable and can be easily operated by a layman even so there is no specific cost involved for the labour using this system as compared to other heavy duty installation required distillation systems. There is almost negligible requirement for the designed system. Only the quarter yearly cost for replacing the RO membrane could be considered. The life span vary from area to area and raw water quality, but roughly it will be workable up to 20-25 years keeping the regular maintenance required for the different parts in mind.

VII. ACKNOWLEDGEMENT

The authors acknowledge the support of Department of Mechanical Engineering, UET Lahore, KSK-Campus for allowing to work under their premises and using their resources.

REFERENCES

- [i] A. M. Bilton, R. Wiesman, A.F.M. Arif, S. M. Zubair and S. Dubosky, "On the feasibility of community-scale photovoltaic-powered reverse osmosis desalination systems for remote locations". *Renewable Energy*, pp. 3246-56, 2011.
- [ii] V. D. Geer , J. A.J. Hanraads and R. A. Lupton, "The art of writing a scientific article". *J Sci Commun*, 2000.
- [iii] A. H. Alami, "Effects of evaporative cooling on efficiency of photovoltaic modules". *Energy Conversion and Management*, Volume 77, pp. 668-679, 2010.
- [iv] E. S. Mohamed, G. Papadakis, E. Mathioulakis and V. Belessiotis, "A direct coupled photovoltaic seawater reverse osmosis desalination system towards battery based system- a technical and economical experimental comparative study". *Desalination*, pp. 17-22, 2008.
- [v] Z. A. Suleimani and V. R. Nair, "Desalination by solar-powered reverse osmosis in a remote area of the Sultanate of Oman". *Applied Energy*, pp. 367-380, 2000.
- [vi] T. Younos, K. E. Tulou, "Energy needs, consumption and sources". *Universities council on water resources, Journal of contemporary water research and education*, pp. 27-31, 2005.
- [vii] A. H. Alami, "Experiments on solar absorption using a greenhouse-effect gas in a thermal solar

- collector". Journal of Renewable and Sustainable Energy, Volume 2, Issue 5, 2010.
- [viii] A. H. Alami, "Mechanical and thermal properties of solid waste-based clay composites utilized as insulating materials". Int. J. of Thermal & Environmental Engineering, Volume 6, Issue 2, pp. 89-94, 2013.
- [ix] R. W. Lee, J. Glater, Y. Cohen, C. Martin, K. Kovace, M. N. Milobar and Dan W. Barteld, "Low-pressure RO membrane desalination of agricultural drainage water". Source: <http://www.water.ca.gov/drainage/grants/drainagereuse/docs/final-reports/UCLA-LowPressureRODesal-Dec122002.pdf>
- [x] G. D. Kang and Y. M. Cao, "Development of antifouling reverse osmosis membranes for water treatment: A review". Water Research, pp. 584-600, 2012.
- [xi] N. P. Cheremisinoff, "Hand book of water and waste treatment technologies". Source: <https://www.crcpress.com/Handbook-of-Water-and-Wastewater-Treatment-Technology/Cheremisinoff/p/book/9780824792770>
- [xii] M. Mulder, "Transport in Membrane". Basic principles of Membrane technology, pp.210-279, 1996.
- [xiii] Ground Water Characteristics, Source: <http://pubs.usgs.gov/wri/wri024094/pdf/mainbodyofreport-3.pdf>
- [xiv] R.W Baker, "Membrane Technology and Applications". pp.149, table 3.7, Source: http://www.separationprocesses.com/Membrane/MT_Ch04d.htm, Dated 16-10-2013
- [xv] Desalination, source: <http://www.iwawaterwiki.org/xwiki/bin/view/Articles/desalinization>
- [xvi] Biography of Aristotle, Source: <http://biography-of.com/aristotle>
- [xvii] Island Desalination by Gilchagas, Source: <http://lego.cuusoo.com/ideas/view/24094>
- [xviii] "Introduction to Desalination Technologies in Australia by URS Australia" Agriculture, Fisheries and Forestry- Australia, pp. 1-33
- Source: <http://www.environment.gov.au/water/publications/urban/pubs/desalination-summary.pdf>
- [xix] Multi Stage Flash Processes, Source: <http://www.sidem-desalination.com/en/Process/MSF/> [Online]
- [xx] Multi-Stage Flash Distillation, Source: http://www.separationprocesses.com/Distillation/DT_Ch07a.html.
- [xxi] R. Semiat, "Multi-Effect Distillation (MED)" Israel Institute of Technology Technion City, Haifa. Source: <http://www.eolss.net/Sample-Chapters/C07/E6-144-44-00.pdf>
- [xxii] J.S Taylor and M. Weisner, "The book for Membrane Selection", Chapter11-Membranes. Source: <http://www.globalspec.com/reference/80710/203279/chapter-11-membranes>
- [xxiii] Overview of Desalination Techniques by Tamim Younos, Kimberly E. Tulou *Virginia Polytechnic Institute and State University* in Universities Council on Water Resources, Journal of Contemporary Water Research & Education, Issue 132, pages 3-10, December 2005
- [xxiv] A. Freshwater, "Desalination in Pacific Island Countries: A preliminary Overview". Drinking Water Safety Planning, SOPAC Water and Sanitation Programme, Deveraux Talagi Attache SOPAC Natural Resource Economics. Source: <https://gsd.spc.int/sopac/docs/SOPAC%20Technical%20Report%20437%20Desalination%20for%20Pacific%20Island%20Countries.pdf>
- [xxv] J. Kucera, "Reverse Osmosis- Industrial Applications and processes". Scrivener Publisher, 2010. Source: <http://www.aiche.org/sites/default/files/cep/20100950.pdf>
- [xxvi] S. P. Beier, "Pressure Driven Membrane Processes", Table 1-Different Pressure Driven Membrane Processes.
- [xxvii] UN Document: Gathering a Body of Global Agreements, A/42/427-Chapter 2, Source: www.documents.net/ocf-02.html.

Section B

ELECTRICAL & ELECTRONICS ENGINEERING

Hybrid Power Analysis Approach for Electronic System Design

Y. A. Durrani¹, A. Ahmad²

¹Electronics Engineering Department, UET, Taxila, Pakistan

²Electrical Engineering Department, UET, Taxila, Pakistan
yaseer.durrani@uettaxila.edu.pk

Abstract—The power estimation in electronic system designs (ESD) has become a significant problem. To keep a balanced approach between the estimation accuracy and speed is the key challenge in the system design. In this paper we present a power analysis method at high abstraction level. We focus on the statistically power dissipation sources of the individual ESD blocks and interconnects/buses of the system. Our hybrid technique combines the regression analysis and look-up-table (LUT) approaches with the non-linear behavioral function. Our algorithm generates input binary signals with five statistical characteristics that help to estimate the average power dissipation. For the power function, we performed Monte-Carlo zero-delay simulation and observed the exact steady-state power behavior of the system. Our power model estimates an accurate power with 10.16% average error. The results are compared with a commercial power estimation tool for the validity of our proposed approach.

Keywords—Low-power, Power estimation, Look-up-table, Register transfer level, CAD/EDA tools

I. INTRODUCTION

Low-Power consumption in electronic system design is becoming an important issue that cannot be ignored. Its flow gives designer a powerful methodology to optimize, estimate and analyze today's increasing power concerns. The rapid growth of transistor density in ESD have made power an important design constraint. At deep submicron level, the reduction of cooling may be the significant factor of integrated circuit (IC) process. ESD is another motivation to investigate the low-power-based system. Power optimization and estimation has nowadays become a difficult task for which the conventional approaches often prove to be inadequate. A key objective in low-power systems is accurate and fast power analysis. Power estimation at high design abstraction level gives new solutions to efficient power problems. Hence, power estimation and optimization approach for low-power is the challenge to a successful design. In order to handle power, commercial electronic design automation (EDA) tools help the designers in the initial stages of the system design

procedures. These tools are useful for minimizing the power dissipation in ESD system. Early power analysis ignores the lengthy procedure to redesign and handles the power budget during the design cycles in the later stages.

As rapid growth of system's complexity and verifications become increasingly difficult and time consuming, power and performance analysis of the design flow are essential for shortening the turn-around time. The design cost and time-to-market of the electronic systems can be greatly reduced through the reuse of predesigned circuits. Power methodology further supports reuse design in a plug-and-play fashion, including buses and hierarchical interconnection infrastructure. Reuse design techniques employing ESD cores cut down on time-to-market, and fast estimation shortens the design evaluation time, which is more efficiently used in design-space exploration. At the initial stage of the pre-design phase, the designers tried to find the possibility of the design exploration space and the power, area, speed requirements. Lot of work has been presented in the past to estimate power of electronic systems at different abstraction levels.

II. LITERATURE REVIEW

A good review of the most effective approaches at different level of the design can be found in [i-ii]. Power analysis models at high-level can be categorized as: linear regression-based, LUT-based or hybrid-based. Regression models estimate power of the individual component with a compact form but it do not deal with the non-linear behavior. Register-transfer level (RTL) cycle accurate model was presented in [iii] to handle with the non-linear behavior with the piecewise regression approach. The improved work of [iii] was further proposed with the automated regression modeling [iv].

LUT-based technique is the most popular approach in the power analysis procedure. Several commercial EDA tools are widely used LUT approach for handling power consumption of each logic block. The impact of the LUT size in the power estimation was discussed in [v]. If the LUT size decreases, then the estimation error increases exponentially. The extended

presented in [vi] to include more independent variables in the model to improve error in the expense of the LUT size.

Hybrid model includes both concepts of regression and LUT approaches. Recently, [vii] demonstrated an efficient hybrid method for the power analysis to minimize the length of the simulation with different levels of the granularity. Such approach uses selectively chooses blocks according to its relative power dissipation to the overall power performance. If it does not effectively influence of the system's power consumption, it may be ignored with some error.

In this work, the two separate hybrid power macro-models are developed for the power estimation of the ESD. These models estimate power for different ESD blocks/buses in the system. These models are only dependent on the environment where blocks and buses are being used. The input signals investigate the accurate power in electronic system. These signals influence the power consumption of ESD blocks and buses in the design. The model uses the average input statistical characteristics for ESD blocks are the transition-density '*TD*', the signal-probability '*SP*', and the spatio-temporal correlation '*ST_C*'. The average input statistical characteristics of buses are the self and coupling transition densities '*STD*', '*CTD*' respectively. These characteristics are used in two separate power models in experiments and achieve comparatively good accuracy. The target is the accurate average total power consumption of a hierarchical blocks and buses under a user-specified application input waveforms.

The paper is organized as follows. In Section III, the detailed background of hybrid power analysis methodology is discussed. In Section IV, the results and discussion is demonstrated. Finally, the Section V summarizes the work.

III. POWER ESTIMATION METHOD

One of the most challenging aspects in the construction of a power macro-model is the choice of the model's characteristics. These characteristics should capture the features that are primarily responsible for a system's dissipation and can thus help in obtaining good estimates of its power dissipation. The flow of high-level power estimation methodology is shown in Fig. 1. The approach consists of the following steps:

1. Characterization of each ESD block/bus at the high-level design library by simulating it under pseudo random signals and fit statistical variables regression curve to the power dissipation results using a least-mean-square (LMS) error fit.
2. Extractions of the power function from parameter model for blocks '*TD*', '*SP*', '*ST_C*' and for buses '*STD*', '*CTD*' using Monte-Carlo simulation approach. The high-level simulator collects the power values for various blocks/buses in the ESD

System.

2. Evaluation of the power model function for block/bus design. These are found in the library by plugging the parameter values in the corresponding model function.

A. Linear Regression Analysis

The proposed hybrid model is the combination of linear regression and LUT approaches. To obtain power model, a linear function in (1) estimates power of the given input signals.

$$P_{Block_avg} = \beta_0 + \beta_1.\alpha_1 + \dots + \beta_{n-1}.\alpha_{n-1} + \beta_n.\alpha_n + \varepsilon \quad (1)$$

where ' P_{Block_avg} ' is the average power dissipation of the individual ESD block, ' $\beta_0, \beta_1, \dots, \beta_{n-1}, \beta_n$ ' are the regression coefficients obtained from the regression analysis, ' $\alpha_0, \alpha_1, \dots, \alpha_{n-1}, \alpha_n$ ' are the statistical characteristics of each input and ε is the error. The parameters of the regression are determined using the linear regression by finding the least-square fit. Equation (1) can be expressed in (2):

$$P_{IP_avg} = \beta_0 + \beta_1.TD + \beta_2.SP + \beta_3.SC + \beta_4.TC + \varepsilon \quad (2)$$

where '*TD*', '*SP*', '*SC*', '*TC*' are the statistical characteristics of our model.

The regression equation in (2) can be computed by applying the set defined input pattern values of '*TD*', '*SP*', '*SC*', and '*TC*'. The determination coefficient p^2 is measured to improve the quality of (2). It measures the proportionality of data set patterns of the input characteristics that helps to predict the accurate power. p^2 varies from 0 to 1 and it is defined in (3):

$$p^2 = 1 - \frac{\varepsilon_s}{r} \quad (3)$$

where ε and r is defined in (4) and (5):

$$\varepsilon_s = \sum (x_i - y_i)^2 \quad (4)$$

$$r = \sum (x_i - \bar{x})^2 \quad (5)$$

with \bar{x} is the mean of the estimated data, x_i predicts the values and y_i is the data set value.

B. LUT-Based Power Estimation for ESD blocks

The power model characteristics are defined in [viii, ix]. We propose an input signal generation algorithm which generates test stimuli with '*TD*', '*SP*', '*ST_C*'. The LUT-based power model estimates the average power dissipation of each ESD block in (6).

$$P_{Block_avg} = f(TD, SP, ST_C) \quad (6)$$

For the given block with the primary inputs width 'w' and the input binary signals length 'l' in (7):

$$l = \{(l_{11}, l_{12}, \dots, l_{1w}), (l_{21}, l_{22}, \dots, l_{2w}), \dots, (l_{n1}, l_{n2}, \dots, l_{nw})\} \quad (7)$$

The $f(\cdot)$ in (6) is the input pattern dependent, so the length and the width in the pattern generation are dependent on the number of primary inputs of the individual block. In most cases, the 'TD' and 'SP' have effective role in the power dissipation due to their characteristics of transition activities of input signals in any digital system. In observations, the correlation factor 'ST_C' is normally dependent on the number of primary inputs and the size (number of gates) of the individual block. Further, in case of 'ST_C', if 'w' increases then spatial-correlation 'SC' are more effective than temporal-correlation 'TC'. Similarly, in case of increases 'l', the 'TC' is more significant than the 'SC' in any input pattern. Hence equation (6) is further modified and introduced two sub-functions in (8) and (9).

$$P_{Block_A_avg} = f(TD, SP, SC_{\rightarrow w}) \quad (8)$$

$$P_{Block_B_avg} = f(TD, SP, TC_{\rightarrow l}) \quad (9)$$

where ' $SC_{\rightarrow w}$ ' and ' $TC_{\rightarrow l}$ ' are the width and length dependent correlation characteristics.

B. LUT-Based Power Estimation for Buses

In the earlier literature, extensive power modeling approaches of interconnects/buses have been introduced [x, xi]. Our LUT-based power model estimates the average power dissipation of interconnects in (10).

$$P_{Interconnect_avg} = f(S_{TD}, C_{TD}) \quad (10)$$

where ' S_{TD} ' and ' C_{TD} ' are the self and coupling transition densities of interconnects. The ' C_{TD} ' depends on the activity between the two adjacent interconnects.

The $f(\cdot)$ in (10) is the input pattern dependent. The input signal generator generates patterns according to the number of interconnects of the individual bus. The $f(\cdot)$ is a mapping-method to be performed during the characterization of the two transition densities. To find function $f(\cdot)$, we must sample a set number of streams with several ' S_{TD} , C_{TD} ' values. The application of the power estimation on each interconnect requires knowledge of the signal characteristics among interconnects. To find an average power dissipation of the local or global shared bus ' P_{Bus_avg} ' depending on the number of interconnects (in the system) can be

computed in (11) using (10).

$$P_{Bus_avg} = f(S_{TD_Bus}, C_{TD_Bus}) \quad (11)$$

where ' S_{TD_Bus} ' and ' C_{TD_Bus} ' are the self and coupling transition densities of bus defined in (12), (13):

$$S_{TD_Bus} = \sum_{i=1}^n S_{TD_i} \quad (12)$$

$$C_{TD_Bus} = \sum_{i=1}^{n-1} S_{TD_{i,i+1}} \quad (13)$$

Here n is the number of interconnects of the bus.

D. Hybrid Power Estimation for ESD

The total power consumption of a system is obtained by adding all its dissipative components. The $f(\cdot)$ in (6), (8), (9), (10) and (11) is a mapping-method to be performed during the characterization of the input signals. To find function $f(\cdot)$, a set pattern of these signals with several values of 'TD, SP, ST_C' and ' S_{TD} , C_{TD} '. The application of the power estimation on each block requires knowledge of the input signal characteristics among individual blocks. The total average power dissipation of the ESD system ' P_{ESD_System} ' is extracted in (14) using (8), (9) and (11).

$$P_{ESD_System} = \sum_{i=1}^n P_{iBlock_avg} + \sum_{i=1}^n P_{iBus_avg} \quad (14)$$

Monte-Carlo zero-delay simulation technique [ix] is used with several sequences of their input signal characteristics given to the ESD block and the power dissipation is estimated to the each sample of the input signals. These power samples are needed to determine whether the entire process is necessary to repeat and full-fill the given criteria. The estimation must satisfy the top-level circuit under the user-specified confidence and error levels. Our power estimation strategy is to sums up the estimates to produce total average power by the macro-model function in (14). The interpolation-scheme [xii] may be performed if the input characteristics do not match their statistics.

IV. RESULTS & DISCUSSION

To validate hybrid power estimation method, the experimental work is evaluated on ESD system as shown in Fig 1. The figure has n number of blocks with different sizes. These blocks are connected with each other through the local and global buses to construct the overall ESD system. The model uses a nonlinear function in (14) to estimate the average power dissipation.

In power estimation procedure, the sequence of an

input pattern is generated for the desired input characteristics ' TD , SP , ST_C ' and ' S_{TD} , C_{TD} ' for ESD blocks and buses respectively. Then using LUT technique, the functional simulations are performed with RTL power simulator and the average power dissipation is extracted by the output waveforms of the individual ESD block or bus. At this stage, the power functions in (6), (8), (9), (10) and (14) can be defined.

This power estimation procedure is divided into two phases: In the first phase, we generate random digital input signals according to the statistical characteristics with the specified probabilistic range between [0-1] for the given block/bus and the average power consumption is estimated using power

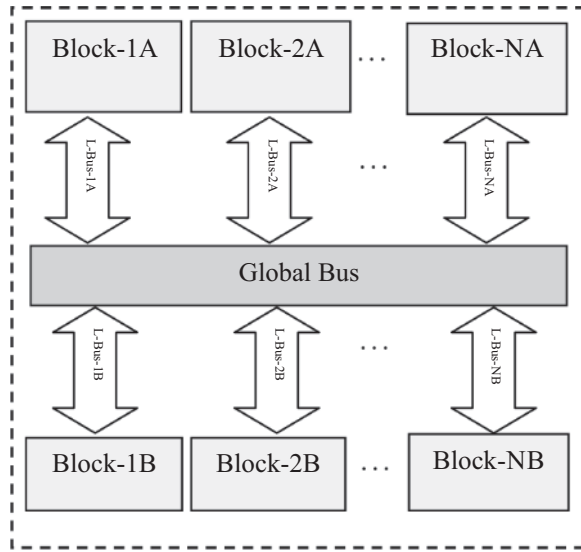


Fig. 1. Example of ESD architecture

function $f(.)$ in (6) or (11). These functions map the input characteristics of each block/bus. In the second phase, a Monte-Carlo zero-delay simulation is performed with several input signals of their statistical properties, whereas the least square fitting is performed for linear regression analysis to find the quality of the power functions P_{Block_avg} and P_{Bus_avg} . Several values are determined by LUT-based approach. Then we estimate the average power results. The accuracy of our power macro-model is tested by running gate-level and RTL simulations. We compare our power results with Xilinx and HSPICE commercial tools. At the end, we compute errors to find the accuracy of our model.

In our preliminary work with ESD system, the hybrid technique intends to reduce large simulations at RTL. Our method allows fast power estimation by a simple addition of all blocks and buses. The average power dissipation of ESD system ' P_{ESD_System} ' is extracted using (14). The main advantage of our hybrid method is that it can provide fast and accurate estimates; thus, it helps designers to explore different complex blocks in real time. We opted for simple functions with low-

order polynomial dependency on $f(.)$ in (6), (8), (9), and (11). We compare our estimated power with simulated power estimation (taken from the power simulator) using (15) and (16) to evaluate the accuracy of our power estimation function. The maximum, minimum, average and root mean square (rms) errors are computed.

In our experiments, we used ESD blocks with different sizes shown in Table 1. Each block may be considered as a single block in a medium VLSI chip. The sizes of our larger blocks are close enough in today's embedded electronic circuits. Hence our power estimation strategy is consistent with individual block-by-block for input pattern generation. The randomly generated sequences have relatively accurate statistics. Our pattern generator can generate a set number of sequences over the entire space range. Therefore, it enables us to perform extensive experiments to reveal the relation between ESD design power dissipation and specific statistics of the input signals. In our study, we used different blocks/buses and for individual block/bus, we generated 400 to 1900 sequences with ' TD , SP , ST_C ' and ' S_{TD} , C_{TD} ' evenly distributed in the three/two dimensional space. Our parameters granularity is 0.2 over the entire space. In practice, much larger sequences should be used for larger circuits. Roughly speaking, for a given block/bus, we empirically observe that sufficiently long input sequences that produce similar steady-state power exhibit similar total power. Given block/bus, for all the input sequences that produce a steady-state power, we believe that hazardous power corresponding to an input sequences have the behavior of a random variable. Furthermore, among all these input sequences that produce a steady-state power, longer sequences tend to have smaller variance than shorter sequences. For the verification of our random sequences, we compared our power results with the functional sequences power results and found a 96% correlation. Synthetic validation is performed by applying a uniform set of stochastically generated test-benches. All the results to be presented were performed with a 3% error-tolerance ($\epsilon = 0.07$) and 98% confidence ($\alpha = 0.03$). Table I and Table II, illustrates the set number of the input vectors and the average relative errors of the estimate values obtained with our macro-model function. For the input characteristics, ' TD , SP , ST_C ', and ' S_{TD} , C_{TD} ' the specified range between [0-1]. The function is more accurate estimating the average power in some cases than others. For example in figure 2, the given input values are more accurate for specifying the range of region between [0.25-0.75] and less accurate of region between [0-0.25] and [0.75-1].

It is evident from Table 1 that the model function $f(.)$ is accurate for estimating the average power for digital block. In Table 1, the first column shows the name of the block. The three dimensional input model estimates the average 6.08%

TABLE I
ACCURACY OF POWER ESTIMATES FOR INDIVIDUAL
BLOCK

Core	$\% \epsilon_{\min}$	$\% \epsilon_{\max}$	$\% \epsilon_{\text{avg}}$	$\% \epsilon_{\text{rms}}$	# gates
Blk-1A	11.20	13.12	11.83	11.78	885
Blk-2A	3.25	4.32	3.56	3.38	463
Blk-3A	14.32	15.30	14.79	14.61	921
Blk-4A	5.14	6.92	5.65	5.54	310
Blk-5A	4.54	6.42	5.56	5.33	456
Blk-6A	7.30	9.35	8.52	8.39	843
Blk-7A	8.23	9.90	8.76	8.64	760
Blk-8A	4.56	6.03	5.67	5.78	658
Blk-1B	6.43	8.12	7.52	7.80	810
Blk-2B	9.12	10.59	9.81	9.93	830
Blk-3B	2.17	3.37	2.84	2.74	420
Blk-4B	4.76	6.16	5.53	5.68	667
Blk-5B	5.57	6.35	5.98	5.86	323
Blk-6B	5.02	6.91	6.04	6.18	644
Blk-7B	1.34	3.07	2.62	2.78	1190
Blk-8B	4.34	5.93	4.94	4.56	944
$\% \epsilon_{\text{avg}}$	6.08	7.62	6.85	6.80	695

TABLE II
ACCURACY OF POWER ESTIMATES OF BUSES

Bus	$\% \epsilon_{\min}$	$\% \epsilon_{\max}$	$\% \epsilon_{\text{avg}}$	$\% \epsilon_{\text{rms}}$	# lines
L-Bus-1A	6.24	8.38	7.45	7.65	16
L-Bus-2A	5.53	7.24	6.25	6.02	16
L-Bus-3A	6.23	8.24	7.19	7.03	16
L-Bus-4A	9.56	11.43	12.01	12.09	16
L-Bus-5A	5.30	7.03	6.49	6.29	8
L-Bus-6A	4.90	6.12	5.37	5.93	8
L-Bus-7A	5.41	6.98	6.38	6.45	8
L-Bus-8A	6.47	7.86	7.16	7.43	8
L-Bus-1B	2.84	3.97	3.21	3.64	16
L-Bus-2B	7.94	10.29	9.01	9.87	16
L-Bus-3B	5.37	8.13	6.35	6.41	16
L-Bus-4B	3.83	5.48	4.46	4.37	16
L-Bus-5B	4.48	6.39	5.49	5.06	8
L-Bus-6B	5.83	7.17	6.57	6.07	8
L-Bus-7B	2.69	4.98	3.15	3.61	8
L-Bus-8B	1.92	3.05	2.69	2.18	8
G-Bus-1	10.54	17.22	14.50	14.44	24
$\% \epsilon_{\text{avg}}$	5.59	7.64	6.69	6.77	12.71

minimum, 7.62% maximum, 6.85% average and 6.80% rms relative errors are demonstrates in columns two, three, four, and five respectively. Columns six gives the number of logic gates of each core consists of 300-1200 logic gates in the ESD system. Our macro-model separately estimates the power consumption of

interconnects/buses among different blocks. In Table II, the first column shows the name of the local or global bus. The two dimensional input macro-model estimates the average 5.59% minimum, 7.64% maximum, 6.69% average and 6.77 rms relative errors are demonstrates in columns two, three, four, and five respectively.. Columns six gives the number of lines/interconnects in each bus consists of 8-24 bits in the ESD system. Figure 2 plots the variation of the power values with the trial interval length (clock cycle) and it demonstrates the length is 1000 for one of the four blocks in the system. The warm-up length is about 400, while the vertical line represents the steady-state value at 800.

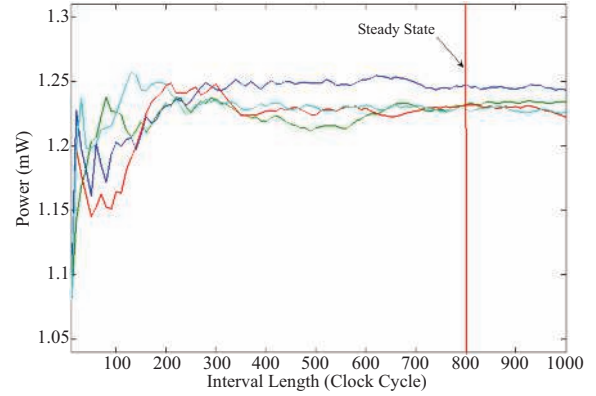


Fig. 2. Power changes with sequence length for different blocks in ESD System

The above results demonstrate that our technique can be implemented to achieve fast and accurate power estimation in the early stage of any ESD design. The average power dissipation of ESD system ' $P_{\text{ESD System}}$ ' is extracted using (14) by a simple addition of all digital blocks and buses. In our experiments, the average error of the entire system is 10.16%. This error may be reduced by using different optimization techniques to improve the power dissipation of the system. One important source of error is due to delay elements such as glitch activities, jitter, skew and other power dissipative elements. In this paper we do not consider these factors and assume zero-delay model approach.

V. CONCLUSION

We have demonstrated a zero-delay power estimation technique at high-level applied to ESD system. In our preliminary work, we extracted two different statistical models to estimate power dissipation for individual blocks and bus in the design. For an entire ESD system, the average power is extracted by a simple addition of all power estimation results of these two models. In our experiments, we measured 10.16% of the average error in the entire system. This error may be reduced by using different optimization techniques to handle the power

dissipative elements such as glitch activities, jitters, skews and other factors. Currently, we are evaluating our approach for more complex ESD systems and are working to further improve its accuracy.

REFERENCES

- [I] X. Liu and M. C. Papaefthymiou, "Incorporation of input glitches into power macromodeling" *Proceeding IEEE international symposium on circuits and systems*, pp. 456-461, 2002.
- [ii] S. Gupta, F. Najm "Power modeling for high-level power estimation", *IEEE Transaction on Very-Large-Scale Integrated System*, vol.8, no. 1, pp. 18-29, 2000.
- [iii] C. Forzan and D. Pandini, "Statistical static timing analysis: A survey," *Journal of VLSI Integration*, vol. 42, no. 3, pp. 409–435, 2009.
- [iv] S. Ravi, A. Raghunathan, and S. Chakradhar "Efficient RTL power estimation for large designs", *International Conference on VLSI Design*, pp. 431-440, 2003.
- [v] S. Gupta, and F. Najm "Analytical models for RTL power estimation of combinational & sequential circuits", *IEEE Transactions on Computer Aided Design*, vol.19, no. 7, pp. 808-814, 2000.
- [vi] M. Barocci, L. Benini, A. Bogliolo, B. Ricco, and D. Micheli "LUT power macro-models for behavioral library components", *IEEE Alessandro Volta Memorial Workshop on Low-Power Design*, pp. 173-182, 1999.
- [vii] N. Bansal, K. Lahiri, A. Raghunathan, and S. Chakradhar "Power monitors: a framework for system-level power estimation using heterogeneous power models", *18th International Conference on VLSI Design*, pp. 579-585, 2005.
- [viii] Y. A. Durrani, and T. Riesgo, "Power estimation technique for DSP architecture", *Elsevier Journal of digital signal processing*, vol. 19, issue 2, pp.213-219, 2009.
- [ix] Y. A. Durrani, and T. Riesgo "High-level power analysis for intellectual property-based digital systems", *Springer Journal of Circuits, Systems & Signal Processing*, vol. 32, no. 6, pp. 1035-1051, 2013.
- [x] Y. A. Durrani, and T. Riesgo "High-level power analysis for IP-based digital systems", *ASP Journal of Low Power Electronics*, vol. 9, no. 4, pp. 435-444, 2013.
- [xi] Y. A. Durrani, T. Riesgo" Power analysis approach and its application to IP-based SoC design " *Emerald International journal of computation and mathematics in electrical and electronic engineering*" vol. 35, issue 3, pp. 1218-1236, 2016.
- [xii] X. C. Li, J. F. Mao, H. F. Huang, and Y. Liu, "Global interconnect width and spacing optimization for latency, bandwidth and power dissipation," *IEEE Transaction on Electron Devices*, vol. 52, no. 10, pp. 2272–2279, 2005.

Section C

MECHANICAL, INDUSTRIAL,
MATERIAL, ENERGY ENGINEERING
AND
ENGINEERING MANAGEMENT

Design and Analysis of Prototype Tesla Turbine for Power Generation Applications

I. Zahid¹, A. Qadir², M. Farooq³, M. A. Zaheer⁴, A. Qamar⁵, H. M. A. Zeeshan⁶

¹Mechanical Engineering & Technology Department, GCU Faisalabad

^{2,4,6}Mechanical Engineering Department, The University of Lahore, Pakistan

^{3,5}Mechanical Engineering Department, UET Lahore, Pakistan

³engr.farooq@uet.edu.pk

Abstract—The objective of the present research is to examines the potential benefits of Tesla Disk Turbine (TDT), a harmless mean of energy conversion from high pressure non-polluting fluid (compressed air, water & steam) to a form of energy e. g. electricity, mechanical power which can be used in various applications. A prototype model of TDT was designed and different experiments were performed with various pressure ranges of compressed air. Theoretical sound (boundary layer theory, adhesion, and viscosity), design, material selection, fabrication, efficiency, power output, advantages, limitations, its applications have been discussed. This model can alternatively be used in different applications of power generation as replacement of batteries & generators. Steam, water and other medium can also be part of this technology by adapting this turbine for large scale energy production. The result obtained from the current research could be utilized as a guide for the further design and operation of the industrial system.

Keywords—Axial flow disc, Boundary layer theory; Compressed air; Flow efficiency; Tesla Turbine.

I. INTRODUCTION

The TESLA, bladeless turbine, uses smooth circular discs instead of vanes and it is placed inside the construction cabinet. Principle of this turbine comes from adhesion and viscosity (Boundary layer effect) [i].

The turbine consists of two main parts, the rotor

and the stator [ii]. The rotor comprises asset of discs placed on the shaft. The stator is the housing of the rotor. A nozzle represents to direct the high speed fluid flow towards the disk's periphery. The fluid flows into the turbine through a tangential inlet and enters the system of spaces in the line of disks. By attrition of the fluid and the disks, the turbine runner is made to rotate. The centrifugal power is affected through the rotation on the turbine rotor between the discs provide its long spiral track [iii]. With growing mechanical load on the turbine, the speed drops, the centrifugal power runs low and the liquid track turns more into the center. This enhances the flow capacity through the mechanism bigger [iv]. Also with the mechanical load off, the higher speed provides the greater centrifugal power. Due to the possible change in speed, the mechanism becomes flexible. Nikola Tesla claimed that total effectiveness of this turbine could reach upto 98% [iv]. Later on, different prototypes design models used compressed air and showed the total effectiveness round about 40% [v]. Numbers of properties of TDT were discussed in current studies. Unlike other conventional ways of power generation, it is environment friendly as it makes the use of non-polluting fluids such as compressed air, water, steam etc. As fluid drags the disc, depends on its viscosity and adhesion of the surface layer of fluid with disc. As the viscosity of these working fluids are close to each other, the bit difference is managed by other properties of fluid like adhesion Hence it is stated as the green energy source [vi]. Fig. 1 shows the implementation of tesla turbine as a green energy resource.

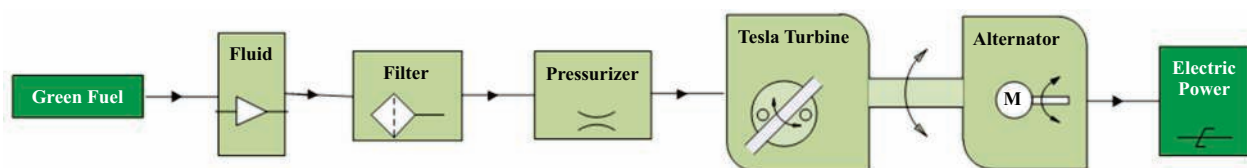


Fig. 1. Tesla Turbine Implementation as a non-conventional energy resource [vii]

Tesla Turbines finds its applications at certain places where the conventional turbine fails to operate as “it can be used to tap geothermal energy from underground salt-brine in locations all over the world” [viii]. It is a

highly efficient rotary engine which has an amazing power and simplicity. This is the sole high power turbine that can be fabricated in expensively using only some simple machining tools; hence it is operationally

advantageous over expensive machines [ix]. Roman in proposed analytical solution method to achieve main objective of design analysis of Tesla Turbine [x]. Krishnan further modified and presented incompressible small as well as medium scale turbine and calculated useful results using ANSYS simulation [xi]. Rice worked for the better performance of Tesla turbine but his experiments were computational base. Guha, Hoya and Deam also presented computational model for small to large scale but could not present analytical solution for the performance of Tesla Turbine [xii-xiv]. After all Carey achieved useful results using analytical solution [xv].

In the present research, the model of tesla turbine has been used for the different applications of power generation as replacement of batteries & generators. For upgraded energy production system, steam, water and other medium could be used for this technology. The result obtained from the current research could be utilized as a guide for the further design and operation of the industrial system.

II. MATERIAL AND METHODS

A. Material Selection

The most important part of the tesla turbine is the rotor (shaft discs) and the nozzle. Material selection for these parts is of the extreme importance. Table I illustrates the various elements of tesla turbine. Ten aluminum discs with 9 spacers of 0.5mm & 16 washers of 5/16" were used as a series of discs in rotor of tesla turbine.

TABLE I
PARTS OF TESLA TURBINE MODEL AND QUANTITY

Parts	Quantity
Plexi glass Sheet	2
Collars	2
Aluminum Shaft	1
Ballbearingsinnerdia1.5cm	2
7"dia&5"lengthplasticpipe	1
5/16"dianutsandbolts	8
Cylinder for storing compressed air	1
Pressure gages with valves(inlet, outlet)	2
Nozzle with control flow valve	1
Rubber hose to supply air	1

Variety of advance materials was used to get control over extreme centrifugal forces inherent to the turbine, such as titanium-impregnated plastic, carbon-fiber and Kevlar-reinforced discs. In present model stainless steel was used for discs, aluminum for collar,

brass for nozzle, steel and aluminum for shaft. Table II shows the size of different parts of tesla turbine based on specific applications.

TABLE II
PARTS AND SIZE OF TESLA TURBINE MODEL

Parts	Size
Turbine diameter	100mm
Disk diameter	6 inches
Disk thickness	2 mm
Disk gap	1.2mm
Number of disks	10
Over base size	(113*185)mm
Total Weight	1420gapprox.
Turbine length (Ex Generator+Mounts)	75mm

B. Design of Tesla Turbine

The important criterion used in the tesla turbine was the designing of rotor, shaft, stator, collarand nozzle. In rotor's designing, a number of discs with same diameter (6 inch) and thickness (2mm) were mounted on a shaft and fixed with a very fine spacing (0.3-0.5mm) between each two. The nozzle slot, compared to the overall width of the rotor, was narrower i.e. the number of the active discs must be less in number than the total discs. For this case turbine with 25 discs, have 23 active discs including the disks with thicker ends. In order to attain more efficiency and overcome losses, nozzle with platinum chamber can be experimented, briefly the geometry of the nozzle can be changed using an interchangeable nozzle insert. As a design compromise it was necessary that the nozzle incorporated a 90° bend just before the exit plane. Using same strategy for inlet, losses could be controlled. The Propelling fluid get pass the outer most active discs. The assembly of rotor was housed inside a cylindrical stator, or within the stationary part of the turbine. In order to house the rotor, the interior format diameter was slightly larger in size than the discs of rotor. Ball bearing for the shaft at each end of the stator was used. Two inlets were contained by the stator, in which nozzles were inserted.

C. Tesla Turbine Prototype

A Tesla Turbine prototype was designed as shown in Fig. 2. This prototype model consists of various parts such as stator, stator outlets, rotor discs, exhaust port and shaft.

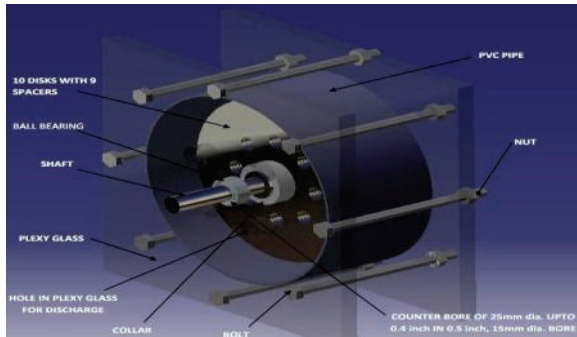


Fig. 2. Prototype Model of Tesla Turbine

D. Working Principle

The principle of Boundary Layer (BL) was followed for the working of Tesla Turbine (TT). According to this principal, molecules which are right next to the surface, stick to the surface as the fluid moves past each disc surface. Those molecules which follow the surface, stick to it and are slowed down in their collision to the molecules stuck to it. These molecules in results slowdown the flow which is just above them. As these molecules move away from these surfaces, the chances of their collisions are reduced with the object surface. Meanwhile, due to viscous forces, the molecules of the fluid resist for separation. These forces become prominent over the inertial forces. This will produce a pulling force that is transferred or moved to the disk, which causes the disk to rotate in the direction of fluid [xvi].

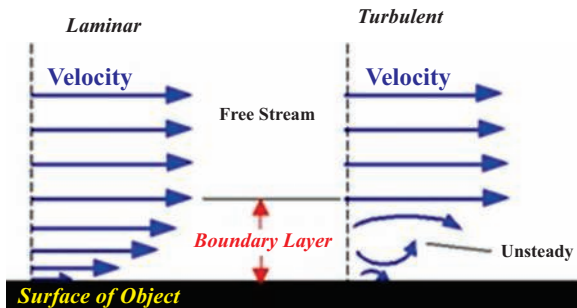


Fig. 3. Boundary Layer Effect [xvi]

The fluid enters the rotor disc spaces in turbulent regime and at the leading edge, stars the formation of boundary layer. Due to the dominating viscous forces,

flow is turned from turbulent to laminar. After the boundary layer build up, the forward transition to the turbulent occurs caused by the increase of velocity. The fluid accelerates in the radial direction and the thickness of the boundary layer decreases. Hence the inertial forces pre dominant and turbulence is expected to increase but with acceleration, the flow current in the turbulent boundary layer became extended and the vortices is dissipated through the viscous effects [xvi].

High speed fluid from the injection nozzle enters the inter-discolor spacing and whirls around bending its flow towards the center of the shaft. It transfers some of its momentum of the rotor discs and ejects through the exhausts lots [v]. Fig. 4 shows the injection of fluid through stator inlets.

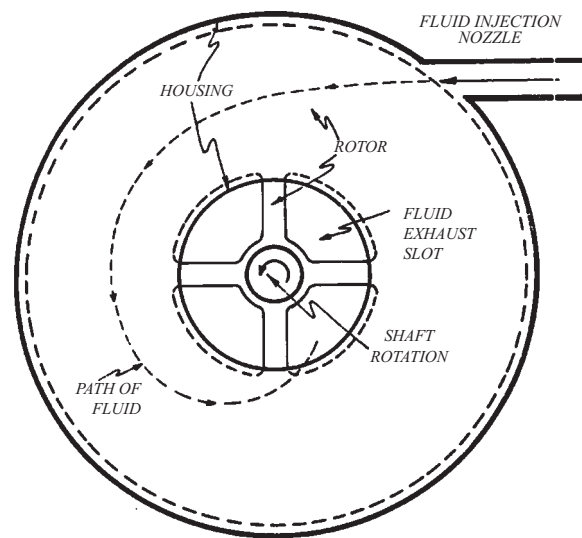


Fig. 4. Flow Path between Discs [xvii]

III. RESULTS AND DISCUSSION

The stator of Tesla turbine contains two or more inlets for nozzles. Through nozzles compressed air at about 272 kPa enters rotor discs results to spin rotor which was coupled with generator and gives output. A tube light of 40 watt was tested and different parameters such as voltage, current and power were observed.

TABLE III
POWER OBTAINED FROM TESLA TURBINE AT DIFFERENT SPEED

Pressure (Kpa)	Rotation (rpm)	Light (Watt)	Voltage (Volts)	Current (Amp)	Efficiency (%)	Power (Watts)
272	1000	40	11	1.5	58	16.5
272	1500	40	12	1.59	58	19.08
272	2000	40	14	1.65	58	23.1
272	2230	40	14	1.72	58	24.08

A. Power Outcome

Power obtained from tesla turbine was analyzed on different speeds. The result shows that the power increased with the increase of speed of rotor of the tesla turbine. There is direct relation between power and number of rotation. Fig. 5 shows the power at different speeds of the turbine. It can be observed that at 1000 rpm power obtained is 16.5 watt which increases linearly by increasing speed.

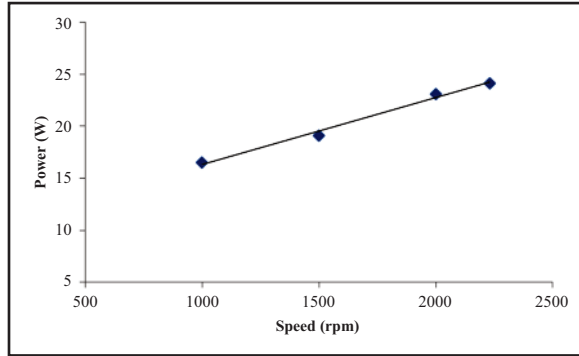


Fig. 5. Relationship between Power and rotation

B. Relation between Voltage & Speed

Fig. 6 depicts the relationship between the voltage and the speed. It is clear that there is almost linear relation between voltage and rpm. As speed decreases from 2230 to 1000 rpm voltage also declined from 14 to 11 volts. Solid line shows the actual behavior while dotted line shows linear relation. There is slight more variation of voltage comparatively at speed of 2000 rpm but still the relationship is linear.

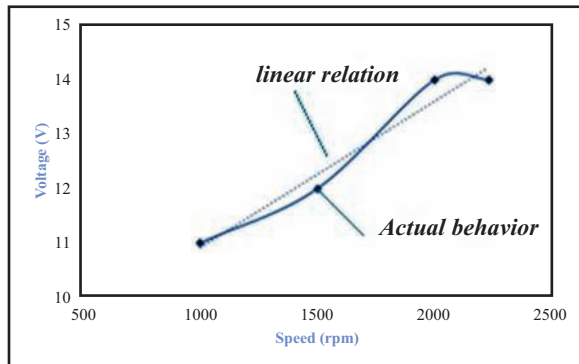


Fig. 6. Relationship between Voltage and rotation

C. Role of Current

The effect of the current with speed is also in accordance with the voltage. Thus also determined from the Ohm's law $V=IR$, where voltages are directly proportional to the current produced. It can be observed from Fig. 7 that at 2230 rpm the value of current that is measured is 1.72 ampere. Hence, the amount of current decreased as number of rpm decreased.

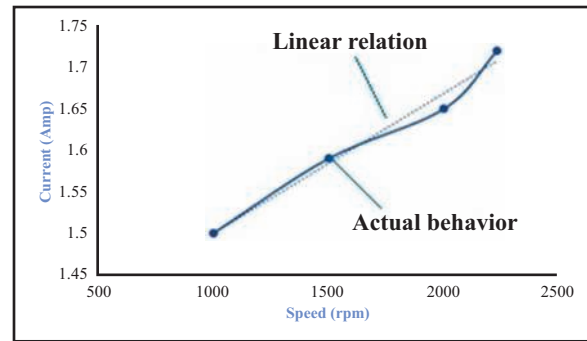


Fig. 7. Relationship between Current and rpm

C. Comparison of Efficiency among different turbines

Three key efficiency points of this turbine are inlet nozzle, disc geometry and the outlet. Disk geometry means the use of compatible material with quite perfect spacing and the accurate number of positions of dividers. Between discs, space must be from 0.032 inch to 0.125 inch. High torque and low horsepower was developed due to narrow spacing and vice versa. Two major functions are performed by inlet nozzle. It transforms gas pressure into the gas kinetic energy and converts the kinetic energy, in parallel streams, into the rotor (turbine disk pack). Figure 8 illustrates comparison of efficiencies of different turbines. The efficiency of bladed turbine is 22 percent and the efficiency of tesla turbine is 58 percent. Among all turbines, Tesla has maximum efficiency where as other turbines like Bladed, Gas Piston, Diesel and Fuel Cell are less in efficiencies of about 22%, 32%, 42% and 45% respectively. It clearly depicts that using Tesla disc turbines could bring more work output by utilizing maximum energy for running turbine. Conventional turbines are mostly reaction and impulse type or both. Tesla turbine is an unconventional turbine that uses fluid properties such as boundary layer and adhesion of fluid on series of smooth disks keyed to a shaft.

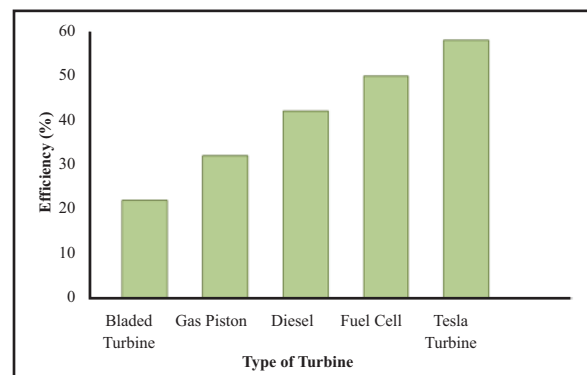


Fig. 8. Percentage Efficiency of Turbine

IV. COMPARATIVE ANALYSIS WITH CONVENTIONAL TURBINE USING CFD

Tesla turbine can generate power for variety of working media like Newtonian fluids, non-Newtonian fluids, mixed fluids, particle laden two-phase flows [xi]. In CFD, tesla turbines results are more clear and broad with lot of advantages seen. Comparative to traditional turbines, typical results of Tesla disc turbines are shown in Fig. 9:

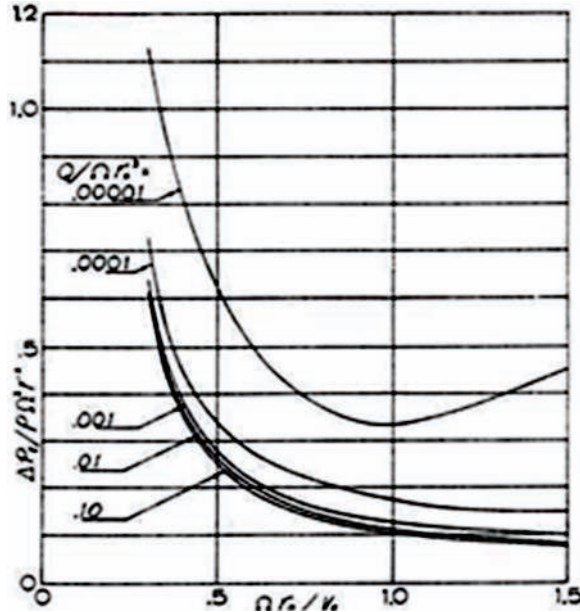


Fig. 9. Percentage Efficiency of Turbine

Whereas CFD analysis shows that it has better results. The three-dimensional flow field and the flow path lines within a Tesla disc turbine have been investigated analytically and computationally. The description of the flow field includes the three-dimensional variation of the radial velocity, tangential velocity and pressure of the fluid in the flow passages within the rotating discs.

Two domains were created in Solidworks 2013. Rotating domain consisted of rotor assembly and the stationary domain consisted of outer casing with a simplified nozzle [xii]. Table iv shows the meshing data for the domain created. Table v presents parameters selected for CFD analysis. Figure vi shows the setup of two domains.

TABLE IV
MESHING DATA FOR DOMAINS OF TESLA TURBINE

Meshing Data	
Rotating Domain	
Nodes	483462
Elements	2011811
Stationary Domain	
Nodes	244141
Elements	1282278

TABLE V
PARAMETERS SELECTED FOR CFD ANALYSIS

Flow State	Transient
Boundary Conditions	Mass flow rate as inlet Atmospheric Pressure at outlet
Turbulence model	K-Epsilon
Mass flow rate	7.2 Kg/sec
Static atmospheric pressure	1 atm (Outlet condition)
Phase	Single(water)
RPM	800

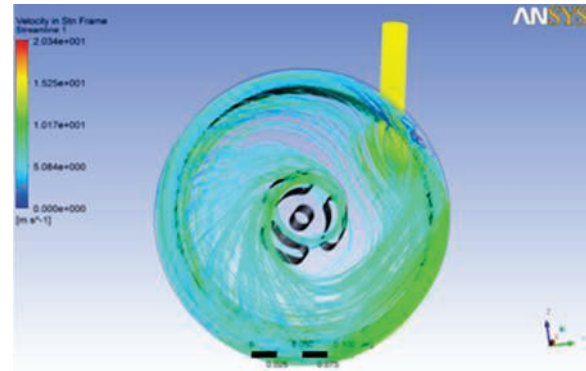


Fig.10. Two domains setup

V. CONCLUSION

In Present research the model of tesla turbine has been used for the different applications of power generation as replacement of batteries & generators. For upgraded energy production system, steam, water and other medium could be used for this technology. It is considered vital to introduce such apparatuses where efficiency is required higher In order to consume those energy resources in which more is the efficiency and less is the cost. This study evaluates that the tesla disc turbine compared to others, operates on high rpm with low vibrations and output is higher with lager velocities. Moreover it works on high velocity. This model can be used in different applications of power generation for the replacement of batteries & generators. Among his lesser-known inventions is a bladeless turbine. The Tesla Turbine differs from typical turbines in that instead of using curved blades like those of a windmill, it uses smooth, parallel disks placed evenly across a shaft, like CD's placed along a stick. By utilizing this phenomena, more modifications in future could bring this world out of the global energy crisis as well as it would let scientists developing systems with more efficiencies. It can replace steam turbines as it has more efficiency and could play an important role as in controlling world's pollution as it is one of the major clean sources of green energy.

REFERENCES

- [i] P. Bloudicek and D. Palousek. "Design of Tesla Turbine" 2007.source: http://dl.uk.fme.vutbr.cz/zobraz_soubor.php?id=341
- [ii] W. Harris "How the Tesla turbine works". Online date: July 14, 2008.source: <http://auto.howstuffworks.com/tesla-turbine2.htm>
- [iii] Tesla turbine, "Principle of Operation" . Source: <http://mve.energetika.cz/jineturbiny/tesla.html>
- [iv] M. E. Crawford and W. Rice. " Calculated Design data for multiple disc pump using incompressible fluid". Journal of Energy and Power, pp. 274-282, 2010.
- [v] V. Krishna. " Design and 'Fabrication of cm scale Tesla Turbines" University of California, 2015. Source:<https://www2.eecs.berkeley.edu/Pubs/TechRpts/2015/EECS-2015-161.html>
- [vi] T. W. Choon, A. A. Rahman, T. S. Li and L. E. Aik. "Tesla turbine for energy conversion: An automotive application" Colloquium on Humanities, Science and Engineering (CHUSER)pp. 816-821, 2012.
- [vii] M. Khan, M. I. Maqsood, E. Ali, S. Jamal and M. Javed. "Proposed applications with implementation techniques of the upcoming renewable energy resource, The Tesla Turbine" Journal of Physics, 2013.
- [viii] Tesla Turbines proposed for geothermal energy from American Antigravity. Online date: March 30, 2007. source: <http://atlanticgeothermal.blogspot.com/2007/03/tesla-turbines-proposed-for-geothermal.html>
- [ix] Tesla turbine builders' organization "Tesla's Geothermal Solution". pp.1-9 Source:www.teslaengine.org/
- [x] V. D. Romanin and V. P. Carey. "An integral perturbation model of flow and momentum transport in rotating micro channels with smooth or microstructured wall surfaces". Physics of fluid, Volume 23, Issue 8, 2011.
- [xi] V. G. Krishnan, Z. Iqbal and M. M. Maharbiz. "A micro tesla turbine for power generation from low pressure heads and evaporation driven flows" Journal of Power and Energy, pp. 1851-1854, 2011.
- [xii] A. Guha and B. Smiley. "Experiment and analysis for an improved design of the inlet and nozzle in tesla disc turbines". pp. 261-267, 2010.
- [xiii] G. P. Hoya and A. Guha. "The design of test rig and study of performance and efficiency of a tesla disc turbine" Journal of Power and Energy. pp. 451-465, 2009.
- [xiv] R. T. Deam, E. Lemma, B. Mace and R. Collins. "On scaling down turbines to millimeter size" Journal of Engineering for Gas Turbines and Power. 2008.
- [xv] V.P. Carey. "Assessment of tesla turbine performance for small scale Rankine combined heat and Power systems" Journal of Engineering for Gas Turbines and Power, 2010.
- [xvi] Boundary layer theory by Glenn Research Center "National Aeronautics and Space Administration" . Source: <https://www.grc.nasa.gov/www/k-12/airplane/boundlay.html>
- [xvii] A. F. R. Landin. "Numerical simulation of the flow field in a friction type turbine" National University of Colombia, Chapter#3 Source:<https://pdfs.semanticscholar.org/6ec1/911086e24a3405a66d25b5b3d28ff6f01849.pdf>
- [xviii] M. J. Traum. "Tesla Turbine Torque Modeling for Construction of A Dynamometer and Turbine" 2011. https://digital.library.unt.edu/ark:/67531/metadc67979/m2/1/high_res.../the_sis.pdf
- [xix] B. P. H. Yan. "Tesla Turbine for Pico Hydro Applications". Guelph Engineering Journal, pp. 1-8, 2011
- [xx] R. Jose, A. Jose, A. Benny, A. Salusand B. Benny "An Experimental Study on the Various Parameters of Tesla Turbine Using CFD". International Advanced Research Journal in Science, Engineering and Technology, pp. 241-244, 2016.

Impact Of Swept Volume Ratio In Designing A Beta Type Stirling Engine

F. A. Siddiqui¹, I. A. Chaudhry^{2,3}, M. Farhan³, I. Sanaullah⁴, M. Asim^{2,3}, M. F. Hanif¹, T. Ambreen⁵

¹ Department of Mechanical Engineering, Bahauddin Zakariya University, Multan, Pakistan.

² School of Mechanical, Aerospace and Civil Engineering, University of Manchester, United Kingdom.

³ Department of Mechanical Engineering, University of Engineering & Technology, Lahore, Pakistan.

⁴ Department of Transportation Engineering and Management, University of Engineering & Technology, Lahore, Pakistan⁵

Department of Mechanical Engineering, COMSATS Institute of Information Technology, Sahiwal, Pakistan

farrukh.siddiqui@bzu.edu.pk

Abstract—A Stirling engine is an external combustion engine operating on a closed regenerative cycle. The working relies on cyclic expansion and compression. The displacer which is meant for shuttling the hot gases from the displacer space may share a part of volume with the piston known as overlap volume. In this paper, an appropriate model for beta type Stirling engine is developed for optimizing its efficiency based on the swept volume ratio (SVR), i.e., the ratio of swept volume of piston space to that of the displacer space. The analysis of impact of SVR on other parameters like phase angle and overlap volume has also been the part of this research. Based on the achieved results, it is observed that an optimum combination of swept volume of displacer and the piston space ensures the efficient working of the beta type Stirling engine and its efficiency increases with the increase of SVR but its impact lessens gradually as the SVR value increases by unity. The influence of phase angle and overlap volume on swept volume ratio is also investigated. The results are represented graphically. From this study, it is concluded that the required efficiency of the beta Stirling engine can be achieved by suitable combination of the discussed parameters.

Keywords—Beta Stirling Engine, Swept Volume Ratio, Work Done, Overlap Volume, Phase Angle

I. INTRODUCTION

Many attempts [i-ii] have been made on renewable energy resources in order to bring the power generating engines according to the needful specifications of input and output limits. Due to continuous increasing demand of energy and the pollution effects, the researchers are much focussed towards the environment friendly techniques [iii-iv] to decrease the gap between demand and supply of energy. Although a lot of studies have been done on existing thermodynamic models of Stirling engines little focus has been given towards parameters designing for targeting the optimum efficiency. In a recent research, discussed in. al. [v] used third order thermodynamic analysis by Fuzzy decision-making method to analyse the efficiency, output power and the pressure drop of a Stirling engine. "The use of regenerative displacer has been proposed in[vi]for replacing solid displacer and stationary regenerator in beta type Stirling engine" and

expected about 20% more power per cubic centimetre. Similarly, development of a theoretical thermodynamic simulation model has been discussed in [vii] for beta Stirling engine with rhombic drive mechanism for improving its performance through periodic parametric variations. These research based developments indicate demand for directing the research towards the optimal design parameters of the Stirling engine. A Stirling engine is operated on cyclic expansion and compression of working fluid such as air or any other gas. Robert Stirling invented the first hot air engine of such kind in 1816. Due to non-breathing nature, Stirling engines are feasible to use in space and machinery working under sea. The energy sources vary and these engines can be operated by any kind of external heat source including coal, solar or waste heat energy from industries. A specific kind of heat exchanger is mounted inside the Stirling engine which acts as a thermal store; a reason for the use of term 'regenerative' for Stirling engine cycle. Out of three types (alpha, beta and gamma)of Stirling engines, the beta type Stirling engine is unique in a sense that both of the displacer and piston are confined to a same cylinder [viii] and normally, both shares the space i.e., the overlap volume. Recently, promising results have been achieved by various researchers for optimizing the engine's design.

For analysing the working of a Stirling engine, the research is still under progress. A dimensionless quantity (power parameter) has been introduced in [ix] for optimizing the Stirling engine performance. However, much of the research on Stirling engine performance is widely based on the classical Schmidt analysis given by x] in 1871. Out of many parameters effecting the performance of a Stirling engine, the ratio of swept volume of piston space and the displacer space is taken as a standard by many researchers[xi-xv].This research highlights the optimal designing of beta type Stirling engine with a special reference to a suitable combination of swept volumes of displacer and piston space respectively. The beta Stirling engine is shown in Fig. 1. As illustrated, the displacer and the power piston are mounted in the same cylinder. For the hot space,

there is a clearance between the displacer and the cylinder walls as the displacer is meant for shuttling the air between hot and cold space. The heat is supplied to the displacer space (hot cylinder) through external source and the displacer pushes the heated air to the piston space (cold cylinder) during the expansion of the working gas as the displacer moves from top dead centre (TDC) to the bottom dead centre (BDC). The work done at this stage is at the cost of heat supplied by

the external source and hence the displacer moves to BDC. It is to be noted that small force is required to move the displacer because there is no seal with the wall and a result a small pressure drop across the heat exchanger and the regenerator will be observed. Since the internal energy of the system remains unaffected while the entropy of the gas increase for an ideal Stirling cycle. In result of the inertial force, the displacer moves up and then pushes the gas towards the

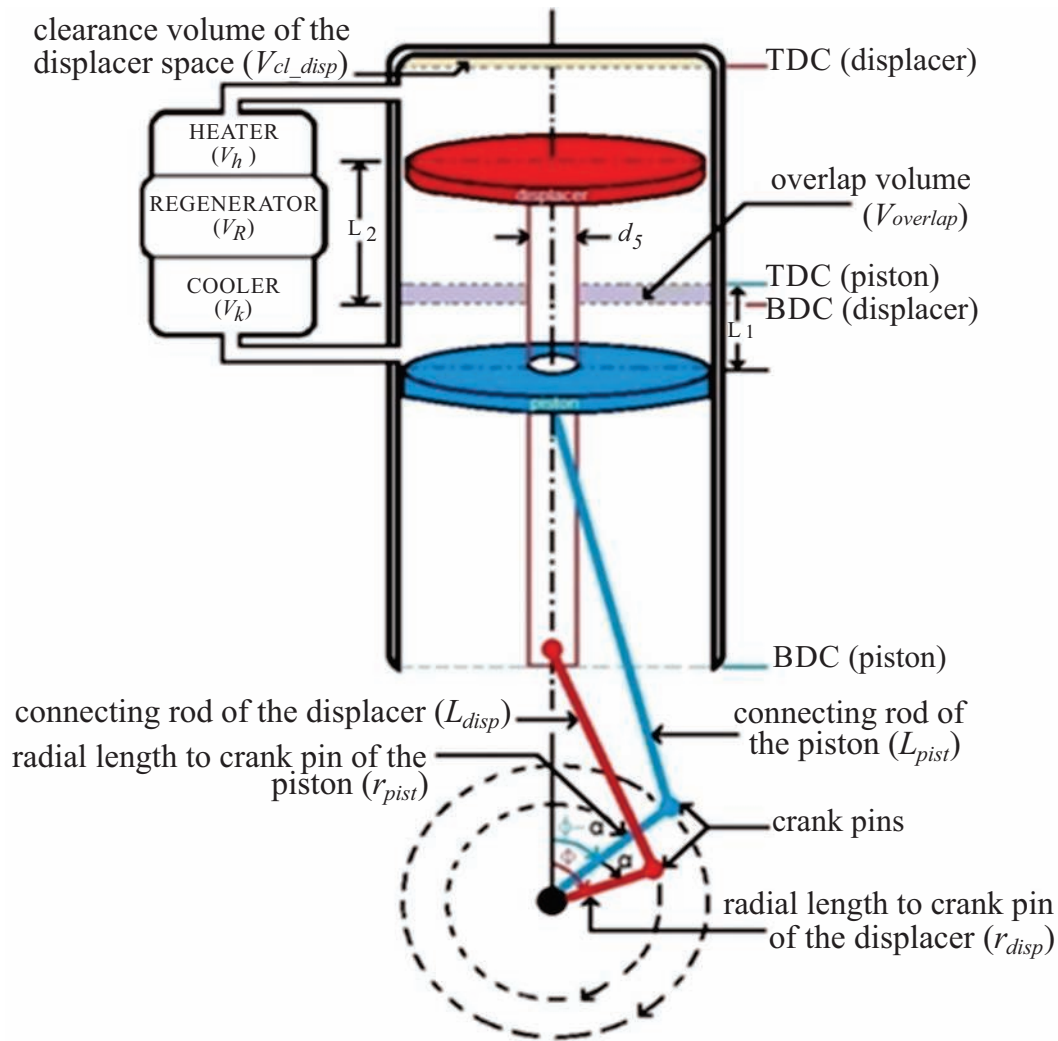


Fig. 1. Schematic volumetric configuration of the beta type Stirling engine

the piston space passing through theregenerator where the heat is abstracted. In cold cylinder, the air is compressed by the piston and the heat is rejected. The work done is equal to the magnitude of rejected heat from the system. There is a decrease in entropy for an

ideal Stirling engine cycle; however, no change in internal energy can be seen. A pseudo model of a Stirling engine along with the temperature profile is depicted in Fig. 2.

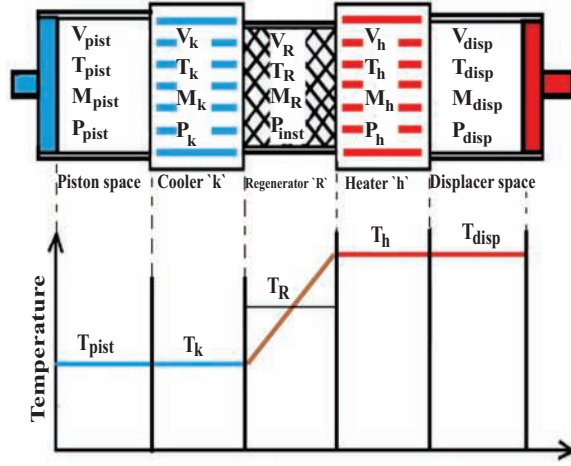


Fig. 2. Pseudo model of a Stirling engine

The work has been done through modelling and simulations by developing a programme on *matlab* software. The results are useful for the further designing of the engine on laboratory as well as on industrial scale.

II. MATHEMATICAL ANALYSIS

A. Calculations for the instantaneous pressure for the working cycle

Based on the model illustrated in Fig. 2, the total mass of the working gas (M_T) for the closed cycle at any instant can be expressed as the sum of the gas components present in all constituent areas.

$$M_T = M_{pist} + M_K + M_R + M_h + M_{disp} \quad (1)$$

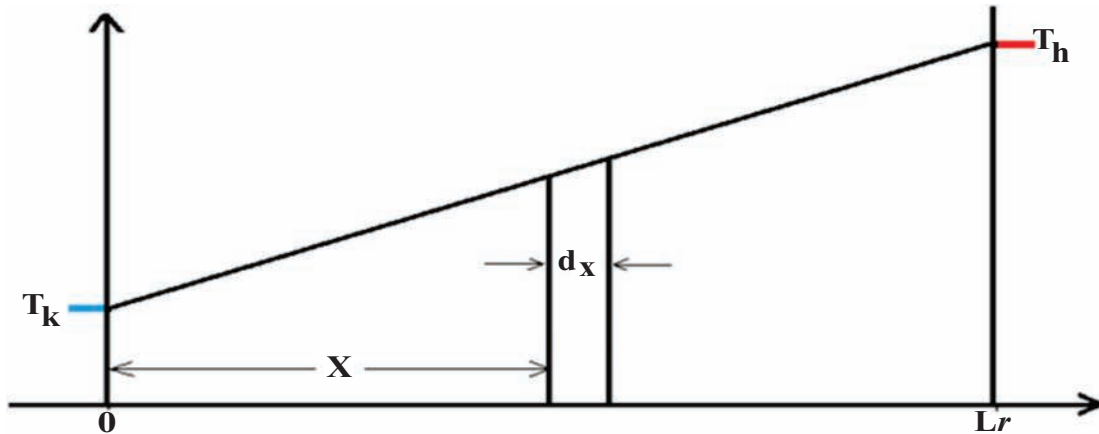


Fig. 3. Linear profile of the regenerator

Through calculations, the temperature profile of the regenerator in Eq. 2 takes the form as given in Eq 3.

$$P_{inst} = \frac{M_T R}{\frac{V_{inst_pist}}{T_K} + \frac{V_K}{T_K} + \frac{V_R \ln(\frac{T_h}{T_k})}{(T_h - T_k)} + \frac{V_h}{T_h} + \frac{V_{inst_disp}}{T_h}} \quad (3)$$

By Universal gas law,

$$M_T = \frac{P_{pist} V_{inst_pist}}{R T_{pist}} + \frac{P_K V_K}{R T_K} + \frac{P_R V_R}{R T_R} + \frac{P_h V_h}{R T_h} + \frac{P_{disp} V_{inst_disp}}{R T_{disp}}$$

Where, T_{pist} , T_K , T_R , T_h and T_{disp} represent the respective instantaneous temperature values in piston space, cooler, regenerator, heater, regenerator and displacer space, respectively while R is the universal gas constant. The instantaneous pressure (P_{inst}) is considered to be similar in all spaces. Therefore,

$$M_T = \frac{P_{inst}}{R} \left(\frac{V_{inst_pist}}{T_{pist}} + \frac{V_K}{T_K} + \frac{V_R}{T_R} + \frac{V_h}{T_h} + \frac{V_{inst_disp}}{T_{disp}} \right)$$

$$P_{inst} = \frac{M_T R}{\frac{V_{inst_pist}}{T_{pist}} + \frac{V_K}{T_K} + \frac{V_R}{T_R} + \frac{V_h}{T_h} + \frac{V_{inst_disp}}{T_{disp}}}$$

The temperature in the displacer and the piston space is similar to that in the heater and cooler, respectively. So, T_{disp} and T_{pist} can be replaced with T_h and T_k like wise.

$$P_{inst} = \frac{M_T R}{\frac{V_{inst_pist}}{T_K} + \frac{V_K}{T_K} + \frac{V_R}{T_R} + \frac{V_h}{T_h} + \frac{V_{inst_disp}}{T_h}} \quad (2)$$

Let ' Lr ' be the regenerator's length and ' x ' be the distance of a particular point from the cooler. The temperature profile of the regenerator can be given in Fig.3:

B. Volumetric analysis

Fig. 2 illustrates the division of the volume of the engine based on its five major components. At any instance, the volume of the working gas present in any of the components of the engine can be analysed. The volume of the displacer space at any instance (V_{inst_disp}) is

given by the Schmidt analysis as (Eq.4),

$$V_{inst_dsp} = (A_{dsp}) \{ (r_{dsp}) (1 - \cos\phi) + L_{dsp} (1 - \sqrt{1 - \left(\frac{r_{dsp}}{L_{dsp}} \sin\phi\right)^2}) \} + V_{Ddsp} + V_{cl dsp} \quad (4)$$

"Where, A_{dsp} and V_{Ddsp} represent the displacer space area and the dead volume of the displacer space, respectively. Dead volume is the total void volume of working fluid (Helium in the present case) enclosed in the overall dead space of the Stirling engine [xvi]." Volumetric configuration in the Fig. 1 is mainly based on the displacer and piston space of the beta type Stirling engine along with other major components. The volume enclosed between the displacer and the piston at any instance is regarded as the instantaneous volume of the piston space (given as V_{inst_pist}). It is to be noted from Fig. 1 that the area of the displacer at the top side is greater than the area at the bottom side. This is due to the displacer rod (with diameter d_s , Fig. 1) attached at the bottom centre of the displacer. Considering A_{dsp_rod} as the area of the displacer rod with radius of ' r_{dsp_rod} ', then the area is given by:

$$A_{dsp_rod} = (r_{dsp_rod})^2$$

The volume enclosed between the piston and its top dead centre (V_{pist_tdc}) at any instant is given as:

$$V_{pist_tdc} = (A_{pist}) \{ (r_{pist}) [1 - \cos(\phi - \alpha)] + L_{pist} [1 - \sqrt{1 - \frac{r_{pist}^2}{L_{pist}^2} \sin^2(\phi - \alpha)}] \}$$

The volume ' V_{pist_tdc} ' is represented as L_1 as the part of stroke length in Fig. 1. Similarly, the volume enclosed between the displacer and its bottom dead centre (V_{disp_bdc}) at any instant is given as:

$$V_{disp_bdc} = (A_{dsp} - A_{dsp_rod}) [(r_{dsp}) (1 + \cos\phi) - L_{dsp} (1 - \sqrt{1 - \frac{r_{dsp}^2}{L_{dsp}^2} \sin^2\phi})]$$

' V_{disp_bdc} ' is indicated as L_2 as part of stroke length in Fig. 1. It is notable that the volume of the piston space (V_{inst_pist}) at any particular moment is determined by calculating the volume between displacer and piston. Keeping clearance and dead volumes in account, the overlap volume ($V_{overlap}$) is subtracted from the sum of following two volume spaces:

- (i) the volume between piston and its top dead centre (TDC). The part of its stroke length is represented as L_1 in Fig.1.
- (ii) the volume between displacer and its bottom dead centre (BDC). The part of its stroke length is represented as L_2 in Fig.1.

Mathematically, it is expressed as:

$$V_{inst_pist} = (A_{pist}) (r_{pist}) \{ [1 - \cos(\phi - \alpha)] + L_{pist} [1 - \sqrt{1 - \frac{r_{pist}^2}{L_{pist}^2} \sin^2(\phi - \alpha)}] \} (A_{dsp} - A_{dsp_rod}) [(r_{dsp}) (1 + \cos\phi) - L_{dsp} (1 - \sqrt{1 - \frac{r_{dsp}^2}{L_{dsp}^2} \sin^2\phi})] - V_{overlap} - V_{cl_pist} - V_{D_pist} \quad (5)$$

In Eq. (5), V_{cl_pist} and V_{D_pist} represent the clearance volume of the piston with reference to displacer motion and the dead volume in the piston space respectively. Considering Fig. 2, the total volume (V) of the engine at any moment is:

$$V = V_{inst_pist} + V_K + V_R + V_h + V_{inst_dsp}$$

Where, V_{inst_pist} , V_K , V_R , V_h and V_{inst_dsp} indicate the instantaneous volume of the piston space, volume of the cooler, regenerator's volume, volume of the heater and the instantaneous volume of the displacer space, respectively.

TABLE I
SPECIFICATIONS OF THE BETA TYPE STIRLING ENGINE

Parameters	Specifications
Volume of the cooler	26.43 cm ³
Volume of the regenerator	7.48 cm ³
Volume of the heater	9.75 cm ³
Volume of min. clearance of piston and displacer	23.09 cm ³
Clearance volume of the displacer space	16.97 cm ³
Dead volume of the displacer space	33.83 cm ³
Output mean pressure	50 bar
Temperature of the hot space	900 K
Temperature of the cold space	300 K
Swept volume ratio	0.5, 1, 2, 3, 4, 5
Swept volume of the piston space	Different combinations
Swept volume of the displacer space	Different combinations
Volume of overlap region	Different combinations
Phase angle	Different combinations

$$\begin{aligned}
V = & (A_{pist}) (r_{pist}) \{ [1 - \cos(\phi - \alpha)] + L_{pist} [1 - \\
& \sqrt{1 - \frac{r_{pist}^2}{L_{pist}^2} \sin^2(\phi - \alpha)}] \} + (A_{disp} - A_{disp_rod}) [(r_{disp}) (1 + \\
& \cos \phi) - L_{disp} (1 - \sqrt{1 - \frac{r_{disp}^2}{L_{disp}^2} \sin^2 \phi})] - V_{overlap} - V_{cl-} \\
& pist + V_{D_pist} + V_{K+} V_h + V_R + (A_{disp}) [(r_{disp}) (1 - \cos \phi) + L_{disp} \\
& (1 - \sqrt{1 - \left(\frac{r_{disp}}{L_{disp}} \sin \phi\right)^2})] + V_{Ddisp} + V_{cldisp}
\end{aligned}$$

The overlap volume shared by the displacer and the piston space is given as:

$$V_{overlap} = \frac{V_{swpt_disp} + V_{swpt_pist}}{2} \frac{\sqrt{(V_{swpt_disp})^2 + (V_{swpt_pist})^2 - 2(V_{swpt_disp})(V_{swpt_pist}) \cos(\alpha)}}{2} \quad (7)$$

C. Calculation of Work done

For calculating work done (W), a programme was set on *matlab software* to observe the impact of any parametrical change. The following expression was used for work done:

$$W = \sum [(V_{i+1} - V_i) * (\frac{P_{i+1} + P_i}{2})] \quad (8)$$

Where, P and V represent the instantaneous values of pressure and volume respectively.

III. RESULTS AND DISCUSSION

Table-I illustrates the specifications of a small beta type Stirling engine. These values are calculated on the basis of optimal application of different parameters in connection with their mutual adjustment. Most of the parameters are limited to be changed or altered consequently.

A *Matlab* programme was designed to analyse the

optimum working conditions. Helium was taken as the standard working gas inside the engine.

A. Swept volume ratio and the Work done

The net work done reflects the efficiency of the engine. The results are analysed through calculating the net work done in a cycle for the instantaneous volume and the pressure. Pressure-Volume (PV) diagrams in Fig. 4 represent the calculated work done at different values of swept volume ratio, i.e., the ratio of swept volume of the piston space to that of the displacer space. The phase angle (ϕ) in each case is taken as 90° to be the optimum value for the other parameters as mentioned in Table 1.

It is notable that the value of calculated work done is being increased as the value of the swept volume ratio is increased. This means that as the swept volume of the piston (cold space) is increased or that of the displacer space (hot space) is decreased, the efficiency of the engine increases. This might have the reason that the hot gas coming from the displacer space through regenerator would have larger space to be cooled down and at larger extent (if not up to 300K). That is the reason that in the modern designed engines, an improvement in adsorption kinetics is obtained by using the finned structure (increased surface area) of heat exchangers^[xvii] which can be seen widely in automobile engines. This improves the cooling capacity of the engine to a larger extent. The Pressure-Volume (P-V) diagram in Fig. 5 indicates the work done at different phase angles ranging from 30 to 150. It reveals that the PV diagram for the phase angle of 90 has the widest area and hence the maximum work will be achieved when the engine would run with the phase angle around 90 (5). With the set program in *matlab software* and generated spread sheets, the value of work done by the beta engine was calculated for phase angle values ranging from 1 to 180° . The results are illustrated graphically in Fig. 4(a)-(f).

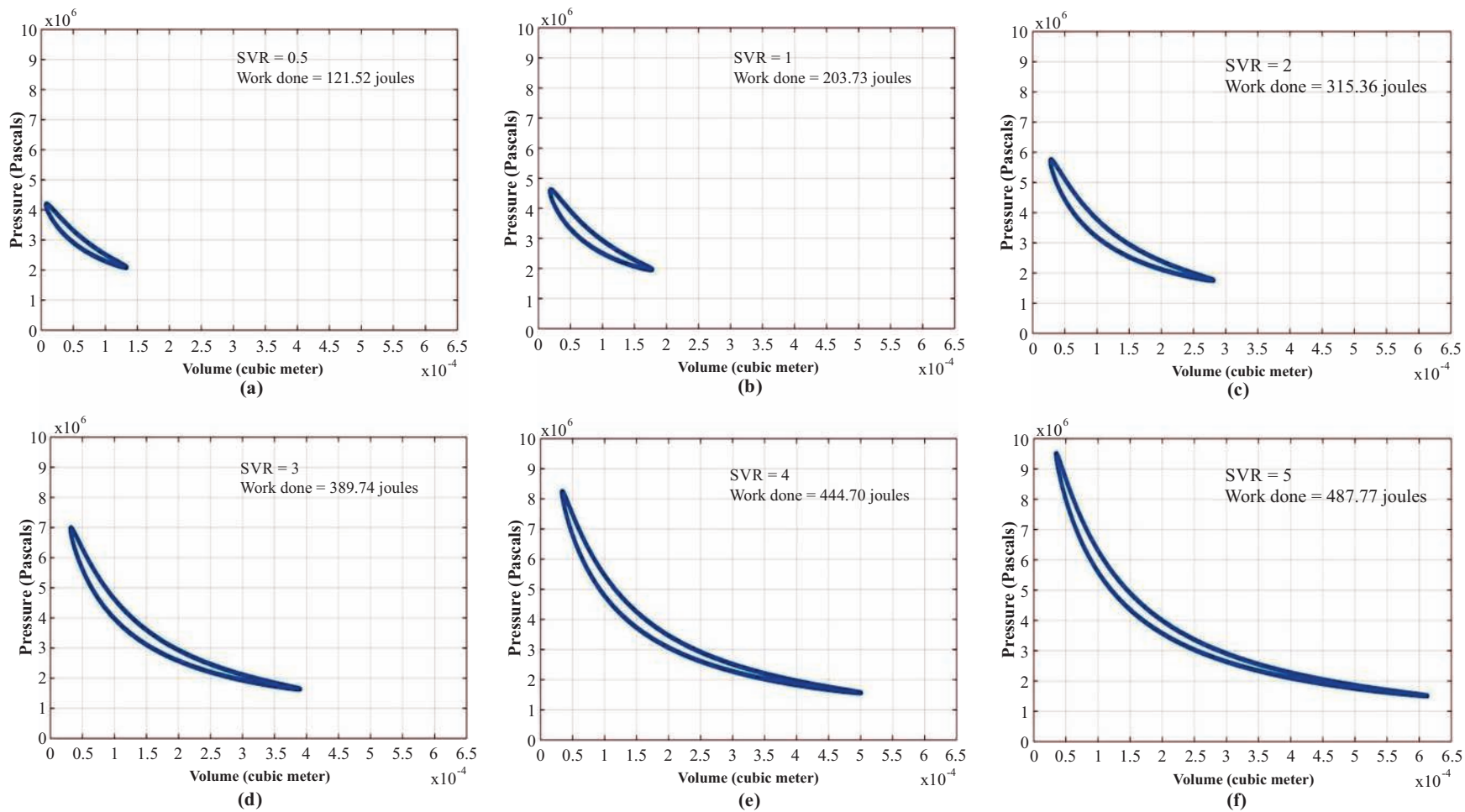


Fig. 4. Pressure–Volume diagrams for the given Beta type Stirling engine at phase angle 90° and swept volume ratio (SVR) of 0.5,1,2,3,4 and 5 respectively

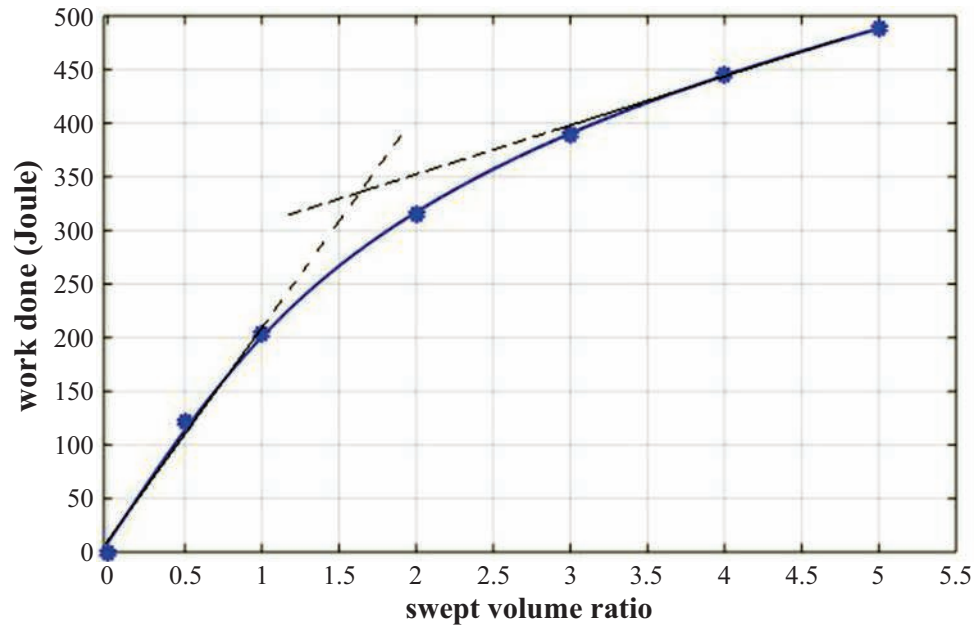


Fig. 5. Work done Vs Swept volume ratio for the beta type Stirling engine for Phase angle 90°

The graphs in Fig. 4 indicate that the efficiency of the engine in the form of work done increases with the increase in swept volume ratio. It is least in Fig. 4 (a) where the swept volume ratio is 0.5 and is found maximum in Fig. 4 (f). Fig. 5 reflects the trend of work done with the swept volume ratio.

It is notable that there is an increasing trend in efficiency in the form of work done with swept volume ratio but the angle of the steep decreases as the SVR crosses beyond unity. This indicates that increasing the SVR by unity may not give as promising results in connection with the efficiency as it remained till SVR value as 1 for the set conditions. Nevertheless, there is impact of many other parameters like phase angle, overlap volume, temperature difference etc., but it is evident that a 'limit' has to be followed for SVR in order to achieve optimum efficiency.

B. Swept volume ratio and the overlap volume

In beta type Stirling engines, the overlap volume is the part of swept volume that is shared by both piston space and the displacer space. Overlap volume can be changed by altering the length of the connecting rod in the slider crank mechanism of either displacer or piston. In order to analyse the impact of overlap volume in connection with the swept volume ratio (SVR), four suitable combinations of overlap volume (7 cm^3 , 14 cm^3 , 28 cm^3 , 35 cm^3) were selected in combination with varying values of SVR. The same impact was also noted for setting the overlap volume as zero. The graph in Fig. 6 depicts the increasing trend of efficiency with increase in SVR at different combinations of overlap volume of the beta type Stirling engine along with indication of change in steep after a specified value of SVR.

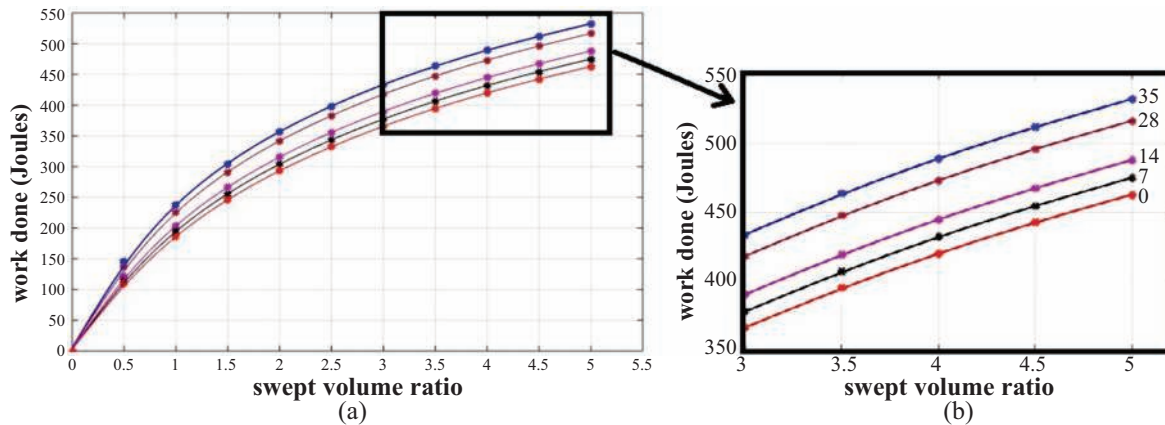


Fig. 6. Work done vs Swept volume ratio for beta Stirling engine at different overlap volumes

In Fig. 6 (a), it is obvious that the efficiency of the engine increases with the increase in swept volume ratio along with the overlap volume. It is indicated more clearly in Fig. 6 (b). The efficiency is at minimum when the engine is set with no overlap volume and attains its maximum value when the overlap volume was set to 35 cm^3 i.e. the highest of the set values. It is further notable that the steep angle for each graph remains almost constant till the value of SVR is 1, after that it decreases gradually. This indicates that increasing the overlap volume for a set value of SVR more than 1 may not promise to follow the same trend of increasing efficiency as it was till unit value of SVR.

This confirms the result obtained previously in 3.1 that optimum value of SVR after which the inclination changes gradually is 1 for the presently set conditions.

C. Swept volume ratio and the phase angle

Phase angle is the angle by which displacer leads the piston for volume variations in beta Stirling engine cycle. Due to its significant role in the efficient working of a beta type Stirling engine, the synergistic effect of phase angle in connection with swept volume ratio are examined. Fig. 7 represents the relationship of SVR with work done at different phase angles.

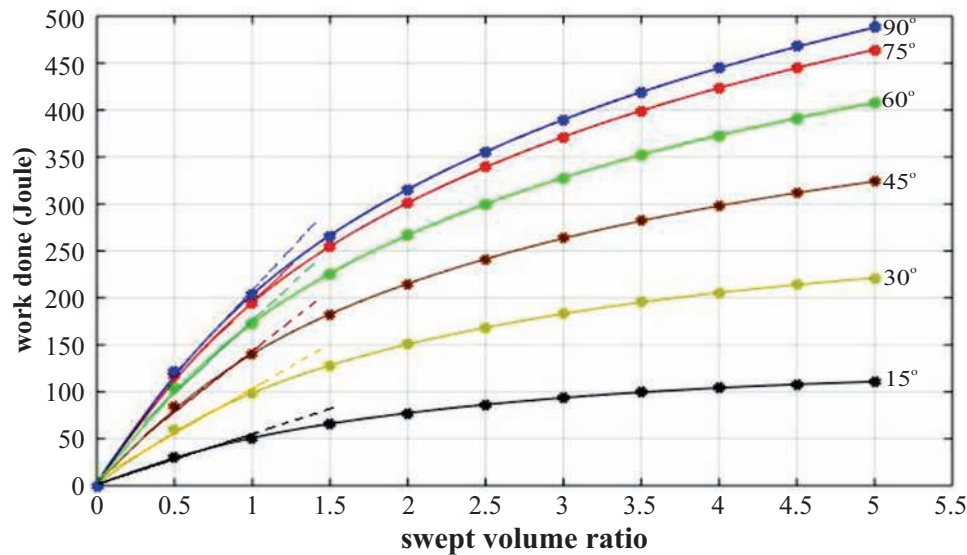


Fig. 7. Work done vs Swept volume ratio for beta Stirling engine at different swept volume ratios

It is evident that the efficiency of the engine increases with the phase angle till 90° after which it decreases gradually in the same manner. However, the steep angle reduces as the swept volume ratio increases; even at lower phase angle, the work done becomes almost independent of higher values of the swept volume ratio i.e. between 4.5 and 5. In Fig. 6, the angle of steep seemed to be unchanged until SVR increases by the value of 1. This again confirms the hypothesis of existence of an optimum value of swept volume ratio in the working of beta type Stirling engine. The optimum phase angle for the beta type Stirling engine detected elsewhere^[9] is around 90° below and above which the efficiency decreases constituting a bell-shaped graph between work done and the phase angle. This also generates a notion that swept volume ratio and the phase angle could ensure the required work done at different combinations compensating each other. Contour plot in Fig. 7 demonstrates this concept for the optimal combination of swept volume ratio and the phase angle for attaining the required efficiency in the form of work done.

From the contour plot in Fig. 8, it is revealed that

the required efficiency (in the form of work done) of the beta type Stirling engine is achievable based on the suitable combination of swept volume ratio and the phase angle; keeping the other parameters in account for their respective role. In the plot, the different coloured patterns represent the set values of work done (in Joules) as according to the numbers mentioned inside the graph. It is notable that the work done becomes almost negligible at the phase angle 0° and 180° . It also confirms that increasing the swept volume ratio, keeping the phase angle constant, increases the work done by the engine. However, at fixed swept volume ratio, the work done increases with the phase angle till its optimal value (i.e. around 90°) and then it decreases in the same way as phase angle increases gradually.

This useful information indicates the synergistic effect of both discussed parameters upon the efficiency of the beta type Stirling engine for designing. It also reveals that one parameter may compensate the other keeping in sight of the other parameters and the other defined limits.

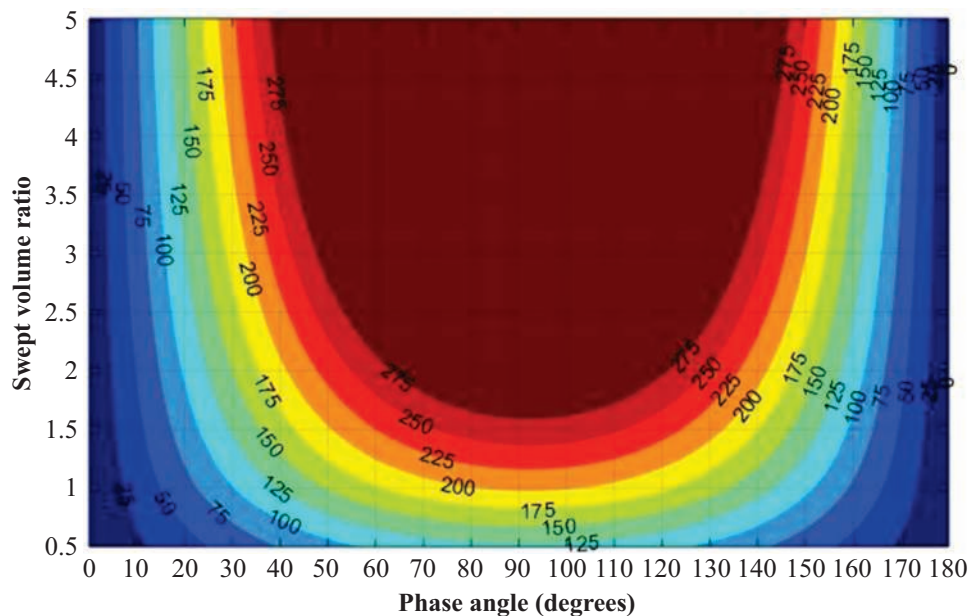


Fig. 8. Work done Vs swept volume ratio of the beta Stirling engine at different phase angles

IV. CONCLUSIONS

- Apart from not being that much popular as internal combustion engine, Stirling engine still appears to grab a promising future due to its simplicity of structure and a high energy to cost ratio. Swept volume relationship between both places of displacer and spacer plays a vital role and a defining parameter for the efficiency of beta type Stirling engine.
- The efficiency of the engine increases with the increase in ratio of swept volume of piston space to that of the displacer space. It was also revealed that this increment remains linear at some particular (optimum) value of swept volume ratio (SVR) and then rate of increment of efficiency with SVR decreases gradually with the further increase in SVR. In present case this optimum value of SVR was found to be unity subject to other parameters in consideration.
- There is a joint impact of swept volume ratio and the overlap volume of piston and displacer space of beta type Stirling engine on its efficiency. Efficiency is found to be increased with the increase in values of both parameters; a limit is always needed to be followed for optimum output though. The targeted efficiency of the beta Stirling engine could be achieved by suitable combination of both parameters as one compensates the other keeping other parameters constant.
- An optimum combination of phase angle with the swept volume ratio promises the effective working of the beta type Stirling engine with maximum output. As indicated by the counter plot in Fig. 8, the required amount of work done is achievable

through suitable combination of both parameters as one parameter compensates the other.

- Targeted efficiency in the beta type Stirling engine is achievable if optimum values of the discussed parameters are selected with a special consideration to the swept volume ratio. This promises the maximum output with less energy consumption.

REFERENCES

- [I] A. Sripakagorn and C.Srikam, "Design and performance of a moderate temperature difference Stirling engine", *Renewable Energy*, 36 (2011) 1728-1733..
- [ii] M. Amjad, F. Fazal, F. Noor, A. Qamar and M. Farooq, "Performance Investigation of a Screw Turbine Operating Under LowHead and Less Flow Rate Requirement", *Technical Journal, UET Taxila, Pakistan*. Volume 20 (SI)No.II(S)-2015.
- [iii] N. Hayat, M. M. A. Bhutta, M. A. M. Qureshi, H. Mughal, A. Rehman and F. A. Siddiqui, "Use ofParabolic Solar collector for Multan: Optimizing Tilt Angle", *Journal of Faculty ofEngineering & Technology, Punjab University* Vol. 21, No.1 (2014).
- [iv] A. R.Tavakolpoura, A.Zomorodiana and A. A.Golneshan, "Simulation, construction and testing of a two-cylinder solar Stirlingengine powered by a flat-plate solar collector withoutregenerator", *Renewable Energy* 33 (2008) 77–87.
- [v] S. Toghayani, A. Kasaeian, S. Hashemabadi and M. Salimi, "Multi-objective optimization of

- GPU3 Stirling engine using third order analysis", *Energy Conversion and Management* 87 (2014) 521–529.
- [vi] E. Eid, "Performance of a beta-configuration heat engine having a regenerative displacer", *Renewable Energy* 34 (2009) 2404 – 2413.
 - [vii] C. Cheng and Y. Yu, "Numerical model for predicting thermodynamic cycle and thermal efficiency of a beta-type Stirling engine with rhombic-drive mechanism", *Renewable Energy* 35 (2010) 2590–2601.
 - [viii] D.J. Shedage, S.B. Kedare and S.L. Bapat, "An analysis of beta type Stirling engine with rhombic drive mechanism", *Renewable energy*, Volume 36, Issue 1, 2011, P: 289–97.
 - [ix] D.W. Kirkley, "Determination of optimum configuration of a Stirling engine", *Journal of Mechanical Engineering Science* 1962 4: 204.
 - [x] G. Walker., *Stirling Engines*, (1980) 17, Oxford University Press.
 - [xi] J.R. Abenavoli, M. Carlini, H. Kormanski, K. Rudzinska and A. Sciaboni, "Nondimensional Schmidt Analysis for Optimal Design of Stirling Engines", *ASME. J. Eng. Gas Turbines Power*. 1996;118(1):8-14. doi:10.1115/1.2816555.
 - [xii] J. R. Senft, "Optimum Stirling engine geometry", *International Journal of Energy Research*, 26 (2002) 1087–1101.
 - [xiii] G.F. Nellis and J.R. Maddocks, "An isothermal model of a hybrid Stirling/reverse-Brayton cryocooler", *Cryogenics* 43 (2003) 31–43.
 - [xiv] S. Zhu and M. Nogawa, "Pulse tube stirling machine with warm gas-driven displacer", *Cryogenics* 50 (2010) 320–330.
 - [xv] C. Cheng and H. Yang, "Optimization of geometrical parameters for Stirling engines based on theoretical analysis", *Applied Energy* 92 (2012) 395–405.
 - [xvi] B. Kongtragool and S. Wongwises, "Thermodynamic analysis of a Stirling engine including dead volumes of hot space, cold space and regenerator", *Renewable Energy* 31 (2006) 345–359.
 - [xvii] A. Hajji and S. Khalloufi, "Improving the performance of adsorption heat exchangers using finned structure", *International Journal of heat and mass Transfer*, 1996; 39(8):1677–86.

Off Shore Wind Turbines: A Solution To Energy Crisis In Pakistan

M. M. A. Bhutta¹, M. A. M. Qureshi², M. A. Ahmad³, S. A. Ahmad⁴, A. A. Bhutti⁵

¹Mechanical Engineering Department, UET, Lahore, Pakistan

²Industrial & Manufacturing Engineering Department, UET, Lahore, Pakistan

³School of Engineering & Technology, ICBS, Lahore, Pakistan

⁴Faculty of Mechanical Engineering, NFC Institute of Engineering and Fertilizer Research, Faisalabad, Pakistan

⁵Petroleum Engineering Department, UET, Lahore, Pakistan

¹bhuttathermo@yahoo.com

Abstract-There is increasing power and energy shortage in Pakistan from last two decades. It is the need of the time to explore new avenues for power production, keeping in view the environmental impact and the concept of sustainability. Utilization of wind energy for production of power become very attractive in current scenario. Massive wind energy potential is available at the coastal areas of Sindh in Pakistan. In this research wind data available from Pakistan Meteorological Department (PMD) is analyzed and it is found that off shore wind turbines having lots of benefits over onshore wind turbines have promising applicability in Karachi coastal areas. Hence with the help of off shore wind turbines the total electricity load of Karachi city i.e. 2500 MW can be handled. For this purpose a practical scheme has also been proposed.

Keywords-Wind Energy, Off Shore Wind Turbine, Feasibility Analysis, Energy Crisis, Power Calculation.

I. INTRODUCTION

During last few decades, Pakistan has been facing serious energy crisis. The major disadvantage of this energy crisis is the slowdown of developing process and it is also affecting overall progress in Pakistan. Therefore, to meet the energy requirements in the country government is planning for renewable energy resources. Pakistan Meteorological Department (PMD) carried out a comprehensive survey to find out the wind Potential along the windy area of the country. The survey report indicates that there is a huge wind potential for collecting wind energy by using the modern technologies, especially in the Sindh coastal areas [i]. In Karachi there is severe power shortage at about 3 to 8 hours per day that causes huge economic losses for the city. Karachi is the greatest industrial city of the country, located at 24.861N and 67.011E along the coastal areas of the Arabian Sea. Karachi is the city of large population of 13 million currently it is facing power shortage problems [ii]. Wind energy is a vast

resource of energy in Pakistan, a huge wind potential is available in Pakistan from which a significant amount of energy can be achieved efficiently [iii]. A survey report presents a huge wind corridor is available in coastal areas of Sindh. For the running of turbine minimum wind velocity required is 3 to 4 m/sec. So luckily in Pakistan at Sindh corridor this wind velocity is 6 to 7.5 m/sec which is perfect to run the turbine. Survey report presented that Pakistan has a huge wind potential for the production of 300,000 MW electricity from wind & solar resource [iv-v]. Pakistan electricity load forecast (MW) from 2007 to 2030 in three categories low, medium and high is given. In 2007 for all three categories demand was 19000 MW. Following Table shows the summary of forecast results.

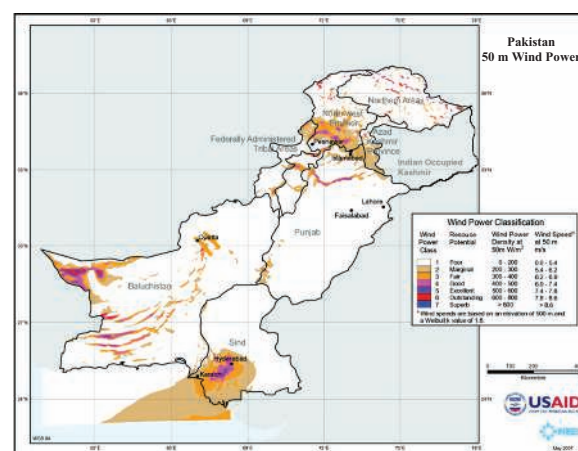


Fig. 1. Wind map of Pakistan

TABLE I
SUMMARY OF FORECAST RESULTS

Description	2007	2010	2015	2020	2025	2030	G.R. (2007-30)
Sale (GWh)							
Low Scenario	83463	112311	176178	261042	370882	500117	8.1%
Medium Scenario	83463	112955	181018	276937	409874	578560	8.8%
High Scenario	92447	113355	185239	295706	470527	735592	9.9%
Generation (GWh)							
Low Scenario	111078	143910	212724	307328	436911	589460	7.5%
Medium Scenario	111078	144711	218448	325740	482080	680330	8.2%
High Scenario	111078	145233	223618	348182	554680	868434	9.4%
Peak Demand (MW)							
Low Scenario	18883	24339	35271	51296	73041	98557	7.4%
Medium Scenario	18883	24474	36217	54359	80566	113695	8.1%
High Scenario	18883	24562	37075	58120	92762	145304	9.3%

Akhlaque AHMED et al. Analyzed data of coastal wind areas for the selected regions, the study was conducted to find out the availability of wind for wind energy generation. Authors studied the distribution of wind with the help of Weibull distribution. They also tested different wind turbines. It was found that, some locations were suitable for wind utilization [vi]. The most comprehensive investigation of the wind potential was undertaken by Pakistan Meteorological Department and it was analyzed that coastal areas of Sindh have larger wind power potential than coastal areas of Baluchistan. The report also indicated that, Sindh coastal areas have comparatively higher wind potentials than other areas of Pakistan [vii]. Due to larger and greater infrastructure cost, connection of small villages to the national grid station is very expensive. Some experts, opinion is that WAPDA (Water and Power Development Authority) has not enough power to provide in these villages. In these villages electricity can be supplied by using wind power, because the wind with greater wind velocity is available round the year in these areas. National Renewable Energy Laboratory (NREL), developed the wind maps that show a greater potential of 346,000 MW in the coastal areas of Pakistan. NREL has discovered the windy coastal areas in the south part of Pakistan. The NREL wind map of Pakistan has given a greater improvement to the wind power generation in the coastal areas with greater power potential. Now this potential area has got much importance for the development of wind energy. In the current study the windy stations like paradise point, French point, Hawks bay, Karachi, Kakapir, Manora beach, Clifton beach and bundle Island were selected. This wind corridor is spread over 60 Km in length.

II. WIND POWER POTENTIAL IN PAKISTAN

To produce electricity through wind power is the rapidly progressing technology. Political, economic and some technical services are developing some procedures and methods to highlight the value of the wind power. In Pakistan there is incredible wind power potential, but unfortunately at present situation the services for power generating through wind potential is not so enough in the country. There is a long coastline area of 1000 km. which is used for the installation of off shore wind turbines like that of Netherlands UK, Japan, Denmark etc. In Pakistan wind power generation started very late, at present no significant power generation projects are in progress. In the same wind power potential and geographical environment as found in Pakistan. India has installed its ten turbines of 55 KW plant at Gujrat in 1986. [8]

In the current study, the project area that is under consideration for wind power potential is 60 Km along the Sindh coastline spread over up to 100 Km deep northward and latitude 25°N approximately.

A. Ongoing Projects in Sindh

Alternative Energy Development Board of federal government has started 9 projects including commissioned and under construction at Jhimpir for total capacity of 484.4 MW, and three projects of 150MW at ghara. All these projects are at different stages. In these projects 84 wind turbines are installed in the villages of Thatta Sindh to supply electricity at 580 homes, besides this in the 49 villages, 3,000 households in the Thatta district. In these 29 projects total Projects Capacity under cost plus regime expected to achieve FC in near future is 50 MW and total projects advanced stage projects capacity is 150 MW and Total Project Capacity below Tariff Stage is 814 MW.

TABLE II
TOTAL COMMISSIONED AND UNDER CONSTRUCTION PROJECTS AT JHIMPIR

Name	M/s FFC Energy Ltd.	M/s Zorlu Enerji Pakistan (Pvt.) Ltd.	M/s Three Gorges Pakistan First Wind Farm (Pvt.) Ltd.	M/s Sapphire Wind Power Company Ltd.	M/s Metro Power Company Ltd.	M/s Yunus Energy Ltd.	M/s Master Wind Energy Pvt. Ltd.	Tapal Wind Energy Pvt. Ltd.	M/s United Energy Pakistan Pvt. Ltd.	Total
Capacity (MW)	49.5	56.4	49.5	50	50	50	50	30	99	484.4

TABLE III
TOTAL COMMISSIONED AND UNDER CONSTRUCTION PROJECTS AT GHARO

Name	M/s Foundation Wind Energy II (Pvt.) Ltd.	M/s Foundation Wind Energy –I Ltd.	M/s Hydro China Dawood Power Pvt. Ltd	Total
Capacity (MW)	50	50	50	150

III. TYPES OF WIND TURBINES

Wind turbines are categorized into two basic types on the basis, on which turbine spins. The turbines which rotate in horizontal axis are mostly used. One of the example is the wind mills, similarly the wind turbine that rotates in vertical axis are the vertical axis turbines. These are not frequently used.

A. Offshore Wind Turbines

Offshore wind turbines are installed inside the sea. Offshore wind is same as that of earthly wind technologies; in the sea the wind potential is stronger and consistent due to this greater wind potential large size wind turbines are to be erected by vessels. The difficulty is to place a structure in a dynamic ocean environment.

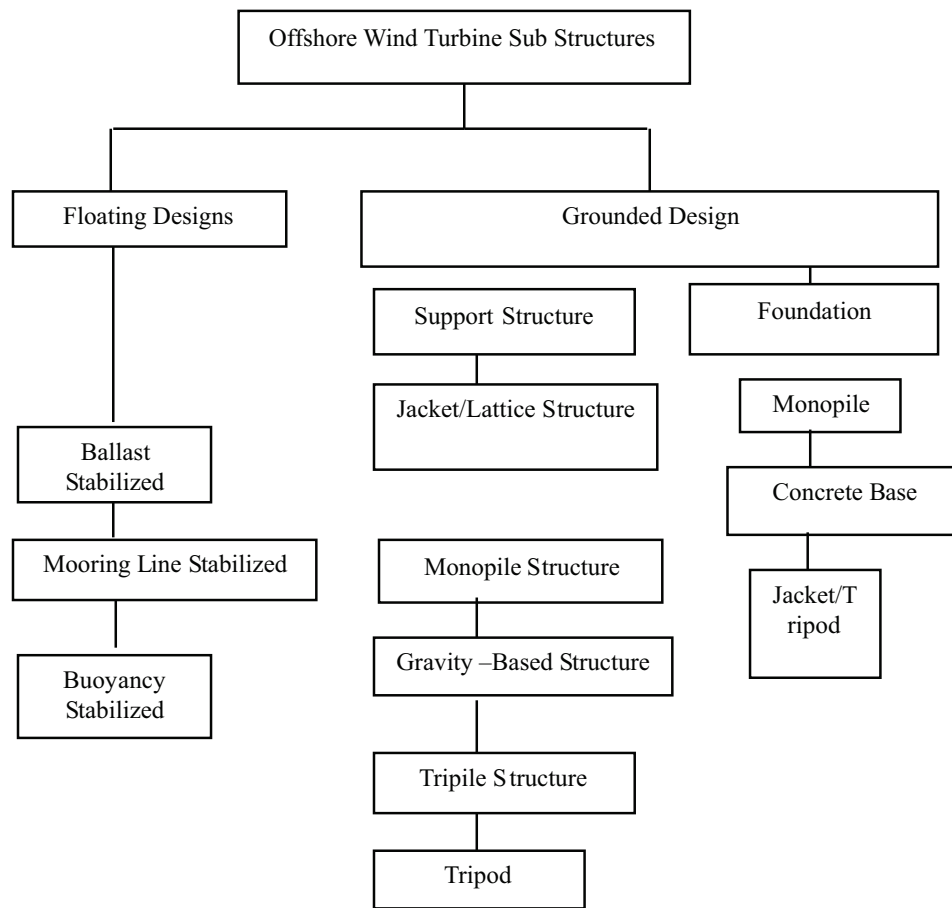


Fig. 2. Types of offshore wind turbines

B. Benefits of offshore wind turbine

Offshore wind turbines have the similar benefits as compared with the onshore wind turbines, wind turbines have not carbon emissions through its whole lifecycle, Fuel is not used in the wind power so it is free of cost as compared to the other electricity generation methods like the conventional power sources. Wind power does not rely on the freshwater [viii]. Offshore winds are stronger and more consistent than onshore winds so it is expected that the turbines can operate at their maximum capacity for a longer period of time[ix]. As the wind power increases, there is possibility to 150% increase in power generation through offshore wind turbines [x]. And the capacity factor of the wind farm also increases from 25 to 40% [xi]. The offshore wind farms are not disturbed with turbine noise as that of onshore wind farm, due to this offshore wind farm can use far larger turbines [xii]. In the sea, using offshore wind power larger turbines are used because there is high and consistent wind velocity that makes the wind turbines more economical and attractive.

C. Comparison of offshore and onshore wind turbines

Offshore wind power projects have one major

advantage over the onshore wind power projects; In the offshore, wind is more powerful and consistent. Some current studies indicated that offshore wind is more powerful so it is very difficult and costly to place infrastructure in the sea. So the installed capacity at sea is very small in comparison with installed capacity on land. Offshore wind energy is renewable and clean, so it reduces the fuels and fossils, due to this it can challenge the air pollution and climate changes. Onshore wind farms have greater negative impact on aesthetics of the landscape compared to offshore wind farms, because the onshore wind farms are mostly visible. The major disadvantage of offshore wind energy farm is a huge construction cost. Offshore wind energy farms are constructed powerfully to bear the rough weather conditions, the cost for installing an offshore wind turbine was \$5 million for 1 MW in 2010, while installing an onshore wind the installing cost is between \$2-2.5 million per megawatt.

D. Global Scenario of offshore wind turbine

From the last decade wind energy has become clean and environment friendly source of energy. This is getting importance worldwide for the availability of basic source and inexpensive technology to convert

the wind into useful energy [xiii]. In Sweden in 1990 first offshore wind turbine was installed. It was a single 220 kW power and 250 m away from the coast at 7 m water Depth and was supported on Tripod. Similarly First Offshore Wind Farm was installed in Denmark 1991. Plant contained 11 turbines of 450 kW power and 1.5 – 3 km from coast at 2-6 m Water Depth and was supported Gravity Foundation. In Japan First offshore wind farm of 16 MW was installed in 2004 and it is expected to upgrade at the power of 1 GW by 2020 [xiv]. Recently in Europe 14 forms of 3.3 GW are under construction, and 7 projects of 1.2 GW are under planning phase. Following figure indicates that in European countries 4995MW, China 509.5 MW and in Japan 33.8 MW power is generated through offshore wind plants. Having the world's 6th largest sea space, According to the Japan Wind Power Association statement, a huge offshore wind power potential is about 600 GW, from which 15% is achieved by the foundation of fixed bottom turbines while the remaining is achieved by using the floating foundation technology [xv]. Most of Japan's potential wind power capacity is located offshore, the most common regions where the floating foundation technology is used are Kyushu Tokyo, and Chubu, while in Tokyo fixed bottom foundation turbines are used.

Global offshore wind energy production

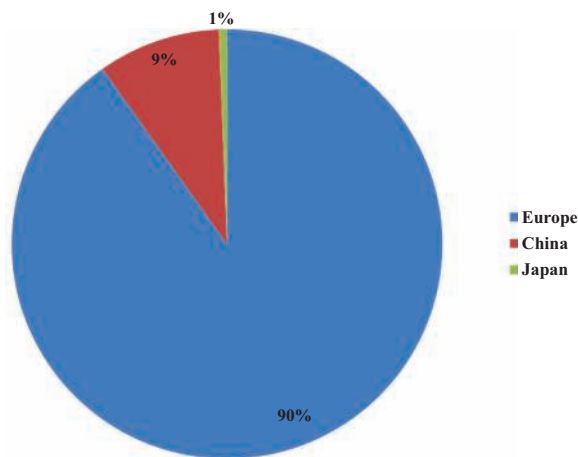


Fig. 3. Global offshore wind energy production

IV. METHODOLOGY; ANALYSIS & DISCUSSIONS

A. Average Wind Speed at Karachi

By using the Log Law and Power Law wind speed at different height is calculated by the following relations.

$$\frac{u}{u_r} = \frac{\ln\left(\frac{Z}{Z_o}\right)}{\ln\left(\frac{Z_R}{Z_o}\right)}$$

Where

U_R is the wind speed at reference height Z_R

Mostly engineers uses Power Law to determine the increase in wind velocity with the available height,

$$U/U_R = (Z - D/Z_R)^\alpha$$

Where:

α is the exponent for power law

$$\alpha = \frac{\ln\left(\frac{Z}{Z_o}\right)}{\ln\left(\frac{Z_R}{Z_o}\right) / \ln(Z/Z_R)}$$

At 50 meters height the wind velocity is computed, and monthly average at 50 meters height, is presented in graph.

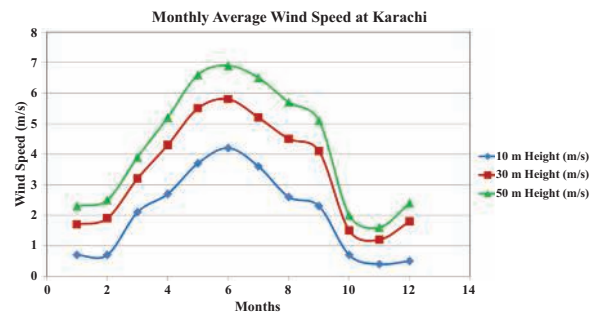


Fig. 4. Monthly average wind speed at Karachi

Table shows monthly average wind speed at different heights of 10, 30 and 50 meters. After computing the results At the height of 10 meters, the average wind speed less than 5 m/s was achieved, The maximum average wind speed recorded in June that was observed 4.2 m/s. At the height of 30 meters. The average wind speed was achieved during May to July that was 5 m/s, while 5.8 m/s was recorded as the maximum average wind speed for the month of June. At the height of 50 meters, a very consistent and high average wind speed was recorded that was ≥ 5.0 m/s during the whole period of 6 months from April to September, The maximum average wind velocity that was recorded is 6.9 m/s in June.

B. Diurnal Wind Speed Variation

Figure shows the annual diurnal wind speed variations at the Karachi sea shore. Wind speed was calculated at different heights of 10, 30 and 50 meters. At 30 meters height the average wind speed varies from wind varies 2.6 m/s to 4.7 m/s and at the height of 50 meters it was recorded from 3.4 m/s to 5.7 m/s.

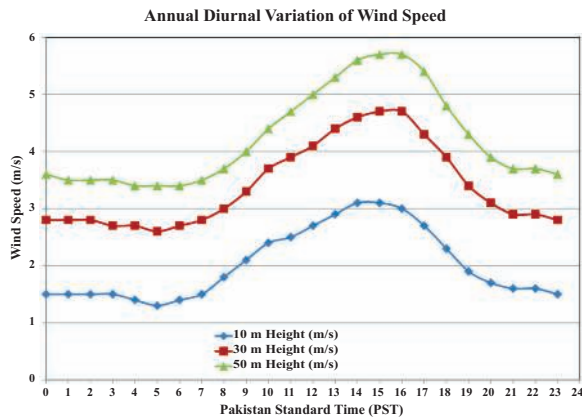


Fig. 5. Monthly Diurnal Variation of wind speed

V. IDEAL WIND POWER CALCULATION

A huge piece of land is required for wind farm at the coastal areas near Karachi. Two projects of 50 MW and 3000 MW required 1283 and 26000 acres respectively, In the current study 50 MW offshore wind farm total 33 turbines of 1.5 MW each is suggested. Theoretically wind power is calculated by the following general equation

$$P_{avail} = C_p \cdot \frac{1}{2} \cdot \rho \cdot A \cdot V^3 \quad (1)$$

Where

C_p = Power coefficient ρ = Density of the oncoming air

A = Swept area of the rotor V = Velocity of the wind

The swept area of the turbine is calculated from the blade length using the area of a circle equation:

$$A = \pi r^2 \quad (2)$$

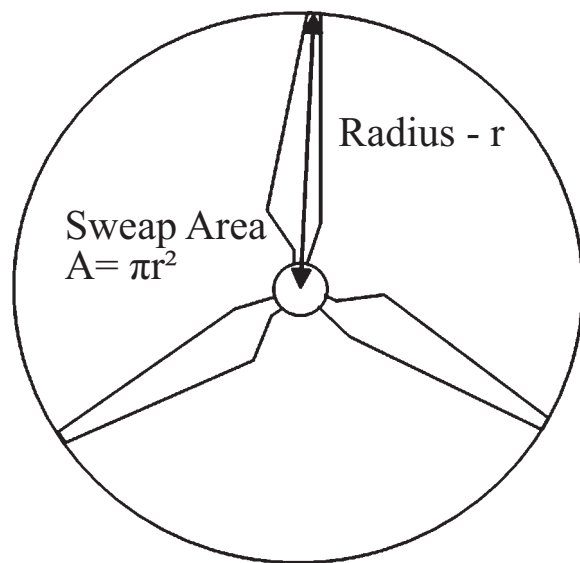


Fig. 6. Blades of Turbines

Tower height= 80 m

Blade Length=38 m

Average wind speed= 6.9 m/s

Power= 1.5 MW

A. Wind Farm Design

When designing the wind farm it is important to combine the wind data with topographical information to design the wind farm. This data may be used for wind flow, sound levels and turbine performance to elevate the location of wind turbines. Access to roads, local electrical network and turbine foundations is also designed

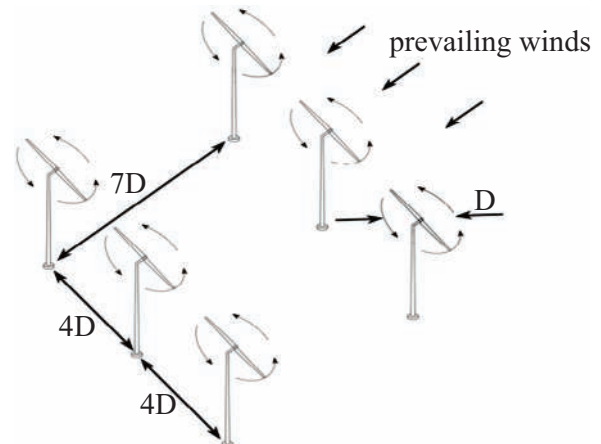


Fig 7: Wind farm Design

B. Foundation Design

Selection of the Foundation for the overall development of offshore wind turbines, the concept plays an important role as a major financial consequences attached to their decisions. Typically, Foundation expenses general expenses 25-34%. Wind turbine foundations are of two types that can be classified as: fixed (or that the seabed is grounded) and floating. Although the system is grounded Foundation supports most of the currently installed or operating turbines, offshore wind turbines (OWTs), due to the shape and form of dynamically sensitive structures because they are slim in the vicinity of the frequency of excitation frequencies by the environmental and mechanical load. The location, the status of the environmental impacts of soil and wind velocity second the monopile design was very suitable for the location of the foundations on the Karachi

1) Loads acting on the foundations

Different types of the loads act on the wind turbine tower, these loads are ultimately converted to the foundation of the tower and this can be of two types: static or dead load and the dynamic loads (a) The load that act at the hub level is the lateral load (b) In near

foundation of the tower load crushed against the substructure of the tower of foundation.. (c) Vibration is generated in the tower due to wind velocity, this

vibration act as a load at the hub level. Because of unbalancing of the rotor, mass and aerodynamics.

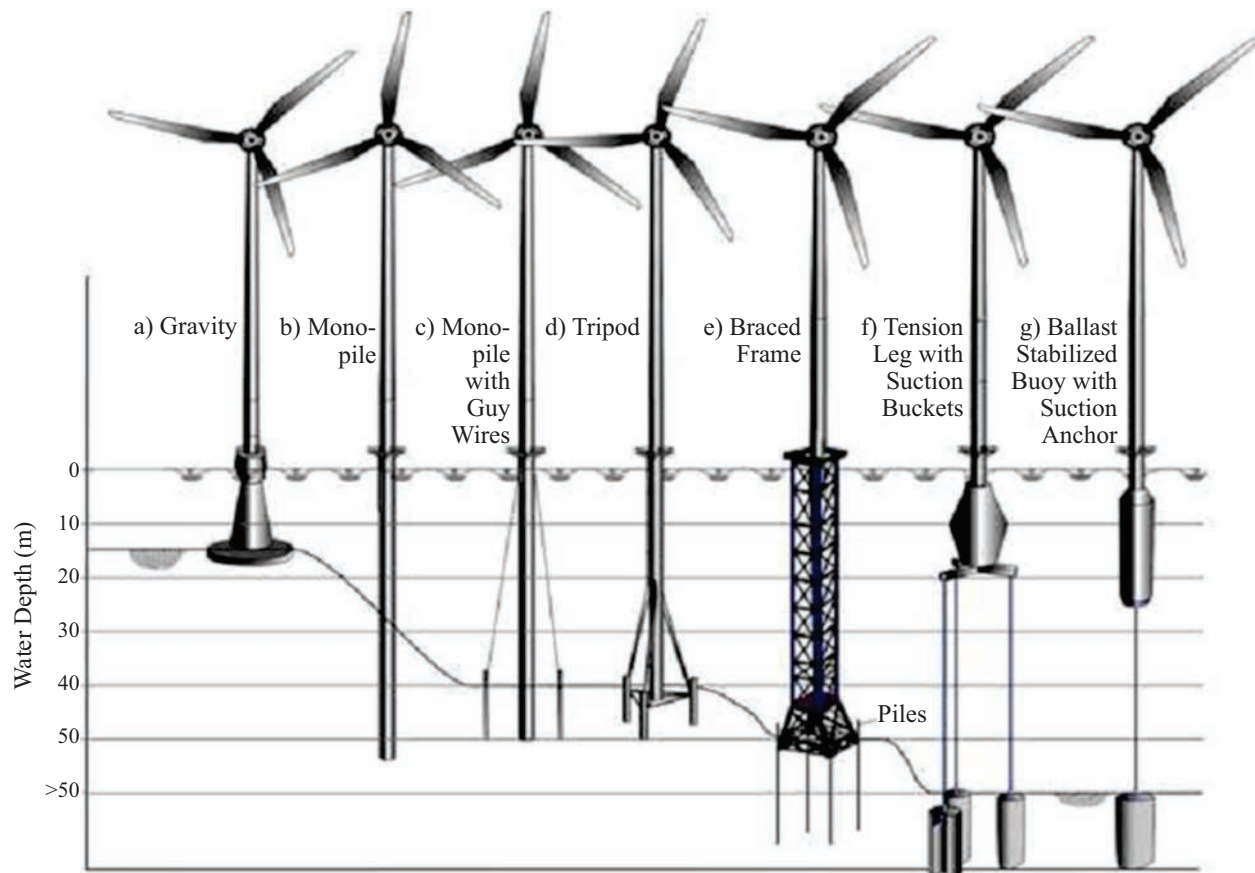


Fig. 8. Various types of support structures and their applicable water depth

VI. RECOMMENDATIONS

Some recommendations are concluded that, enough space is provided by the ports to accommodate installation of the turbines. For the installation of turbines Self-installing systems must be developed to minimize the installation costs. Practical knowledge and Training courses should be developed, a strong collaboration between the different companies should be developed for the new projects. Since the wind turbines are designed on the basis of size and the foundation structure [xii]. There is a need to develop such a control system where all these basic needs are to be met. New SOPs techniques and tools should be developed for the promotion of the wind farms. More tests/surveys are to be conducted to locate the proper sites (small and large scales) near the coastal areas.

VII. CONCLUSIONS

There is shortage of power in Pakistan, so government is adopting different methods to fulfill the

requirements. To get the electricity through wind energy by using offshore wind turbine is one of them. In the current research the wind corridor near Karachi that is in length of 60 Km where wind speed was calculated. From the results it is concluded that there is a huge power potential in this wind corridor where average wind velocity is 7 m/s. On behalf of this data, a proposed wind power is also calculated. It is also concluded that off shore wind turbine farm is suggested near Karachi to meet the power requirements.

REFERENCES

- [i] Dr. Q. Z. Chaudhry & H. Mir, M. Afzaal (Technical Report No. PMD-11/2004) Pakistan Metrological Department.
- [ii] S. M. Hassan Ali, M. Jibran S. Zuberi, "A study to incorporate renewable energy technologies into the power portfolio of Karachi, Pakistan" Renewable and Sustainable Energy Reviews 47 (2015) 14-22.
- [iii] M. S. Malkani., "A Review of Coal and water resources of Pakistan", Pakistan (Quetta), Sci.,

- Tech. and Dev., 31:202-218, (2012).
- [iv] T. Muneer, M. Asif., “Prospectus for Secure and sustainable electricity Supply for Pakistan”, Renewable and sustainable energy reviews 11(2007)654-671.
- [v] M. A. Ahmed, F. Ahmed and M. W. Akhtar., “Wind Characteristics And Wind Power Potential For Southern Coasts Of Sindh, Pakistan”, ISSN: 1814-8085, Vol. 6, No 2, 163-168, (2010).
- [vi] M. A. Ahmad, F. Ahmad and M. W. Akhtar “Assessment of Wind Power Potential for Coastal Areas of Pakistan” Turk J Phys 30 (2006), 127-135 TUBITAK.
- [vii] Pakistan Meteorological Department report (2009).
- [viii] Nayyer A. Z., Professor & Director “Prospects of renewable energy resources in Pakistan. Proceedings of COMSATS Conference 2004 on Renewable Energy Technologies & Sustainable Development, 2005.
- [ix] IEA. Offshore wind experiences. Paris; 2006.
- [x] Vattenfall. Horns rev offshore wind farm; 2007.
- [xi] M. Junginger, A. Faaij. W. C. Turkenburg “Cost reduction prospects for offshore wind farms”. Wind Engineering 2004; 28(1):97–118.
- [xii] W. Musial, S. Butterfield. “Future for offshore wind energy in the United States:” preprint. In: Energy Ocean 2004. Palm Beach FL; 2004.
- [xiii] W. E. Alnaser and A. Al. Karaglisuli, Renewable Energy, 21, (2000), 247.
- [xiv] European Wind Energy Association (EWEA) Report 2013.
- [xv] Japan Wind Power Association, 2012) (Sasebo Heavy Industries, 2013) reports.

Load Dispatch Management Using Trend Analysis of Demand and Generation in Pakistan

A. Ali¹, M. A. Chaudhary², S. Khushnood³, M. Hussain⁴

^{1,3}Faculty of Mechanical & Aeronautical Engineering, University of Engineering and Technology, Taxila

²Namal College, Mianwali

⁴Faculty of Management Sciences, Capital University of Science & Technology, Islamabad.

¹enr_akram@hotmail.com

Abstract-Load management has been an enigma despite the adequate level of production of electricity. This research focuses on the short-term evaluation of the maximum output of various electricity generation facilities to meet the required system load at minimum possible cost without disrupting the regular power supply to the end users and aimed to give overview of the economic load dispatch problem regarding abrupt variations in monthly load demand and generation throughout the year. The research analysis was conducted by using daily data regarding the generation, load demand across the country and power system constraints of generation and transmission. The aspect of reduction in share of Hydel generation during canals closure at water scarcity season every year has also been taken into account. By analyzing both the actual and predicted values at load dispatch center, it provides monthly trend of generation, consumer demand and load shed at the same time. Daily and monthly data figures of the last 06 years in MW/GWh is analyzed and executed. Values have been plotted in graphs to understand the monthly/annual variations in total generation and total demand. Research is aimed to improving the quality of power dispatch and deriving workable solutions.

Keywords-Load Dispatch Management (LDM), Economic Dispatch(ED), Demand Side Management (DSM), Unit Commitment (UC), Mega Watts(MW), Giga Watt Hours (GWh).

I. INTRODUCTION

Pakistan is one of the countries that is seriously facing energy crisis due to increase in energy demand as of globally. Though there are many factors but the most common include increase in population size, luxurious standards of living, and reduction in availability of energy resources in developing countries [i]. Some future assumptions concluded from researches, show that by year 2040 the overall population of world may increase from 7 billion to 9 billion due to which energy demand can be increased

up to 35% than current requirement [ii-iii]. There are many causative factors for Residential energy usage like increasing population, increasing urbanization and upgraded living standards [iv-vii]. The installed electricity generation capacity of Pakistan was 22,797 MW in 2013 whereas the average demand was 17,000 MW and hence, the shortfall was between 4,000 and 5,000 MW. The percentage share of sources of generation was as about Oil (35.2 per cent), Hydel (29.9 per cent), Gas (29 per cent) Nuclear, solar and imported (6 per cent). As per our analysis, the electricity demand during peak hours will rise by 4 to 5 percent in the next 10 years, roughly 1,500 MW. This depressing forecast is the product of a lopsided energy mix, fading indigenous fuel reserves, expanding circular debt and transmission hold-ups. At the current stage, economic growth depends on the availability and affordability of sustained energy supplies and vice versa [viii]. In Pakistan, the energy demand is also increasing exponentially due to a rapidly growing population and the number of households. Pakistan stands at six amongst the most populous countries in the world, having a population over 180 million in 2013, and the future estimates show over 350 million citizens in 2035 [ix]. The gas reserves in Pakistan are close to exhaustion. The price hike in imported oil affect the budget considerably and therefore, it is not practically possible to ensure its constant supply. Hydel power seems to be the only probably solution to meet the upcoming energy challenges but the inherent and obvious political and environmental issues make building dams a farfetched opportunity. In the current scenario, perhaps, reducing excessive reliance upon oil and adopting environment friendly and low-cost alternatives are the best options. Presently in Pakistan there are severe energy crises having devastating effects on economic growth [x]. This results in increasing unemployment and mental stress. Activities related to public or community welfare services have also met a decline.

Maintaining a sound balance between demand and generation is certainly an integral operational function in the modern day energy management system. The reason behind use of the LD is to identify the maximum

generation within the existing operating units and identification of ways through which the total generation cost gets minimized without affecting the power balance equation and eradicating the other constraints affecting power supply in the system. During analysis of the existing literature on the ED issue and probable solutions it is realized that the traditional techniques and strategies to counter the issues prove to be excessively complicated while dealing with complex dispatch problems. Also evident was the fact that the lack of robustness and efficiency was prevalent in numerous practical applications. An Efficient and optimum electric load dispatch in centralized power supply systems has always held an important position in the electric power industry. Over the past few decades, it has become highly important to ensure that the power systems function face minimum interruptions and consistent power supply is maintained to satisfy consumers throughout the year. Keeping the generation system updated and in optimal condition are also important concerns. Considering the small number of efficient generating units in terms of production costs and increasing power supply demand, fuel cost and supply limitation, it is important that the committed units generate the expected load. Also, it is vital that the expected load generation remains undeterred by fluctuations in fuel cost and varying load demand at various time intervals [xi-xiv].

The primary objective of LD of electric power generation is to program the committed generating unit outputs in order to meet the load demand while utilizing minimal operating cost as well as satisfying all equality and inequality constraints in units and system. The LD issue has been addressed by different researchers already and the issue is an extensive one involving different problems. Some of the main problems include the Unit Commitment or Pre-Dispatch issue, which involves selection of most efficient generating sources to meet the expected load demand and ensure a specified margin of operating reserve within specific time duration. Another problem is the on-line committed dispatch of load, which involves extended distribution to the end users. In centralized LD, the electricity supply is not fixed because it is received via different generation units. However, the units are allowed to take values again with specific limits to fulfill a certain load demand with minimal fuel consumption [xv-xvi].

Load Management is basically the process of balancing electrical load with the electricity supply on the network by adjusting or controlling the load instead of controlling the power station output, which is also referred to as demand side management (DSM). This is achieved by real-time direct interference of the utility using frequency sensitive relays triggering the circuit breakers (ripple control) via time clocks or alternately, by utilizing especial tariffs to modify consumer behavior. Through Load Management, utilities can

minimize electricity demand during peak hours and this resultantly, reduces costs by eradicating the need for tweaking power plants. Additionally, power plant optimization is a time-consuming process as the requirement of bringing them on-line and addressing of challenges in case a plant goes off-line unexpectedly. Load management also helps in reducing harmful emissions because peaking plants or backup generators are less efficient, less environment-friendly and unreliable options than base load power plants. Latest load-management technologies are being developed and modified continually by both private and public sectors.

Real-time dispatch can be computed in two stages. The first stage involves solving of a unit commitment (UC) problem for selecting generating units in order to meet the required per hour load demand [xvii-xviii]. The second stage involves solving of an ELD problem for computing the power outputs of the committed units for meeting the required load. This decision is usually taken minutes to hours before the implementation time. Current studies on UC have focused on planning purposes to accommodate load and generation forecasting challenges.

National load dispatch center is the department responsible for controlling and monitoring of the country's power supply mechanism. The primary tasks include the Dispatching power from available sources of generation and Consistent processing of the power transmission network. This center is based at Islamabad and is required to conduct generation, dispatch and operation of 500/220 kV primary transmission network. On the other hand, is responsible for maintaining the quality of power in terms of frequency and voltages.

Dispatching of electricity is indeed a dynamic task and control center is responsible for performing this daunting task along with addressing the technical, seasonal, financial and social aspects that affect power dispatch. The department controls electricity generation through hydro-thermal coordination considering the water releases from the dams as sanctioned by IRSA. It could be affected by anything, a public holiday, a Pak-India cricket match, abrupt and uncalled for weather changes or sudden changes in power demand during the month of Ramadan. Load dispatch management center faces a new challenge every day in maintaining consistent power supply and meeting regular demand. Apart from this, the center is responsible for conducting studies on power system to evaluate load flow and contingency analysis, load forecasting and short to medium term operational planning. It also has to examine, analyze and schedule the maintenance shutdowns of generation units and transmission equipment as well as ensuring system's stability and security for uninterrupted load management.



Fig. 1. Power System Structure of Dispatch Center

The two fundamental components of load dispatch are described below:

A. Planning for Tomorrow's Dispatch

- Proper scheduling of generation units for every hour of the next day's dispatch according to the forecast load.
- Selection of most appropriate available generating units for operation to dispatch load for the next day (operating day).
- Recognizing capacity of each generating unit.
- Ramping rate (The response time of any generator in case it is put in operation)
- Recognizing maximum and minimum generation levels of each Generating unit.
- Recognizing value of minimum time limit the generating unit must stay off when once turned off.

2. Dispatching for the Power System Today

- By using Automatic Generation Control (AGC) for the purpose to change generation dispatch as needed, monitor and maintain system frequency at 60 Hz
- Monitor each hour dispatch plans for ensuring balanced dispatch in every hour
- Observing transmission system flows
- Ensuring that transmission flows remain in reliable limits
- Ensuring that voltage levels are within reliability ranges
- Controlling new power flow timetables
- Restraining current power flow timetables
- Altering the dispatch
- Shedding Load.

In electrical power sector, the Load Dispatch mechanism is a critically important job because it involves ensuring balanced and uninterrupted power supply to the end users within minimal cost. Since the

efficiency of the new generating units is higher than the older ones, therefore, the economic dispatch has to be resolved efficiently and tactfully to reduce the power generation cost. Load dispatch problems are here analyzed in last 06 years data of generation, demand and load shed. Maximum computed demands in a month and corresponding capabilities of Private Power Plants, Thermal and Hydel sources are analyzed, which results in a good idea of load management with respect to generating capability of plants connected to WAPDA system and consumer demand throughout the year. Conclusions are arrived which finally leads to an outline of the future directions for research and development efforts in this particular area.

II. METHODOLOGY

However, in Pakistan, the higher order cost functions for (a) improved curve fitting for running cost, (b) lower estimation, (c) much practical, precise and reliable results, regression analysis for last 06 years is done for load dispatch center. In this paper numerical data from NTDC and WAPDA Power Plants (64), Generating Units (496), 500 kV Stations (17), 220 kV Stations (35), 132 / 66 / 33 kV Station (900), 500 kV Transmission Lines (5183) KM, 220 kV Transmission Lines (9104) KM, 132 / 66 / 33 kV Transmission lines, (28,892) KM is used. We analyzed and compare the period of mismatch between demand and generation throughout the year, uncertainty of availability of electricity generated by Hydel, thermal and nuclear from both generation and demand perspective over a variety of times scales. How load dispatch management mainly keeps balance between total generation and total power demand, the difference is named as load shedding or load management. So six years data is analyzed on daily and monthly basis for better regression analysis. The general form of the estimated regression equation for modeling the linear trend in the energy generation is $Y_t = b_0 + b_1Y$ also satisfied. Where, Y_t is forecast of energy generation in period t and Y is the number of year i.e. 1 for 2009, 2 for 2010 and so on. Also multiple regression equation for modeling both the month wise seasonal effects and the linear trend in the energy generation time series is discussed in equation, $Y_t = b_0 + b_1M_1 + b_2M_2 + \dots + b_{12}M_{12} + b_{13}t$. Where Y_t is forecast of energy generation in period t and $M_1 \dots M_{12}$ are the number of months i.e. 1 for January and 12 for December is taken, if period t correspond to January then 1 otherwise 0 and so on for each month. Time period t i.e. considering time in fiscal years July 2009 is 1 and June 2015 is taken as 72. In results the equations clearly shows the difference between actual and predicted values of demand, generation and load shed by the load dispatch center.

III. DATA TREND ANALYSIS AND DISCUSSIONS

All the data daily, monthly and annual is taken and analyzed, the results taken are as under:

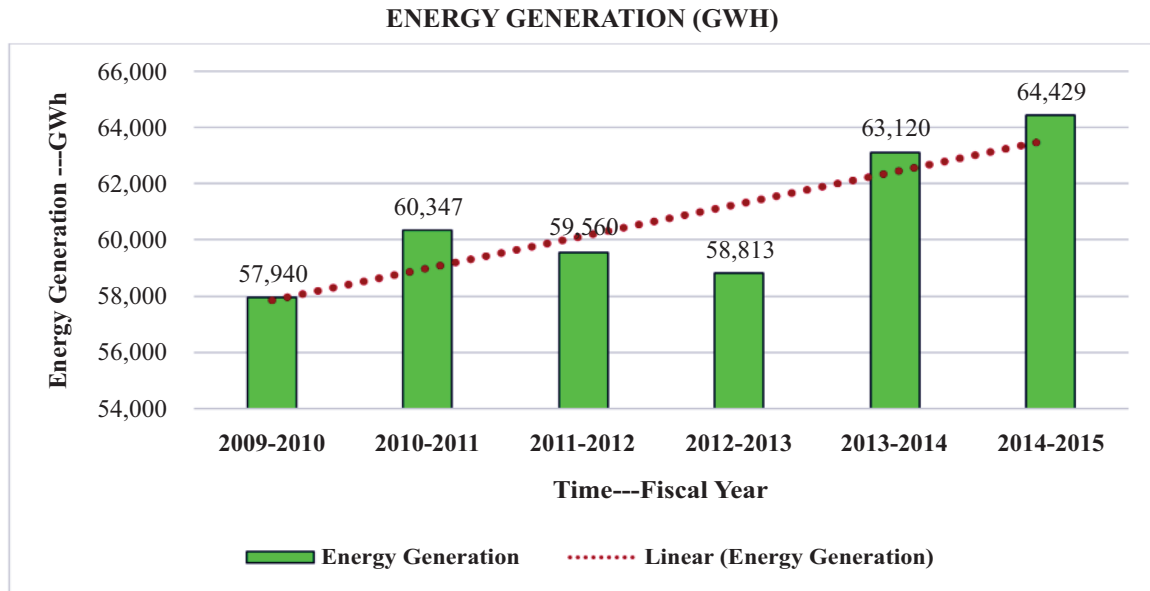


Fig. 2. Actual annual Growth in Net Energy Generation

The general form of the estimated regression equation for modeling the linear trend in the energy generation is as follows:

$$Y_t = b_0 + b_1 Y$$

Where

Y_t is forecast of energy generation in period t and Y is year number i.e. 1 for 2009, 2 for 2010 and so on.

In Fig.2, the mean of above data is 60,701 GWh

having range of 6,489 GWh from 57,939 GWh to 64,428 GWh. The data covers six years from July 2009 to June 2015. Standard deviation of the data is 2,544 GWh and data is slightly skewed positively to right by 0.666. Slope of the line is 1,143.4, whereas intercept is 56,700. Hence the linear equation is $y = 56,700 + 1,143.4 (Y)$. R^2 of the data is 0.7068, which reflect that data is quite closer to the trend line. This aspect is also clearly evident from the Energy Generation Graph in Fig. 2.

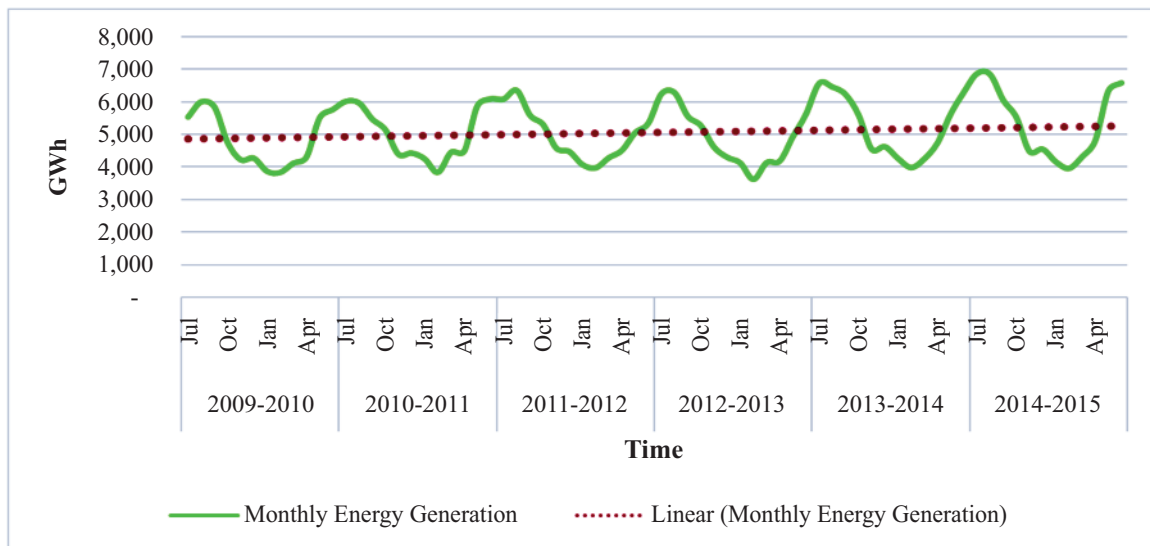


Fig. 3. Monthly Energy Generation

In Fig. 3, We have observed a clear pattern of movement in the monthly energy generation chart during the each six months of a year. That is, from February to July, the energy generation increases and declines linearly from August to January. Slope of the data is 5.21 whereas intercept is at 4867.14. R2 of the data is 0.015, which reflects large variation of data around trend line and it is also clear from monthly energy generation chart in Fig.3 that data crossed the trend twice in a year.

The general form of the estimated regression equation for modeling the linear trend in the energy generation is as follows:

$$Y_t = b_0 + b_1 M$$

Where

Y_t is forecast of energy generation in period t and M is month number i.e. 1 for July 2009 and 72 for June 2015.

The linear equation concluded from this data is $y = 4867.14 + 5.21 (\text{Month})$

In order to further investigate the pattern of energy generation and to confirm the understanding that there

is a seasonal effect and linear trend, regression is applied on the data. Then the estimated multiple regression equation for modeling both the monthly seasonal effects and the linear trend in the energy generation time series is as follows:

$$Y_t = b_0 + b_1 M_1 + b_2 M_2 + \dots + b_{12} M_{12} + b_{13} t$$

Where

Y_t is forecast of energy generation in period t and $M_1 \dots M_{12}$ are month numbers i.e. 1 for January and 12 for December, if period t corresponds to January then 1 otherwise 0 and so on for each month

T is time period i.e. July 2009 is 1 and June 2015 is 72

Based on the regression model using dummy variable, following equation has been drawn to compute energy generation for any month in a year. Results of the regression model are reasonably good. R2 of the data is 0.93, which shows the strength of linear equation:-

$$y = 5613.64 + 359.15 \text{ Jul} + 450.62 \text{ Aug} - 86.48 \text{ Sep} - 623.36 \text{ Oct} - 1431.23 \text{ Nov} - 1469.21 \text{ Dec} - 1796.59 \text{ Jan} - 2061.80 \text{ Feb} - 1675.79 \text{ Mar} - 1435.90 \text{ Apr} - 388.87 \text{ May} - 0 \text{ Jun} + 7.96 \text{ Period}$$

In Fig. 4. below are the graphical results of the equation concluded above. It is evidently apparent that

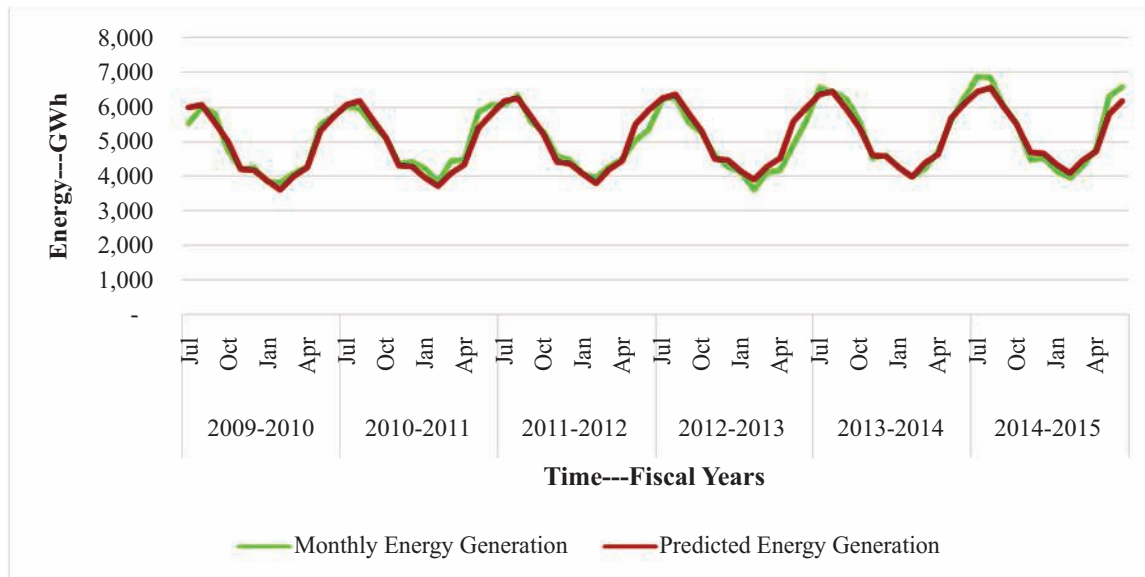


Fig. 4. Monthly Energy Generation Actual vs. Predicted

IV. LOAD DEMAND

Tremendous increment in electricity demand has been dubbed as the most prominent factor contributing to the obstinate demand-supply gaps. This has been proven by various studies conducted on the issue of power crisis involving aspects like governance, transmission, distribution losses and circular debt etc. During the past three decades there has been enormous

upsurge in the electricity demand most probably due to factors like industrialization, urbanization, rural electrification, agriculture and service sector growth, increasing domestic demand and rising per capita income, actual demand was never fully anticipated due to the lackluster forecast and future planning. It is important to upgrade old plants and to set up new generating stations in the face of constantly increasing electricity demands.

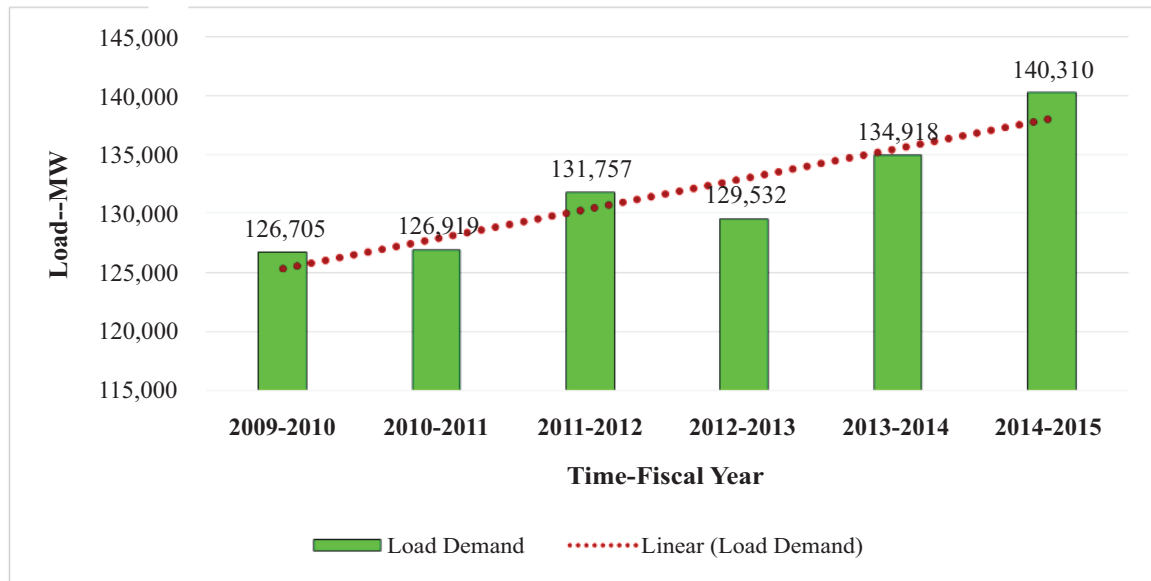


Fig. 5. Yearly Load Demand by Consumers

Six year's period from Jul 2009 to Jun 2015 has been used to analyze load demand. Mean of load demand is 131,690 MW, whereas range of data is 126,705 MW to 140,310 MW (13,605). Standard deviation of the data is 5,234 MW and skewness of the data is slightly positive i.e. 0.9, which shows growing trend.

The general form of the estimated regression equation for modeling the linear trend in the energy demand is as follows:

$$Y_t = b_0 + b_1 Y$$

Where

Y_t is forecast of energy demand in period t and Y is the year number i.e. 1 for 2009, 2 for 2010 and so on.

Slope of the annual demand is 2565.54 MW, whereas intercept is at 122,710 MW. R^2 of the data is 0.84, which shows the strength of linear equation. Following linear equation has been calculated to predict annual load demand:

$$Y = 122,710 + 2565.54 (x \text{ Year})$$

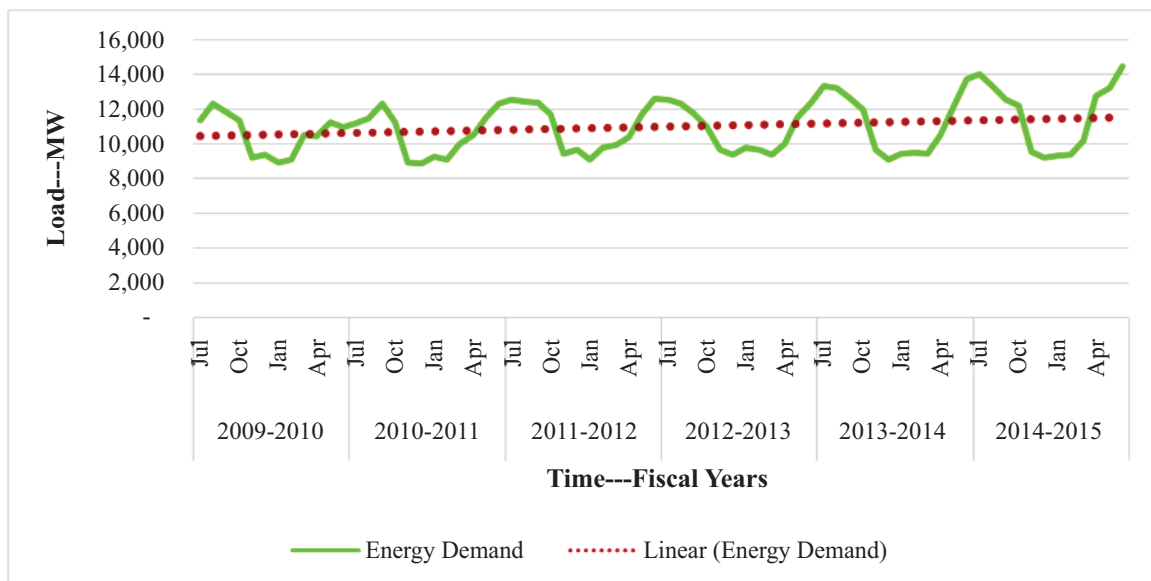


Fig. 6. Monthly Trend of Load Demand By Consumers

The monthly data of energy demand has been analyzed to observe the trend in demand and the graphical results revealed that there is a linear trend in six years. An interesting point to be discussed is the seasonal effects in energy demand, which is also clear from the monthly energy demand chart.

The general form of the estimated regression equation for modeling the linear trend in the energy demand is as follows:

$$Y_t = b_0 + b_1 M$$

Where

Y_t is forecast of energy demand in period t and M is month number i.e. 1 for July 2009 and 72 for June 2015. In fig.6 the Slope of the data is 15.26, intercept is 10417.33 so the best fit line equation is:-

$$y = 10417.33 + 15.26 (x \text{ month})$$

However, the R^2 of the data is 0.044, which reflects variation of data around trend line and it is also clear from monthly energy demand chart that data crossed the trend twice in a year. In order to conclude strong results and seasonal impacts, data has been further analyzed.

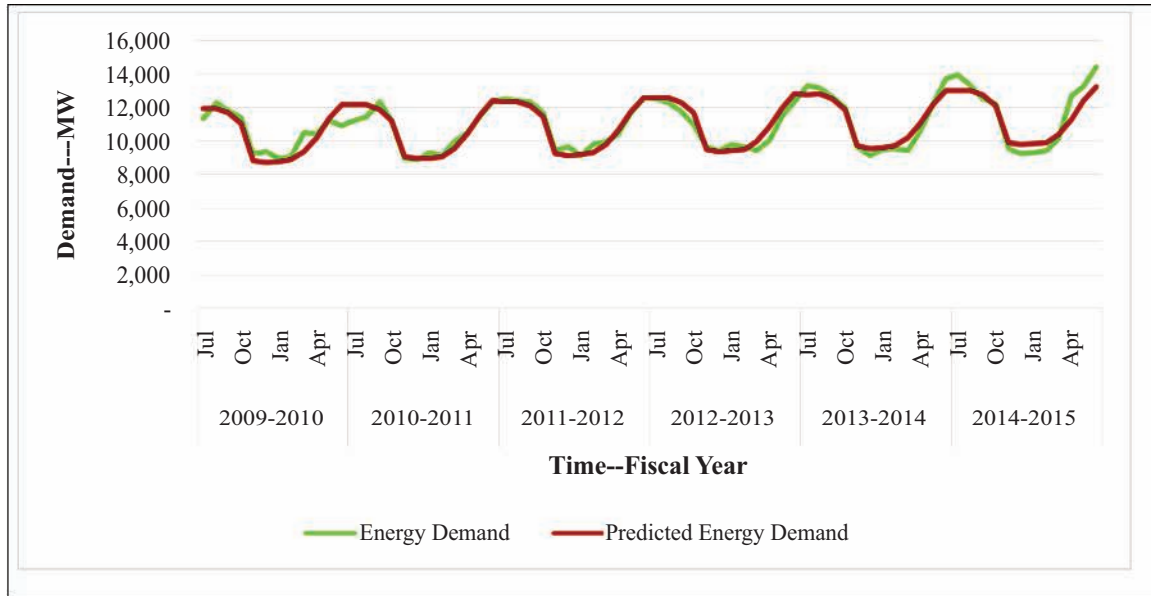


Fig. 7. Variations in actual and predicted monthly demand

The data has been regressed to analyze the seasonal impacts and the results are remarkably positive. After incorporating the seasonal impacts, the predicted values are very close to the actual values, which is clear from above Fig. 7.

The general form of the estimated multiple regression equation for modeling both the monthly seasonal effects and the linear trend in the energy demand time series is as follows:

$$Y_t = b_0 + b_1 M_1 + b_2 M_2 + \dots + b_{12} M_{12} + b_{13} t$$

Where

Y_t is forecast of energy demand in period t and M_1, \dots, M_{12} are number of months i.e. 1 for January and 12

for December, if period t corresponds to January then 1 otherwise 0 and so on for each month, Time period T , i.e. July 2009 is 1 and June 2015 is 72. R^2 of the data is 0.88, which shows the strength of linear equation given below:

$$\begin{aligned} Y = & 12000.57 + 17.81 \text{ Period} - 43.31 \text{ Jul} \\ & - 51.63 \text{ Aug} - 337.51 \text{ Sep} \\ & - 1010.22 \text{ Oct} \\ & - 3207.53 \text{ Nov} \\ & - 3359.13 \text{ Dec} - 3331.8 \text{ Jan} \\ & - 3244.58 \text{ Feb} - 2783.44 \text{ Mar} \\ & - 1932.94 \text{ Apr} - 818.01 \text{ May} \\ & + 0 \text{ Jun.} \end{aligned}$$

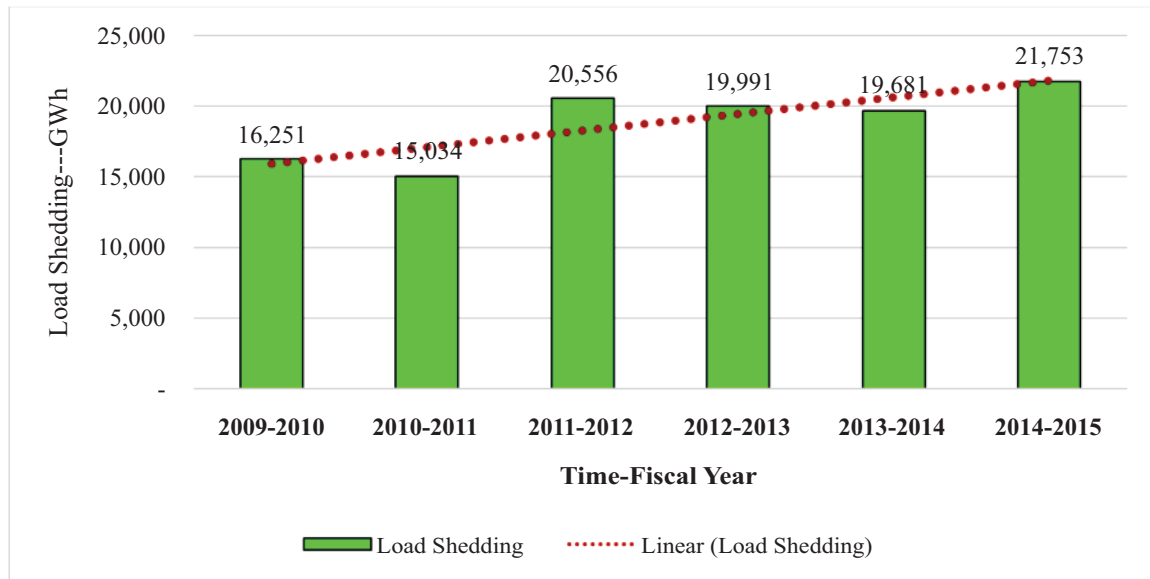


Fig. 8. Load Shedding (Annual Trend)

The range of the data is from 15,034 Gwh to 21,753GWh (i.e. 6,719), mean is 18,878 Gwh and standard deviation of the data is 2,632GWh. This reflects the variation of data around mean.

The general form of the estimated regression equation for modeling the linear trend in the energy load shedding is as follows:

$$Y_t = b_0 + b_1 Y$$

Where

Y_t is forecast of energy load shedding in period t and Y is year number i.e. 1 for 2009, 2 for 2010 and so on.

In Fig. 8, Slope of the annual energy load shedding is 2,565, intercept is 122,710GWh and R^2 of the data is 0.84. The strength of linear equation is quite well. The equation computed is $y = 2,565 + 122,710(x \text{ year})$.

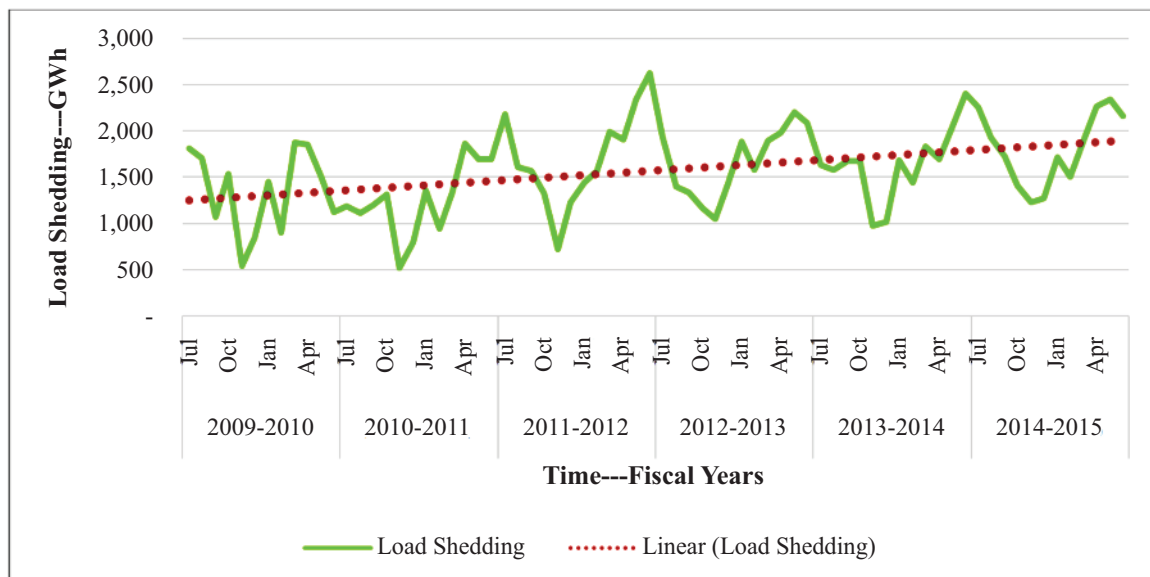


Fig. 9. Monthly Variations in Actual Load Shedding

In order to gain deeper insight of load shedding, monthly load shedding data has been analyzed to assess the trends and seasonal variation. In fig. 9, it is clear that Load shedding data also has seasonality effects. The general form of the estimated regression equation for modeling the linear trend in the energy load shedding is as follows:

$$Y^t = b_0 + b_M$$

Where

Y^t is forecast of load shedding in period t and M is month number i.e. 1 for July 2009 and 72 for June 2015. The equation drawn for monthly load shedding is given below. However, R^2 of the data is 0.17, which is quite low and reflect the variation of data around the linear line:-

$$Y = 9.2 + 1,237 (x \text{ month})$$

To analyze the effects of seasons the data is being further analyzed below.

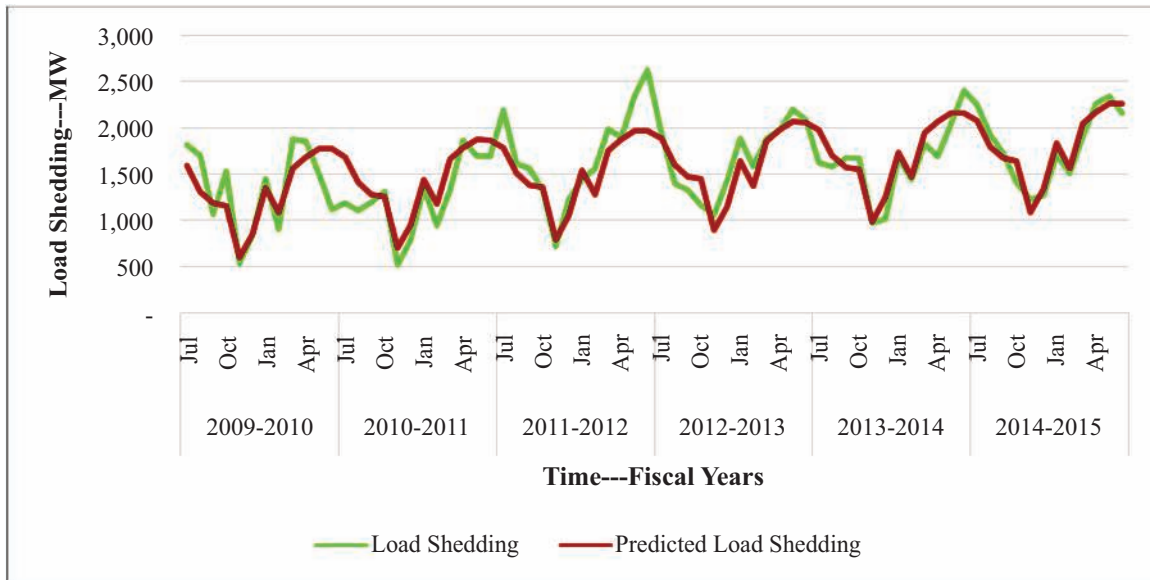


Fig. 10. Monthly Load Shedding Trend – Actual Vs Predicted

The data has been regressed to analyze the seasonal impacts, after incorporating the impacts, the predicted values are very close to the actual values, which is clear from above figure 10. The general form of the estimated multiple regression equation for modeling both the monthly seasonal effects and the linear trend in the energy load shedding time series is as follows:

$$Y^t = b_0 + b_1M_1 + b_2M_2 + \dots + b_{12}M_{12} + b_{13}t$$

Where

Y^t is forecast of energy load shedding in period t

and $M_1 \dots M_{12}$ are the month numbers i.e. 1 for January and 12 for December, if period t correspond to January then 1 otherwise 0 and so on for each month, Time period T , i.e. July 2009 is 1 and June 2015 is 72. R^2 of the data is 0.75, which shows the strength of linear equation given below:-

$$\begin{aligned} Y &= 1678.77 \\ &+ 8.11 \text{ Period} - 91.96 \text{ Jul} - 379.72 \text{ Aug} - 516.61 \text{ Sep} - 547.97 \\ &\text{Oct} - 1120.24 \text{ Nov} \\ &- 870.39 \text{ Dec} - 385.86 \text{ Jan} - 660.65 \text{ Feb} - 187.22 \text{ Mar} - 72.59 \\ &\text{Apr} + 12.26 \text{ May} + 0 \text{ Jun.} \end{aligned}$$

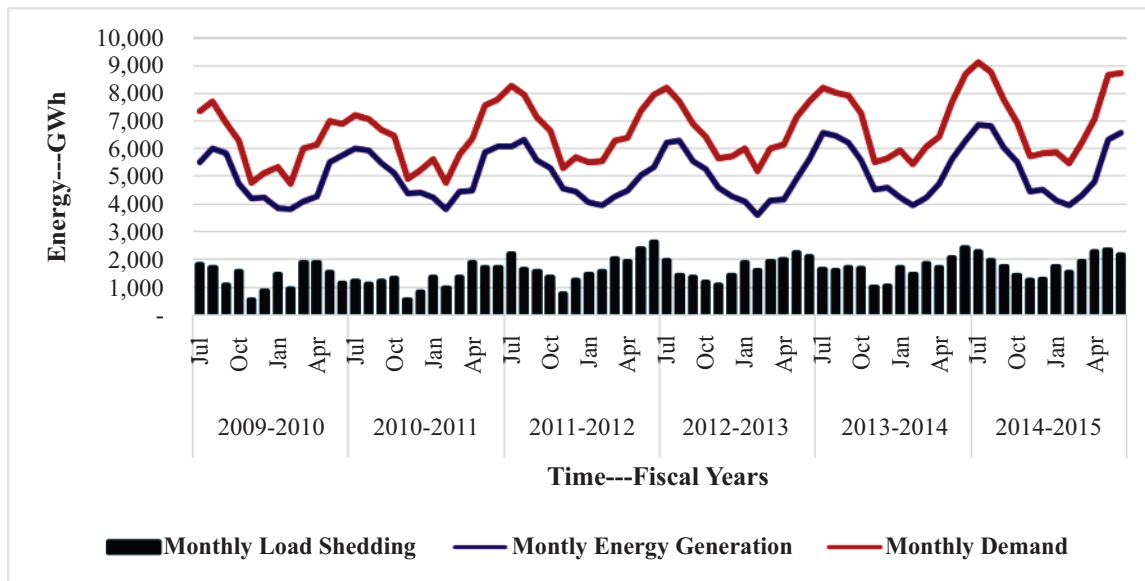


Fig. 11. Comparison of Energy Generation, Demand and Load Shedding

V. CONCLUSION

The analyzed research data of a period of 6 years from WAPDA's own power plants generation, Private Power plants and purchased from KESC has shown a significant room of improvement in load dispatch system. Different Load management measures were implemented in last 6 years to address the load management issues with different constraints and certain power system impediments. The major impediments steered with the whole load management systems were, less hydel generation due to canal closure in January of each year, sudden forced outage of WAPDA, Thermal and IPP's, transformation due to scheduled and emergency maintenance of power plants. The permanent impediment is the less hydel generating potential due to lower reservoir level with fewer outflows to meet the water indents allocated by IRSA and occasional transmission/transformation bottlenecks that further provokes for better load management opportunity. Results show generation increases in 4 years whereas decreases in 2 years. Each of the resulting values corresponds to previous year. The results on demand side show unsteady growth as 7.89%, 0.16 %, 3.87 %, 3.72 % and 3.93 % rise in years, 2009-2010, 2010-2011, 2011-2012, and 2013-2014 respectively, whereas, a decrease at the rate of 1.53% during the year 2012-2013. This research will be a future guideline for economic dispatch centre to address the concurrent and future issues with comprehensive load management planning. For future, the solar and windmill generation will be a significant contributor in energy generation after net metering and should be considered for future research.

REFERENCES

- [i] Gertler, C.W.O.S.P. How will energy demand develop in the developing world? *Journal of Economic Perspectives*, American Economic Association, 2012, 26, 119-138.
- [ii] Corporation, E. M. The outlook for energy: A view to 2040. 2014.
- [iii] Department of Economic and Social Affairs. World population prospects: The 2012 revision. (Medium variant); Population Division, United Nations.
- [iv] C. Sun, X. Ouyang, H. Cai, Z. Luo, A. Li, Household pathway selection of energy consumption during urbanization process in china. *Energy Conversion and Management* 2014, 84, 295-304.
- [v] F. Fu, L. Ma, Z. Li, K. R. Polenske, The implications of china's investment-driven economy on its energy consumption and carbon emissions. *Energy Conversion and Management* 2014, 85, 573-580.
- [vi] H. Ceylan, H. K. Ozturk, Estimating energy demand of turkey based on economic indicators using genetic algorithm approach. *Energy Conversion and Management* 2004, 45, 2525-2537.
- [vii] Census of electricity establishments (cee) 2005-06. Government of Pakistan, S. D., Federal Bureau of Statistics, September 2007, Ed.
- [viii] M. H. Sahir, A. H. Qureshi, Specific concerns of Pakistan in the context of energy security issues and geopolitics of the region. *Energy Policy* 2007, 35, 2031-2037.
- [ix] Economic survey of Pakistan 2008-09. Finance Ministry, Government of Pakistan, <http://www.finance.gov.pk>: 2009.

- [x] Institute of Public Policy, B. N. U. Pulling back from the abyss 2010; p (p. 66).
- [xi] J. Wood and B. F., "Wollenberg, Power generation, operation and control", New York: John Wiley Inc., 1984.
- [xii] R. Balamurugan† and S. Subramanian, "An Improved Dynamic Programming Approach to Economic Power Dispatch with Generator Constraints and Transmission Losses", *Journal of Electrical Engineering & Technology*, 3 (3), pp. 320~330, 2008
- [xiii] G. Sreenivasan, C. H. Saibabu, S. Sivanagaraju, "Solution of Dynamic Economic Load Dispatch (DELD) Problem with Valve Point Loading Effects and Ramp Rate Limits Using PSO International", *Journal of Electrical and Computer Engineering (IJECE)*, 1(1), September 2011
- [xiv] H. H. Happ, "Optimal power dispatch – a comprehensive survey", *IEEE Trans. Power Apparatus Syst.* PAS-96 (3)(1977) 841–854.
- [xv] B. H. Chowdhury, S. Rahman, "A review of recent advances in economic dispatch", *IEEE Trans. Power Syst.* 5 (4) (1990) 1248–1259.
- [xvi] W. G. Wood, "Spinning reserve constraints static and dynamic economic dispatch", *IEEE Trans. Power Apparatus Syst.* PAS-101 (2) (1982) 338–1338.
- [xvii] Han Yu and Rosehart, W. D, "An Optimal Power Flow Algorithm to Achieve Robust Operation Considering Load and Renewable Generation Uncertainties," *IEEE Trans. Power Syst.* vol. 27, no. 4, pp. 1808–1817, Nov. 2012.
- [xviii] B. C. Lesieutre, D. K. Molzahn, A. R. Borden, and C.L. DeMarco, "Examining the limits of the application of semi definite programming to power flow problems," in *Proc. 49th Annual Allerton Conf., Allerton House, IL, USA, Sep. 2011*, pp. 1492–1499.

Knowledge Management: Awareness And Adoption In The Oil And Gas Automation Industry In Pakistan

M. P. Mughal¹, B. Ahmad²

^{1,2}Engineering Management Department, UET Lahore, Pakistan.

²bilal_ahmed81@hotmail.com

Abstract-Competition in the business world has forced the organizations to build competitive advantage. In this context, resource based view of the firm has gained popularity where human capital and knowledge management (KM) is deemed important for building a competitive advantage. Oil & Gas automation industry is characterized by intense competition, whereby different international players compete with each other on the basis of their expertise and capabilities. This study investigates awareness and adoption of KM within Oil & Gas automation sector corporations having some presence in Pakistan. Both end users and service providers within the sectors are sought their opinion regarding adoption and awareness of the KM in the industry. Moreover, perceptual differences of the service providers and end users are also sought in the study pertaining to the awareness, importance and implementation of KM. The study further highlights the barriers to KM implementation and also establishes relationship between KM and organizational performance. The findings of the study highlight KM as a multi functional concept, which contributes towards efficiency and effectiveness of an oil & gas organization in many ways. Further, implementation of KM is also deemed to be a multi-faceted task, which requires behavioral, cultural, managerial and resource based support both from individuals within an organization and from organization as an institution. Finally, the study confirms a positive impact of KM on organizational performance within Oil & Gas automation sector.

Keywords-Knowledge Management, Automation, Performance, Competitive Advantage

I. INTRODUCTION

The era of information technology emerged after the era of industrial revolution, which essentially was characterized by hostile trends like increasing competition, saturating markets, globalization, and emergence of services based industry. In order to cope up with these complexities, strategic view of business emerged where survival of the organizations in the marketplace became dependent upon building and

exploiting some core competencies. This necessitated effective management all of organizational resources in order to build some core competencies. With time the organization focus also shifted from tangible assets to intangible assets. One of such intangible asset is knowledge possessed by the organizations and its people [i]. The management of the knowledge has been a hot area of debate. Its value as a strategic asset is widely propagated both in literature and in practice [ii-iii]. The concept although is not new as according to [iv], KM also prevailed in ancient civilizations, in an informal manner. The concept of craftsmanship and apprenticeship in pre-industrialized era also indicate towards the knowledge possessed by the master. The master used to transfer the knowledge among the generations of apprentices over the time. The formalization of the concept started after the propositions of [v] who highlighted the resource based view of the firm. After that, KM became buzzword in context of the corporate strategy and organizations around the globe started to pursue KM in a formal manner. As a result various key positions relating to KM were added to organizational hierarchy and structure [vi].

Thus, in modern era, organizational success is associated with the ability of the firm to exploit its explicit and tacit knowledge [vii]. So, an effective framework of knowledge transfer is deemed for effective exploitation of the knowledge [viii]. The traditional benefits of KM and KM system include the ability of organizations to be more responsive, more flexible, more productive, more innovativeness and better decision making [iii]. The authors stated that KM has become need of the era and it is derived by the urge to disseminate best practices, share tactical knowledge and to encourage continuous improvement. This in turn, supports in new product and service developments, reduce rework and enable the organization to be more responsive to its clients [ix]. KM also provides an evolutionary platform for the emergence of new technologies. Furthermore, it improves existing processes of an organization. This on the whole, is considered beneficial for the organization [x].

But implementation of KM is not a simple task and requires considerable effort, support and resources from people (human resource), technology, processes and culture of organization [xi]. [xii] on the other hand identified three forces that influence KM in an organization. These forces include managerial influences, resource influences and environment influences. Manager influences are further divided into four factors i.e. exhibition of leadership in KM activities, coordination of KM activities, controlling KM activities and measurement of KM activities. Resource influences pertain to the financial resources, human resources or material resources. Lastly, environmental resources are related to the external environment of the organization such like time, technology, market, fashion, competition and climate (educational, social, political, economic and governmental). The authors stressed that KM initiatives should have managerial support, appropriate financial resources, budgets and infrastructure to ensure the success of such indicatives [xiii]. Finally, eleven critical success factors were identified for the adoption of KM i.e. management leadership & support, culture, information technology, strategy & purpose, measurement, organizational infrastructure, processes & activities, motivational aids, resources, training & education and human resource management [xiv].

The propagation on the value of the Km has increased over time, but there have been confusions on the nature and conception of KM [xv,xxi]. There is also evidence that awareness of benefits of KM do not lead towards systematic implementation of KM [xix]. [xxv] points out that there is no one size fit all solution of KM implementation. Further, complexity on conception and implementation of KM also undermine its usability as a strategic asset [xix]. [xxvi] further elaborate the problems of Pakistani firm, which are unable to manage their knowledge assets and intellectual capital to better ends.

This study in tis regard provides first hand evidence into the oil & gas automation industry of Pakistan. The focus of the study is perceptions of end users and service providers of the industry. This would help practitioners and managers to understand the perceptual gaps on the KM and also explore the value of KM as a strategic asset. This study would further help them to use, channelize and manage KM for better ends.

II. RESEARCH METHODOLOGY

The purpose of this research is to explore perceptions and opinions of the individuals working in the Oil & Gas automation industry with regard to KM, its importance and implementation within the sector. Survey design is deemed suitable data collection technique for the study as this design enables the researcher to collect information regarding the

perceptions of the respondents in an appropriate manner. Thus, a questionnaire instrument was developed to collect the data. Questions included in the instrument were based on the past studies on the subject [xiii, iii, xv, xvi, xvii, xviii, xix, xx]. The questionnaire was composed of seven parts; where first part of the questionnaire was related to the general familiarity of respondents for the term and basic concept of KM, second part of the questionnaire contained questions relating to the importance of the KM, third part asked respondent regarding the implementation of KM system, fourth part contained the questions for the measurement of KM, fifth part had measurement scale of performance and sixth part solicited the responses of the respondents on the barriers relating to KM while the last part of the questionnaire contained questions relating to the demographics of the respondents. Questions included in section 2 to section 5 of questionnaire were asked on five point likert scale.

The questionnaires were floated among the service providers and end users within the Oil & Gas automation industry. It was ensured that the respondent's organization has some representation in Pakistan. Out of 200 total questionnaires floated 132 valid responses were generated (Response rate = 66%). Out of these 132 responses; 81 were service providers and remaining 51 were end users of the industry.

The collected data is analyzed using simple frequency distributions and descriptive statistics. Chi Square and independent sample t-test are also used to find difference of opinion between service providers and end users. Regression analysis is used to relate KM with organizational performance. Following hypothesis is tested in the study:

- H0: There is no significant impact of KM on organizational performance in oil & gas automation industry.
- H1: There is a significant impact of KM on organizational performance in oil & gas automation industry.

III. ANALYSIS

The analysis of the paper is divided into four sections, whereby first section provides demographical characteristics of the respondents, second section provides descriptive statistics on importance of KM, implementation of KM and barriers to KM implementation, third section established the perceptual differences of end users and service providers on KM importance and implementation and last section assesses the impact of KM on performance of organizations in oil & gas automation industry.

A. Demographical distribution of respondents

The demographical questions asked from the respondents were related to their gender, job nature and work experience. Most of the respondents were males

as only 3 females were found in the sample who were also from service provider category and remaining 129 respondents were male out of which 78 were from service provider group and remaining 51 were from end user group. Regarding the nature of the job, 30 respondents belonged to the managerial cadre (18 service providers & 12 end users) and remaining 102 respondents were of non-managerial responsibilities (63 service providers & 39 end users). With regard to the total work experience service providers on average had 6.22 (Standard Dev. = 7.31) years of work experience and end users had on average of 11.15 (Standard dev. = 4.98) years of work experience and average experience of service providers with the current organization was 2.59 years (standard dev. = 3.79) and of end users was 4.24 years (standard dev. = 2.65).

B. Descriptive Statistics: Importance & Implementation of KM

Firstly, respondents were asked about their knowledge on KM. Out of total 81 service providers 69 knew about it, while 12 did not know about it. Entire 51 end-users seemed to know about the KM. Pearson Chi-Square of 8.311 (p -value < .01) indicated that there exist significant differences among the service provider and end user group with regard to their general awareness on KM. End users seemed to be more aware of the KM as compared to the service providers.

Secondly, respondents were asked as to whether their organization has implemented some system of KM or not. Out of 78 service providers who responded to this question 69 confirmed to have some KM system in their organization, while remaining 9 respondents responded otherwise. Out of total 51 service providers, 48 also accepted to have some KM system in their organization. Pearson Chi-Square value of 1.169 does not indicate any significant differences among both respondent groups i.e. service providers and end users. Functions of KM, like reduction in work, service improvements, quality improvements, better responsiveness improvements in decision-making and KM as strategic asset were deemed most important by the respondents, while functions like reduction in litigation cost, better conflict management and strengthening the relationship with suppliers and customer were considered least important by the respondents.

TABLE I
IMPORTANCE OF KM

	Mean	Std. Deviation
Reduction in rework	4.00	0.89
Service improvements	3.98	0.82
Quality improvements	3.98	0.84
Better responsiveness	3.98	0.97
Improvement in decision making	3.93	0.78

KM as strategic asset/ competitive advantage	3.93	0.78
Improvement in delivery time	3.79	0.87
Improvements in profits	3.71	0.87
Strengthening the relationship with suppliers & customers.	3.57	0.97
Better conflict management	3.57	0.92
Reduction in litigation cost.	3.47	0.90
Overall Importance Score	3.81	0.63

Table II provides the essentials of the implementation of KM in Oil & Gas automation industry. For implementation of KM, factors like supportive and encouraging culture and development of strategy with KM objective were deemed most important, while factor of appointment of KM manager was considered least important by the respondents.

TABLE II
ESSENTIALS OF IMPLEMENTATION OF KM

	Mean	Std. Deviation
Supportive and encouraging organizational culture	4.16	0.81
Development of a strategy outlining KM objectives	3.96	0.77
Integrated KM information system	3.84	0.91
Top management involvement & support	3.79	0.99
Preparation of budgets and allocation of resources	3.71	0.87
Appointment of KM manager	3.51	0.99
Overall Implementation Score	3.82	0.66

Table III provides further elaboration of the implementation of the KM system within the Oil & Gas automation industry by exploring the barriers to the effective implementation of the KM system. Overall, individual factors such like lack of will, lack of leadership and employee involvement are more significant barriers towards KM implementation.

TABLE III
BARRIERS OF KM IMPLEMENTATION

	Mean	Std. Deviation
Lack of will.	4.07	.97
Lack of proper leadership in the organization	3.79	1.08
Lower involvement of employees.	3.71	1.24
Lack of formal training.	3.61	1.06
Fear of people that sharing	3.52	1.10

knowledge would undermine their importance in the organization.		
Lack of trust between members of the organization.	3.44	1.25
Tendency of high potential people to work individually.	3.43	1.14
Time & costs constraints	3.36	1.13

C. Perceptual differences of end users and services providers

Table IV provides difference of opinion of service providers and end users with regard to the overall importance and implementation of KM system in the Oil & Gas automation industry. A significant t-value indicates that, the implementation of the KM system in Oil & Gas automation industry was perceived differently by service providers and end users, while importance of the KM was not perceived differently by end users and service providers. Thus, null hypothesis of 'there are no significant differences between perceptions of end users and service providers for importance and implementation of KM' was rejected in case of implementation of KM only.

TABLE IV
DIFFERENCE OF PERCEPTIONS OF SERVICE PROVIDERS AND END USERS

Perceptual Category	Groups	Mean	Std. Dev.	Mean Diff.	Prob.
Importance	Service Provider	3.79	.74	-.04 [.39]	.69
	End User	3.83	.42		
Implementation	Service Provider	3.73	.76	-.23 [2.29]	.02**
	End User	3.96	.41		

**Significant at 5% level of significance.

D. Assessment of impact of KM on performance

In order to assess the impact of KM on organizational performance, regression analysis is deemed suitable. It assumes KM as independent variable and statistically establishes its impact on organizational performance in oil and gas industry.

Tables V provide results of regression analysis of the study. R square indicates that almost 46.4% of the variation in the performance of the organization is explained by the KM in Oil & Gas automation industry.

The F statistics of the model is indicates that model is good fit at 1% level of significance.

TABLE V
REGRESSION RESULTS

Model	Unstandardized Coefficients	Standardized Coefficients	T	Prob.
	B	Std. Error Beta		
1 (Constant)	1.475	.194	7.624	.000
KM	.584	.055	10.614	.000
R-Square	.464	F-Statistics	112.658(Prob. < .01)	

a. Dependent Variable: Performance

The results indicate a positive and significant impact of KM on performance of the organizations in Oil & Gas automation industry. Thus, null hypothesis (H0) is rejected and alternate (H1) is accepted.

Overall, this study found significant differences between service providers and end users with regard to the awareness of the KM and also regarding the implementation of KM in oil & gas automation industry. KM overall seem to have multifaceted implicates for the contemporary organizations in the Oil & Gas automation industry, where KM effects various efficiency and performance related facets of the organization including reduction in rework, service & quality improvements, increased responsiveness & profits and better decision making. KM could also be proved to be strategic asset for the organization. The implementation of KM seem a bit complicated where factors like supportive culture, clear objectivity, integrated information system, top management support and budget allocations were deemed important factors for the better implementation of KM system. This entails that KM as a multifaceted concept requires integrated implementation efforts from all aspects of the organization. Various personal factors like lack of will, less leadership support, lack of employee involvement, no formal training and reluctance of people to share knowledge seemed significant barriers in implementation of KM system and practices within Oil & Gas automation industry. Further, KM was found associated with the organizational performance. These findings are consistent with the previous literature on the topic which deem KM as a strategic asset of the organization and deem KM beneficial for various aspects of the organizational efficiency and performance [xxi, iii, x, xvi, xvii). KM as a multifaceted concept having confusion is also widely elaborated [xxi, xxii, xxiii] and implementation of KM has always been considered tricky requiring support from people, culture, technology and other resources [xxi-xxiii]. Lastly, studies also support the notion of a positive impact of KM on firm performance [xxiv, xvi]. Thus implementation of the KM although is a daunting, tricky and complex task; it could be very beneficial for the long-term survival and sustainability of the organization in a competitive marketplace.

IV. CONCLUSION

This study was conducted with an aim to investigate dynamics of KM within the Oil & Gas automation industry. The respondents of the study were both service providers and end users within the industry. The study indicated that KM has much importance for the Oil & Gas automation industry where the concept has multidimensional implications regarding various performance and efficiency related aspects of the organizations. It further was found that the implementation of the KM within the Oil & Gas automation sector a tricky task where by supportive culture, clear objectivity, integrated information system, top management support and budget allocations were deemed important factors for KM implementation. Further, significant perceptual differences were found between service providers and end users of the Oil & Gas automation industry with regard to the implementation and awareness of KM. The study also confirms a positive impact of KM on organizational performance in Oil & Gas automation industry. This study overall establishes the importance of the KM in Oil & Gas automation industry as a strategic asset or success factor but there lie many ambiguities regarding the conception and implementation of KM both as a concept and as a tool. Further research is necessary to explore the potential and implications of KM in various industries and there is also a need to draw a systematic procedure to implement the KM system within the organization. The conceptualization of the construct also needs clarifications and awareness with regard to the true conceptualization of the term is also important.

REFERENCES

- [I] I. W. Kang, "KMPI: measuring knowledge management performance", in *Information & Management*, vol. 42, no. 3, 2005, pp. 469-482.
- [ii] G. Gartner, "Grappling with e-knowledge". *Computer world*, vol. 32, No. 1, 1998, pp. 43.
- [iii] M. Alavi, and D. E. Leidner, "Knowledge management systems: issues, challenges, and benefits". *Communications of the AIS*, 1(2es), 1999, pp. 1.
- [iv] B. Bergeron, "Essentials of knowledge management", Vol. 28, 2003, John Wiley & Sons.
- [v] E. Penrose, "The theory of the growth of the firm". 1959 Oxford University Press.
- [vi] K. Metaxiotis, K. Ergazakis and J. Psarras, "Exploring the world of knowledge management: agreements and disagreements in the academic/practitioner community". *Journal of knowledge management*, vol. 9, no. 2, 2005, pp. 6-18.
- [vii] J. Glass, "A best practice process model for hybrid concrete construction", *Construction Management and Economics*, vol. 23, no. 2, 2005, pp. 169-184.
- [viii] H. Abdul-Rahman, I. A. Yahya, M. A. Berawi and L. W. Wah, "Conceptual delay mitigation model using a project learning approach in practice", *Construction Management and Economics*, vol. 26, no. 1, 2008, pp. 5-27.
- [ix] H. S. Robinson, P. M. Carrillo, C. J. Anumba, and A. M. Al-Ghassani, "Perceptions and barriers in implementing knowledge management strategies in large construction organisations", In *Proceedings of the RICS Foundation Construction and Building Research Conference, 2011*, pp. 451-460. Glasgow Caledonian University, UK.
- [x] C. O. Egbu, S. Hari, and S. H. Renukappa, "Knowledge management for sustainable competitiveness in small and medium surveying practices" *Structural Survey*, vol. 23 no. 1, 2005, pp. 7-21.
- [xi] P. Quintas, P. Lefrere and G. Jones, "Knowledge management: a strategic agenda". *Long range planning*, vol. 30, no. 3, 1997, pp. 385-391.
- [xii] C. W. Holsapple, and K. D. Joshi, "An investigation of factors that influence the management of knowledge in organizations" *The Journal of Strategic Information Systems*, vol. 9, no. 2, 2000, pp. 235-261.
- [xiii] H. S. Robinson, P. M. Carrillo, C. J. Anumba and A. M. Al-Ghassani, "Knowledge management practices in large construction organisations", *Engineering, Construction and Architectural Management*, vol. 12, no. 5, 2005, pp. 431-445.
- [xiv] K. Y. Wong and E. Aspinwall, "An empirical study of the important factors for knowledge-management adoption in the SME sector". *Journal of Knowledge Management*, vol. 9, no. 3, 2005, pp. 64-82.
- [xv] W. David and L. Fahey "Diagnosing cultural barriers to knowledge management", *The Academy of management executive*, vol. 14, no. 4, 2000, pp. 113-127.
- [xvi] P. Carrillo and P. Chinowsky, "Exploiting knowledge management: The engineering and construction perspective". *Journal of Management in Engineering*, vol. 22, no. 1, 2005, pp. 2-10.
- [xvii] L. R. Yang, J. H. Chen and H. W. Wang, "Assessing impacts of information technology on project success through knowledge management practice", *Automation in Construction*, vol. 22, 2012, pp. 182-191.
- [xviii] A. H. Gold, A. Malhotra and A. H. Segars, "Knowledge management: an organizational capabilities perspective", *Journal of Management Information Systems*, vol. 18, no. 1, 2001, pp. 185-214.

- [xix] N. Forcada, A. Fuertes, M. Gangoellis, M. Casals, and M. Macarulla, "Knowledge management perceptions in construction and design companies". *Automation in construction*, vol. 29, 2013, pp. 83-91.
- [xx] M. Alavi, T. R. Kayworth, and D. E. Leidner, "An empirical examination of the influence of organizational culture on knowledge management practices". *Journal of management information systems*, vol. 22, no. 3, pp. 191-224.
- [xxi] M. Y. Cheng, H. S. Peng, C. M. Huang, and C. H. Chen, "KM-oriented business process reengineering for construction firms". *Automation in Construction*, 21, 2012, pp. 32-45.
- [xxii] M. A. Peteraf, "The cornerstones of competitive advantage: A resource-based view". *Strategic management journal*, vol. 14, no. 3, 1993, pp. 179-191.
- [xxiii] U. R. Kulkarni, S. Ravindran, and R. Freeze, "A knowledge management success model: theoretical development and empirical validation". *Journal of Management Information Systems*, vol. 23, no. 3, 2007, pp. 309-347.
- [xxiv] C. López-Nicolás and A. L. Meroño-Cerdán, "Strategic knowledge management, innovation and performance". *International Journal of Information Management*, vol. 31, no. 6, 2005, pp. 502-509.
- [xxv] A. Styhre, "Managing Knowledge in the Construction Industry", *Spon Research*, Abingdon, Oxon, UK, 2009.
- [xxvi] M. Khalique, N. Bontis, J. Abdul Nassir bin Shaari, and A. Hassan Md. Isa, "Intellectual capital in small and medium enterprises in Pakistan". *Journal of Intellectual Capital*, vol. 16, no. 1, 2015, pp. 224-238.

Questionnaire

Dear Sir

I am conducting a research to understand the dynamics of Knowledge Management (KM) in Automation industry. Knowledge has become a driving force for organizational competence and effectiveness and managing this knowledge possessed by the organization through its people, processes, culture and technology could prove to be a competitive advantage in competitive environment today. Knowledge brings competence and competence enable the organization to better serve its customer's needs and demands. This research is being conducted to understand the perceptual gap among the service provider and service receiver in Automation industry with regard to knowledge management and the role it could play in growth and efficiency of the organizations operating in automation industry. The information collected through this questionnaire will remain confidential and would only be used for research purpose. Your assistance is highly appreciated.

Thank you!

Please answer the following questions before proceeding.

1	Do you know about Knowledge Management (KM)?	Yes	No
2	Does your organization have some knowledge management system in place?	Yes	No

Please proceed if the answer to above question is yes; leave the survey otherwise.

Use following scale to record your response

(1= Strongly Disagree) (2= Disagree) (3= Neutral) (4= Agree) (5= Strongly Agree)

Importance of KM

1	KM improves decision making within the organizations of automation industry.	1	2	3	4	5
2	KM improves the delivery time of the organizations in automation industry.	1	2	3	4	5
3	KM brings service improvements in the organizations of automation industry.	1	2	3	4	5
4	KM strengthens the relationship of the organizations in automation industry with both their suppliers and their customers.	1	2	3	4	5
5	KM brings quality improvements for the organizations in automation industry.	1	2	3	4	5
6	KM enables an organization to respond to customers in a quick manner in automation industry.	1	2	3	4	5
7	KM reduces rework in automation industry.	1	2	3	4	5
8	KM could prove to be a strategic asset/ competitive advantage in automation industry.	1	2	3	4	5
9	KM improves profits of the organizations in automation industry.	1	2	3	4	5
10	Knowledge management makes conflict management easier.	1	2	3	4	5
11	Proper implementation of knowledge management may result in reduction of litigation cost.	1	2	3	4	5

Implementation of KM system

1	An integrated KM information system is necessary for the implementation of KM system in the automation industry.	1	2	3	4	5
2	Appointment of KM manager is essential for the effective implementation of KM system in automation industry.	1	2	3	4	5
3	Top management involvement & support is required for effective implementation of KM system in automation industry.	1	2	3	4	5

4	A supportive and encouraging organizational culture is must for a better implementation of KM system in automation industry.	1	2	3	4	5
5	Preparation of budgets and allocation of resources is essential for effective implementation of KM system in automation industry.	1	2	3	4	5
6	Development of a strategy which outlines objectives of KM system is important for successful KM implementation in automation industry.	1	2	3	4	5
KM						
1	My company recognizes value of knowledge management as strategic asset.	1	2	3	4	5
2	We discuss and reevaluate our position on lost business opportunities; which are caused by inappropriate exploitation of available knowledge.	1	2	3	4	5
3	In my organization, knowledge management makes work easy and more productive.	1	2	3	4	5
4	Knowledge management makes it easier for us to monitor undergoing projects.	1	2	3	4	5
5	Knowledge management has brought flexibility into the working of my organization.	1	2	3	4	5
6	Knowledge management has improved our flexibility relating to the project works.	1	2	3	4	5
Performance						
Over the past two years, my organization has improved its ability to...						
1	Innovate new products and services.	1	2	3	4	5
2	Identify new business opportunities.	1	2	3	4	5
3	Co-ordinate the development efforts of different units.	1	2	3	4	5
4	Anticipate potential market opportunities for new product/ services.	1	2	3	4	5
5	Rapidly commercialize new innovations.	1	2	3	4	5
6	Adapt quickly to unanticipated changes.	1	2	3	4	5
7	Anticipate surprises and crises.	1	2	3	4	5
8	Quickly adapt its goals and objectives to industry/ market changes.	1	2	3	4	5
9	Decrease market response time.	1	2	3	4	5
10	React to the new information about the industry or market.	1	2	3	4	5
11	Be responsive to new market demands.	1	2	3	4	5
12	Avoid overlapping development of corporate initiatives.	1	2	3	4	5
13	Streamline its internal processes.	1	2	3	4	5
14	Reduce redundancy of information and knowledge.	1	2	3	4	5
Barriers						
What might be the barriers to the effective implementation of knowledge management system in any organization?						
1	Time & costs constraints	1	2	3	4	5
2	Lack of proper leadership in the organization.	1	2	3	4	5
3	Lack of will.	1	2	3	4	5
4	Lack of formal training.	1	2	3	4	5
5	Lower involvement of employees.	1	2	3	4	5
6	Lack of trust between members of the organization.	1	2	3	4	5
7	Tendency of high potential people to work individually.	1	2	3	4	5
8	Fear of people that sharing knowledge would undermine their importance in the organization.	1	2	3	4	5

Demographics

Gender: 1. Male 2. Female

Nature of Job: 1. Managerial 2. Non-managerial

Work Experience (Total): _____

Work Experience (With current organization): _____

Name of Current Organization (optional): _____

List of Responding Companies

Sr #	Company Name
1	Akzonobel
2	Chevron
3	Intech Process Automation
4	Interloop
5	Pall Corporation
6	RasGas Qatar
7	Sadara
8	Tengiz

Process Improvement for PET Bottles Manufacturing Company Using Six Sigma Approach

M. Ullah¹, A. M. Khan², R. Nawaz³, R. Akhtar⁴

^{1,3,4}Industrial Engineering Department, University of Engineering and Technology Peshawar, Pakistan

²Mechatronics Engineering Department, UET Taxila Sub-Campus, Chakwal, Pakistan

¹misbah@uetpeshawar.edu.pk

Abstract-Rejection in production processes cannot be ignored in industries in general, and in manufacturing organizations in particular. Six sigma has been considered an organized and scientific approach for the last few decades in order to reduce the number of rejections in processes. This paper has focused the injection molding process in PET bottles manufacturing industry in Pakistan. The paper aims to reduce the number of rejected products produced during the injection molding process and highlight the significant factors and their level that severely affect the molding process. Different type of defects were observed in the injection molding process. Statistical approach using hypothetical analysis and experimental design techniques were used to conclude significant factors and their levels. Injection pressure, melting temperature, and resin type were observed as the most significant factors that affect the number of defective products produced during the PET bottles manufacturing. The joint interaction effect of pressure and temperature was also significant in comparison to all other interaction effects during this process.

Keywords-Six Sigma, Design of Experiment, Quality Control

I. INTRODUCTION

Six sigma has been considered as measure of quality in manufacturing and service industries for the last few decades. It is a disciplined and result oriented approach that eliminate defects by keeping the production or service processes near to the level of perfection. Linderman et al. define six sigma as "(...) an organized and systematic method for strategic process improvement and new product and service development that relies on statistical methods and the scientific method to make dramatic reductions in customer defined defect rates" [i]. The "sigma" terminology was introduced for the first time by Walter Shewhart in 1922 with the introduction of three standard deviations with mean. They highlighted that products falling outside the means, can be considered

as defect[ii].

Six Sigma has been considered as customer-driven approach that eliminates waste, increase quality and improve organizational performance. Its main objective remain the identification of causes for poor performance or reduced productivity. Major causes are identified and preventive measure for process improvement are carried out in order to reduce defects and variations in processes. Although six sigma has been introduced and implemented in the manufacturing sector, however, it has also been common tool used in the service sector [iii]. The authors in [iv] highlighted the importance of Define-Measure-Analyze-Improve-Control (DMAIC) process based on potential parameters where the actual strength of this DMAIC process exists. They emphasized the fact that practitioner need to understand the strengths and limitations of the said six sigma problem solving approach. Six sigma is similar in functional approach as total quality management for solution of problems in manufacturing industries, such as PDCA i.e., Plan-Do-Check-Act and the Seven Step method of Juran and Gryna[v].

DMAIC can be considered as meta-routine in order to establish new routines by changing the existing ones [vi]. Six sigma has been basically applied to the generic situations in service and manufacturing processes to reduce variations in processes [vii]. Six sigma has been used as a basic for process improvement[viii]. Process can be considered as more consistent with greater number of sigma's within the defined specification limits and reduced number of defects. It is not cost-effective to achieve six sigma level in all processes in an operation; therefore, one must focus on the most critical ones that are relevant to the customer requirements.

The PET bottles manufacturing process is also among those processes where tremendous improvements can be made in order to reduce defects produced in the process and increase company's profits. Different approaches and techniques are applied to know the reasons behind the causes and significant

factors that affect the process output. Application of these products are numerous and are extensively used in day-to-day life. Polyethylene terephthalate commonly abbreviated as PET, is a thermoplastic polymer resin of the polyester family and is used in synthetic fibers such as beverage, food and other liquid containers, thermoforming applications, and engineering resins often in combination with glass fiber.

The majority of the world's PET production is for synthetic fibers around more than 60% with bottle production accounting for around 30% of global demand. Polyester makes up about 18% of world polymer production and is the third-most-produced polymer; polyethylene (PE) and polypropylene (PP) are first and second respectively. PET consists of polymerized units of the monomer ethylene terephthalate, with repeating $C_{10}H_8O_4$ units. PET is commonly recycled and is referred as symbol number "1" for its recycling characteristics.

A. PET bottles manufacturing process

Two basic molding methods used for PET bottles, the one-step "hot preform" method and the two-step "cold preform" method.

A two-step method has been used in the examined industry at industrial estate Hayatabad, Peshawar, KPK, Pakistan to produce PET bottles. The two-step method uses two separate machines. The first machine; an injection molding machine, injection molds the preform, which resembles a test tube, with the bottle-cap threads already molded into place. The body of the tube is significantly thicker, as it will be inflated into its final shape in the second step using stretch blow molding. In the second step, the blow molding machine reheats the preforms and is then inflated against a two-part mold to form them into the final shape of the bottle. This method is most suited in medium to large-scale production.

The generalized process of bottle manufacturing can be outlined as shown in Fig. 1. Dehumidifying drying agents are used for drying purposes before processing as PET may absorb moisture from the atmosphere. Dried PET pellets are then compressed and melted by a rotating screw. Molten PET is injected into the injection cavity and cooled rapidly to form a "Preform" (The test-tube-like cavity from which bottles are blown). The temperature of the preform is adjusted to the correct profile for blowing. The hot preform is simultaneously stretched and blown into a shaped blow mold to form a tough, lightweight container. The finished container is then ejected from the mold.

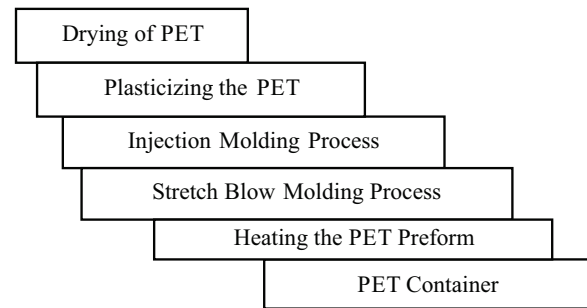


Fig. 1. Process flow diagram for PET bottles.

B. Problem formulation and process diagram

The company produced PET bottles using two-step method including injection molding and blow molding processes. PET products produced during the processes results in rejection rate due to different types of defects. Quality control section of the company rejects these products due to these defects. It has been observed that the rejection rate is 11.24 preforms per hour in the injection molding process. These rejections have a significant impact on the medium range industry where financial impact rises up to 0.8 Million rupees per annum due to this process only. The management of the company is interested to reduce the number of rejected preforms produced in the process and increase company profits by reducing the associated loss. Technical personnel are focused to define major factors that affect the injection molding process and set levels of these factors such that the number of rejections are reduced.

C. 1) Process Flow Chart

Figure 2 shows the basic flow chart of the processes being carried out from raw material i.e., PET resins to the finished product i.e. PET bottles. The PET resins are received from the supplier and are then checked by the Quality Control (QC) department. If the resins are rejected by QC, they are returned to the supplier and if the resins are approved by QC, they are shifted to the raw material store. Then from the raw material store, these resins are issued to injection molding machines for preform production. There are two injection molding machines named as, Huskey's machines (H-1 and H-2). H-1 machine has 48 cavities and produces perform of different weights such as (19, 25, 28, 39, 45, 48) gm. While H-2 has 96 cavities and produces perform of weights (17, 19, 25, 28, and 39) gm. After the production of perform, they are checked by the QC department. The rejected performs are sent to the crush unit for recycling and the approved performs are shifted to raw material store. After this, the approved performs are issued to the blow molding in order to produce PET bottles from the performs. PET bottles produced are checked by QC section. The rejected bottles are sent to the crush unit for recycling and the approved bottles are packed and kept in the store and are dispatched to the customers when orders

are received. The rejects from both injection molding and blow molding are sent to the crush unit for recycling and then the recycled material is issued to

injection molding and the same process continues again and again.

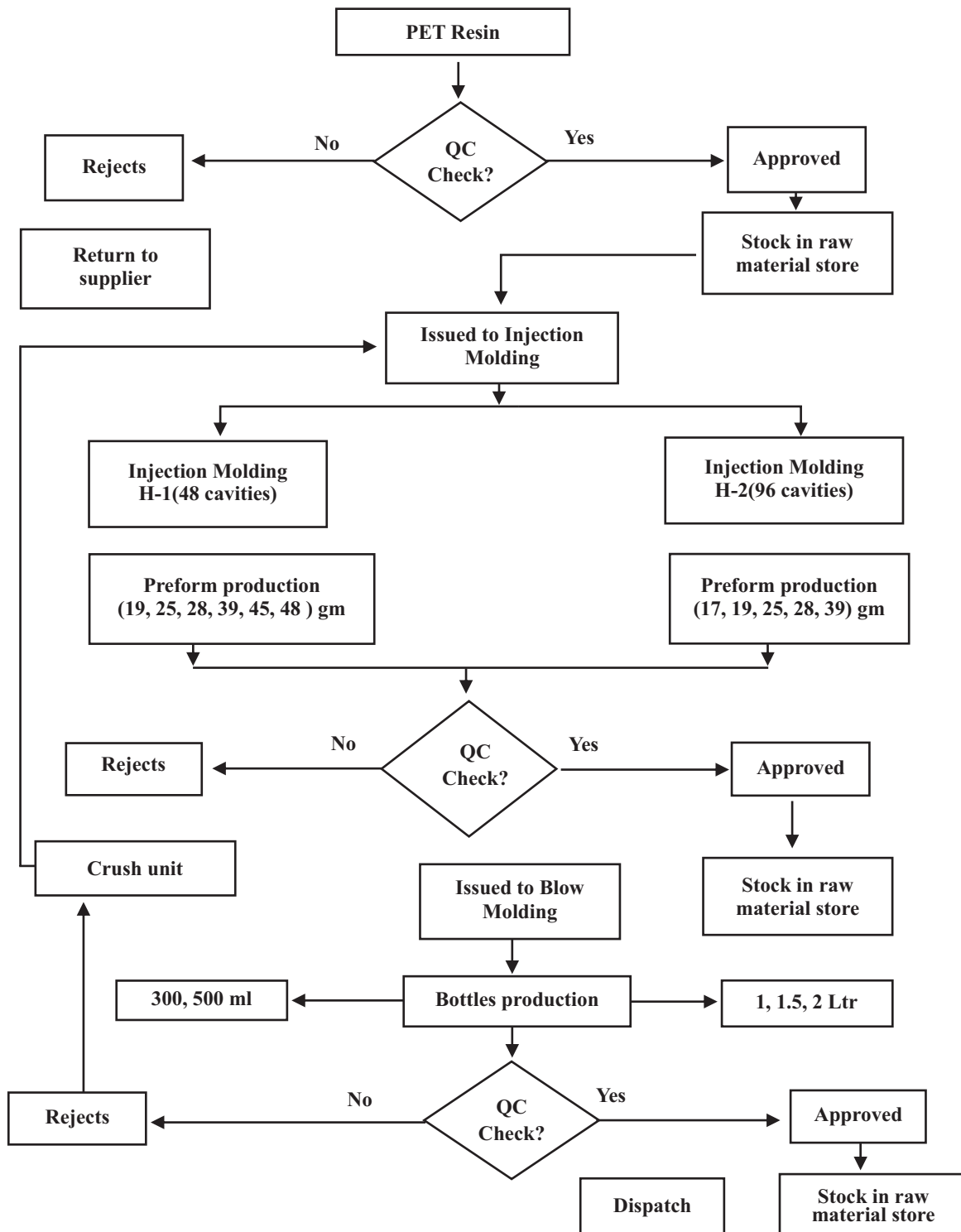


Fig. 2. Flow chart PET bottles manufacturing process.

2) Types of defects

Defects were commonly observed in the injection molding process. The injection molding process was focused for further analysis to figure out significant

factors that results in increased defect rate. Defects observed in the process could be in different forms. Major types have been listed below.

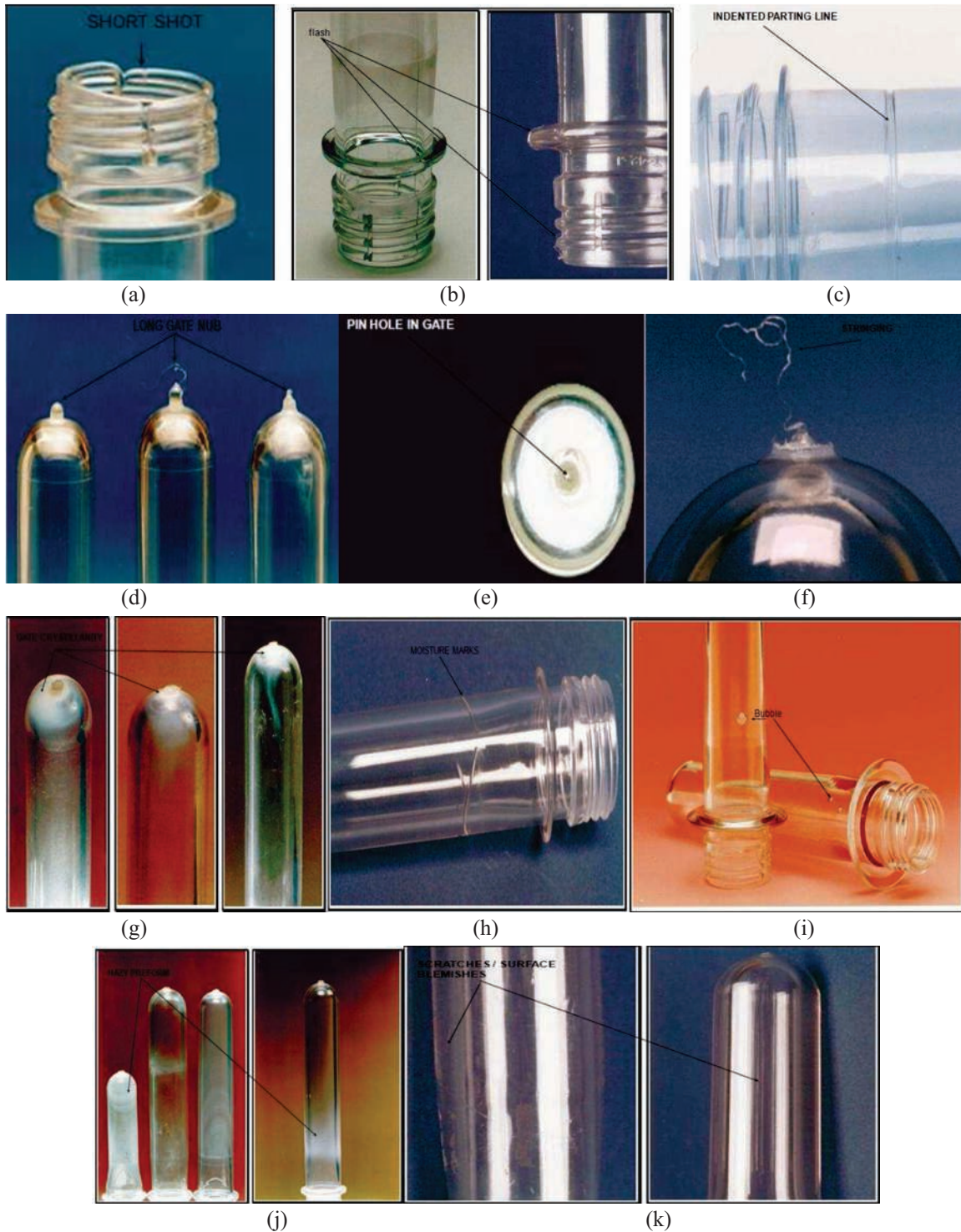


Fig. 3. Types of Defects in PET bottle production processes: (a) Short Shot (b) Flash on thread (c) Parting line flash (d) Long gate (e) Gate pin hole (f) Gate stringing (g) gate crystallization (h) moisture marks (i) air bubbles (j) Hazy Preform (k) Scratches.

II. STATISTICAL ANALYSIS AND DISCUSSION

Following factors have been identified in order to improve the process output.

1. Types of resin
2. Operator line
3. Melting temperature
4. Injection pressure

Resin type were differentiated on the basis of shape and size i.e., circular (type A) and rectangular (type B). There were two injection molding machines in operation which were named as operator line 1, and operator line 2. As per the PET bottles manufacturing company common practices the acceptable range for the melting temperature is 250°C-310°C and for the injection pressure is 40 Pa-70 Pa. There were also some nuisance factors which are:

1. Moisture Content
2. Color of Preform

Above four factors were chosen for the experimentation purpose leaving the nuisance factors as the nuisance factors cannot be controlled in the given conditions. Data was collected as number of rejects per hour for each of the four factors, two different levels were selected for each factor as shown in Table I.

TABLE I
FACTORS LEVELS

Factors	Level 1	Level 2
Type of resin	Type A (circular)	Type B (rectangular)
Operator line	Line 1	Line 2
Melting temperature	250 C	310 C
Injection pressure	40 Pa	70 Pa

A sample of 100 hours data was collected at each level for all the factors. A normal probability plot of the residuals gives an indication of whether or not the assumption of the normality of the random errors is appropriate. A normal probability plot of the residuals is shown in Fig. 4, which shows that the normal probability plot is not far from the straight line which indicates that the normality assumption is satisfied for the data.

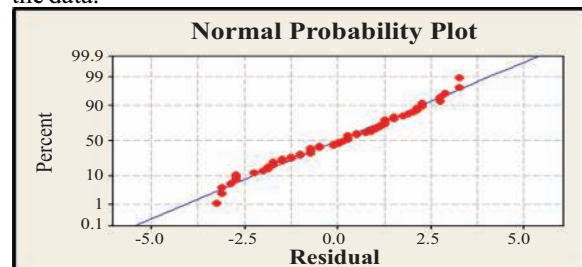


Fig. 4. Normal probability plot for residuals

A. Significant factors identification

Following hypothesis are made in order to know whether these two levels of each factor are of significance.

Hypothesis are rejected based on P-value. Null hypothesis are rejected if the P-value is less than the level of significance. It is assumed that the level of significance (α) is taken as 5 %.

The null and the alternative hypotheses are stated as:

H_0 = Variance of the two levels of each factor are equal.

H_1 = Variance of two levels of each factor are not equal.

An F-test is used to test if the variances of two samples are equal. This test can be a two-tailed test or a one-tailed test. The two-tailed version tests against the alternative that the variances are not equal. The one-tailed version only tests in one direction, that is the variance from the first sample is either greater than or less than the second sample variance.

Table II shows the results of the F-test conducted for the types of resin,

TABLE II
F-TEST FOR TYPES OF RESINS

Test and CI for Two Variances: Number of Defect in A, Number of Defect in B				
Method				
Null hypothesis	$\text{Sigma}(\text{Number of Defects in A per Hour}) / \text{Sigma}(\text{Number of Defects in B per Hour}) = 1$			
Alternative hypothesis	$\text{Sigma}(\text{Number of Defects in A per Hour}) / \text{Sigma}(\text{Number of Defects in B per Hour}) \text{ not } = 1$			
Significance level	Alpha = 0.05			
Statistics				
Variable	N	StDev	Variance	
Number of Defects in A per Hour	25	4.173	17.417	
Number of Defects in B per Hour	25	6.281	39.457	
Distribution of Data	CI for StDev		Variance Ratio	
Normal	(0.441, 1.001)		(0.198, 1.002)	
Continuous	(0.446, 1.038)		(0.199, 1.070)	
Test				
Method	DF1	DF2	Statistic	P-Value
F Test (normal)	24	24	0.44	0.625

Since the p-value = 0.025 < $\alpha=0.05$, therefore, the Null hypothesis (H_0) is rejected in the favor of alternative hypothesis (H_1) and it is concluded that the variance for two types of resin is not equal. For the operator lines (L_1 and L_2)

TABLE III
F-TEST FOR OPERATOR LINES

Test and CI for Two Variances: Line 1, Line2				
Method				
Null hypothesis	$\text{Sigma}(\text{Line 1}) / \text{Sigma}(\text{Line2}) = 1$			
Alternative hypothesis	$\text{Sigma}(\text{Line 1}) / \text{Sigma}(\text{Line2}) \text{ not} = 1$			
Significance level	Alpha = 0.05			
Statistics				
Variable	N	StDev	Variance	
Line 1	100	4.266	18.196	
Line2	100	3.453	13.344	
Distribution of Data				
	CI for StDev	Variance Ratio		
Normal	(0.958, 1.424)	(0.917, 2.027)		
Continuous	(0.937, 1.451)	(0.878, 2.192)		
Method				
	DF1	DF2	Statistic	F-Value
F Test (normal)	99	99	1.36	0.0622

Since the p-value = 0.0622 > $\alpha=0.05$, therefore, the null hypothesis H_0 cannot be rejected.

For melting temperatures

Since the $p(F<=f) = 0.594 > \alpha=0.05$. The null hypothesis H_0 is true in this case, which means that the variance of the two levels of temperature is equal.

TABLE IV
F-TEST FOR MELTING TEMPERATURE

Test and CI for Two Variances: Low Temperature, High Temperature				
Method				
Null hypothesis	$\text{Sigma}(\text{Low Temperature}) / \text{Sigma}(\text{High Temperature}) = 1$			
Alternative hypothesis	$\text{Sigma}(\text{Low Temperature}) / \text{Sigma}(\text{High Temperature}) \text{ not} = 1$			
Significance level	Alpha = 0.05			
Statistics				
Variable	N	StDev	Variance	
Low Temperature	100	4.231	17.899	
High Temperature	100	4.464	19.928	
Distribution of Data	CI for StDev		Variance	
	Ratio		Ratio	
Normal	(0.777, 1.155)		(0.604, 1.335)	
Continuous	(0.740, 1.138)		(0.547, 1.295)	
Method	DF1	DF2	Statistic	P-Value
F Test (normal)	99	99	0.90	0.594

For low and high pressures

TABLE V
F-TEST FOR INJECTION PRESSURE

Test and CI for Two Variances: Low Pressure, High Pressure					
Method					
Null hypothesis	$\text{Sigma}(\text{Low Pressure}) / \text{Sigma}(\text{High Pressure}) = 1$				
Alternative hypothesis	$\text{Sigma}(\text{Low Pressure}) / \text{Sigma}(\text{High Pressure}) \text{ not} = 1$				
Significance level	$\text{Alpha} = 0.05$				
Statistics					
Variable	N	StDev	Variance		
Low Pressure	100	4.604	21.194		
High Pressure	100	6.229	38.794		
Distribution of Data	CI for StDev Ratio	CI for Variance Ratio			
Normal	(0.606, 0.901)	(0.368, 0.812)			
Continuous	(0.640, 1.039)	(0.409, 1.079)			
Test					
Method	DF1	DF2	Statistic	P-Value	
F Test (normal)	99	99	0.55	0.003	

Since the $p\text{-value} = 0.003 < \alpha=0.05$. Therefore, the null hypothesis can be rejected in the favor of H_1 and concludes that the variance for two levels of injection pressure is not equal.

The t-test assesses whether the means of two samples are statistically different from each other. This analysis is appropriate whenever we want to compare the means of two samples.

T-test is performed for the data collected to know whether the means of the two levels of each factor are equal or not. For this, the null and the alternative hypotheses are stated as:

H_0 = means are equal

H_1 = means are not equal

We will reject the null hypothesis, if the p-value is less than or equal to level of significance ($\alpha=0.05$).

Factors having p-value less than the level of significance α , will be having a significant effect on the number of rejects.

For types of resin (A and B)

Table VI shows the difference in means and variance between the types of resin. It is based on hypothesis test since the p-value is less than alpha (α)

level of 0.05, i.e., $P(T \leq t) = 0.001 < \alpha=0.05$. Therefore, we reject the H_0 in the favor of H_1 and conclude that the mean for two types of resin is not equal. Thus the inference from the hypothesis test is that there is a significant difference between the two types of resin and that contributes to the number of preform rejection rate.

For the operator lines (L_1 and L_2)

Table VII shows the difference in means and variance between the operator lines. It is based on hypothesis test since the p-value is greater than α (0.05), i.e. $p(T \leq t) = 0.057 > \alpha=0.05$. Therefore, fail in rejecting the null hypothesis H_0 and therefore the alternative hypothesis H_1 is rejected and concludes that the mean for two operator lines is equal. Thus the inference from the hypothesis test is that there is no significant difference between the two operator lines and that doesn't contribute much to the number of Preform rejects.

TABLE VI
T-TEST FOR TYPES OF RESIN

Two-Sample T-Test and CI: Number of Defects in A p, Number of Defects in B p				
Two-sample T for Number of Defects in A per Hour vs Number of Defects in B per Hour				
	N	Mean	StDev	SE Mean
Number of Defects in A p	25	6.80	4.17	0.83
Number of Defects in B p	25	12.04	6.28	1.3
Difference = μ (Number of Defects in A per Hour) - μ (Number of Defects in B per Hour)				
Estimate for difference: -5.24				
95% CI for difference: (-8.27, -2.21)				
T-Test of difference = 0 (vs not =): T-Value = -3.47 P-Value = 0.001 DF = 48				

TABLE VII
T-TEST FOR OPERATOR LINES

Two-Sample T-Test and CI: Line 1, Line2				
Two-sample T for Line 1 vs Line2				
	N	Mean	StDev	SE Mean
Line 1	100	9.92	4.27	0.43
Line2	100	11.36	3.65	0.37
Difference = μ (Line 1) - μ (Line2)				
Estimate for difference: -1.440				
95% CI for difference: (-2.548, -0.332)				
T-Test of difference = 0 (vs not =): T-Value = -2.56 P-Value = 0.057 DF = 193				

For melting temperatures

Table VIII shows the difference in means and variance between the two levels of melting temperature. It is based on hypothesis test since the P-value is less than Alpha (α) level of 0.05, i.e. $P(T \leq t) = 0.001 < \alpha=0.05$. So we reject the H_0 in the favor of H_1 and concludes that the mean for the two levels of melting temperature is not equal. Thus the inference from the Hypothesis test is that there is a significant difference between the two levels of melting temperature and that contributes to the number of Preform rejects.

For low and high pressures

The t-test figure for the low and high pressures is given below:

Table ix shows the difference in means and variance between the two levels of injection pressure. It is based on hypothesis test since the p-value is less than alpha (α) level of 0.05, i.e. $p(T \leq t) = 0.001 < \alpha = 0.05$. So we reject the H_0 in the favor of H_1 and concludes that the mean for the two levels of injection pressure is not equal. Thus the inference from the Hypothesis test is that there is a significant difference between the two levels of injection pressure and that contributes to the number of Preform rejects.

From the F-test and t-test results, we have identified three controllable factors which are material, injection pressure and melting temperature. We took two levels of each of these factors and a full factorial experimental design was used and a total of 8 experimental runs were required. We made 8 replicates of each run, giving a total of 64 runs. Experimental design matrix was constructed, so that, when the experiment was conducted, the response values could be recorded on the matrix.

TABLE VIII
T-TEST FOR TYPES OF MELTING TEMPERATURE

Two-Sample T-Test and CI: Low Temperature, High Temperature				
Two-sample T for Low Temperature vs High Temperature				
	N	Mean	StDev	SE Mean
Low Temperature	100	12.00	4.23	0.42
High Temperature	100	9.97	4.46	0.45
Difference = μ (Low Temperature) - μ (High Temperature)				
Estimate for difference: 2.030				
95% CI for difference: (0.817, 3.243)				
T-Test of difference = 0 (vs not =): T-Value = 3.30 P-Value = 0.001 DF = 197				

TABLE IX
T-TEST FOR INJECTION PRESSURE

Two-Sample T-Test and CI: Low Pressure, High Pressure				
Two-sample T for Low Pressure vs High Pressure				
	N	Mean	StDev	SE Mean
Low Pressure	100	12.28	4.60	0.46
High Pressure	100	15.56	6.23	0.62
Difference = μ (Low Pressure) - μ (High Pressure)				
Estimate for difference: -3.280				
95% CI for difference: (-4.808, -1.752)				
T-Test of difference = 0 (vs not =): T-Value = -4.23 P-Value = 0.001 DF = 182				

TABLE X
MATRIX FOR DOE RUNS

Run#	Run Order	A	B	C	D-AB	E-AC	F-BC	G-ABC	R1	R2	R3	R4	R5	R6	R7	R8	Ave.	Std.Dev.
1	1	-	-	-	+	+	+	-	12	18	17	12	15	16	16	15	15.1	2.17
2	2	+	+	+	-	-	-	+	10	11	12	8	9	12	10	14	10.8	1.91
3	3	-	+	-	+	-	+	+	21	19	18	22	23	24	21	18	20.8	2.25
4	4	+	-	+	-	+	-	-	16	18	16	19	18	17	17	19	17.5	1.20
5	5	-	-	+	-	-	+	+	6	8	7	8	5	7	6	9	7.0	1.31
6	6	+	+	-	+	+	-	-	4	5	6	4	3	3	3	2	3.8	1.28
7	7	-	+	+	-	-	+	+	14	18	15	17	19	19	15	18	16.9	1.96
8	8	+	-	-	+	+	-	-	9	14	10	13	12	10	14	8	11.3	2.31

In the above matrix, A represents Material type, B represents injection pressure, C represents melting temperature, AB for the interaction effect of material type & injection pressure, AC for material type & melting temperature, BC for injection pressure & melting temperature and ABC for material type, injection pressure & melting temperature. Minus (-) sign represents the level 1 while plus (+) sign represents the level 2 of each factor.

In the first run we took material type A, injection pressure 40 Pa and melting temperature 250°C, and initiated the experiment. We collected the data as number of Preform rejects per hour and recorded on the matrix. We ran the same experiment 8 times and calculated the mean and standard deviation. Similarly in the next run, material type was changed to B while keeping the pressure and temperature the same. The same procedure was applied to all the possible combinations by changing the levels of factors to identify their effect on the response variable (number of Preform rejects). A more clear understanding of the data is illustrated from the cube plot of the data means.

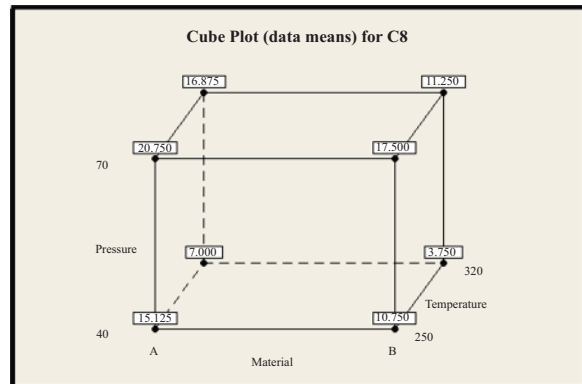


Fig. 5. Cube plot of the data means

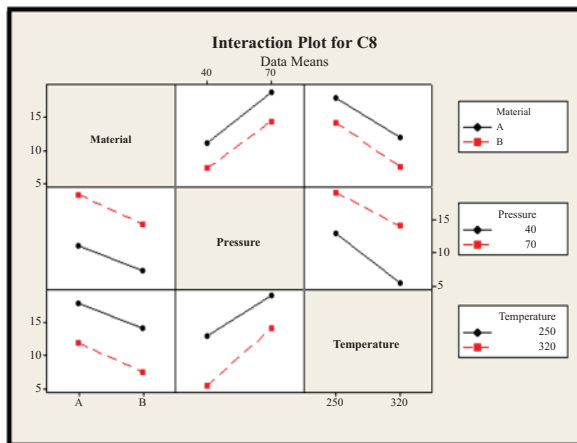


Fig. 6. Interaction plot for the significant factors.

The cube plot in Fig. 5, represents the mean values of the interactive effects at different levels of each factor from the data collected by conducting the DOE runs. The lowest value i.e. 3.750 rejects per hour observed at combination of Material type B, injection pressure 40 Pa and melting temperature 320°C which means that this is the optimal condition for the lowest number of Preform rejects.

The interaction plot Fig. 6, highlights the fact that strong interaction among the three factors does not exist in the given levels. Similar kind of analysis can be observed in the Pareto chart shown in Fig. 7.

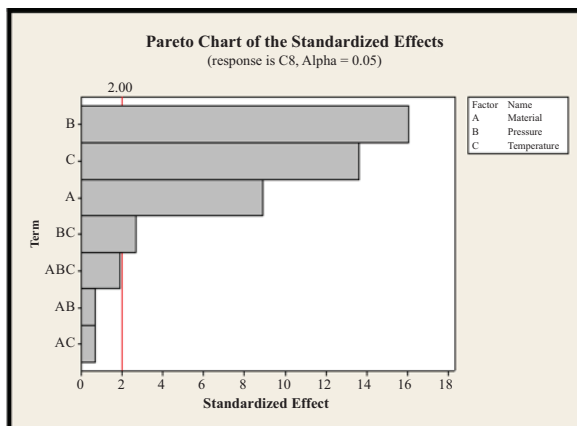


Fig. 7. Pareto chart for the standardized effects of factors.

The Pareto chart in Fig. 7 shows that the most significant factors and interacting are B, C, A, and BC respectively. Other interaction factors can be considered as non-significant. Therefore, the optimal conditions are as under

TABLE XI
OPTIMAL CONDITIONS

Factor	Value/Type	Optimal Setting
PET resin type	B	B
Melting temperature	310 °C	High(+)
Injection pressure	40 Pa	Low(-)

Given the above optimal conditions, the process was carried out for another 100 hours and the number of rejects reduced to an average of 3.750 rejects per hour from 11.24 rejects per hour.

V. CONCLUSIONS

The paper focused the injection molding process for PET bottles manufacturing in a selected company using six sigma approach. The rejection rate has been controlled significantly by highlighting significant factors statistically and set the optimum levels for the significant factors using experimental design approach. Hypothesis were made and analysis was performed based on F-test and t-tests to analyze the data variance and means. Statistical analysis showed that injection pressure, melting temperature, resin type and the interaction effect of pressure and temperature remain significant during the control of rejection rate in the processes. It was further shown that resin type B, high melting temperature, and low pressure resulted in reduced average number of rejections per hour. These optimal settings are strongly recommended for practitioners in the said field. The study was limited to the injection molding process in the PET bottles manufacturing process. The research findings are useful for PET bottles manufacturers especially for defect rate reduction. The methodology and sequence of tests used in this project can also be repeated for a specific type of rejects. For instance, the most common rejects in the selected industry was short shots so the whole projects can be repeated for this specific type of rejects. The research can be further extended to other relevant areas of manufacturing processes for process improvement.

REFERENCES

- [i] K. Linderman, R.G. Schroeder, S. Zaheer, A.S. Choo, "Six Sigma: a goal-theoretic perspective," *Journal of Operations Management*, vol. 21, 2003, pp. 193-203.
- [ii] B. Nakhai, J.S. Neves, "The challenges of six sigma in improving service quality," *International Journal of Quality & Reliability Management*, vol. 26, 2009, pp. 663-684.
- [iii] J. Antony, "Six sigma for service processes," *Business Process Management Journal*, vol. 12, 2006, pp. 234-248.
- [iv] J. de Mast, J. Lokkerbol, "An analysis of the Six

- Sigma DMAIC method from the perspective of problem solving," *International Journal of Production Economics.*, vol.139,2012,pp.604-614.
- [v] A. Balakrishnan, R. Kalakota, P.S. Ow, A.B. Whinston, "Document-centered information systems to support reactive problem-solving in manufacturing," *International Journal of Production Economics.*,vol.38, 1995,pp.31-58.
- [vi] R. G. Schroeder, K. Linderman, C. Liedtke, A.S. Choo, "Six Sigma: Definition and underlying theory," *Journal of Operations Management.*, vol. 26,2008,pp.536-554.
- [vii] R. McAdam, B. Lafferty, "A multilevel case study critique of six sigma: statistical control or strategic change?," *International Journal of Operations & Production Management.*, vol.24,2004,pp.530-549.
- [viii] S. S. Chakravorty, "Six Sigma programs: An implementation model," *International Journal of Production Economics.*,vol.119,2009,pp.1-16.

Casagrande Liquid Limit Testing Of Jamshoro Soil By One Point Method

M. Aslam¹, S. N. R. Shah², S. H. Otho³

¹Civil Engineering Department, University of Malaya, Kuala Lumpur, 50603, Malaysia

^{2,3}Civil Engineering Department, Mehran University of Engineering & Technology, SZAB Campus, Khairpur Mir's, Pakistan

¹aslam_bhanbhro13@yahoo.com

Abstract-The Liquid limit (LL) tests are considered essential to determine the index properties of soil. Casagrande liquid limit test is one of these tests and universally recognized for soil testing. The purpose of this research work is to introduce the constant values of index (e) and Number of Blows for A-7-6 (AASHTO Classification) clayey shale type soils using one point formula. 100 samples of A-7-6 soil were collected from Jamshoro (Pakistan) zone and multi point Casagrande liquid limit laboratory tests were performed. After obtaining test results, samples were squeezed out with appropriate range of LL covering maximum number of samples. Suitable range of number of blows was chosen and the most appropriate index (e) value for selected soil samples was calculated. The experimental results were compared with one point formula results. The reliability of LL between experimental results and one point formula results exhibited excellent relationship.

Keywords-Jamshoro, Liquid Limits, Casagrande, Clayey Soil, One Point Formula, Index Value.

I. INTRODUCTION

The liquid limit (LL) and plastic limit (PL) of soil, also called consistency limits or Atterberg limits, are very important physical parameters for soil science [i-iii]. Atterberg observed that soil is less resistant against moulding at specified quantity of water. Furthermore, the cracks may be developed in the soil at lower moisture content [iv]. In order to distinguish the states of soil or clay, Atterberg introduced that at lowest water content, (expressed in mass percent of the clay dried at 120 °C) the body can be rolled into threads without failure and this state is called the plastic limit of soil. The liquid limit is defined as a state in which the body takes the shape of fluid after processing through a specified equipment [iv-v]. Later, Reed [vi] used the term “consistency” referring to the states of ceramic raw materials relying on water content. According to Reed [vi], the quantity of water required to change normal clay into plastic state is referred to as plastic limit. The initial effect of adding water to dry clay is the increase in cohesion of molecules which gradually

reaches to the removal of air from voids between particles. Adding more water into the voids tends the body to easily fail under deformation. Slurry system is established at high water contents body starts to flow. That phase is referred to as liquid limit of that body. The difference in the quantity of water at two limiting points, related to the dry mass of the clay, is expressed as the “plasticity index” (PI), [vi]. The liquid and plastic limits define the transitions between liquid and plastic behavior. These limits can give significant information about the behavior of soil [vii].

In order to determine plastic and liquid limits of soil, Casagrande investigated various soil types using an innovative method to determine the plasticity of clayish and non-clayish materials [viii]. Casagrande method is widely used to evaluate Atterberg's limits. However, it utilizes large number of variables which results in a complex comprehensive relationship between the parameters and performance of soil. This problem was solved by a probabilistic approach put forwarded by Gutiérrez (2006). He used regression analysis and expressed linear behavior of consistency limits for soil [ix].

The most commonly used methods to evaluate the liquid limit of soil are multipoint test and one-point tests methods [x]. Multipoint test method is recommended to obtain highly précised results. Multipoint tests are performed for organic soils or the soils existing in marine environment. The one-point liquid limit test is based on the experience that the slope of the liquid limit flow line for soils within a given geologic environment is essentially a constant on a logarithmic plot. Thus, the liquid limit can be determined provided that the constant defining the slope has been established from correlations on the soil in question. The one-point liquid limit test is preferred in areas where the soils are geologically similar. Moreover, adequate correlations defining the slope of the liquid limit flow line are required to be made and consistency required to cause closure at 20-30 blows. One-point method demands vigilant observation of duration taken by the specimen to achieve its liquid limit. Therefore, inexperienced technicians generally avoid one-point testing. One-point method does not require high cost, however, the lack of accuracy is a

limitation of this method which limits its use in controlling materials [xi].

Established to designate fine grained soils as clay and silt, universally accepted standard test methods have been solely performed on soils sieved through # 40 mesh. Because consistency limits are characteristic to fine-grained soils, and the material passing through # 40 mesh may include a significant amount of sand, the use of a # 40 sieve for this purpose may lead to significant errors regarding the class or plasticity level of a soil. The Atterberg limits are the basic parameters for classifying the plastic soils. Two main approaches are available in the literature to find the liquid limit values: the percussion method (originally proposed by Casagrande) [xii], and the fall cone method (originally suggested by Geotechnical Commission of Swedish State Railways (GCSSR) [xiii]). Based on the fundamentals of the above mentioned two methods, several methods were developed and implemented worldwide. The Bureau de normalization du Quebec, and then, the Canadian Standards Association, defined their own standards concerning these tests according to the devices and procedures described by Swedish Commission and Casagrande, for fall cones and percussion methods, respectively [viii-xiv]. They also proposed simple and new Single Point Method for determining the Liquid limit values by using Casagrande and fall cone methods. Canadian scientists prefer the fall cone method due to its advantages defined by Garneau and Le Bihan [xv]. Sanzeni et al. [xvi] examined the specific surface and hydraulic conductivity of fine-grained soils. They applied several testing methods and the one point method showed better performance. Kumar and Kumar [xvii] used various industrial wastes and examined the stabilization of clayey type soil. The results showed that fly ash has a significant impact on the liquid limit of soil.

In general, the purpose of this research work is to introduce the constant values of index (e) and Number of Blows for A-7-6 clayey shale type soils used in One Point Formula of Liquid limit by Casagrande method. Such soil exists in the Jamshoro (Pakistan) zone. The soil samples have been taken from different parts of Jamshoro. This research will minimize the efforts and will provide easiness and time saving for the researchers and designers in Jamshoro zone to calculate the liquid limit of soil existing in that area. The liquid limit values calculated in this research can be used directly without performing several liquid limit laboratory tests every time. A comparison of the experimental and one point formula results is presented to ensure the authenticity of findings.

II. METHODOLOGY

A. Liquid Limit Apparatus

The Casagrande liquid limit instrument, as shown

in Fig. 1, suggested by Indian standards [xviii- xix], was selected for performing the laboratory tests on the specimens. The drop height adjustment of the cup was 10 mm. The crank was turned at 2 revolutions per second while holding the guage in position against the tape and cup in order to check the adjustment. The grooving tool with a tip width and depth of 2.5 mm and 8.0 mm, respectively, was used. The soil samples were sieved through a 20.3 cm diameter (No. 40) sieve, in accordance with the requirements of ASTM Specification [viii] with a rim of 5 cm above the mesh. Balance of capacity was 500 grams and sensitivity was 0.01gram. Thermostatically controlled oven with a capacity up to 250 °C was used for drying the soil samples at controlled temperature. Porcelain evaporating dish of 12-15 cm diameter was used and the spatula used for mixing was flexible with 8 cm long and 2 cm wide blade. Palette knives of 20 cm long and 3 cm wide blade were utilized to properly mix and fill the testing cup. Containers were kept air-tight and non-corrodible for determination of moisture content.

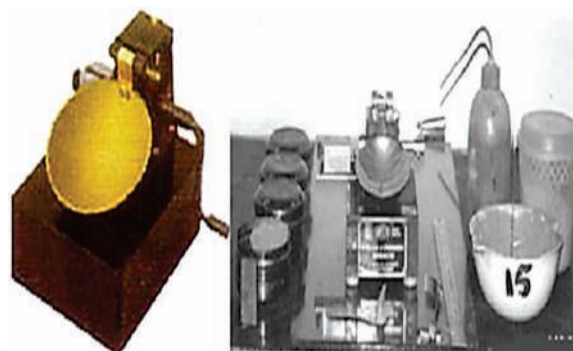


Fig. 1. Casagrande apparatus

B. Mixture details

The ground was excavated up to 3 ft with the help of available instruments and labor and 100 samples of clayey soil were collected. The samples were placed in the oven for 24 hours. The dried samples were then sieved using # 40 meshes to achieve a 300 gram sample. It was observed that the sample has no material retained on the 425-urn (No. 40) sieve. A mixture was prepared by adding distilled water to the samples on the glass plate using the spatula. Initial mixing time was 30 minutes. The prepared mixture was placed in open air to achieve the desired moisture content. Water content of the soil was brought to a consistency by 15 to 25 blows of the liquid limit device to close the groove. The soil was re-mixed 24 hours before the tests and LL was determined.

I. RESULTS

After the collection of all the samples, the liquid limit test was performed. The experimental procedure was repeated for all the 100 samples and 100 graphs

were plotted following the procedure suggested by [xx]. The flow curve of one sample as a typical curve is shown in Fig. 2. The typical curve was plotted by considering number of blows and the water content of the sample. After the sample was cut and groove was made, the crank device was rotated at 2 revolutions per second. The number of blows (N) were counted that caused the sample closure (make the paste so that N begins with a value higher than 35). When N was in the range of 15 to 40, the sample was collected and weighed. When soil was not dried as per requirement, the mixture was exposed to fan and continuous mixing was performed, rather than adding more soil. Then, the cup was cleaned after each trial. A minimum of three trials with values of $N \sim 15$ to 40 were performed and after 24 hours, the corresponding water content (%) was determined. The resultant flow curve was plotted as shown in Fig. 2. However, as per suggested by codes, the liquid limit values of all the samples were selected at 25 number of blows. Meanwhile, the liquid limit values of all the samples with their respective number of blows are shown in Table I.

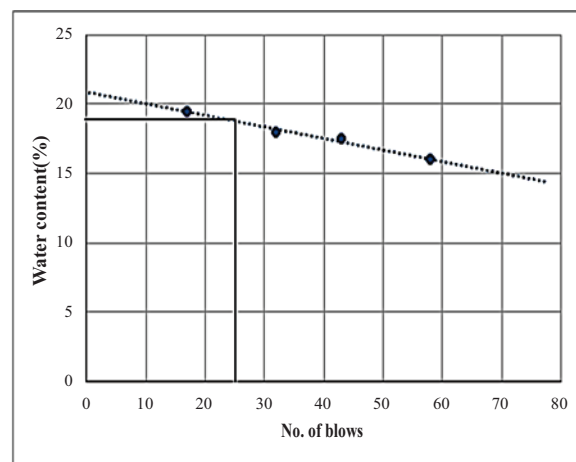


Fig. 2. Typical flow curve of the liquid limit for one sample

TABLE I
LIQUID LIMIT VALUES AND NUMBER OF BLOWS OF ALL THE SAMPLES

Sample No.	Number of Blows	Liquid Limit (%)	Sample No.	Number of Blows	Liquid Limit (%)
01	25	18	51	25	43
02	25	42	52	25	19
03	25	44	53	25	45
04	25	16	54	25	52
05	25	26	55	25	23
06	25	28	56	25	50
07	25	21	57	25	52
08	25	33	58	25	22
09	25	21	59	25	52
10	25	21	60	25	28
11	25	40	61	25	16
12	25	57	62	25	24
13	25	36	63	25	16
14	25	21	64	25	28
15	25	52	65	25	18
16	25	29	66	25	22
17	25	25	67	25	19
18	25	18	68	25	18
19	25	19	69	25	18
20	25	29	70	25	19
21	25	17	71	25	18
22	25	22	72	25	19
23	25	26	73	25	20
24	25	44	74	25	18
25	25	18	75	25	18
26	25	18	76	25	20
27	25	52	77	25	43
28	25	24	78	25	42
29	25	19	79	25	26
30	25	53	80	25	28

31	25	46	81	25	51
32	25	17	82	25	58
33	25	19	83	25	52
34	25	46	84	25	33
35	25	26	85	25	87
36	25	19	86	25	40
37	25	18	87	25	20
38	25	19	88	25	36
39	25	22	89	25	42
40	25	56	90	25	38
41	25	22	91	25	20
42	25	16	92	25	18
43	25	16	93	25	30
44	25	22	94	25	55
45	25	17	95	25	20
46	25	16	96	25	16
47	25	18	97	25	19
48	25	20	98	25	30
49	25	18	99	25	52
50	25	28	100	25	42

As can be seen in Table I, the results indicate variations in the readings for the liquid limits. In order to precise the results, the samples are divided into different groups according to the similarity exists in the values of liquid limits. Fig. 3 shows 56 samples out of 100, which contains the liquid limit range from 16 to 26. The major reason to select this range of the liquid limit was obtained from the literature. As it was observed that most of researchers have reported that the liquid limit range of Jamshoro soil is 15-25 [xxi-xxiv]. Therefore, authors believe that the 16-26 is the most suitable range to compute and investigate the various parameters of the liquid limit for the Jamshoro region. The detailed liquid limit values of the selected 56 samples are presented in Table II.

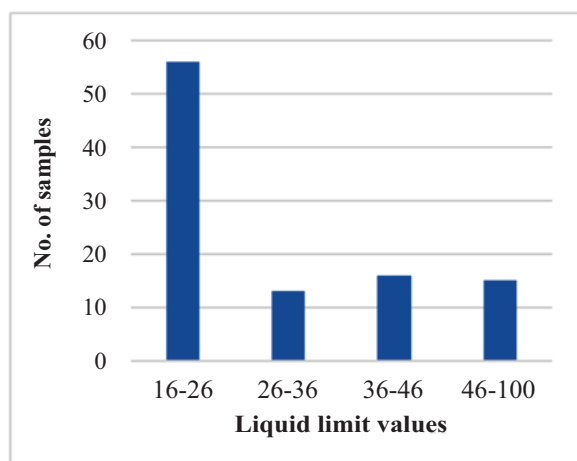


Fig. 3. Number of samples in Different LL ranges

TABLE II
LIQUID LIMIT VALUES OF SELECTED 56 SAMPLES

No.	Liquid Limit Values	No. Of Samples
1	16	6
2	17	3
3	18	14
4	19	9
5	20	6
6	21	4
7	22	6
8	23	1
9	24	2
10	25	1
11	26	4

III. COMPUTATION OF INDEX (e) VALUES

A range of number of blows between 20 and 30 was selected as suggested in [xvi]. From this range, the values of 20, 26 and 30 number of blows were further selected to calculate the index (e) values. The water content values were 19%, 16% and 16%, respectively, which were computed from the liquid limit graphs as shown in Fig. 4. The water content values for the rest of the samples were also drawn from the previously prepared liquid limit graphs in a similar manner.

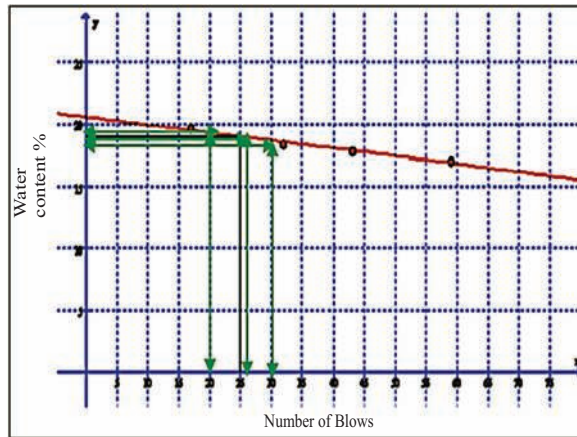


Fig. 4. Water content values @ different number of blows

A. Index (e) values @ 20-26-30 blows

Eq. 1 (One Point formula of liquid limit) is used to find the index (e) values.

$$LL = W * (N/25)^e \quad (1)$$

Now by rearranging this formula,

$$e = \log(LL/w) \log(N/25) \quad (2)$$

Where;

LL= Liquid Limit Values, W= Water Content (%), N= Number of Blows and e= Index (slope of the flow line).

At 20, 26 and 30 number of blows, the calculated index (e) values of the selected samples having Liquid Limits 16, 17, 18, 19, 20, 21, 22, 24 and 26 are given in Tables III-X, respectively. The comparison of obtained index values of all 56 specimens in the range 16-26 is presented in Fig. 5.

TABLE III
INDEX (e) VALUES OF LL=16 AT 20, 26 & 30
NUMBER OF BLOWS

S. No.	LL	W @ 20 Blows	W @ 26 Blows	W @ 30 Blows	Index (e) @ 20 Blows	Index (e) @ 26 Blows	Index (e) @ 30 Blows
1.	16	19	15.8	14	0.770	0.320	0.732
2.	16	17.5	15.6	15.8	0.401	0.646	0.068
3.	16	16.5	15.75	15.5	0.138	0.402	0.174
4.	16	17	15.67	15.2	0.271	0.531	0.281
5.	16	16.5	15.9	15.58	0.138	0.159	0.146
6.	16	16.5	15.85	15.5	0.138	0.240	0.174

TABLE IV
INDEX (e) VALUES OF LL=17 AT 20, 26 & 30
NUMBER OF BLOWS

S. No.	LL	W @ 20 Blows	W @ 26 Blows	W @ 30 Blows	Index (e) @ 20 Blows	Index (e) @ 26 Blows	Index (e) @ 30 Blows
1.	17	18	16.6	16.15	0.2561	0.607	0.2813
2.	17	18.5	16.7	16.5	0.3789	0.453	0.1637
3.	17	17.3	16.8	16	0.0783	0.301	0.3325

TABLE V
INDEX (e) VALUES OF LL=18 AT 20, 26 & 30
NUMBER OF BLOWS

S. No.	LL	W @ 20 Blows	W @ 26 Blows	W @ 30 Blows	Index (e) @ 20 Blows	Index (e) @ 26 Blows	Index (e) @ 30 Blows
1.	18	19	17.75	17.75	0.2422	0.3566	0.0767
2.	18	19.1	17.8	17	0.2658	0.2848	0.3135
3.	18	19.2	17.85	16.5	0.2892	0.2133	0.4772
4.	18	19.3	17.88	16	0.3125	0.1705	0.6460
5.	18	18.4	17.9	16.2	0.0984	0.1420	0.5778
6.	18	18.5	18	17.5	0.1227	0	0.1545
7.	18	19.5	17.98	17.58	0.3587	0.0283	0.1294
8.	18	18.08	17.88	17.65	0.0198	0.1705	0.1077
9.	18	19	17.78	17.4	0.2422	0.3135	0.1859
10.	18	19.1	17.82	17	0.2658	0.2562	0.3135
11.	18	19.5	17.92	16.5	0.3587	0.1136	0.4772
12.	18	19	17.88	17.2	0.2422	0.1705	0.2493
13.	18	19.8	17.9	17.9	0.4271	0.1420	0.0305
14.	18	18.1	17.68	17.52	0.0248	0.4573	0.1482

TABLE VI
INDEX (e) VALUES OF LL=19 AT 20, 26 & 30
NUMBER OF BLOWS

S. No.	LL	W @ 20 Blows	W @ 26 Blows	W @ 30 Blows	Index (e) @ 20 Blows	Index (e) @ 26 Blows	Index (e) @ 30 Blows
1.	19	20.1	18.5	17	0.2522	0.6799	0.6100
2.	19	20	18.7	18	0.2298	0.4058	0.2965
3.	19	19.4	18.6	17.5	0.0933	0.5425	0.4510
4.	19	20.2	18.65	18.5	0.2744	0.4740	0.1462
5.	19	19.7	18.85	18.58	0.1621	0.2020	0.1226
6.	19	19.9	18.88	18	0.2074	0.1615	0.2965
7.	19	19.1	18.87	18.7	0.0235	0.1750	0.0872
8.	19	19.5	18.9	18.7	0.1164	0.1345	0.0872
9.	19	19.85	18.92	18.1	0.1961	0.1075	0.2661

TABLE VII
INDEX (e) VALUES OF LL=20 AT 20, 26 & 30
NUMBER OF BLOWS

S. No.	LL	W @ 20 Blows	W @ 26 Blows	W @ 30 Blows	Index (e) @ 20 Blows	Index (e) @ 26 Blows	Index (e) @ 30 Blows
1.	20	20.2	19.5	19	0.045	0.646	0.281
2.	20	21	19.6	18	0.218	0.515	0.578
3.	20	22	19.6	18.2	0.427	0.450	0.517
4.	20	20.3	19.7	18.5	0.067	0.385	0.427
5.	20	20.5	19.8	19	0.110	0.256	0.281
6.	20	20.8	19.9	19.5	0.175	0.128	0.138

TABLE VIII
INDEX (e) VALUES OF LL=21 AT 20, 26 & 30
NUMBER OF BLOWS

S. No.	LL	W @ 20 Blows	W @ 26 Blows	W @ 30 Blows	Index (e) @ 20 Blows	Index (e) @ 26 Blows	Index (e) @ 30 Blows
1.	21	21.7	20.5	19	0.146	0.614	0.548
2.	21	21.2	20.75	20	0.042	0.305	0.267
3.	21	21.5	20.7	20.5	0.105	0.366	0.132
4.	21	21.9	20.9	20.5	0.188	0.121	0.110

TABLE IX
INDEX (e) VALUES OF LL=22 AT 20, 26 & 30
NUMBER OF BLOWS

S. No.	LL	W @ 20 Blows	W @ 26 Blows	W @ 30 Blows	Index (e) @ 20 Blows	Index (e) @ 26 Blows	Index (e) @ 30 Blows
1.	22	22.5	21.7	21	0.101	0.350	0.255
2.	22	22.3	21.6	20.5	0.0607	0.467	0.387
3.	22	23.1	21.8	21.5	0.2186	0.232	0.126
4.	22	22.23	21.85	21	0.0466	0.174	0.255
5.	22	22.5	21.9	21.65	0.102	0.116	0.088
6.	22	23.5	21.87	20	0.2955	0.151	0.522

TABLE X
INDEX (e) VALUES OF LL=24 AT 20, 26 & 30
NUMBER OF BLOWS

S. No.	LL	W @ 20 Blows	W @ 26 Blows	W @ 30 Blows	Index (e) @ 20 Blows	Index (e) @ 26 Blows	Index (e) @ 30 Blows
1.	24	25.1	23.7	22	0.200	0.321	0.477
2.	24	25.5	23.8	23.5	0.271	0.213	0.115

TABLE XI
INDEX (e) VALUES OF LL=26 AT 20, 26 & 30
NUMBER OF BLOWS

S. No.	LL	W @ 20 Blows	W @ 26 Blows	W @ 30 Blows	Index (e) @ 20 Blows	Index (e) @ 26 Blows	Index (e) @ 30 Blows
1.	26	26.5	25.7	25	0.085	0.296	0.296
2.	26	27.3	25.8	23.5	0.218	0.196	0.196
3.	26	28	25.88	24	0.332	0.118	0.118
4.	26	26.85	25.92	25.80	0.144	0.078	0.078

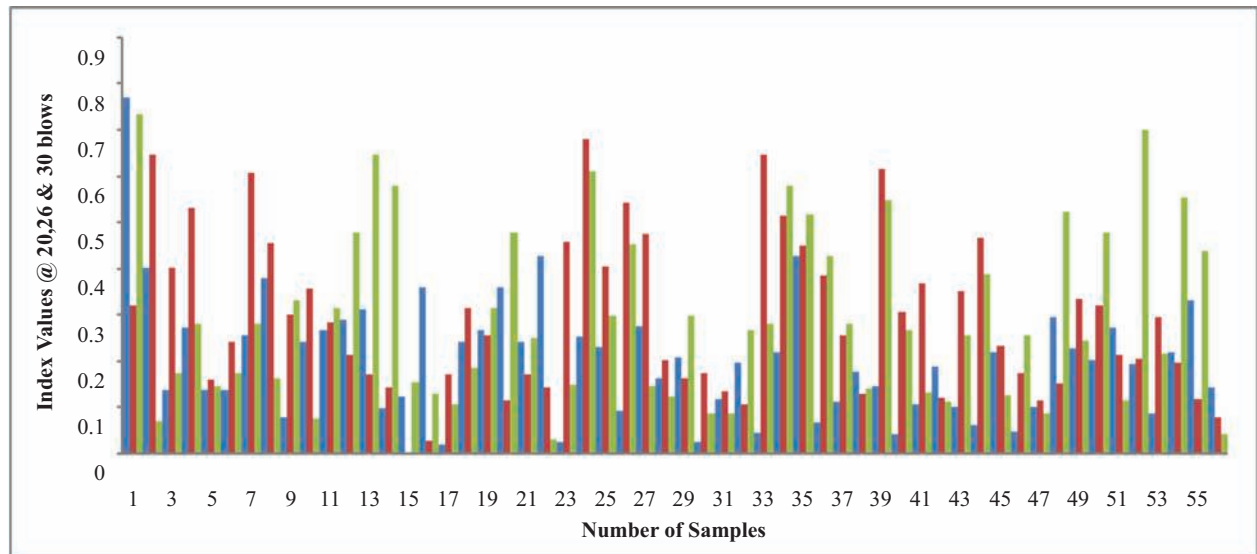


Fig. 5. All 56 Index (e) values @ 20, 26 & 30 Number of Blows

B. Index (e) values for soil specimens

The most appropriate value of index can be calculated by finding out the average of available index values at selected number of blows.

The average value of index (e) at 20 number of blows = $e_{20} = 0.20393$

The average value of index (e) at 26 number of blows = $e_{26} = 0.29301$

The average value of index (e) at 30 number of blows = $e_{30} = 0.29131$

The average of these three values of index (e) will finally give the required value:

$$e_{RK} = (e_{20} + e_{26} + e_{30}) / 3$$

$$e_{RK} = (0.20393 + 0.29301 + 0.29131) / 3$$

$$e_{RK} = 0.26275$$

$$e_{RK} = 0.263$$

IV. VALIDATION

After the computation of the index (e) values at 20, 26 and 30 number of blows, the values are utilized to compute liquid limit values using one point formula and to validate the reliability. The values of liquid limit and index (e) at 20, 26 and 30 number of blows are explained in Tables XII, XIII, and XIV, respectively. The graphical comparison of liquid limit and index (e)

at 20, 26 and 30 number of blows are shown in Figs. 6, 7 and 8, respectively.

TABLE XII
COMPARISON OF LIQUID LIMIT BY ONE POINT &
EXPERIMENTAL RESULTS @ 20 BLOWS

No.	W	N	e @ 20 Blows	LL by One Point Value	LL by Exp: Results
1.	19	20	0.263	17.91704	16
2.	17.5	20	0.263	16.50254	16
3.	16.5	20	0.263	15.55953	16
4.	17	20	0.263	16.03104	16
5.	16.5	20	0.263	15.55953	16
6.	16.5	20	0.263	15.55953	16
7.	18	20	0.263	16.97404	17
8.	18.5	20	0.263	17.44554	17
9.	17.3	20	0.263	16.31394	17
10.	19	20	0.263	17.91704	18
11.	19.1	20	0.263	18.01134	18
12.	19.2	20	0.263	18.10564	18
13.	19.3	20	0.263	18.19994	18
14.	18.4	20	0.263	17.35124	18
15.	18.5	20	0.263	17.44554	18
16.	19.5	20	0.263	18.38854	18
17.	18.08	20	0.263	17.04948	18
18.	19	20	0.263	17.91704	18
19.	19.1	20	0.263	18.01134	18
20.	19.5	20	0.263	18.38854	18
21.	19	20	0.263	17.91704	18
22.	19.8	20	0.263	18.67144	18
23.	18.1	20	0.263	17.06834	18
24.	20.1	20	0.263	18.95434	19
25.	20	20	0.263	18.86004	19
26.	19.4	20	0.263	18.29424	19
27.	20.2	20	0.263	19.04864	19
28.	19.7	20	0.263	18.57714	19
29.	19.9	20	0.263	18.76574	19
30.	19.1	20	0.263	18.01134	19
31.	19.5	20	0.263	18.38854	19
32.	19.85	20	0.263	18.71859	19
33.	20.2	20	0.263	19.04864	20
34.	21	20	0.263	19.80304	20
35.	22	20	0.263	20.74605	20
36.	20.3	20	0.263	19.14294	20
37.	20.5	20	0.263	19.33154	20
38.	20.8	20	0.263	19.61444	20
39.	21.7	20	0.263	20.46315	21
40.	21.2	20	0.263	19.99164	21
41.	21.5	20	0.263	20.27455	21
42.	21.9	20	0.263	20.65175	21
43.	22.5	20	0.263	21.21755	22
44.	22.3	20	0.263	21.02895	22
45.	23.1	20	0.263	21.78335	22
46.	22.23	20	0.263	20.96294	22
47.	22.5	20	0.263	21.21755	22
48.	23.5	20	0.263	22.16055	22
49.	24.2	20	0.263	22.82065	23
50.	25.1	20	0.263	23.66935	24
51.	25.5	20	0.263	24.04655	24
52.	26.1	20	0.263	24.61236	25
53.	26.5	20	0.263	24.98956	26
54.	27.3	20	0.263	25.74396	26
55.	28	20	0.263	26.40406	26
56.	26.85	20	0.263	25.31961	26

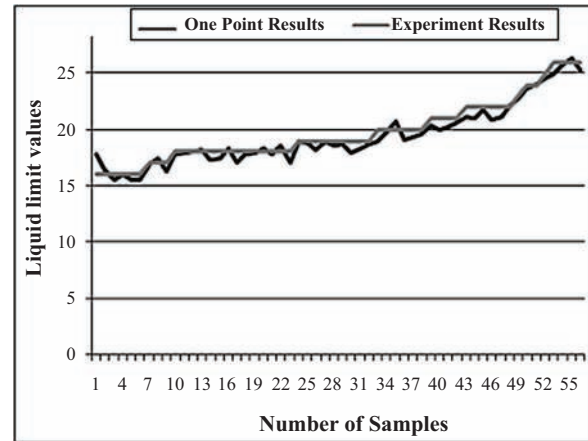


Fig. 6. Comparison of LL b/w One Point & Experimental Results @ 20 number of Blows

TABLE XIII
COMPARISON OF LIQUID LIMIT BY ONE POINT &
EXPERIMENTAL RESULTS @ 26 BLOWS

No.	W	N	e @ 20 Blows	LL by One Point Value	LL by Exp: Results
1.	15.8	26	0.263	15.96382	16
2.	15.6	26	0.263	15.76175	16
3.	15.75	26	0.263	15.9133	16
4.	15.67	26	0.263	15.83247	16
5.	15.9	26	0.263	16.06486	16
6.	15.85	26	0.263	16.01434	16
7.	16.6	26	0.263	16.77212	17
8.	16.7	26	0.263	16.87315	17
9.	16.8	26	0.263	16.97419	17
10.	17.75	26	0.263	17.93404	18
11.	17.8	26	0.263	17.98456	18
12.	17.85	26	0.263	18.03508	18
13.	17.88	26	0.263	18.06539	18
14.	17.9	26	0.263	18.08559	18
15.	18	26	0.263	18.18663	18
16.	17.98	26	0.263	18.16642	18
17.	17.88	26	0.263	18.06539	18
18.	17.78	26	0.263	17.96435	18
19.	17.82	26	0.263	18.00477	18
20.	17.92	26	0.263	18.1058	18
21.	17.88	26	0.263	18.06539	18
22.	17.9	26	0.263	18.08559	18
23.	17.68	26	0.263	17.86331	18
24.	18.5	26	0.263	18.69182	19
25.	18.7	26	0.263	18.89389	19
26.	18.6	26	0.263	18.79285	19
27.	18.65	26	0.263	18.84337	19
28.	18.85	26	0.263	19.04544	19
29.	18.88	26	0.263	19.07576	19
30.	18.87	26	0.263	19.06565	19
31.	18.9	26	0.263	19.09596	19
32.	18.92	26	0.263	19.11617	19
33.	19.5	26	0.263	19.70218	20
34.	19.6	26	0.263	19.80322	20
35.	19.65	26	0.263	19.85374	20
36.	19.7	26	0.263	19.90426	20
37.	19.8	26	0.263	20.00529	20
38.	19.9	26	0.263	20.10633	20
39.	20.5	26	0.263	20.71255	21

40.	20.75	26	0.263	20.96514	21
41.	20.7	26	0.263	20.91463	21
42.	20.9	26	0.263	21.1167	21
43.	21.7	26	0.263	21.92499	22
44.	21.6	26	0.263	21.82396	22
45.	21.8	26	0.263	22.02603	22
46.	21.85	26	0.263	22.07655	22
47.	21.9	26	0.263	22.12707	22
48.	21.87	26	0.263	22.09676	22
49.	22.7	26	0.263	22.93536	23
50.	23.7	26	0.263	23.94573	24
51.	23.8	26	0.263	24.04677	24
52.	24.8	26	0.263	25.05714	25
53.	25.7	26	0.263	25.96647	26
54.	25.8	26	0.263	26.06751	26
55.	25.88	26	0.263	26.14833	26
56.	25.92	26	0.263	26.18875	26

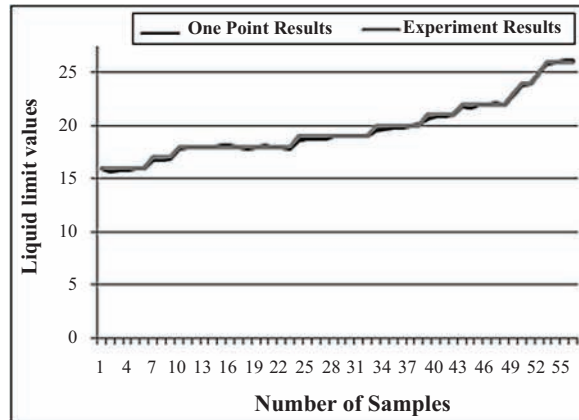


Fig. 7. Comparison of LL b/w One Point & Experimental Results @ 26 Number of Blows

TABLE XIV
COMPARISON OF LIQUID LIMIT BY ONE POINT & EXPERIMENTAL RESULTS @ 30 BLOWS

No.	W	N	e @ 20 Blows	LL by One Point Value	LL by Exp: Results
1.	14	30	0.263	14.68766	16
2.	15.8	30	0.263	16.57608	16
3.	15.5	30	0.263	16.26134	16
4.	15.2	30	0.263	15.94661	16
5.	15.58	30	0.263	16.34527	16
6.	15.5	30	0.263	16.26134	16
7.	16.15	30	0.263	16.94327	17
8.	16.5	30	0.263	17.31046	17
9.	16	30	0.263	16.7859	17
10.	17.75	30	0.263	18.62186	18
11.	17	30	0.263	17.83502	18
12.	16.5	30	0.263	17.31046	18
13.	16	30	0.263	16.7859	18
14.	16.2	30	0.263	16.99572	18
15.	17.5	30	0.263	18.35958	18
16.	17.58	30	0.263	18.44351	18
17.	17.65	30	0.263	18.51695	18
18.	17.4	30	0.263	18.25467	18
19.	17	30	0.263	17.83502	18
20.	16.5	30	0.263	17.31046	18
21.	17.2	30	0.263	18.04484	18

22.	17.9	30	0.263	18.77923	18
23.	17.52	30	0.263	18.38056	18
24.	17	30	0.263	17.83502	19
25.	18	30	0.263	18.88414	19
26.	17.5	30	0.263	18.35958	19
27.	18.5	30	0.263	19.4087	19
28.	18.58	30	0.263	19.49263	19
29.	18	30	0.263	18.88414	19
30.	18.7	30	0.263	19.61852	19
31.	18.7	30	0.263	19.61852	19
32.	18.1	30	0.263	18.98905	19
33.	19	30	0.263	19.93326	20
34.	18	30	0.263	18.88414	20
35.	18.2	30	0.263	19.09396	20
36.	18.5	30	0.263	19.4087	20
37.	19	30	0.263	19.93326	20
38.	19.5	30	0.263	20.45782	20
39.	19	30	0.263	19.93326	21
40.	20	30	0.263	20.98238	21
41.	20.5	30	0.263	21.50694	21
42.	20.58	30	0.263	21.59086	21
43.	21	30	0.263	22.03149	22
44.	20.5	30	0.263	21.50694	22
45.	21.5	30	0.263	22.55605	22
46.	21	30	0.263	22.03149	22
47.	21.65	30	0.263	22.71342	22
48.	20	30	0.263	20.98238	22
49.	22	30	0.263	23.08061	23
50.	22	30	0.263	23.08061	24
51.	23.5	30	0.263	24.65429	24
52.	22	30	0.263	23.08061	25
53.	25	30	0.263	26.22797	26
54.	23.5	30	0.263	24.65429	26
55.	24	30	0.263	25.17885	26
56.	25.8	30	0.263	27.06726	26

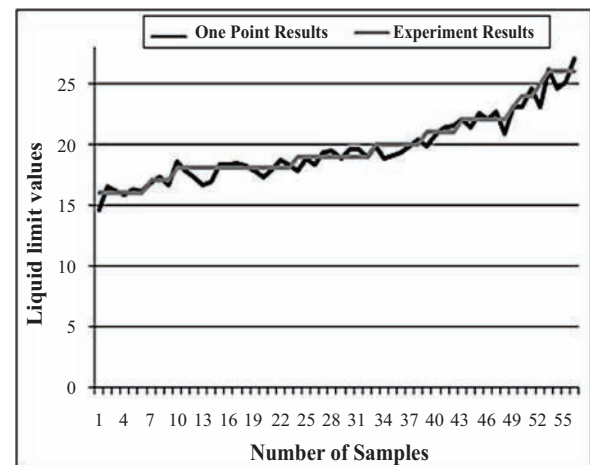


Fig. 8. Comparison of LL b/w One Point & Experimental Results @ 30 Number of Blows

A. Reliability of the results

To validate the reliability of the test results, the variance and standard deviation of results were also calculated. The difference of both quantities is represented in Fig. 9.

The Reliability @ 20 Blows = 87%.

The Reliability @ 26 Blows = 99.97%.

The Reliability @ 30 Blows = 99.94%.

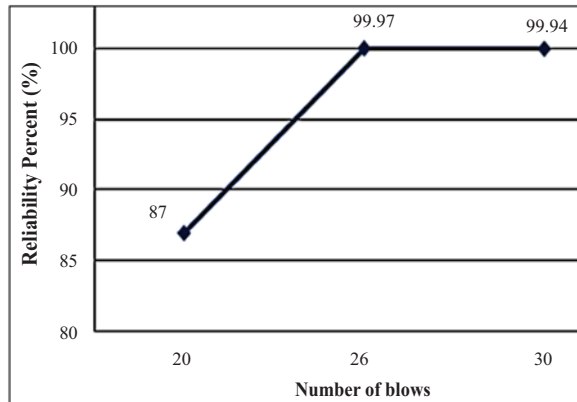


Fig. 9. Comparisons of Reliability of LL b/w One Point and Experimental Results @ 20, 26 & 30 Number of Blows

V. CONCLUSIONS

The purpose of this research work is to introduce the constant values of index (e) and Number of Blows for A-7-6 (AASHTO Classification) clayey shale type soils using one point formula. 100 samples of A-7-6 soil were collected from Jamshoro (Pakistan) zone and multi point Casagrande liquid limit laboratory tests were performed. The 20-30 number of blows were determined as best in the light of literature and placed constant for One Point Formula. Experimental results were validated with one point formula results and an excellent relationship was observed. The index (e) value obtained by this research was found different from that suggested by Punmia et al. (2005) (ranging between 0.068-0.121) [xviii]. The calculated value was verified on all collected samples and fairly accurate results were obtained using this index (e) value. Based on the laboratory investigation and research work, it was found that for Jamshoro soil, the Index value (e_{RK}) is 0.263. This evaluated index value and calculated quantity of number of blows will help the user to avoid performing liquid limit laboratory tests on proposed soil.

REFERENCES

[I] A. Namdar, A.K. Pelko, 2010. "Liquid and plastic limits evaluation of mixed soil matrices". *E-Journal of Science & Technology (e-JST)*. Vol. 3(5), 2010; pp. 1-8.

[ii] Y. Guo, Q. Wang, "Experimental research on fall cone test to determine liquid limit and plastic limit of silts". *Rock and Soil Mechanics*. Vol. 9, 2009, pp. 09.

[iii] C. Venkatasubramanian, G. Dhinakaran, "Effect of Bio-Enzymatic soil stabilisation on unconfined compressive strength and California

Bearing ratio". *Journal of Engineering and Applied Sciences*, vol. 6 (5), 2011, pp. 295-298.

- [iv] A. Atterberg, "Die plastizität der tone". *Internationale Mitteilungen für Bodenkunde*. Vol. 1 (1), 1911, pp. 10-43.
- [v] F. Bergaya, G. Lagaly, "General introduction: clays, clay minerals, and clay science". *Handbook of clay science*. Vol. 1, 2006, pp. 1-18.
- [vi] J. S. Reed, "Principles of Ceramic Processing". 2nd ed. Wiley, New York, 1995.
- [vii] L. Jefferson, C. F. D. Rogers, "Liquid limit and the temperature sensitivity of clays". *Engineering Geology*. Vol. 49 (2), 1998, pp. 95-109.
- [viii] A. Casagrande, "Notes on the design of the liquid limit device". *Geotechnique*. Vol. 8 (2), 1958, pp. 84-91.
- [ix] A. Gutierrez, "Determination of Atterberg limits: uncertainty and implications". *Journal of geotechnical and geoenvironmental engineering*. Vol. 132 (3), 2006, pp. 420-424.
- [x] American Standards D-4318-05. "Standard Test Methods for Liquid Limit, Plastic Limit and Plasticity Index of Soils". American Society for Testing Materials, 2005.
- [xi] V. Domenech, E. Sanchez, V. Sanz, J. Garcia, F. Gines, "Assessing the Plasticity of Ceramic masses by determining indentation force". *Qualicer*, Spain, 1994.
- [xii] K. Kayabali, "Determination of Consistency Limits". A Comparison between #40 and #200. Materials Ankara University, Geological Engg. Dept. Ankara, Turkey, 2011, pp. 1547-1560.
- [xiii] J. Bradford, R. Grossman, "In-situ measurement of near-surface soil strength by the fall-cone device". *Soil Science Society of America Journal*. Vol. 46 (4), 1982, pp. 685-688.
- [xiv] K. Terzaghi, "The influence of modern soil studies on the design and construction of foundations". In *Building Res. Congress*, 1951.
- [xv] S. Leroueil, J.P. Le-Bihan, "Liquid limits and fall cones". *Canadian Geotechnical Journal*. Vol. 33 (5), 1996, pp. 793-798.
- [xvi] A. Sanzeni, F. Colleselli, D. Grazioli, "Specific surface and hydraulic conductivity of fine-grained soils". *Journal of Geotechnical and Geoenvironmental Engineering*, Vol. 139(10), 2013, pp. 1828-1832.
- [xvii] B. N. N. Kumar, M. A. Kumar, "Soil stabilization with fly ash and industrial waste". *International Journal of Scientific Research in Science and Technology*, Vol. 2(2), pp. 198-204.
- [xviii] A. K. Misra, R. Mathur, Y. V. Rao, A. P. Singh, P. Goel, "A new technology of marble slurry waste utilization in roads". *Journal of Scientific & Industrial Research*, Vol. 69, 2010, pp. 67-72.
- [xix] S. Nayak, B. M. Sunil, S. Shrihari, "Interactions

- between soils and laboratory simulated electrolyte solution”. Geotechnical and Geological Engineering, Vol. 28(6), 2010, pp. 899-906.
- [xx] B. Punmia, A. K. Jain, “Soil mechanics and foundations”. *Firewall Media*, 2005.
- [xxi] A. Kumar, G.B. Khaskheli, P. A. Muhammad, “Effect of Marble Powder on Various Geotechnical Properties of Jamshoro Soil”. *Advancing Civil, Architectural and Construction Engineering & Management, ICCIDC–III*, (2012).
- [xxii] S. B. Osman, F. I. Siddiqui, M. Y. Behan, “Relationship of Plasticity Index of Soil with Laboratory and Field Electrical Resistivity Values”. *Applied Mechanics and Materials*, Vol. 353, 2013, pp. 719-724.
- [xxiii] A. Kumar, G. B. Khaskheli, “Effect of cement content on unconfined Compressive strength of Jamshoro soil”. *International Symposium on Sustainable Geosynthetics and Green Technology for Climate Change (SGCC)*, 20-21 June (2012). Bangkok, Thailand.
- [xxiv] A. M. Sahito, Z. A. Almani, “Liquefaction Susceptibility Evaluation of Hyderabad Soil”. *International Journal Of Modern Engineering Research*, Vol. 5(8), 2015, pp. 9-15.

Section D

COMPUTER, SOFTWARE,
TELECOMMUNICATION, ENGINEERING
COMPUTER SCIENCE

Classification of Brain States using Subject-Specific Trained Classifiers

N. Irtiza¹, H. Farooq²

¹Electrical Engineering Department, Bahria University, Karachi, Pakistan,

²Computer Science Department, Bahria University, Karachi, Pakistan,

¹navinza@hotmail.com

Abstract—One of the key components to develop a usable Electroencephalography (EEG) based Brain Computer interface (BCI) is the efficient classification of EEG patterns using Machine Learning classifiers. This paper presents a comparison of Linear Discriminant Analysis (LDA), Naïve Bayes and Decision Tree classifiers by applying to the EEG data. The classifiers are applied on BCI Competition III: Dataset V that consists of three cognitive tasks, namely, right and left hand imagery movement and the imagination of any word starting from a given random letter. The BCI experiments for this data have been performed with three subjects. For subjects 1 and 2, the Naïve Bayes classifier provides best results while for subject 3 the maximum accuracy is achieved from LDA classifier. In order to improve the accuracy further, it has been proposed to apply combination of classifiers based on Multiple/Ensemble Classifier System concept on data for single subject with different sessions of data recording. By combining the classifiers LDA and Decision Tree, maximum accuracies of 81%, 70% and 56% for subjects 1, 2 & 3 respectively have been achieved that are comparable with the accuracies achieved by the winner of the competition. It is concluded that instead of employing single classifier, the approach for using combination of classifiers significantly improves the performance of a BCI system.

Keywords—Brain Computer Interfacing, Machine Learning, Electroencephalography, Classification, Multiple Classifier System

I. INTRODUCTION

A communication system that transmits signals from brain without using any muscular activity to a machine or a computer is termed as Brain Computer Interface (BCI) [i]. The Electroencephalography (EEG) based signal generated by a human brain performing a particular cognitive task or brain activity like imagination of hand or movement or observing several auditory or visual stimuli can be helpful to determine the intention and emotion of the user. The most common approach for designing a BCI system is to perform analysis and interpretation of EEG signals

in such a manner that they vary the state of a machine [i]. The EEG signal captured from brain consists of six different oscillations having specific frequency bands. The oscillations based on frequency ranges as well as location of their origin are categorized. They are delta (less than 4 Hz), theta (4-7 Hz), alpha (8-15 Hz), beta (12- 30 Hz), mu (8-12Hz) and gamma (32+Hz). Based on BCI System, various computer based applications have been designed [ii, iii]. Motor imagery is defined as a cognitive task by which a subject simulates any specific action in her mind without actually performing the movement. Motor imagery has been widely considered as a major scenario in BCI related studies [iv-vi]. The Berlin Brain Computer Interface group in Germany has developed a BCI application named as the P300 or Hex-O speller which is a EEG signal based spelling application in which the user has to control the size and rotation of the arrow displayed on the screen using motor imagery. He has to select a cell in a hexagon that consists of 6 cells such that each cell consists of either a letter or group of letters [ii].

Efficient classification of different electroencephalogram (EEG) patterns plays instrumental role in designing a usable BCI System. The purpose of the classification stage in a BCI device is to assign automatically a class or label to the feature vector that has been previously extracted. A classifier is defined as a function that partitions a set of data or objects into two or multiple classes. Thus, in machine learning the purpose of the classification is to develop a rule based on a set of samples or observations that allocate an observation or a sample x to one of multiple classes. Here, x denotes a feature vector of N -dimensional data. For the simplest case, there can be only two different binary classes. In such case, a classifier can be formulated as a decision function $f: \mathbb{R}^N \rightarrow \{-1, +1\}$, that assigns an instance x to one of the classes, assigned by $+1$ and -1 [vii]. The predicted class label represents the state of user's mind while performing the BCI experiment.

In this paper, we aim to validate one of the stages of our proposed methodology in our previous work to find out the neural correlates of Neuroception [viii]. The proposed work specifically focuses on the problem of assessment of neural correlates for fear-induced EEG

activity acquired while user's brain is functioning unconsciously to differentiate among the states of safety vs. dangerous. We proposed that LDA will be used to perform classification of the cognitive state of the subject if he is in state of fear or not. To validate this statement, initially the LDA classifier is applied on the dataset BCI Competition III: dataset V from Berlin BCI group. In addition to LDA, Naïve Bayes and Decision tree are applied on the same dataset for comparison. In order to improve the performance of the classifier, concept of Multiple / Ensemble Classifier has been applied and it is found that the approach has significantly improved the results. Employing the combination of LDA and Decision tree, the prediction accuracy has remarkably increased.

The rest of the paper is arranged as follows. Section II explains some BCI studies emphasizing on what feature extraction and classification techniques have been used. Section 3 consists of methodology with description of dataset and EEG feature based on Power Spectral Density (PSD). Details are given regarding how LDA, Naïve Bayes (NB) and Decision Tree (DT) classifiers are used in this work. The approach combining LDA with Decision Tree is also presented. The Section IV mentions the results obtained from each of the classifiers. Section V discusses the results and the performance with the existing results is compared. Finally, the paper is concluded in Section VI.

TABLE I
STUDIES SHOWING MACHINE LEARNING TECHNIQUES FOR BCI APPLICATIONS

Authors' work	Features Extracted	Machine learning classifiers	Performance Measure / Value
[ix]	<ul style="list-style-type: none"> • Power Spectrum • Wavelet • Entropy • Fractal Dimension 	<ul style="list-style-type: none"> • LDA • PCA • SVM 	Classification Accuracy / 91.77%-
[x]	<ul style="list-style-type: none"> • Wavelet 	<ul style="list-style-type: none"> • Independent Component Analysis (ICA) 	
[iii]	<ul style="list-style-type: none"> • Event Related Potential 	<ul style="list-style-type: none"> • Linear FDA 	<ul style="list-style-type: none"> • Offline binary classification / 77.7% • Online multiclass accuracy / 89.37%
[xii]	<ul style="list-style-type: none"> • Power Density 	<ul style="list-style-type: none"> • Short term fourier transform (STFT) • Genetic Algorithm (GA) 	Classification Error Rate / 20%

The rest of the paper is arranged as follows. Section II explains some BCI studies emphasizing on what feature extraction and classification techniques have been used. Section III consists of methodology with description of dataset and EEG feature based on Power Spectral Density (PSD). Details are given regarding how LDA, Naïve Bayes (NB) and Decision Tree (DT) classifiers are used in this work. The approach combining LDA with Decision Tree is also presented. The Section IV mentions the results obtained from each of the classifiers. Section V discusses the results and compared the performance with existing work. Finally, the paper is concluded in Section VI

II. RELATED WORK

In any BCI application, the features extracted from acquired EEG signals are translated into interpretable

commands. For this purpose, different algorithms from machine learning have been employed for the past several years [ix, xiii]. Some of the techniques and the features extracted in BCI systems are mentioned in Table I. A study [ix] is conducted to identify the specific characteristics associated with emotions using EEG signals. Furthermore, pattern of emotion changes while the subject is experiencing during the BCI experiment are also investigated. For this purpose, different movie clips are designed to induce emotions of subjects. From EEG signals captured, three different features based on power spectrum, non-linear dynamical analysis and wavelets are extracted. Support Vector Machine (SVM) is used for classification purpose. In order to achieve reduction in features dimensionality, Principal Component Analysis (PCA) and Linear Discriminant Analysis (LDA) are applied and compared. The best classification accuracy of 91.77% is achieved in this work [ix].

A computer game to find out cortical oscillatory dynamics associated with three different nature of social behavior including aggressive, avoidant and friendly is designed in [x]. In this work, EEG responses are analyzed using wavelet transform. For feature extraction and classification, the technique of Independent Component Analysis (ICA) is used.

A novel method using auditory evoked potentials for designing a multiclass spelling BCI application is proposed in [iii]. In this study, the subjects have focused their attention to different auditory stimuli varying both in pitch and direction. The signals operating the text entry application are categorized on the basis of nine different control signals. The proposed method was named as PASS2D that achieved information transfer rate (ITR) of 0.8 characters per minute. For classification purpose, fisher discriminant analysis (FDA) is used. In case of offline binary classification, 77.7% accuracy is achieved. While for online multiclass scenario, 89.37% decisions were correctly classified [iii].

Extraction of optimal feature set based on power density of EEG response is performed in [xii]. Pre-processing is conducted using spatial and temporal filters for short-time fourier transform (STFT) to extract time-frequency features. Genetic algorithm (GA) is then applied for selection of optimal features. In this work, the datasets from BCI competition III and IV are used. In addition, BCI experiments are also performed to apply the proposed approach. SVM is applied for classification and achieved the classification error rate to 20% [xii]

A. Multiple/Ensemble Classifier System

Multiple classifier systems (MCSs), classifier committees or ensemble classifiers perform the task of classification not based on a single classifier but based

on a combined decision of a set of at least two classifiers [xvi]. Various studies have used this approach. In [xix] Support Vector Machine (SVM) and decision tree have been integrated for understanding and prediction of trans-membrane segments.

In [xx] the performance evaluation of three ensemble algorithms for EEG signal classification of tasks for mental imagery has been performed. Using k-nearest neighbor as base classifier, combined with decision tree and SVM, classification is performed on real EEG recordings. Experimental results suggest the practicability of ensemble classification methods for EEG Signals classification [xx]. In [xxi] combination of LDA, ADABOOST and Decision tree classifiers to detect different cases of occluded as well as non-occluded faces is used. The ensemble of LDA and decision tree combines the outputs from each of the individual classifiers.

The two architectures used in the design of MCS are illustrated in Fig. 1. Firstly, in parallel topology, each classifier is given same data as input, so that the final outcome from the combined classifiers is made based on the outputs of the individual classifiers obtained individually. On the other hand, in the conditional or serial architecture, individual classifiers are applied one by one in sequence, implying some specific ordering or ranking for them. When the base or primary classifier cannot be trusted to classify a given data or object for example may be because of the low confidence or support in its outcome, then the data is fed to a secondary classifier, adding classifiers in sequence. This technique is suitable when the cost of classifier exploitation is significant, so that the base classifier is computationally cheapest one and secondary classifiers have comparatively larger exploitation cost.

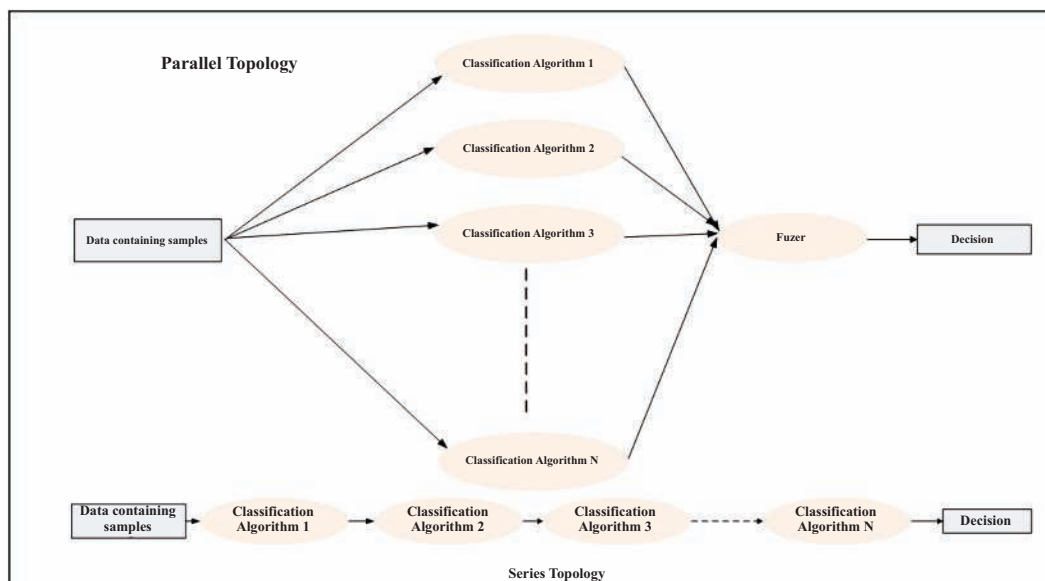


Fig. 1. Parallel & Series Topologies for Multiple / Ensemble Classifiers [xvi]

III. METHODOLOGY

This paper is extension of our previous proposed work [viii] as already mentioned in Section I. Since the experiments that are to be performed to get the EEG data will consider oscillatory rhythms, the objective of this paper is to apply different Machine learning Classifiers using Matlab on the EEG dataset that consists of EEG signals from three normal subjects during three labeled sessions consisting of repetitive self-paced right or left hand movement imagery, and the imagination of words starting with the given specific random letter.

A. Precomputed Features - PSD

Firstly, the raw EEG potentials were spatially filtered using a surface Laplacian filters. Then, at the rate of 16 times per second i.e. every 62.5 ms -- the power spectral density (PSD) in the frequency band of 8-30 Hz is evaluated over the last second of EEG data having the frequency resolution of 2 Hz for the 8 centro-parietal electrodes C3, Cz, C4, P3, Pz, CP1, CP2, and P4. The resulting EEG sample is a 96-dimensional feature vector (product of 8 electrodes and 12 frequency components). The organizers of the competition have provided the data in this pre-computed form [xxiii]. The Power Spectral Density (PSD) can be computed from the Fourier transform of the Auto correlation function of a signal. It basically elaborates how the signal squared value or the signal power is spread in terms of frequency [xxiv].

Fig. 2 shows the flowchart of each stage of the methodology out of which the steps till feature extraction have been done by the competition organizers. The stage of classification to predict classes from extracted features is performed in this work. As

per the requirements of the competition, firstly the average has been calculated for each 0.5 second [xxii]. The Statistical Toolbox of Matlab is used for this work. LDA, Decision Tree and Naïve Bayes classification algorithms are applied and compared for the given dataset.

B. Linear Discriminant Analysis (LDA)

Let $X_1 = \{x_1^1, x_1^2, \dots, x_1^l\}$ and $X_2 = \{x_2^1, x_2^2, \dots, x_2^l\}$ be samples from two different classes. Linear discriminant is given by the vector w which maximizes

$$J(w) = \frac{w^T S_B w}{w^T S_W w} \quad (1)$$

where

$$S_B := (m_1 - m_2)(m_1 - m_2)^T$$

$$S_W := \sum \sum (x - m_i)(x - m_i)^T$$

are the between and within class scatter matrices and m_i determines the direction that maximizes the projected class means (numerator) whereas minimizing the classes variance (the denominator) [xiv]. LDA works on following three assumptions [xv]:

- Features belonging to each class are Gaussian distributed
- The Gaussian distributions for each class have same covariance matrix.
- True class distributions are already known.

In this work the LDA classifier computes the sample mean of each of the three classes. As per equation (1), the sample covariance matrix is computed by first subtracting the mean of each class from samples of that class and then the empirical covariance matrix is evaluated.

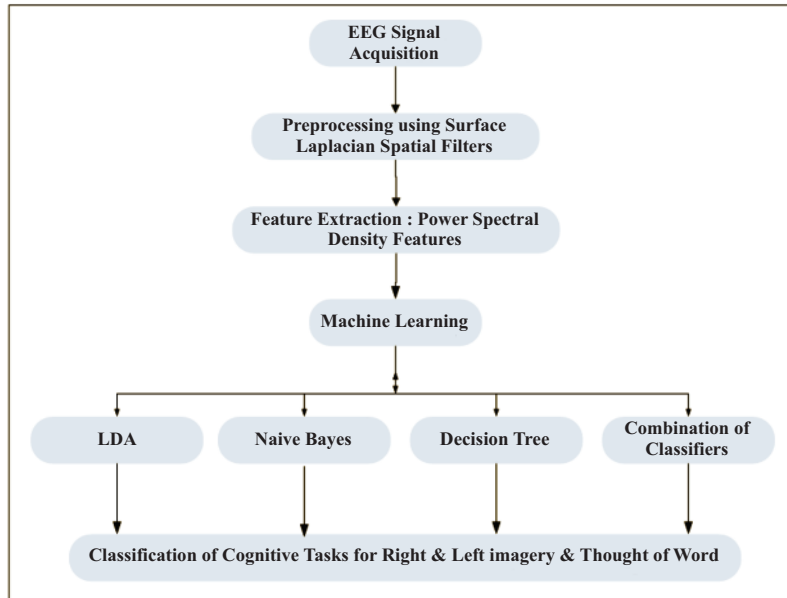


Fig. 2. Flowchart explaining the complete methodology

A. Naïve Bayes

A naive bayes classifier is one of the methods of supervised learning algorithms that is based on applying bayes theorem which says:

$$p(c_j | d) = \frac{p(d | c_j) p(c_j)}{p(d)}$$

where

$p(c_j | d)$ is the probability of instance d being in class c_j ,

$p(d | c_j)$ is the probability of generating instance d given

class c_j ,

$p(c_j)$ is the probability of occurrence of class c_j , and

$p(d)$ is the probability of instance d occurring

It is a simplified Bayesian probability model which assumes that the features are independent and the probability of one attribute will not affect the probability of other attribute. It works well on classification but it states that the error occurs due to three factors including bias, variance and training data noise [xvii]

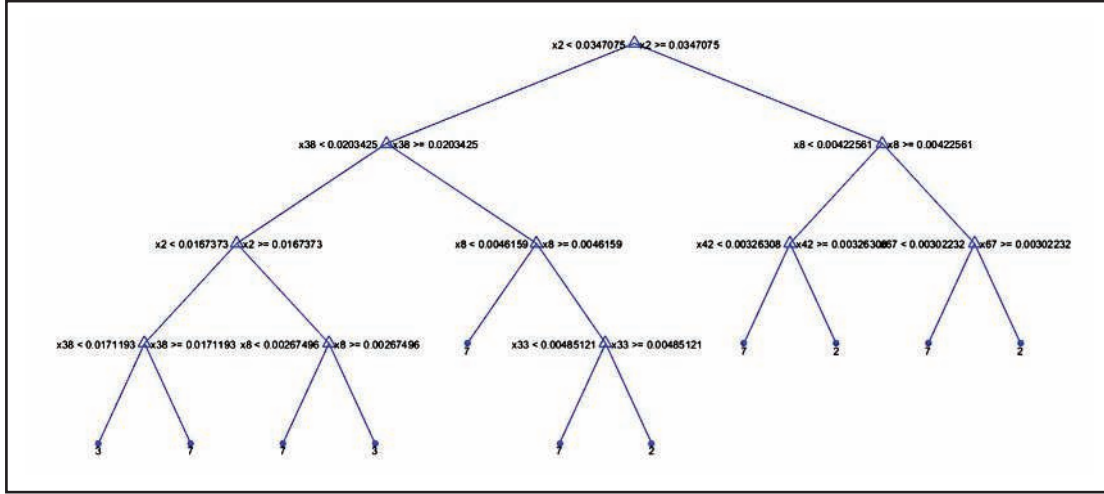


Fig. 3. Decision Rules based on initial setting for 10 splits

D. Decision Tree

Decision Tree is one of the non-parametric supervised learning algorithms used for classification and regression. A decision tree illustrates graphically the decisions to be taken, the events that may take place, and the outcomes associated with different combinations of events and decisions. Probabilities are allocated to the events, and values are evaluated for each outcome. Using this approach, complex decisions are split into simpler decisions. Structure resembling a tree is formed as a result of this classification method. [xviii]. Decision tree (DT) can lead to instability since small variations in data may form an entirely different tree that was earlier generated. This problem can be generally catered by combining decision tree classifiers using an ensemble approach.

In this work, Classification And Regression Tree (CART), one of the widely used DT algorithms is used. CART is a technique that uses tree structure in binary form having two branches at each node. The first

internal node also called the root node is the point where the process of tree building initiates such that the entire data is split into two subsets. The splitting of each subset is based on a parameter for predefined criterion. According to this criterion, a test is conducted at each step to find out the most suitable feature that gives the best separation of the training samples [xxv]. This work uses the GINI index criterion to build the tree. The Gini index provides a measure of the impurity degree in a dataset. For any dataset, the Gini's Diversity Index (gdi) or Gini index of a node is computed using

$$1 - \sum_i p^2(i),$$

where the summation term is over the classes i at the node, whereas $p(i)$ is the fraction of classes for class i that reach the node. A node with only one class has Gini index 0 is termed as a pure node. Other than pure node, the Gini index is always positive.

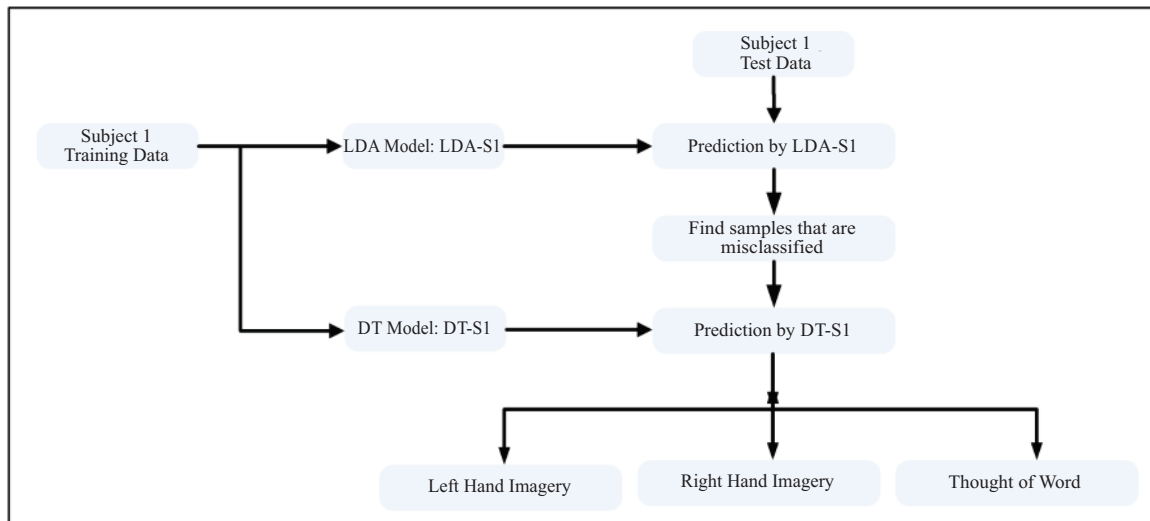


Fig. 4. Architecture for Ensemble Classifier based on LDA as base and Decision Tree as secondary classifier

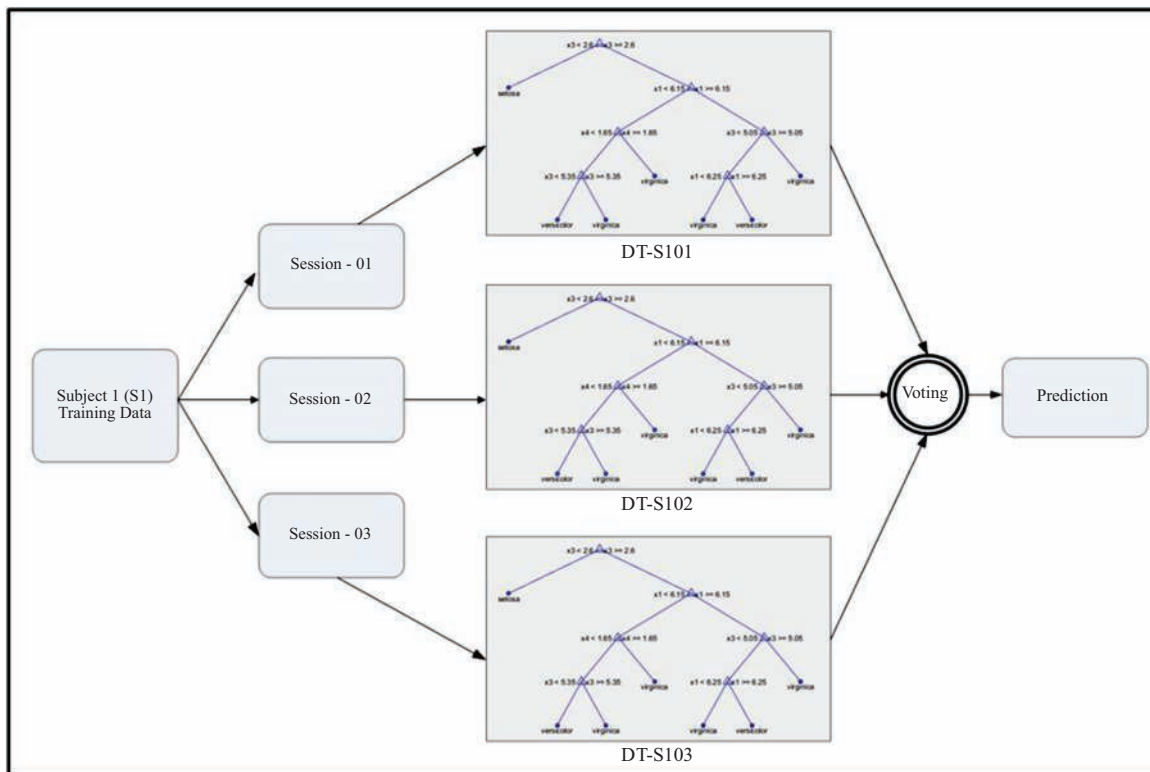


Fig. 5. Framework for Ensemble Model based on Random Forest

Followings steps are performed to generate decision tree in this work:

1. Beginning with entire input data, examine possible binary splits for each predictor
2. A split having best optimization criterion based on GINI index is selected
3. Splitting is stopped whenever any of the following is achieved: Either the node is pure or the parameter for 'Maximum Number of Splits' (MaxNumSplits) is achieved

4. Split is imposed.

5. Same procedure is repeated for the two child nodes.

In this work, firstly the MaxNumSplits is set to 10. The decision rules based on this criterion are mentioned in Fig. 3. Initially, out of 96 features, few are retained by the classifier as obvious from the figure. In order to improve the accuracy, the splits increased and decision rules are modified.

E. Multiple / Ensemble Classifier System based approach

In order to improve the performance of the classifiers, the approach to combine classifiers based on Multiple classifier system is proposed and applied as shown in Fig. 4. The approach used in [xxi] for face detection in case of various types of occluded faces has been followed. Combination of LDA and decision tree classifiers is used to combine the results from individual classifiers where LDA is used as base or primary classifier while the decision tree is integrated as secondary one. Firstly, the LDA and decision tree classifier models are trained by providing the same training set. The test data is then provided to the LDA trained classifier. The samples or instances that are misclassified by LDA are fed to the decision tree classifier.

The classifiers based on decision tree are ensembled by means of random forest (RF). A RF classifier defined as an ensemble of several decision trees where each casts a vote for a majority decision for the class selection of input data sample. Each session of a subject produced specific decision tree classifiers.

In Fig. 4, the approach of combination of classifiers for Subject 1 has been elaborated. Firstly, the training data from session 1 for Subject 1 is fed as input to the classifiers LDA and named as LDA-S1. Then training data from session 3 of the same subject is given as test data to the trained classifiers LDA-S1 for the prediction of the class of the mental task produced by the subject. The outcome is compared with the actual class labels and those instances that are misclassified by LDA-S1 are retained only for the input to the secondary classifier based on the decision tree ensemble. Each session of subject 1 is used to train random forest named as DT-S1. Thus, DT-S1 in turn comprised of ensembles of random forests trained from other two sessions of specific subject. Fig. 5 presents the framework of proposed ensemble based on random forest. Subject I is considered where random forests are trained from other sessions. For the three sessions of subject 1, they are termed as DTS101, DTS102 and DTS103. If session 3 is considered as test data, the ensemble will consider DTS101 and DTS103 for prediction Voting is performed for final decision of the predicted class label.

TABLE II
RE-SUBSTITUTION ERROR FOR EACH TRAINING
SESSION FOR THREE SUBJECTS

Subject 1:

Classifier	Training Data 01	Training Data 02	Training Data 03
LDA	.0963	.0737	.0695
NB	.2431	.2419	.2489
Decision Tree	.0619	.0323	.0426

Subject 2:

Classifier	Training Data 01	Training Data 02	Training Data 03
LDA	.1682	.1574	.1290
NB	.2788	.2477	.2788
Decision Tree	.0853	.0648	.0691

Subject 3:

Classifier	Training Data 01	Training Data 02	Training Data 03
LDA	.1963	.1495	.2023
NB	.3879	.2780	.3070
Decision Tree	.0724	.0467	.0744

IV. RESULTS

Classifiers based on LDA, NB and Decision Tree algorithms are applied on the EEG dataset described in following section.

A. Dataset

BCI Competition III, Dataset V is obtained from the BCI Competition III website [xxii] provided by the IDIAP Research Institute in Switzerland [xxiii]. It consists of EEG signals from three normal subjects during three labeled sessions (each session is 4 minutes long) without feedback. During each session, the subject performed three brain activities (in random manner) for almost 15-20 seconds duration, resulting in more or less 16 repetitions of each cognitive task that consisted of repetitive self-paced right or left hand movement imagery, and the imagination of words starting with the given specific random letter. EEG recordings were performed with using a Biosemi system having a cap with 32 EEG electrodes placed at standardized positions as per the International 10-20 system. 512 Hz is set as the sampling rate. Signals are recorded at full DC having no incorporation for artifact correction or rejection.

The classification accuracy of each model is depicted and then their respective accuracies are compared. For each of these classification procedures, the performance is measured by means of two parameters: the resubstitution error and cross validation error. The re-substitution error also known as misclassification error has been computed for each of three training session for all three subjects as shown in Table II.

TABLE III
RE-CROSS-VALIDATION ERROR FOR EACH OF THE
THREE SUBJECTS

Subject 1:

Classifier	Training Data 01	Training Data 02	Training Data 03
LDA	.2271	.2166	.2197
NB	.2936	.3065	.2915
Decision Tree	.3394	.3641	.3049

Subject 2:

Classifier	Training Data 01	Training Data 02	Training Data 03
LDA	.3710	.2986	.2972
NB	.3618	.3125	.3456
Decision Tree	.4447	.3657	.3502

Subject 3:

Classifier	Training Data 01	Training Data 02	Training Data 03
LDA	.4369	.3107	.4442
NB	.5140	.3949	.4605
Decision Tree	.5397	.4673	.6000

The cross-validation errors for each of the subjects are shown in Table III. In order to validate the model, 10 fold cross-validation is performed in which the data is randomly split into ten (10) almost equal-sized partitions, and 9 out of 10 folds are used as training data while the remaining one is retained as the validation set so that in the end, every sample or instance has been used exactly once for testing purpose.

Furthermore, statistical parameters including sensitivity, specificity and confusion matrix are also used for performance evaluation of the classifiers. Specificity is defined as the measurement of fraction of negatives that are correctly identified as such (e.g., the percentage of samples of left hand movement imagination that are correctly identified as not having this state). It is also called the true negative rate. Sensitivity is defined as the measurement of fraction of positives that are correctly identified as such. For example, the percentage of samples of left hand movement imagination that are correctly identified as having this state. Sensitivity is also called true positive rate. In terms of formula, they can be written as:

$$\text{Sensitivity} = \frac{TP}{TP + FN}$$

$$\text{Specificity} = \frac{TN}{TN + FP}$$

where, TP, TN, FP and FN denote true positives, true negatives, false positives, and false negatives, respectively.

Confusion matrix and statistical measures are mentioned in Table IV and V respectively. Table VI lists the maximum accuracies obtained from each of the classifier as well as ensemble classification algorithm for each subject. The accuracies obtained by the winner of the BCI competition III dataset V are also mentioned [xxii].

V. DISCUSSION

From Table II, the least resubstitution error is obtained in case of Decision tree algorithm while LDA has lesser to that of Naïve Bayes. So, it apparently seems that DT has produced the best results but if the comparison is performed using cross validation error, it is found that here LDA outclasses DT. The cross-validation errors for each of the subjects are shown in Table III. Due to difference between resubstitution and cross-validation errors of DT, it can be inferred that the decision tree has overfitted the data. It seems that the tree classifies the original training data in good manner, but design of the tree is little sensitive to the specific training set that's why its performance on any new test dataset may likely to debase.

While comparing the results from each of the single classifiers, it is observed that Naïve Bayes has performed best for the given dataset as shown in Table II. For subjects 1 and 2, the Naïve Bayes classifier produces highest accuracy while for subject 3 the maximum accuracy is achieved from LDA classifier. From Table II, it is also cleared that the results does not depend only the classifier, but also on the training session of given subject. If the user is feeling lethargic during that session, the performance can degrade significantly.

TABLE IV
CONFUSION MATRICES OF THE CLASSIFIERS FOR
SUBJECT 1 SESSION 3
(LABELS 2, 3 AND 7 SHOW LEFT HAND, RIGHT HAND
AND RANDOM WORD IMAGINATIONS RESPECTIVELY)

Classifiers	True Labels	Predicted Labels		
		2	3	7
LDA	2	89	13	9
	3	15	85	34
	7	38	24	139
DT	2	79	16	11
	3	31	81	27
	7	32	25	144
NB	2	109	30	15
	3	15	77	20
	7	18	15	147
Ensemble	2	106	24	12
	3	18	101	3
	7	8	19	155

A. Statistical Measures

The confusion matrices presenting the results of the classifiers applied are given in Table IV. Labels 2, 3 and 7 show left hand, right hand and random word imaginations respectively. From these matrices, we can tell the frequency by which an EEG sample is misclassified as another. To find out, how well each class is identified by the classifier, we need to look at Table V for sensitivity and specificity values. From Table V, it is obvious that samples for random word generation are more identifiable as compared to other instances. Sensitivity for each classifier in case of class 7 achieve highest values. And for the proposed classifier attains the highest value 91.18%. The Naïve Bayes classifier identifies class 2 labels more efficiently as compared to class 3 samples. Similarly, the proposed approach outperforms other classifiers for identification of label 3 and achieved highest sensitivity of 80.33%.

TABLE V
STATISTICAL MEASURES OF THE CLASSIFIERS

Classifiers	True Labels	Statistical Parameters (%)		
		Sensitivity	Specificity	Classification Accuracy
LDA	2	62.68	91.06	70.18
	3	69.67	82.31	
	7	76.37	73.73	
DT	2	55.63	89.29	68.16
	3	66.39	79.36	
	7	79.12	73.73	
NB	2	76.76	83.27	74.66
	3	63.11	87.97	
	7	80.77	84.93	
Ensemble	2	80.30	87.67	81.16
	3	70.14	92.55	
	7	91.18	88.46	

B. Comparison with State of the Art

Table VI lists the maximum accuracies obtained from each of the classifier for each subject. Here we will only talk about the maximum accuracy obtained for a particular subject across different training samples. In Table VII, the accuracies obtained by the winner and 1st runner up of the BCI competition III dataset V, are also mentioned to compare our results with them [xxiii]. Here, it is observed that by

combining the classifiers for the same training data, the accuracies are improved significantly and can be compared with the one obtained by the winner of the competition. The winner works with the precomputed samples. It has been trained off-line with data of first three sessions and it is structured in three stages: preprocessing and feature extraction statistical discrimination, and online discrimination improvement. First of all, before any analysis data are transformed by means normalizing of each PSD sample. Each spectral component of channel i from sample t is normalized dividing by the energy of $PSD_t(i)$. With data normalized, the feature extraction process is guided by canonical variates transform (CVT), a generalization of Fisher's linear discriminant function to more than two groups. This transformation permits the projection of a p -dimensional dataset X to be classified into c classes in a $(c-1)$ -dimensional feature space where classes separation is maximized [xxii-xxiii].

Results of the first runner up are also mentioned in Table VII. In this work the r^2 values are plotted to select good discriminative component of the input data as input feature for the purpose of classification. The features are normalized to an interval $[0,1]$. Support Vector Machine (SVM) classifier is obtained from the training data and five fold cross-validation is applied [xxii-xxiii].

In our approach, firstly LDA as a weak classifier performs classification. By introducing randomness in building random forests, the classifiers become robust and cause them to have a good performance when the data have many outliers which is our case. Predictions from random forests are considered on the basis of majority voting approach resulting in significant increase in classification accuracy. Results mentioned in Table VII are plotted in Fig. 6.

TABLE VI
MAXIMUM CLASSIFICATION ACCURACIES

Classifier	Sub. 1	Sub. 2	Sub. 3
• LDA	70.17	55.07	51.16
• NB	74.66	60.13	46.49
• Decision Tree	68.16	56.68	46.26
• Ensemble - LDA combined with DT	81.16	70.27	56.51

TABLE VII
COMPARISON WITH STATE OF THE ART

Classifier	Sub. 1	Sub. 2	Sub. 3
Author's Results based on Ensemble - LDA combined with DT	81.16	70.27	56.51
Winner Result based on CVT [xxii-xxiii]	79.60	70.31	56.02
1 st Runner Up result based on SVM [xxii-xxiii]	78.08	71.66	55.73

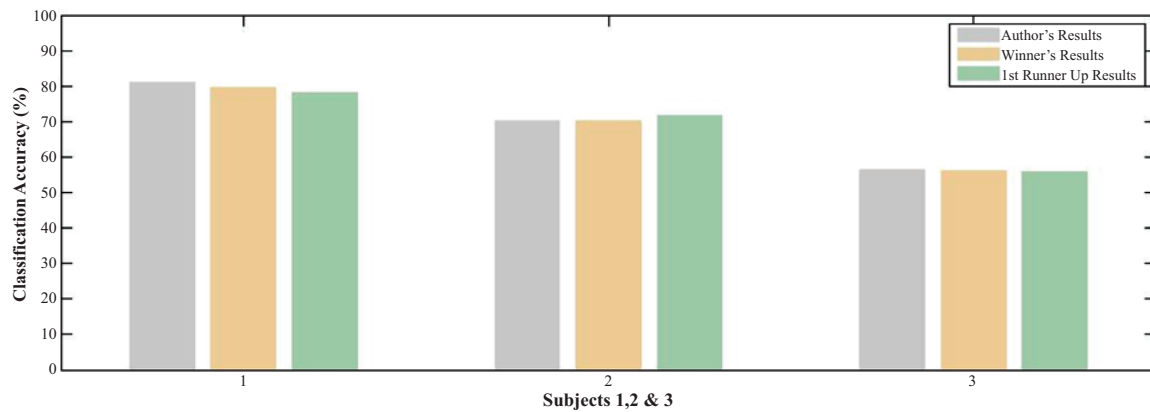


Fig. 6. Results from Table VII are plotted as bar chart

VI. CONCLUSION & FUTURE WORK

The main objective of this study is to demonstrate the application and comparison of machine language techniques using LDA, Naïve Bayes and Decision Tree to predict the cognitive state of the subject. The dataset V from BCI Competition III is used for this purpose. The features based on Power Spectral Density have been given as input to the classifiers. In order to further improve the accuracy, combination of classifier is used where LDA is used as the primary classifier while decision tree from random forests as the secondary one. The results are compared with that of the winner of the competition and it is found that the classification accuracies obtained after the combination of classifier has improved significantly. While comparing the results from each of the single classifiers, Naïve Bayes has performed best. Two parameters are used to assess the performance of the classifier namely resubstitution error and cross-validation error. For statistical analysis, sensitivity and specificity for each classifiers are evaluated.

In future these machine learning algorithms can be applied for the classification stage of our proposed work [viii]. And it will be evaluated if the results are obtained accordingly as we have found in this work using BCI Competition dataset.

Acknowledgments. This work is funded by Higher Education Commission (HEC), Pakistan and is being conducted and supervised under the 'Intelligent Systems and Robotics' research group at Computer Science (CS) Department, Bahria University, Karachi, Pakistan..

REFERENCES

- [I] F. Lotte, "Study of electroencephalographic signal processing and classification techniques towards the use of brain-computer interfaces in virtual reality applications," INSA de Rennes, 2008.
- [ii] B. Blankertz, M. Krauledat, G. Dornhege, J.

Williamson, R. Murray-Smith, and K.-R. Müller, "A note on brain actuated spelling with the Berlin brain-computer interface," in *Universal Access in Human-Computer Interaction. Ambient Interaction*, ed: Springer, 2007, pp. 759-768.

- [iii] J. Höhne, M. Schreuder, B. Blankertz, and M. Tangermann, "A novel 9-class auditory ERP paradigm driving a predictive text entry system," *Frontiers in neuroscience*, vol. 5, p. 99, 2011.
- [iv] M. C. F. Castro, A. Araujo Masiero, F. Theoto Rocha, and P. T. Aquino, "Motor imagery recognition and its cerebral mapping," in *Biosignals and Biorobotics Conference (2014): Biosignals and Robotics for Better and Safer Living (BRC), 5th ISSNIP-IEEE*, 2014, pp. 1-5.
- [v] R. Chai, S. H. Ling, G. P. Hunter, and H. T. Nguyen, "Mental non-motor imagery tasks classifications of brain computer interface for wheelchair commands using genetic algorithm-based neural network," in *Neural Networks (IJCNN), The 2012 International Joint Conference on*, 2012, pp. 1-7.
- [vi] M. Naeem, C. Brunner, and G. Pfurtscheller, "Dimensionality reduction and channel selection of motor imagery electroencephalographic data," *Computational intelligence and neuroscience*, vol. 2009, 2009.
- [vii] S. Lemm, B. Blankertz, T. Dickhaus, and K.-R. Müller, "Introduction to machine learning for brain imaging," *Neuroimage*, vol. 56, pp. 387-399, 2011.
- [viii] N. Irtiza and H. Farooq, "The study of fear-induced power modulations for Cognitive Man-Machine Communication," in *Cognitive Informatics & Cognitive Computing (ICCI* CC), 2015 IEEE 14th International Conference on*, 2015, pp. 346-351.
- [ix] X.-W. Wang, D. Nie, and B.-L. Lu, "Emotional state classification from EEG data using machine learning approach," *Neurocomputing*, vol. 129, pp. 94-106, 2014.

- [x] G. G. Knyazev, J. Y. Slobodskoj-Plusnin, A. V. Bocharov, and L. V. Pyrkova, "Cortical oscillatory dynamics in a social interaction model," *Behavioural brain research*, vol. 241, pp. 70-79, 2013.
- [xi] S. Dähne, F. C. Meinecke, S. Haufe, J. Höhne, M. Tangermann, K.-R. Müller, and V. V. Nikulin, "SPoC: a novel framework for relating the amplitude of neuronal oscillations to behaviorally relevant parameters," *NeuroImage*, vol. 86, pp. 111-122, 2014.
- [xii] P. Chum, S.-M. Park, K.-E. Ko, and K.-B. Sim, "Optimal EEG feature selection by genetic algorithm for classification of imagination of hand movement," in *IECON 2012-38th Annual Conference on IEEE Industrial Electronics Society*, 2012, pp. 1561-1566.
- [xiii] F. Lotte, M. Congedo, A. Lécuyer, F. Lamarche, and B. Arnaldi, "A review of classification algorithms for EEG-based brain-computer interfaces," *Journal of neural engineering*, vol. 4, p. R1, 2007.
- [xiv] B. Scholkopf and K.-R. Mullert, "Fisher discriminant analysis with kernels," *Neural networks for signal processing IX*, vol. 1, p. 1, 1999.
- [xv] B. Blankertz, S. Lemm, M. Treder, S. Haufe, and K.-R. Müller, "Single-trial analysis and classification of ERP components—a tutorial," *NeuroImage*, vol. 56, pp. 814-825, 2011.
- [xvi] M. Woźniak, M. Graña, and E. Corchado, "A survey of multiple classifier systems as hybrid systems," *Information Fusion*, vol. 16, pp. 3-17, 2014.
- [xvii] G. Keerthika and D. S. Priya, "Feature Subset Evaluation and Classification using Naive Bayes Classifier," *Journal of Network Communications and Emerging Technologies (JNCET)* www.jncet.org, vol. 1, 2015.
- [xviii] U. R. Acharya, R. Yanti, J. W. Zheng, M. M. R. Krishnan, J. H. TAN, R. J. Martis, and C. M. Lim, "Automated diagnosis of epilepsy using CWT, HOS and texture parameters," *International journal of neural systems*, vol. 23, p. 1350009, 2013.
- [xix] J. He, H.-J. Hu, R. Harrison, P. C. Tai, and Y. Pan, "Transmembrane segments prediction and understanding using support vector machine and decision tree," *Expert Systems with Applications*, vol. 30, pp. 64-72, 2006.
- [xx] S. Sun, C. Zhang, and D. Zhang, "An experimental evaluation of ensemble methods for EEG signal classification," *Pattern Recognition Letters*, vol. 28, pp. 2157-2163, 2007.
- [xxi] K. Ichikawa, T. Mita, O. Hori, and T. Kobayashi, "Component-based face detection method for various types of occluded faces," in *Communications, Control and Signal Processing, 2008. ISCCSP 2008. 3rd International Symposium on*, 2008, pp. 538-543.
- [xxii] B. C. III. (2004/2005). *BCI Competition III 2004/2005*. Available:<http://www.bbci.de/competition/iii/results/#martigny>
- [xxiii] B. Blankertz, K.-R. Müller, D. J. Krusienski, G. Schalk, J. R. Wolpaw, A. Schlögl, G. Pfurtscheller, J. R. Millan, M. Schröder, and N. Birbaumer, "The BCI competition III: Validating alternative approaches to actual BCI problems," *Neural Systems and Rehabilitation Engineering, IEEE Transactions on*, vol. 14, pp. 153-159, 2006.
- [xxiv] A. B. Benevides, T. F. Bastos Filho, and M. Sarcinelli Filho, "Pseudo-Online Classification of Mental Tasks Using Kullback-Leibler Symmetric Divergence," *Journal of Medical and Biological Engineering*, vol. 32, pp. 411-416, 2012.
- [xxv] W. Y. Loh, "Classification and regression trees," *Wiley Interdisciplinary Reviews: Data Mining and Knowledge Discovery*, vol. 1, pp. 14-23, 2011.

Co-Design of Dual-Band Low Noise Amplifier Operating in 900MHz/1800MHz Bands for Multi-standard Wireless Receiver

S. Mudassir¹, J. Muhammad², J. Akbar³, T. Mir⁴, R. Zeeshan⁵

^{1,2,4,5}Faculty of Information & Communication Technology, BUITEMS, Quetta-Pakistan

³Physics Department, Hazara University Mansehra-Pakistan

²Jan.Muhammad@buitms.edu.pk

Abstract—In this paper the design of a fully concurrent dual-band (900/1800MHz) low-noise amplifier (LNA) is presented, the main aim is to bring the noise figure below 3dB to improve the performance of modern receivers. Two single band LNAs operating at GSM 0.9GHz and Digital Cellular System (DCS) 1.8GHz are separately designed using traditional method first then both single-band matching networks are merged, one dual-band matching network (MNs) of the dual band LNA is designed at (900MHz and 1800MHz). This is a single stage amplifier. The dual band LNA is designed to provide low noise figure. The fully concurrent LNA circuit designed using BFG520 Transistor technology, and simulated in Advance Design System (ADS) of version 2009A. For use in multi-standard wireless receiver frontend the proposed design is very useful because the noise figure obtained is suitable for the better performance. The simulation results show that single band LNA at 900 MHz gives the Noise figure of 1.2dB while at 1800MHz it is increased to 2.6dB, the dual band design provides the Noise figure of 1.19dB and 2.71dB for 900MHz and 1800MHz respectively, using 100mA current from 9V power supply with the power consumption of 0.9 Watt.

Keywords—Low Noise Amplifier, Matching Network

I. INTRODUCTION

In the recent years the telecommunication sector is developing swiftly and this development provided growth in radio frequency (RF) operated systems. The demand for high performance and low noise communication circuits has been increased. The LNAs are widely used in the RF and microwave receivers. The LNA is an important component in the front-end of RF receivers [i]. New-generation radio receivers are capable of operating at different frequency bands. Low noise Amplifiers (LNAs) working at wide frequency band and with multi operating standards are required. It is important to design Low Noise Amplifiers operating at different frequency bands. In the receiver chain LNA is the first active element so the overall noise figure

(NF) of the receiver depends on the noise figure (NF) of LNA, which controls output Signal to noise ratio (SNR) and sensitivity of receiver [ii]. LNAs are a frontend device of any receiver system used in wireless communications and normally LNAs are inserted just after the antenna [iii, iv]. The wireless communication input signal is weak and unprotected against noise so the primary task while designing the Low Noise Amplifier is to enhance the signal power and minimizing the introduction of noise. In designing circuits for Low Noise Amplifier the major problem is to reduce noise figure as well as to provide a stable 50Ω input match for maximum power transfer [v].

Initially, two single band LNAs operating at 900MHz and 1800MHz are designed separately. One dual-band matching network (MNs) of the dual band LNA is designed at 900MHz and the other at 1800MHz finally both the networks are combined. This is a single stage amplifier [vi]. The results indicate that the co-design version has a performance similar to that of the cascade version, with the number of passive components reduced to nearly half. In this method, no separate mode control switch is required for channel selection. The values of passive devices in the dual-band Matching Network are determined by the formulae given in this manuscript.

II. BACKGROUND

Key elements in LNA are Noise figure, return loss and the gain, the performance of the system is strongly affected by low NF without adequate gain, and with high gain without low NF [vii, viii].

In the modern receivers, the power of the signal received is usually very low and needs to be properly amplified for further processing like base band operation, so the purpose to design LNA at the frontend is to amplify the signal received and to reduce the noise Fig. 9.

Overall noise figure of the receiver depends on the noise figure of LNA [x], output Signal-to-noise ratio (SNR) and sensitivity of the receiver is controlled by noise figure of LNA [xi], because of these reasons

LNA is considered the most important element of any wireless receiver. To optimize the gain and noise figure number of topologies have been used to implement LNAs, for example single stage LNA in CMOS processes for a standard wireless receiver and for multistandard wireless receivers concurrent and non-concurrent dual band LNAs are developed [xiii].

In a dual band non-concurrent topology anyone of the single band is operated at specific operating frequency [xiii], in another topology two or more single bands working in parallel mode can consume more power in concurrent configuration. Wide band amplifiers are another topology but unwanted signals are also amplified with the input frequency band of interest which degrades the overall performance of the receiver [xiv].

14dB of Voltage gain has been achieved with noise figure of around 2dB for concurrent LNA operating at 900MHz/2.4GHz for multi-standard wireless receiver [v]. To implement multiband LNA there are number of approaches available like wide band, switch mode, parallel mode and concurrent mode LNA [ix, xv].

In this paper the approach followed is concurrent LNA using band pass filter in which the signal is fed to the LNA through band pass filter where the input and output impedance matching is specially considered, when compared with parallel LNA, concurrent LNA topology reduces the chip area or the module area as there would be only one driver circuit for all the frequency bands of choice, and could save the power consumption by reducing the number of passive components on chip. In wide band LNA, strong undesirable blockers are amplified together with the desired frequency bands and receiver sensitivity is significantly degraded [v, xiv].

III. PROCEDURE FOR CO-DESIGN

A. Primary matching network design

Suppose that ω_1 and ω_2 are the two operating angular frequencies for target Band pass filter BPF and LNA where ($\omega_1 < \omega_2$). First, according to method in [iv], BPF is designed, then single band input and output Matching Network(MN) are designed for two single band LNAs.

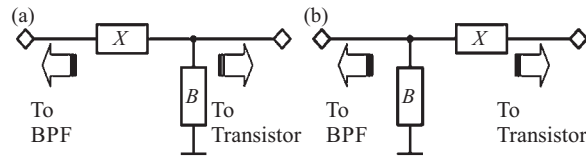


Fig.1. Two types of L-type Matching Networks [vi]

The schematic shown in Fig. 1 (a) and Fig. 1 (b) shows the series reactance and shunt susceptance values at ω_1 and ω_2 as X_1 , B_1 and X_2 , B_2 , respectively. Identical types of single-band Matching Networks MNs for both ω_1 and ω_2 will be used. The

next step is to combine these matching networks into dual band MNs. The general form of dual band matching network is shown in Fig 2.

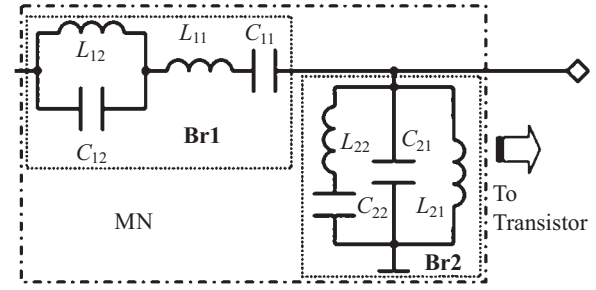


Fig. 2. Two branches of dual-band Matching Network [vi]

If the basic elements of X and B in Fig. 1 have the structure of branches (**Br1**) and (**Br2**) depicted in Fig.2, respectively, it can replace both circuits in Fig. 1 as a dual-band MN in Fig. 2 for the dual-band LNA. The value of each element of branches 1 and 2 in dual-band MN shown in Fig. 2 can be calculated using the following procedure [vi].

B. Translation of single band MNs into Dual band MN

Two single band matching networks designed for ω_1 and ω_2 can be converted into one dual band matching network having structure of Fig. 1 by using the following formulas.

First of all, find out values of each element in the series branch (**Br1**) of the dual-band MN, the elements are L_{11} , C_{11} , L_{12} and C_{12} . Equation 1 and equation 2 give the relationship of these elements with a single band MNs series branch [xvi].

$$\omega_1 L - \frac{1}{\omega_1 C_{11}} + \frac{\omega_1 L_{12}}{1 - \omega_1^2 L_{12} C_{12}} = X_1 \quad (1)$$

$$\omega_2 L_{11} - \frac{1}{\omega_2 C_{11}} + \frac{\omega_2 L_{12}}{1 - \omega_2^2 L_{12} C_{12}} = X_2 \quad (2)$$

Taking further combination and resolving the expressions the current through L_{12} can be given as

$$C_{12} L_{12} = \frac{1}{\omega_1 \omega_2} \quad (3)$$

The values of L_{11} , C_{11} and C_{12} are dependent on L_{12} once it is calculated we can determine L_{11} , C_{11} and C_{12} from Equation 1–3. For L_{11} , C_{11} and C_{12} to be non-negative L_{12} should be minimum, L_{12min} can be given as;

$$L_{12min} = \max\left[0, \frac{(\omega_2 - \omega_1)(X_1 \omega_1 - X_2 \omega_2)}{\omega_1 \omega_2 (\omega_1 + \omega_2)}, \frac{(\omega_2 - \omega_1)(X_1 \omega_2 - X_2 \omega_1)}{\omega_1 \omega_2 (\omega_1 + \omega_2)}\right] \quad (4)$$

L_{12} is located to the smallest possible value. By putting value of L_{12} in equation (3) it can be able to calculate C_{12} which can be used to calculate L_{11} and C_{11} from equation (1).

In the same way, for the shunt branch (Br2) in the dual-band MN, the equations used to conclude L_{22} , C_{22} , L_{21} and C_{21} can be acquired as [xvi]

$$\omega_1 C_{21} - \frac{1}{\omega_1 L_{21}} + \frac{\omega_1 L_{22}}{1 - \omega_1^2 L_{22} C_{22}} = B_1 \quad (5)$$

$$\omega_2 C_{21} - \frac{1}{\omega_2 L_{21}} + \frac{\omega_2 L_{22}}{1 - \omega_2^2 L_{22} C_{22}} = B_2 \quad (6)$$

$$C_{22} L_{22} = \frac{1}{\omega_1 \omega_2} \quad (7)$$

$$C_{22} \min = \max \left[0, \frac{(\omega_2 - \omega_1)(B_1 \omega_1 - B_2 \omega_2)}{\omega_1 \omega_2 (\omega_1 + \omega_2)}, \frac{(\omega_2 - \omega_1)(B_1 \omega_2 - B_2 \omega_1)}{\omega_1 \omega_2 (\omega_1 + \omega_2)} \right] \quad (8)$$

Above formulas provide mathematical background for the design of dual band LNA, this is implemented in circuit designing and the theory is used to obtain our results [vi]

IV. BIASING NETWORK DESIGN

The approach is implemented in Advance Design System (ADS) to obtain the simulation results [xvii]. DC Voltage of 9V is applied to the transistor BFG 520 which is used in circuit. Biasing network is shown in Fig 3, with appropriate plan of biasing resistors, desired operating voltage and current were accomplished.

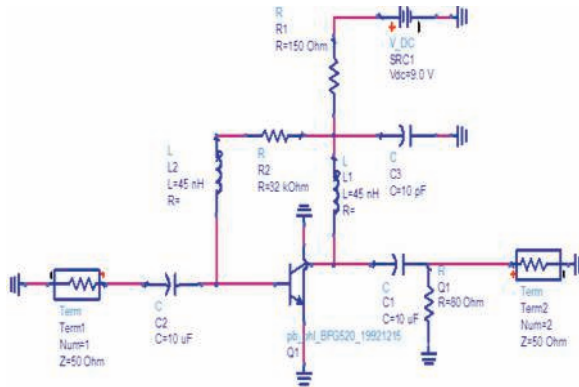


Fig 3. Schematic of biasing network

In this circuit the capacitors C1, C2 force that no direct current travels to the input and output portion of RF path. The C3 capacitor is used as a filter which prevents the unwanted noise and high frequency ripple signals from the direct current power supply, a capacitor of 10uF capacitance is more suitable in this circuit for blocking the DC. Two inductors L1 and L2 prevent the radio frequency signals travelling into the biasing network of circuit. These inductors L1 and L2 chokes are used to separate the radio frequency from the biasing network circuit. After analyzing the results, it was analyzed that to increase the maximum gain it is possible to set all the reactive components.

V. SINGLE BAND LNAS

First step in circuit of dual band low noise amplifier design is to design two single band low noise amplifiers at 900MHz and 1800MHz.

A. LNA design at 900MHz

Fig 4. Depicts the circuit diagram of LNA at 900MHz. Design includes a shunt capacitor of 4.43pF and a series inductor of 5.19nH as input matching network. Output matching network contains a shunt inductor of 55.5nH. These components make the proposed LNA design perfectly matched at 50Ω at both input and output ports.

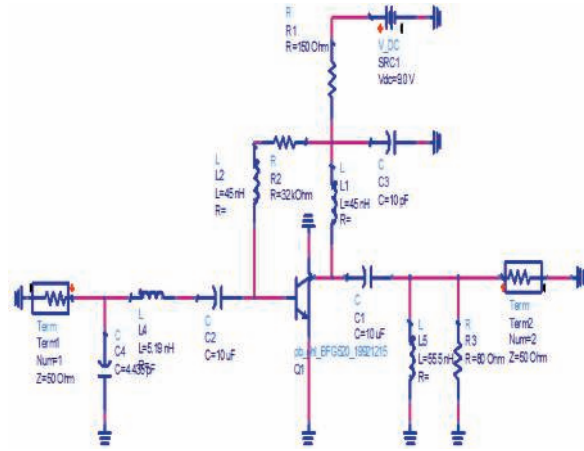


Fig 4. Matching Network Design of LNA at 900MHz

B. LNA design at 1800MHz

The circuit diagram of LNA at 1800 MHz is depicted in Fig 5. Design includes a shunt inductor of 3.35nH and a series capacitor of 2.82pF as input matching network. Output matching network contains a shunt inductor of 14.93nH. These components make this LNA design perfectly matched at 50Ω at both input and output ports at the desired operating frequency i.e. 1800MHz.

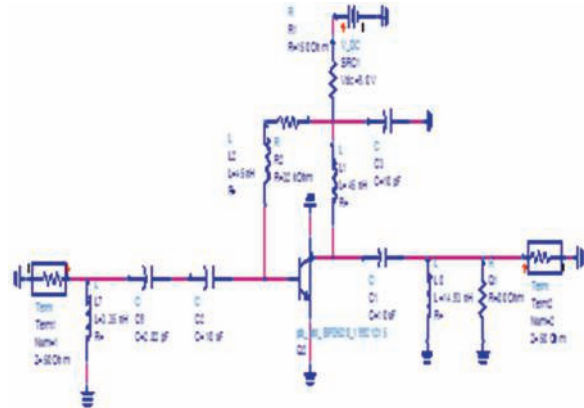


Fig 5. Matching Network Design of LNA at 1800MHz

C. Results of 900MHz LNA

In order to analyze the behavior of the RF devices or networks at a given frequency we need scattering parameters or S-parameter. Fig. 6 describes the curve of S-Parameter $S(2, 1)$ it is the forward transmission of input at port1 and output at port2. Marker indicated the results of $S(2, 1)$ at 900MHz. Forward transmission is taken in dB, in the biasing network and set the all values of components for high gain result, low noise and stability of the circuit. Fig. 6 shows that the gain of 14.138dB at 900MHz is obtained.

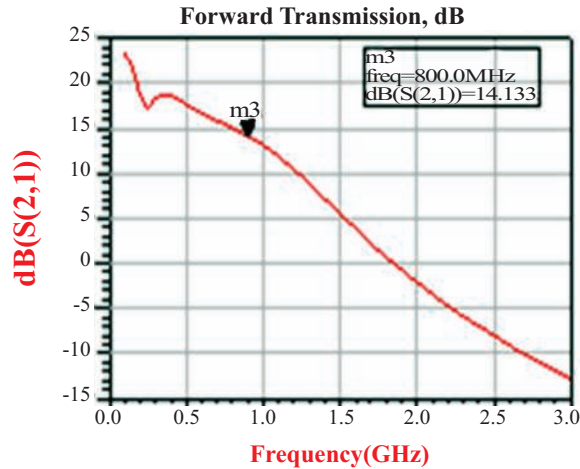


Fig. 6. Graph showing Forward transmission at 900MHz

Fig. 7. Shows the result of S-Parameter $S(1, 2)$, which is the input transmission at port2 and output is port1. Marker M2 shows the result of $S(1, 2)$ at 900MHz, which is around -27dB.

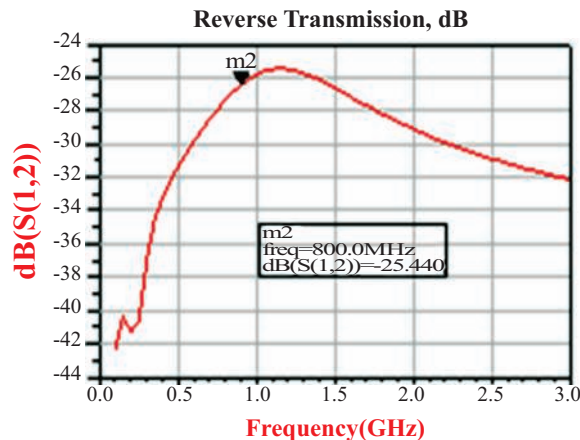


Fig. 7. Graph showing Reverse Transmissions at 900MHz

Input and output Coefficients of reflection are important for the maximum power transfer, Fig 8 shows the plots of input reflection coefficient on smith chart. The Marker (M1) in Fig. 8 shows that amplifier is

matched at 900MHz, since it has no imaginary part at the output port.

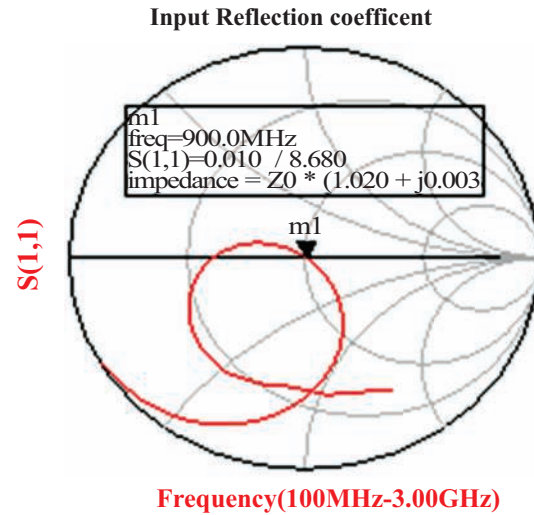


Fig. 8. Input reflection coefficient smith chart at 900MHz

Fig. 9 shows the plot of output reflection coefficient on smith chart. Marker shows that amplifier is matched at 900MHz, since it has no imaginary part at output port.

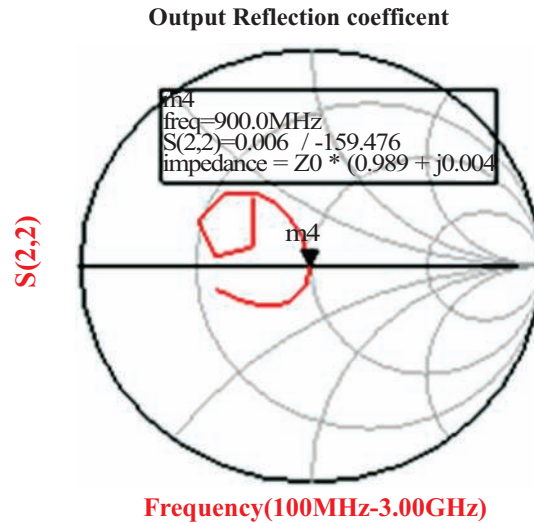


Fig. 9. Output reflection coefficient on smith chart at 900MHz

As depicted in Fig. 10, is the curve of minimum noise figure and the actual noise figure of design at 900MHz. The two curves blue and red shows the curve of minimum noise figure for the frequency between of 100MHz to 3.0GHz and the actual noise figure of the designed circuit network for the same frequencies respectively. Values of minimum noise figure and the actual noise figure at 900MHz is 1.01 and 1.208 respectively are also shown.

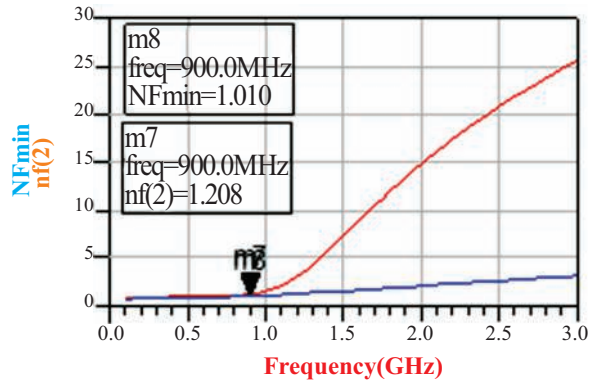


Fig. 10. Showing minimum and actual noise figure at 900MHz

The curve of stability function ' μ ' after designed the matching network is shown in Fig 11. The red and blue lines in the plot stand for Stability Factor ' μ ' (Load) and ' μ ' (Source).

$\mu > 1$
is the condition for unconditional stability as shown in the graph represents that amplifier is stable.

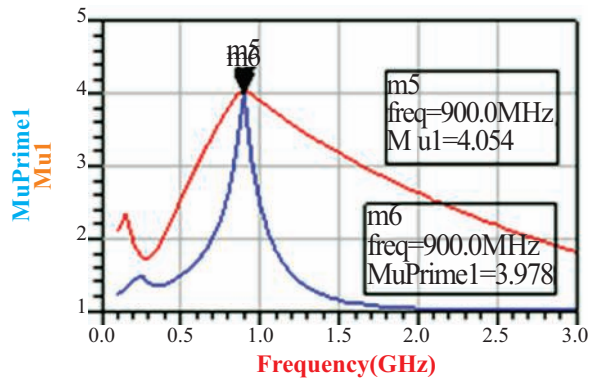


Fig. 11. Unconditionally stable at 900MHz

Fig. 12 demonstrates the plot for input reflection coefficient in the linear scale region below 10dB from 700MHz to 1.050GHz. These are the two boundary points of bandwidth; it is observed that frequency ranges of input and output return losses are less then -10dB.

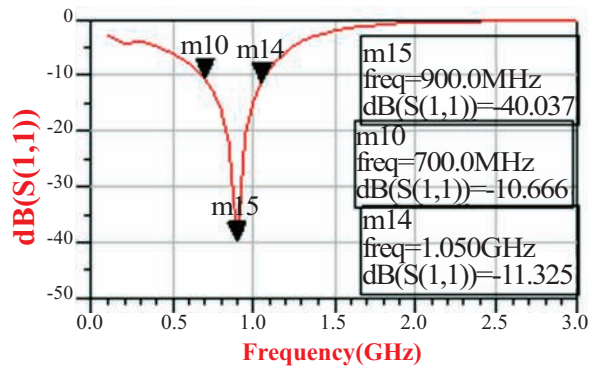


Fig. 12. Bandwidth at 900MHz

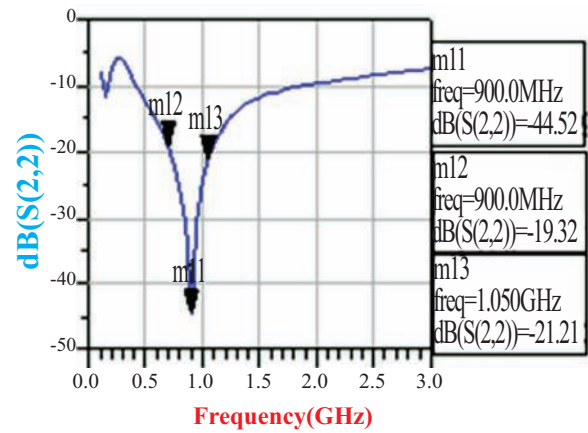


Fig. 13. Output reflection coefficients at 900MHz

The result of Output Reflection Coefficient (ORC) is demonstrated in Fig 13. The markers are positioned at the required points of bandwidth.

D. Results of 1800MHz LNA

Fig 14 represents the curves of S-Parameter S (2, 1). It is the Forward Transmission (FT) input at port1 and output is port2. Marker indicates the result of S (2, 1) at 1800MHz. Design the biasing network and set all the values of components for high Gain, Low noise and Stability. Fig 14 shows that the gain at 1800MHz is 8.577dB.

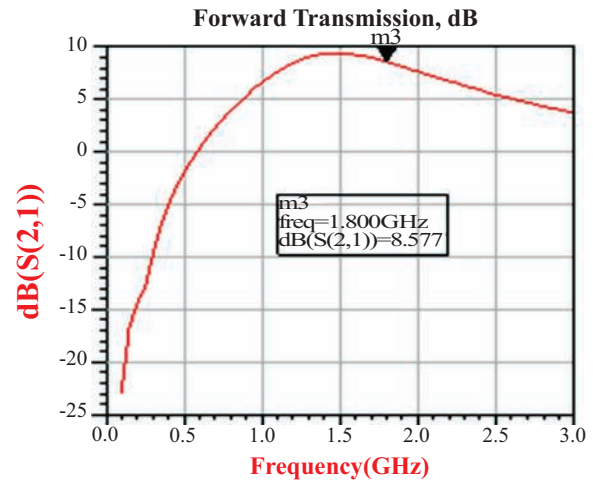


Fig. 14. Graph showing Forward transmission at 1800MHz

The Fig. 15 depicts the curve of S-Parameter S (1, 2) It is the transmission of input at port2 and output at port1. Marker(M4) shows the result of S (1, 2) at 1800MHz. Reverse transmission (RT) is taken in dB. The designed biasing network and all the set values of passive components the reverse transmission at port 1 is -20.324 dB at 1800MHz.

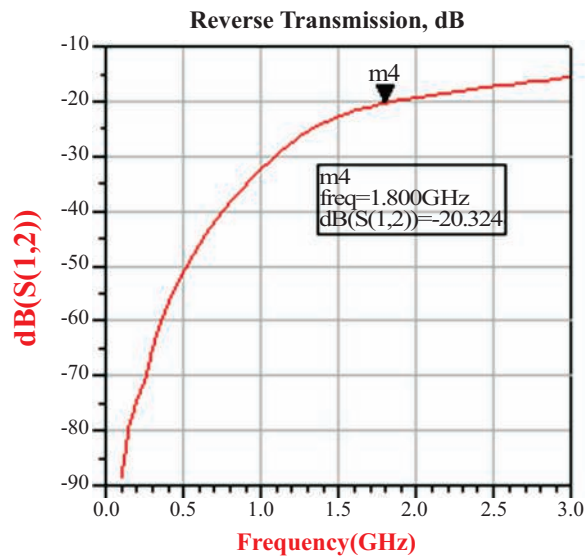


Fig. 15. Graph showing Reverse Transmissions at 1800MHz

The plots shown in Fig. 16 and 17 are the input reflection and output reflection coefficient on smith chart at 1800MHz respectively. Markers indicate that the amplifier is matched at 1800MHz as it has no imaginary part at input as well as output port.

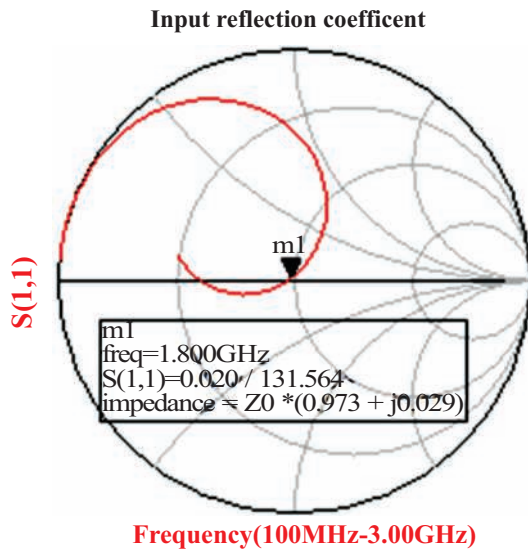


Fig. 16. Shows Input reflection coefficient smith chart at 1800MHz

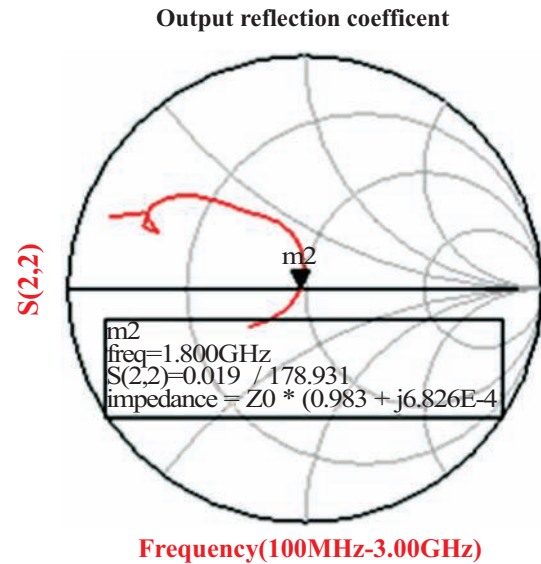


Fig. 17. Shows Output reflection coefficient on smith chart at 1800MHz

In Fig. 18 the curve of minimum noise diagram and the actual noise diagram of design at 1800MHz are depicted. Two curves in blue and red color show the curve of minimum noise diagram in the frequency range from 0GHz to 3.0GHz and the actual noise diagram of designed network for the same frequencies, respectively. Values of min noise diagram and the actual noise diagram at 1800MHz are 1.847 and 2.625 dB, respectively.

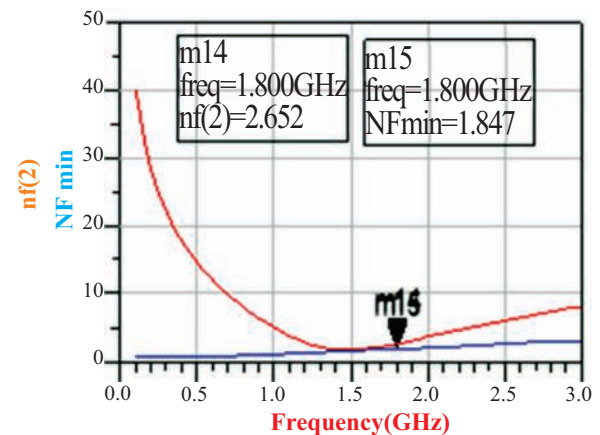


Fig. 18. Noise Figure at 1800MHz

Fig. 19 shows the condition for unconditional stability, graph shows that amplifier is stable.

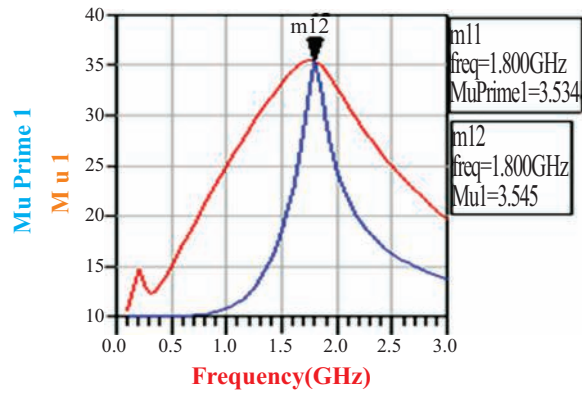


Fig. 19. Unconditionally stable at 1800MHz

Fig. 20 demonstrates the plot of input reflection coefficient in the linear scale in region below 10dB from 1.550GHz to 2.250GHz. These are the two boundary points for bandwidth. For these results both input and output return losses are less than -10dB.

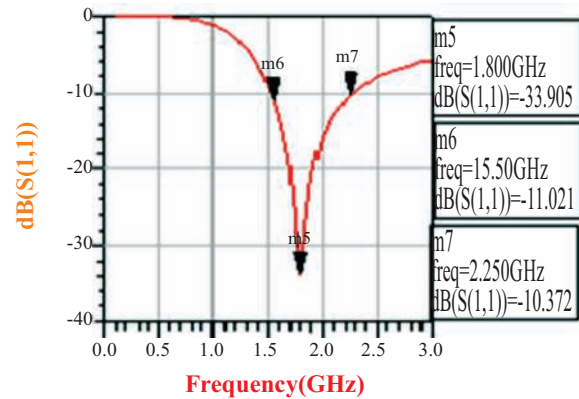


Fig. 20. Shows Bandwidth at 1800MHz

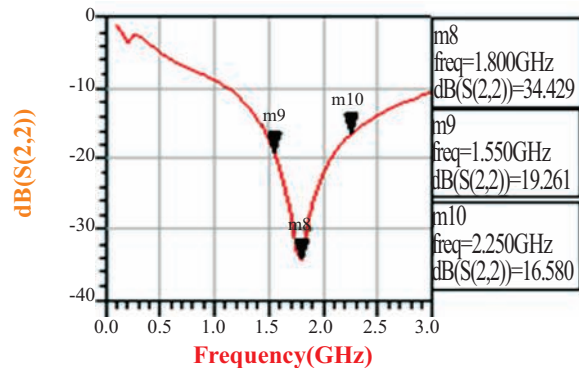
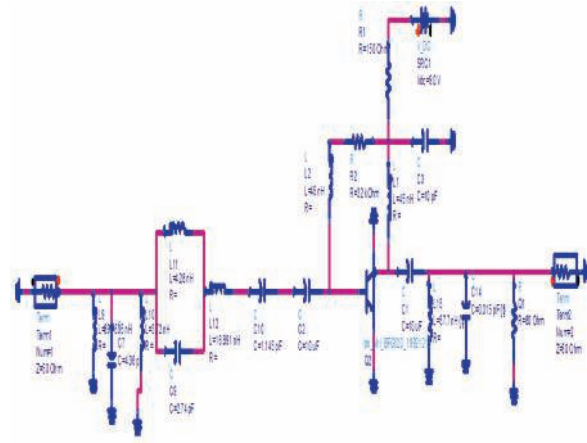


Fig. 21. Shows Output reflection coefficients at 1800MHz

The result of Output Reflection Coefficient is demonstrated in Figure 21. Markers positioned at required bandwidth and preferred frequency.

VI. DUAL BAND LNA

As discussed earlier, we designed the Dual Band matching network from the two single Band matching network circuits with operating frequencies at 900MHz and 1800MHz. This describes the results of the final Dual Band Low Noise Amplifier working at both 900 MHz and 1800MHz concurrently. The circuit diagram shown in Fig. 22 is used for making Dual Band Low Noise Amplifier.



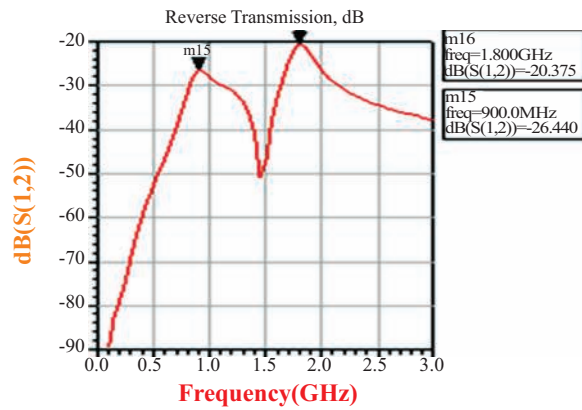


Fig. 24. Graph showing Reverse transmission

Fig. 24 shows Reverse Transmission (RT), by designing the biasing network and setting all the values of components for Low noise amplifier, the values of RT obtained are -26.44 dB and -20.375 dB at 900MHz and 1800MHz respectively.

Figures 25 and 26 depict the results of output reflection and input reflection coefficients respectively on Smith Chart at 900MHz and 1800MHz.

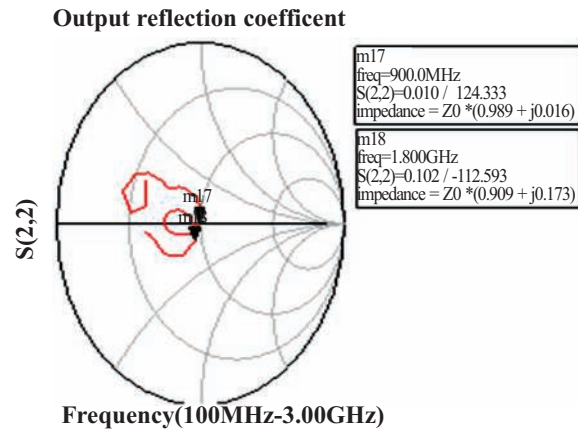


Fig. 25. Output reflection coefficient on smith chart

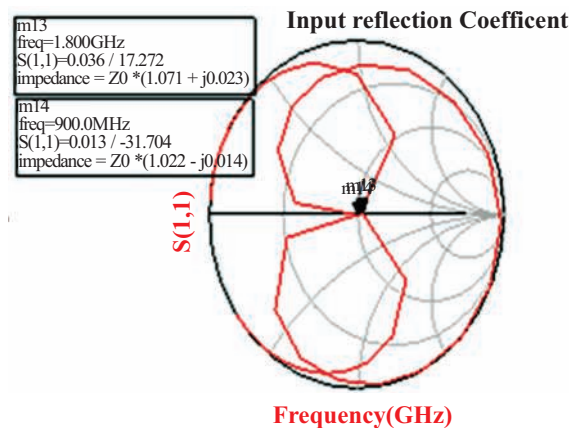


Fig. 26. Input reflection coefficient on smith chart

Fig. 27 shows the curve of minimum noise and the actual noise of dual band design at 1800MHz and 900MHz. Two curves (blue and red) show the curve of minimum noise in between frequency ranges of 0GHz to 3.0GHz and the actual noise of designed network of similar frequency ranges, respectively. Value of minimum noise figure and the actual noise figure at 1800MHz is 1.847 and 2.717 respectively and values of minimum noise and the actual noise at 900MHz is 1.01 and 1.195 respectively.

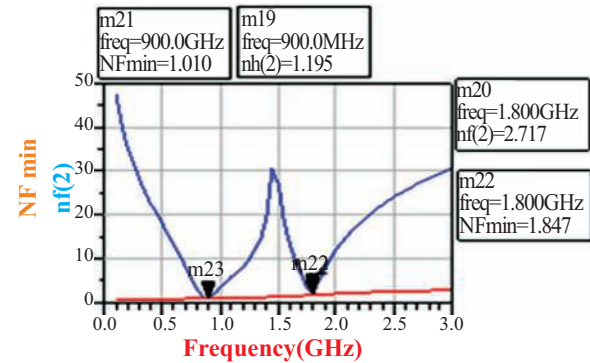


Fig. 27. Graph shows Noise Figure

For the stability check following plot in Figure 28 shows that the LNA is stable for desired frequency range.

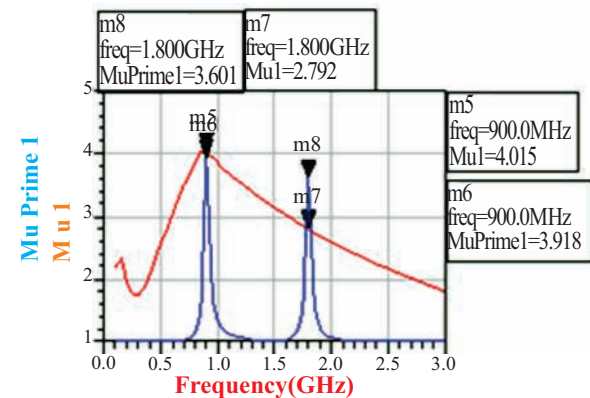


Fig. 28. Graph shows unconditionally stable

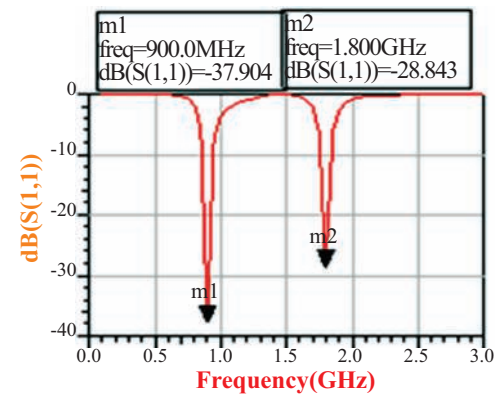


Fig. 29. Shows Bandwidth

Fig. 29. Shows the two operating bands of dual band LNA marked at 900MHz and 1800MHz.

VII. RESULTS AND DISCUSSIONS

The results obtained are summarized in table I and II respectively, the single band LNA at 900 MHz achieved the noise figure of 1.2dB while at 1800MHz it is 2.6dB and our dual band design has provided the noise figure of 1.19dB and 2.71dB for 900MHz/1800MHz respectively drawing 100mA current from 9V power supply with power consumption of 0.9 Watt. Signal gain for 900MHz/1800MHz achieved the values of 14.13dB and 8.52 dB.

The results clearly elaborate performance of dual band single stage LNA, the appropriate input and output matching network for the given amplifier has provided efficient gain and minimum noise figure. The design of Low Noise Amplifier is completed using ADS simulations.

Moreover, an RF dual band LNA with working frequency of 900MHz and 1800MHz was designed, simulated, and built. The results suggest that the amplifier have a comparatively high gain which keeps the amplifier intrinsically stable at all the frequencies.

TABLE I
SUMMARY OF VOLTAGE GAIN AND NOISE FIGURE

Frequency	0.9 GHz	1.8 GHz
Voltage Gain	14.138dB	8.577dB
Noise Figure	1.19dB	2.71dB
DC Current	100mA	100mA

TABLE II
SUMMARY OF CONCURRENT DUAL BAND LNA PERFORMANCE

Specification Name	LNA at 900 MHz	LNA at 1800MHz	Dual Band LNA at 900MHz and 1800MHz	
Center Frequency	900 MHz	1800MHz	900 MHz	1800MHz
Bandwidth	>300MHz	>300MHz	100MHz	100MHz
Small signal Gain	14.13 dB	8.57 dB	14.13 dB	8.52 dB
Return loss (input, output)	-40 dB	-34 dB	-37.9 dB	-28.8 dB
Noise Figure	1.2 dB	2.6 dB	1.19 dB	2.71 dB
Supply Voltage	9V			
DC current	100mA			

VIII. CONCLUSIONS

Aim of this research is to model a conventional design for the Low Noise Amplifier, which is efficient

Co-design procedure for Dual-band Low Noise Amplifier.

Small signal gain is achieved above 14 dB with the noise figure of 1.19 dB and 2.71 dB for 900MHz and 1800MHz respectively.

If the less lossy RF substrate and high quality factor (Q) inductors are available, it will be possible to design true concurrent LNAs with better performance.

We plan to extend this design for tunable multi-band LNAs with more selective load filter using high quality factor (Q) inductors and minimizing the power consumption.

REFERENCES

- [i] R. Ma and W. Zhang "Co-design of Dual-band Low Noise Amplifier and Band-pass Filter", International Journal of Electronics, April, 2010.
- [ii] H. T. Friss "Noise Figure of Radio Receivers", Proc. IRE, vol. 32, pp.419-422 1944.
- [iii] J. J. Wang and Y. P. Zhang "Circuit model of microstrip patch antenna on ceramic land grid array package for antenna-chip co-design of highly integrated RF transceivers", IEEE Trans. Antennas Propag., vol. 53, no. 12, pp.3877-3883 2005
- [iv] W. Wang, Y. P. Zhang, '0.18- μ m CMOS push-pull power amplifier with antenna in IC package," IEEE Microwave and Wireless Components Letters, Vol. 14, No. 1, pp. 13-15, 2004.
- [v] SS. Datta , K. Datta, A. Dutta, T. K. Bhattacharyya, "Fully Concurrent Dual-Band LNA Operating in 900 MHz/2.4 GHz Bands for Multi-Standard Wireless Receiver with sub-2dB Noise Figure", IEEE Third International Conference on Emerging Trends in Engineering and Technology, 2010.
- [vi] S. Datta; A. Dutta, K. Datta, T. K. Bhattacharyya, "Pseudo Concurrent Quad-Band LNA Operating in 900 MHz/1.8 GHz and 900 MHz/2.4 GHz Bands for Multi-Standard Wireless Receiver," IEEE 24th International Conference on VLSI Design (VLSI Design), 2011.
- [vii] A. Victor and J. Nath, "An Analytic Technique for Trade-Off of Noise Measure and Mismatch Loss for Low Noise Amplifier Design", Wireless and Microwave Technology Conference (WAMICON), IEEE 11th Annual. IEEE, 2010
- [viii] H. A. Haus "Optimum noise performance of linear amplifiers", Proc. IRE, vol. 46, no. 8, pp.1517-1539
- [ix] H. Hashemi and A. Hajimiri, "Concurrent Multi-Band Low-Noise Amplifiers-Theory, Design and Applications", IEEE Trans. On Microwave Theory and Techniques, vol. 50, No.

- 1, pp. 288-301, Jan. 2002.
- [x] H. T. Friis, "Noise Figure of radio receivers," Proc. IRE. pp. 419-422, July 1944.
- [xi] K. L. Fong, "Dual-band high-linearity variable-gain low-noise amplifiers for wireless applications," in Int. Solid-State Circuits Conf. Tech.Dig., Feb. 1999, pp. 224–225.
- [xii] J. Ryyanen, K. Kivekas, J. Jussila, A. Parssinen, and K. Halonen, "A dual-band RF front-end for WCDMA and GSM applications," in Proc. IEEE Custom Integrated Circuits Conf., May 2000, pp. 175–178.
- [xiii] R. Magoon, I. Koullias, L. Steigerwald, W. Domino, N. Vakilian, E. Ngompe, M. Damgaard, K. Lewis, and A. Molnar, "A triple-band 900/1800/1900MHz low-power image-reject front-end for GSM," in Int. Solid-State Circuits Conf. Tech. Dig., Feb. 2001, pp. 408–409.
- [xiv] J. Janssens, J. Crols, and M. Steyaert, "A 10 mW inductorless, broadband CMOS low noise amplifier for 900 MHz wireless communications," in Proc. IEEE Custom Integrated Circuits Conf., May 1998, pp.75–78.
- [xv] S. Datta, K. Datta, A. Dutta, T. K. Bhattacharyya, "Pseudo Concurrent Quad-Band LNA operating in 900 MHz, 1.8 GHz and 900 MHz, 2.4 GHz bands For Multi-Standard Wireless Receiver", IEEE International Conference on Communications and Electronics, Aug 2010.
- [xvi] I. Akhchaf, S. Khouliji, M. Essaidi, & M. L. Kerkeb, "Study, Modeling and Characterization of Dual-Band LNA Amplifiers Receivers for Wireless Microwaves Communication Systems", Journal of Wireless Networking and Communications, 2012.
- [xvii] <http://www.keysight.com/en/pc1297113/advanced-design-system> (last visited Dec, 2014)



Technical Journal

Website: www.uettaxila.edu.pk

University of Engineering and Technology, Taxila-Pakistan

CALL FOR PAPERS

Researchers and Academia are invited to submit the research articles to Technical Journal of UET Taxila. It is a peer reviewed, broad-based open access journal. It covers all areas of engineering sciences and engineering management.

Technical Journal is a quarterly publication of UET Taxila recognized by HEC in “Y” category. It is published regularly with a key objective to provide the visionary wisdom to academia and researchers to disseminate novel knowledge and technology for the benefit of society. Technical Journal is indexed by well recognized international database such as PASTIC Science Abstracts, AGRIS Data Base, ProQuest Products, EBSCO Data Bases, Library of Congress and various other nineteen (19) HEC approved abstracting and indexing agencies.

For enquiries, submissions of articles or any other information please visit our website <http://web.uettaxila.edu.pk/techjournal/index.html> or contact the Editorial Office on the following number: +92-51-9047896

e-mail: technical.journal@uettaxila.edu.pk

Submission of paper remains open round the year. Researchers and Academia can submit their papers at any time which they deem fit. Presently there are no charges for publication of research paper in Technical Journal.

It will be highly appreciated if the information is forwarded to interested colleagues from Pakistan as well as abroad.

Looking forward to receiving the research papers on behalf of Technical Journal Editorial Office.

Dr. Hafiz Adnan Habib

Chief Editor

Technical Journal,

UET, Taxila

Instruction for authors for publishing in Technical Journal UET Taxila

General

Papers may be submitted any time throughout the year. After receipt of paper it will be sent to concerned referees, at least one from a technology advanced countries. Papers reviewed and declared fit for publication will be published in the coming issue. The journal is quarterly publication, having four issues annually. A soft copy of paper must be submitted through online submission system by using the following link:-

<http://tj.uettaxila.edu.pk/index.php/technical-journal/about/submissions>

Authors are required to read the following carefully for writing a paper.

Manuscript Preparation

Text should be type-written with M.S word, Times New Roman Font size 10, at single space and with margins as 1 inch top, 1 inch left, 0.5 inch right, and 1 inch bottom, on an A-4 size paper. The manuscript should be compiled in following order:-

Title Page

The Title page should contain:

- Paper title
- Author names and affiliations
- Postal and email addresses
- Telephone/Cell and fax numbers
- One author should be identified as the Corresponding Author

Abstract

An abstract up to maximum of 200 words should be written in the start of paper. The abstract should give a clear indication of the objectives, scope, methods, results and conclusions.

Keywords

Include at least five keywords (Title Case) in a separate line at the end of the abstract.

Body of the Paper

Body of the paper may include introduction and literature review, materials and methods, modeling/experimentation, results-discussions and conclusions etc.

- Define abbreviations and acronyms the first time they are used in the text, even after they have already been defined in the abstract. Do not use abbreviations in the title unless they are Unavoidable.
- Use zero before decimal places: "0.24" not ".24".
- Avoid contractions; for example, write "do

not" instead of "don't."

- If you are using *Word*, use either the Microsoft Equation Editor or the *MathType* add-on (<http://www.mathtype.com>) for equations in your paper (Insert | Object | Create New | Microsoft Equation or Math Type Equation). Number equations consecutively with equation numbers in parentheses flush with the right margin, as in (1). Refer to "(1)," not "Eq. (1)" or "equation (1)," except at the beginning of a sentence: "Equation (1) is ..."
- Symbols used in the equations must be defined before or immediately after it appears.
- Use SI units only.

Originality

Only original contributions to Engineering, Science and Management literature should be submitted for publication. It should incorporate substantial information not previously published.

Length

Research paper should be consisting of 5-8 pages as per specifications given above.

Accuracy

All the technical, scientific and mathematical information contained in the paper should be checked with great care.

Figures

All figures should be at least 300 dpi in JPG format. It is to be also ensured that lines are thick enough to be reproduced conveniently after size reduction at the stage of composing. All figures (graphs, line drawings, photographs, etc.) should be numbered consecutively and have a caption consisting of the figure number and a brief title or description of the figure. This number should be used when referring to the figure in the text. Figure may be referenced within the text as "Fig. 1" etc.

Tables

Tables should be typed in a separate file using M.S. Word 'table' option. All tables should be numbered in Roman numerals consecutively. Tables should have a caption in Upper Case, must be centered and in 8 pt. consisting of the table number and brief title. This number should be used when referring to the table in text. Table should be inserted as part of the text as close as possible to its first reference.

When referencing your figures and tables within your paper, use the abbreviation "Fig." Even at the beginning of a sentence. Do not abbreviate "Table." Tables should be numbered with Roman Numerals.

Acknowledgments

All individuals or institutions not mentioned elsewhere in the work who have made an important contribution should be acknowledged.

References

Reference may be cited with number in square brackets, e.g. "the scheme is discussed in [iii]". Multiple references are each numbered with in bracket. e.g. the scheme is discussed in [iv-vii]. Do not use "Ref." or "reference" except at the beginning of a sentence: "Reference [xi] illustrates..."

Please do not use automatic endnotes in Word, rather, type the reference list at the end of the paper using the "References" style. Reference list/bibliography and in text references, both will be cited in roman alphabet. "Within text citations must be in chronological order in the first appearance. The subsequent appearance(s) of the same may be random as per need of the paper."

Note: For template of paper please visit our journal's page:

<http://web.uettaxila.edu.pk/techjournal/index.html>

Check List

Sr. No.	Description	Yes/No																												
1	<p>Undertaking signed by all authors that the research paper has not been submitted to any other journal for publishing and submitted research work is their own original contribution is required as per following format.</p> <table border="1"> <tr> <td colspan="4">Paper Titled:</td> </tr> <tr> <td colspan="4">Authorship and Contribution Declaration</td> </tr> <tr> <td>Sr.#</td> <td>Author-s Full Name</td> <td>Contribution to Paper</td> <td>Author-s Signature</td> </tr> <tr> <td>1</td> <td>Mr./Dr./Prof. Alpha (Main/principal Author)</td> <td>Proposed topic, basic study Design, methodology and manuscript writing</td> <td></td> </tr> <tr> <td>2</td> <td>Mr./Dr./Prof. Bravo(2nd Author)</td> <td>Data Collection, statistical analysis and interpretation of results etc.</td> <td></td> </tr> <tr> <td>3</td> <td>Mr./Dr./Prof. Charlie (3rd Author)</td> <td>Literature review & Referencing, and quality insurer</td> <td></td> </tr> <tr> <td>⋮</td> <td>⋮</td> <td>⋮</td> <td></td> </tr> </table>	Paper Titled:				Authorship and Contribution Declaration				Sr.#	Author-s Full Name	Contribution to Paper	Author-s Signature	1	Mr./Dr./Prof. Alpha (Main/principal Author)	Proposed topic, basic study Design, methodology and manuscript writing		2	Mr./Dr./Prof. Bravo(2 nd Author)	Data Collection, statistical analysis and interpretation of results etc.		3	Mr./Dr./Prof. Charlie (3 rd Author)	Literature review & Referencing, and quality insurer		⋮	⋮	⋮		
Paper Titled:																														
Authorship and Contribution Declaration																														
Sr.#	Author-s Full Name	Contribution to Paper	Author-s Signature																											
1	Mr./Dr./Prof. Alpha (Main/principal Author)	Proposed topic, basic study Design, methodology and manuscript writing																												
2	Mr./Dr./Prof. Bravo(2 nd Author)	Data Collection, statistical analysis and interpretation of results etc.																												
3	Mr./Dr./Prof. Charlie (3 rd Author)	Literature review & Referencing, and quality insurer																												
⋮	⋮	⋮																												
2	Pictures are placed on paper at proper places and separate pictures in JPEG format are provided in a separate file with their caption as well.																													
3	Technical Journal UET Taxila follow IEEE format. Please submit your paper according to required format i.e. double column, tables and figures captions & numbers, indentation and particularly in-text citation and bibliography according to IEEE format.																													
4	"Time New Roman" font shall be used in legends, captions of Figures, Graphs and Tables etc.																													
5	Complete contact information of the corresponding author:- Name: _____, Designation: _____ Institute Name: _____, Email: _____ Cell: _____, Ph No. and Fax (if any) _____																													
6	Main area of Research paper e.g. Electrical, Mechanical etc. shall be mentioned																													
<p>Note: Ensure that all requirements have been met before submitting the paper http://tj.uettaxila.edu.pk/index.php/technical-journal/about/submissions For any query please visit: http://web.uettaxila.edu.pk/techJournal/index.html</p>																														

EDITORIAL OFFICE: Correspondences should be made on the following address:

Asif Ali

Editor, Technical Journal Editorial Office

Central Library, University of Engineering and Technology (UET) Taxila, Pakistan

Tel: +92 (51) 9047896 Email: technical.journal@uettaxila.edu.pk

